Université de Strasbourg

École Doctorale des Sciences de la Vie et de la Santé

Thèse présentée par :

Beatriz Alejandra Macias Garcia

Pour obtenir le grade de

Docteur de l'Université de Strasbourg

Discipline : Sciences du vivant

Spécialité : Aspects Moléculaires et Cellulaires de la Biologie

Déficit en Ikaros: de LAL-T à la maladie auto-immune

Soutenue publiquement le 8 Octobre 2012

Membres du Jury:

Rapporteur Interne/Président du Jury: Dr. Anne-Sophie Korganow

Rapporteur Externe : **Dr. Françoise Pflumio**

Rapporteur Externe : **Dr. Bertrand Nadel**

Directeur de Thèse : **Dr. Susan Chan**

I would like to thank…

…Susan and Philippe to give me the opportunity to be part of their nice lab, for their trust in me to work in different areas, for all their support and their discussions

…the jury members Anne-Sophie Korganow, Francoise Pflumio and Bertrand Nadel for agreeing to read my thesis and judge my work

…the former members of the lab, the lady Qi Cai for all the FACS advice and the nice conversations in the lab, my dear Notch team Robin for showing me how to take care of the cell lines and the sick mice and to Mac for replaying my countless questions and his great assistance in the B cell stimulation when he came for a Thanks-giving dinner…

…the actual members of the lab: Apos, Kate, Rose-Marie, but specially to Jerome, the other member of the Notch team for all the work and the time that we spend together to get the paper, to Deepika and Peggy for all their discussion and support for the LICs project, and even more specially to Beate for all her discussion about B cells, the revision of my English, and her support when I lost my patience, I will not be the worst person if you are around ;o) and to Attila, who showed me how fast the weather can change in Strasbourg, I have never seen before indoor snow, and for his support in the scientific and personal aspects

…Patricia and Claudine for their technical support in the lab and with the FACS and for the delicious cakes and cookies for the emotional support

…all the IGBMC services especially to Alex and William for their help with the mice, their patience in teaching me how to handle the mice and all the bleeding they did for me

…my friends, for their support despite the distance

…my parents and my brothers, for all their love and for always being there

…Manuel, without whom I would not be here, thanks to his care, to all his supporting and to share this incredible experience together

TABLE OF CONTENTS

ABBREVIATIONS

5'FU	5'fluorouracil
ABC	ATP-binding cassette
AID	Activation-Induced cytidine Deaminase
ALL	Acute Lymphoblastic Leukemia
AML	Acute Myelogenous Leukemia
ANA	Antinuclear antibodies
APL	Acute Promyelocytic Leukemia
ATL	Adult T cell Leukemia/lymphoma
BAFF	B cell activator of the TNF family
B-ALL	B-Acute Lymphoblastic Leukemia
BCR	B Cell Receptor
BLNK	B cell linker protein
BM	Bone Marrow
Btk	Bruton's tyrosine kinase
C-	Carboxy
CD	Cluster of Differentiation
CDR	Complementary Determining Regions
CFSE	Carboxyfluorescein succinimidyl ester
CGH	Comparative Genomic Hybridization
CLP	Common Lymphoid Progenitors
CML	Chronic Myeloid Leukemia
CNA	Copy Number Alteration
CNS2	Conserved Non-coding Sequence 2
CRAC	calcium release activated calcium
CSC	Cancer Stem Cell
CSR	Class Switch Recombination
CtBP	C terminal Binding Protein
CtIP	CtBP Interacting Protein
DAG	Diacylglycerol
Dll-1	Delta-like ligand (1,3,4)
dn	dominant negative
DN	Double negative (CD4$^-$CD8$^-$)
DNA	Deoxyribonucleic Acid
DP	Double positive (CD4$^+$CD8$^+$)
E5	Embryonic day 5
EBF1	Early B cell Factor 1
EC	Extracellular
ELISA	Enzyme-Linked ImmunoSorbent Assay
ER	Endoplasmic Reticulum

4

ERK	Extracellular signal-Regulated Kinase
ETP	Early T-cell Precursors
FACS	Fluorescence-Activated Cell Sorting
FCS	Fetal Calf Serum
FO	Follicular B cells (B220$^+$CD23^{hi}CD21^{med})
Fr	Fraction
GSI	γ-secretase inhibitor
GSK-3	Glycogen Synthase Kinase-3
HC	Heavy Chain
HD	Heterodimerization
HEL	Hen Egg Lysozome
Hes-1	Hairy and enhancer of split-1
HSC	Hematopoietic Stem Cells
ICN	Intracellular Notch1
Ig	Immunoglobulin
IGF1R	Insulin-like Growth Factor Receptor 1
Igh	Immunoglobulin heavy chain
Ik	Ikaros
Ik$^{L/L}$	Ik hypomorphic mouse line with LacZ knocked into the Ikaros gene *(Ikzf1)*
IL-4	Interleukin-4
INC	Ik$^{L/L}$ Notch1$^{f/f}$ CD4-Cre mice
IRC	Ik$^{L/L}$ RBP-J$^{f/f}$ CD4-Cre mice
ISP	Immature Simple Positive
ITAM	Immunoreceptor Tyrosine Activation Motifs
ITIMS	Immunoreceptor Tyrosine Inhibitory Motifs
JNK/SAPK	c-Jun NH2-terminal kinase/Stress activated protein kinase
LC	Light Chain
LIC	Leukemia Initiating Cell
Lin	Lineage markers
LMPP	Lymphoid primed Multi-Potent Progenitors
LSK	Lin negative Sca-1 positive c-Kit positive
LT- HCS	Long-Term HCS
M	Methionine
MAP	Mitogen Activated Protein
MAPK	MAP Kinase
MAPKK	MAPK Kinase
MAPKKK	MAPK Kinase Kinases
M-CSF	Macrophage Colony-Stimulating Factor
mIg	Membrane-bound Immunoglobulin
MLL	Mixed-Lineage-Leukemia
MRL/lpr	Lupus susceptible mouse line with defective Fas expression

N-	Amino
N1C	Ik$^{+/+}$ Notch1$^{f/f}$ CD4-Cre mice
NF-AT	Nuclear Factor of activated T cells
NF-κB	Nuclear Factor κB
NK	Natural Killer
NOD/SCID	Non-Obese Diabetic/SCID
NRR	Negative Regulatory Region
NSG	NOD/it-SCID/IL-2R gamma null
NuRD	Nucleosome-Remodelling Deacetylase
Opn	Osteopontin
PCR	Polymerase Chain Reaction
Ph	Philadelphia chromosome
PI-3K	Phosphatidylinositol-3 kinase
PIP$_2$	Phosphatidylinositol-4,5-bisphosphate
PIP$_3$	Phosphatidylinositol-3,4,5-trisphosphate
PKC	Protein Kinase C
PLCγ2	Phospholipase-Cγ2
PTK	Protein Tyrosine Kinases
RAG	Recombination Activating Gene
RBP-J	Recombination site Binding Protein J
RNA	Ribonucleic Acid
RSS	Rag Signal Sequences
RT-PCR	Real Time PCR
S1	Site (1, 2,3)
SCID	Severe Combined Immunodeficiency
SCLL	Stem Cell Leukemia/Lymphoma
SH2	SCR homology 2
s-HEL	soluble hen egg lysozome
SLC	Surrogate Light Chain
SLE	Systemic Lupus Erythematosus
SLEDAI	SLE Disease Activity Index
SNP	Single Nucleotide Polymorphisms
SP	Single Positive
Syk	Spleen tyrosine kinase
T1	Transitional 1 (2,3)
TACE	Tumor necrosis factor-α-converting enzyme
T-ALL	T-Acute Lymphoblastic Leukemia
TCR	T Cell Receptor
TdT	Terminal deoxynucleotidyltransferase
T$_H$	T helper
TM	Transmembrane
WT	Wild type

MOUSE LINES

Ik$^{L/L}$	Ikaros deficient mouse generated by the insertion of the LacZ reporter into exon2 of the IKZF1 gene. The Ik$^{L/L}$ mouse express truncated but functional Ikaros proteins (~10% of WT levels). It is a germ-line mutation.
Ik$^{L/L}$ Notch1$^{f/f}$ CD4-Cre	Mice bearing a T cell specific Notch1 deletion starting from the DN4 stage in the Ik$^{L/L}$ background
Ik$^{L/L}$ Notch3 KO	Mice bearing a Notch3 deletion in the Ik$^{L/L}$ background
Ik$^{L/L}$ RBP-J$^{f/f}$ CD4-Cre	Mice bearing a T cell specific RBP-J deletion starting from the DN4 stage in the Ik$^{L/L}$ background
Ik$^{f/f}$	The Ik$^{f/f}$ mice contain floxed Ikaros allele in which the last exon encoding the dimerization domain was flanked by loxP sites. The deletion of the dimerization domain by Cre recombinase results in a "null" allele
Ik$^{f/f}$ CD21-Cre	Mice bearing a mature B cell specific Ikaros deletion under the control of the CD21 promotor
Ik$^{f/f}$ CD19-Cre	Mice bearing an immature B cell specific Ikaros deletion under the control of the CD19 promotor
Ik$^{f/f}$ Rosa26-CreERT2	Mice bearing an inducible Ikaros deletion after the administration of tamoxifen

During my PhD studies, I was involved in three different projects related to the Ikaros function in T and B cells. I worked with the Ikaros$^{L/L}$ (Ik$^{L/L}$) mouse line that was generated in the lab, which expresses low levels of truncated but functional Ikaros protein (to be described in detail in section I). Two of the projects involved the Ik$^{L/L}$ tumor, the Notch dependence for their development and the analysis of the leukemia initiating cells present in these tumors. In the third project I studied the link between Ik$^{L/L}$ B cell activation and the auto-immune symptoms found in the Ik$^{L/L}$ mice. Therefore, my dissertation is divided in 4 different sections:

1) General Introduction. To introduce you to the main subject, there is a brief summary about Ikaros and its function.

2) The development of the Ik$^{L/L}$ tumor is Notch dependent. This section will include an introduction of acute lymphoblastic leukemia (ALL) and the Ikaros mutations found in human and mouse ALL, as well as in the Ik$^{L/L}$ tumors. It includes also a brief introduction of the Notch signaling pathway and its implication in ALL. Following this, I show the published results: Oncogenic activation of the Notch1 gene by deletion of its promoter in Ikaros-deficient T-ALL (Jeannet et al., 2010). To finish, I close with a short discussion about our results.

3) Analysis of the leukemia initiating cells in a mouse model of T-ALL deficient for Ikaros. With an introduction about the leukemia initiating cells and their characteristics, I present the data obtained for this goal. To complete this section, there is a discussion about these results.

4) B cell activation and the auto-immune symptoms in the Ik$^{L/L}$ mice. After an introduction about the Ik$^{L/L}$ mature B cells, B cell receptor activation, B tolerance, and the systemic lupus erythematosus, I show the results obtained for this project with the manuscript: Ikaros deficiency promotes autoantibody production and activation of the MAPK pathway in B cells. To conclude, a brief discussion will follow the results obtained.

Section I. **GENERAL INTRODUCTION**

I.1. Ikaros

I.1.1. The Ikaros Family

The Ikaros transcription factor family, comprises 5 members, Ikaros (*Ikzf1*), Helios (*Ikzf2*), Aiolos (*Ikzf3*), Eos (*Ikzf4*) and Pegasus (*Ikzf5*). They are characterized by two sets of highly conserved zinc finger motifs that are involved in either protein-nucleic acid or protein-protein interactions (Molnar et al., 1996; Rebollo and Schmitt, 2003).

The zinc finger motif located at the amino (N)-terminus plays a role in the binding to specific DNA sequences (Rebollo and Schmitt, 2003). All family members, except Pegasus, contain four DNA binding zinc fingers that recognize the canonical sequence "GGAAA" (Molnar and Georgopoulos, 1994). Pegasus, with three DNA binding zinc fingers, recognizes the sequence "GNNNGNNG" (Perdomo et al., 2000). The second zinc finger motif (composed of 2 zinc fingers) is found at the carboxy (C)-terminus and allows the protein to form homodimers or heterodimers with the other members of the family (Georgopoulos et al., 1992; Hahm et al., 1994).

Ikaros, the founding member was initially described as LyF-1. The study of the transcriptional control of the murine terminal deoxynucleotidyltransferase (TdT) gene identified LyF-1, a 50 kDa sequence-specific DNA-binding protein, that was enriched at most stages of B and T cell differentiation (Lo et al., 1991). The amino acid sequences of this protein revealed that LyF-1 and Ikaros are the same gene (Hahm et al., 1994).

Ikaros is expressed by all hematopoietic cells. The other family members are likewise expressed mainly in hematopoietic cells such as Helios and Aiolos (Hahm et al., 1998; Wang et al. 1996), or broadly expressed like Eos (brain, liver, myeloid, megakaryocytic and monocytic cells) and Pegasus (mature hematopoietic cells, brain, heart, skeletal muscle, kidney and liver) (Perdomo et al., 2000).

I.1.2. Ikaros expression

Ikaros was initially described as a transcription factor expressed in early B and T cell development (Lo et al., 1991; Georgopoulos et al., 1992). Ikaros is abundantly expressed during early embryonic hematopoiesis in mice, including hematopoietic stem cells (HSCs) from embryonic day 5 (E5) and in lymphoid precursors in the fetal thymus (E10.5) (Georgopoulos et al., 1992; Molnar et al., 1996) Later, it was shown to be expressed in pluripotent HSC, in multipotent progenitors with erythro-myeloid and lymphoid potential (Georgopoulos et al., 1997), in erythroid precursors (Lopez et al., 2002) and in myeloid precursors (Georgopoulos et al., 1994, Wang et al., 1996; Dumortier et al., 2003; Papathanasiou et al., 2003).

The *Ikzf1* gene contains 7 exons which give rise to a 431 amino acid protein. By alternative splicing, Ikaros pre-mRNA can generate at least 8 isoforms (Fig. I.1) (Molnar and Georgopoulos, 1994; Hahm et al., 1994). They share the protein-interaction domain and differ in components of the DNA-binding domain. Ikaros isoforms with functional DNA binding domains (at least three zinc fingers) can bind the motif "GGAAA" (Ik1-3). The Ik-4 isoform, with only two N-terminal zinc fingers can bind to tandem recognitions sites that share this sequence, indicating that isoforms may have both unique and common gene targets (Molnar and Georgopoulos, 1994). In contrast, isoforms that lack a functional DNA binding domain (one or no N-terminal zinc fingers) have dominant negative (dn) functions (Ik5-8), as they can dimerize with other Ikaros isoforms (and family members) and inhibit their DNA binding (Georgopoulos et al., 1997). Thus, differential expression of Ikaros isoforms modulates the DNA binding potential of its protein products and therefore may regulate the expression of different Ikaros target genes.
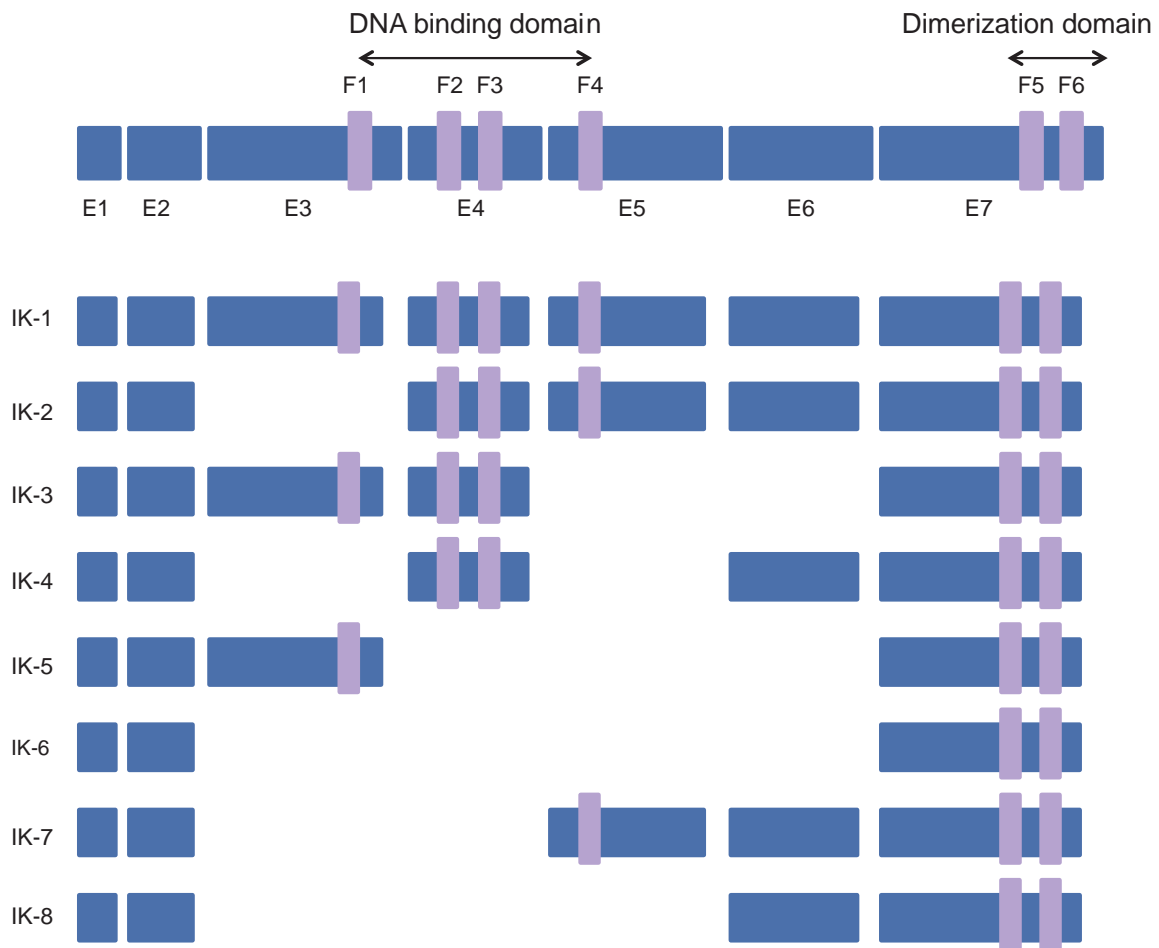
Figure I.1. Structure of the Ikaros proteins. Structure of the Ikaros proteins with 4 N-terminal zinc fingers (F1-F4) that comprise the DNA binding domain and two C-terminal zinc fingers (F5-F6) for dimerization with other Ikaros isoforms or other members of the Ikaros family. Alternative splicing of the 7 exons generates multiple Ikaros isoforms, all of them conserve the dimerization domain and different components of the DNA-binding domain. Blue boxes represent the exons, the zinc fingers are shown in purple.

I.1.3. Ikaros targeted mouse models

Different mouse models have been used to explore Ikaros function. Here, I give a brief introduction of the Ikaros targeted mouse models to describe the main effect of Ikaros deficiency for B and T cell development as well as in the tumor development for these mice. The Ik$^{L/L}$ mouse is described in more detail as my work is based on this mouse model. The description of the Ik$^{L/L}$ tumor is in section II. The Ik$^{L/L}$ mature B cells is in section IV. A summary of the mice models is depicted in table I.1.

I.1.3.1. Dominant negative Ikaros mice (Ik^{dn} mice)

The deletion of exons 3 and 4 by homologous recombination generated mutant Ikaros proteins with an altered DNA binding domain that function as dominant negative isoforms. The Ikaros proteins in Ik$^{dn/dn}$ mice cannot bind DNA but they retain their ability to homo and heterodimerize with other family members. The Ik$^{dn/dn}$ mice display an early and complete block in the development of all lymphoid lineages, including T cells, during both fetal and adult hematopoiesis. The severe lymphoid cell defects results in death after 1-3 weeks from severe infections (Georgopoulos et al., 1994). The heterozygote Ik$^{+/dn}$ mice develop clonal T cell expansion after one to two months of age and are concomitant with the loss of the wild type (WT) allele (Winandy et al., 1995). Thus, the severe defects for lymphopoiesis in the Ik^{dn} mice demonstrate the key role of Ikaros for normal lymphocyte development and the potential redundancy in function of the other Ikaros family members.

I.1.3.2. Ikaros null mice (Ik$^{-/-}$ mice)

The Ikaros null mice harbor a mutation in the C-terminal region (deletion of exon 7). These mice do not express Ikaros proteins, and lack B cells and their earliest precursors. T cell precursors are absent during fetal hematopoiesis, however, the Ik$^{-/-}$ mutant mice develop T cells between 3 to 5 days after birth. All the Ik$^{-/-}$ mice develop leukemia. The Ik$^{-/-}$ T cells show skewed differentiation into the CD4^{+} lineage and undergo clonal expansion in the thymus around 4 weeks of age. These aberrant clonal T cell populations are detectable at later timepoints in the spleens of older mutants. The analyses of this mutant mouse suggest distinct roles of Ikaros during the development of hematopoietic precursors in the fetus and in the adult. Also, these analyses establish Ikaros as a tumor suppressor gene acting during thymocyte differentiation (Wang et al., 1996; Chari et al., 2010).

I.1.3.3. Hypomorphic Ikaros mice (Ik$^{L/L}$ mice)

The Ik$^{L/L}$ ("L" for LacZ) mouse bears a hypomorphic Ikaros mutation due to the insertion of the LacZ reporter into exon 2 of *Ikzf1* (Ikaros gene*)* via homologous recombination in ES cells (Fig. I.2A). The analysis of the Ikaros protein expression in the WT, Ik $^{+/L}$ and Ik$^{L/L}$ mice revealed that the major isoforms, Ik1 and Ik2, were detected in the WT, reduced in the Ik$^{+/L}$ and absent in the Ik$^{L/L}$ bone marrow (BM), spleen or thymus. However, two smaller

polypeptides (Ik1* and Ik2*) were weakly detected in the spleen and thymus from the Ik$^{L/L}$ mice (Fig. I.2B). Cloning and sequence analyze showed that exon-1 sequences were aberrantly spliced to those of exon-3, leading to the production of Ikaros isoforms lacking exon-2-encoded amino acids. The expression of lower amounts of Ikaros protein allows a less severe defect in lymphopoiesis compared to the previous Ikaros mutant mice. The Ik$^{L/L}$ mice develop B cells after birth from a small number of precursors (Kirstetter et al., 2002). In line with the Ik$^{+/dn}$ and Ik$^{-/-}$ mice, the Ik$^{L/L}$ mice develop T-lymphomas with 100% penetrance (Dumortier et al., 2006). Ikaros* proteins are functional and show punctate nuclear localization similar to WT Ikaros protein. They also, inhibit proliferation and rescue the deregulated gene expression in Ik$^{L/L}$ tumor-derived cell lines (Dumortier et al., 2006), as well as the defect in class switch recombination (Sellars et al., 2009). In addition, Ikaros* proteins can bind to Ikaros motifs by gel shift. Thus, the Ik $^{L/L}$ mutation results in the low expression (~10-20% of WT levels) of truncated but functional Ikaros protein.
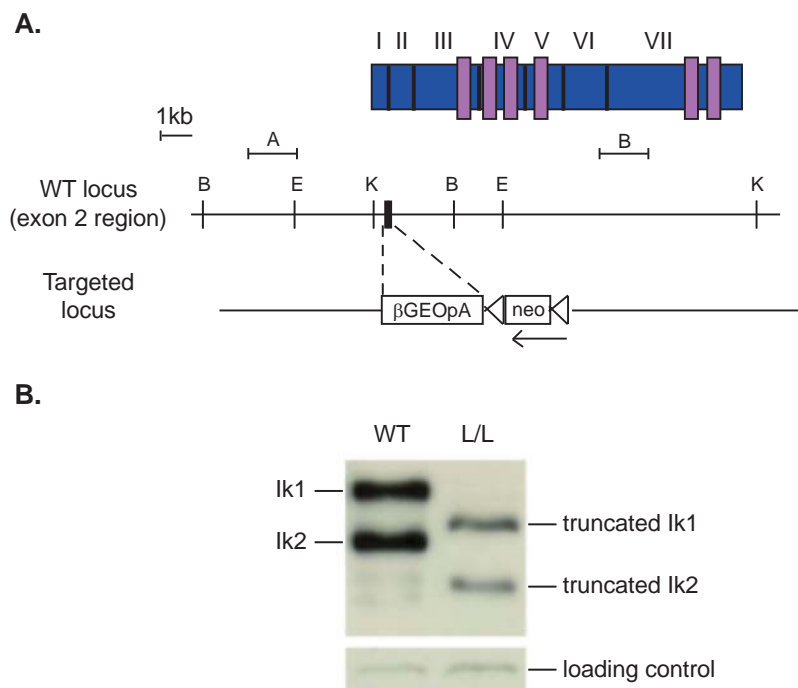

Figure I.2. The Ik$^{L/L}$ mouse model. A. The LacZ reporter was introduced into exon 2 of *Ikzf1* (Kirstetter et al., 2002). B. Ikaros expression in WT and Ik$^{L/L}$ CD43$^-$ spleen B cells by western blot. Truncated Ikaros (Ikaros*) proteins are expressed at ~10-20% of WT levels.

I.1.3.4. Ikaros plastic mice (Ik$^{plstc/plstc}$ mice)

Using the chemical mutagen N-ethyl-N-nitrosourea, Papathanasiou et al. (2003), generated a point mutation in the 3rd zinc finger that disrupts DNA binding but preserves efficient assembly of the full length protein into higher order complexes. The homozygous mutation in mice is embryonically lethal with several defects in terminal erythrocyte and granulocyte differentiation, excessive macrophage formation, and blocked lymphocyte development. The heterozygote Ik$^{+/plstc}$ mice display a partial block in lymphocyte differentiation and develop T cell lymphomas at high frequency. The Ik$^{+/plstc}$ mice show, in the thymus, normal mature T cells at 4 weeks post-natal, however, they contain increased numbers of T cells in the spleen, cosistent with a preleukemic stage. In the B cell lineage, the Ik$^{+/plstc}$ mice display an accumulation of pro-B cells. Nevertheless, the cells overcame this block and a normal mature B cell compartment is established in adult mice. (Papathanasiou et al., 2003).

Table I.1. Ikaros targeted mouse models.			
Mouse line	Mutation	Genotype	Phenotype
Ik^{dn} (Dominant negative)	Δ zinc fingers 3-4 (DNA binding)	dn/dn	↓HSCs 100x
			Lack NK, B, T cells and DCs
		+/dn	↑ TCR mediated proliferation
			T cell malignancies
Ik$^{-/-}$ (Null)	Δ zinc fingers 6-7 (dimerization domain; very little protein expression)	-/-	↓ HSCs 30-40x
			↑myeloid, ↓γδ-T cells and erythrocytes
			Lack NK, B and fetal T cells
			Clonal T cell expansion
			Delayed in embryonic to adult β-globing switching
Ik$^{L/L}$ (hypomorphic)	LacZ → Exon2 Exon 2 deletion (truncated protein at 10% WT levels)	L/L	No fetal B cells, partial postnatal block
			T cell malignancies
			T and B cells hyper-proliferation
			No mature pDCs
Ik$^{Plstc/Plstc}$ (Plastic; likely dominant negative)	H191R (Zinc finger 3) ↓DNA binding	Plstc/Plstc	Embryonic lethal
			↑ myeloid, ↓erythroid (FL) cells
			No T, some B precursors cells
		+/Plstc	No Fetal T or B cells
			Pro-B to pre-B block (adult)
			T cell malignancies (65% penetrance)

NK, Natural Killer; DC, dendritic cells; TCR, T cell receptor; pDC, plasmatic dendritic cells. (Georgopoulos et al., 1994; Winandy et al., 1995; Wang et al., 1996; Lopez et al., 2002; Kirstetter et al., 2002 ; Dumortier et al., 2006 ; Allman et al., 2006 ; Papathanasiou et al., 2003)

The analysis of the Ikaros targeted mouse lines showed that Ikaros is crucial for long-term HSC (LT-HSC) function (Nichogiannopoulou et al., 1999) and for lymphoid development (Wang et al. 1996). Loss of Ikaros affects the postnatal development of T cells, as the Ik$^{-/-}$ mice show defects in pre-T cell receptor (TCR) and TCR checkpoints and CD4 vs. CD8 lineage choice (Avitahl et al., 1999; Urban and Winandy, 2004; Winandy et al., 1999). Similarly, Ikaros controls the activation threshold to antigen receptor stimulation in mature B cells (Kirstetter et al., 2002, Results section 3). Ikaros is also involved in the differentiation of conventional and plasmacytoid dendritic cells, natural killer (NK) cells, neutrophils and erythrocytes (Allman et al., 2006; Bogget al., 1998; Dumortier et al., 2003; Lopez et al., 2002; Wu et al., 1997). Thus, Ikaros is a central regulator of the hematopoietic system, from HSCs to mature hematopoietic cells (Fig. I.3).
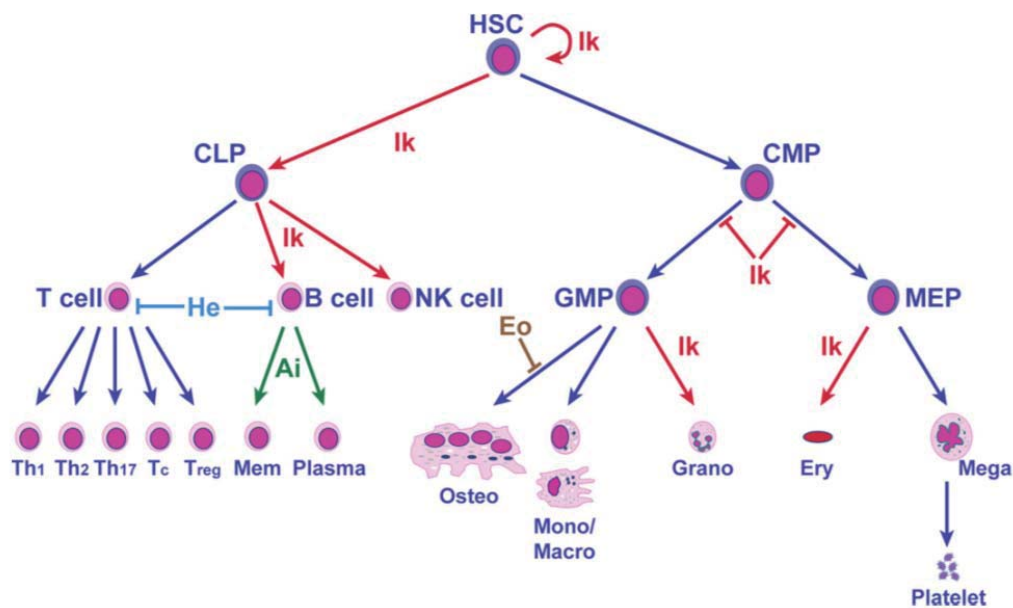
Figure I.3. Role of Ikaros family proteins in hematopoietic cell-fate decisions. (John and Ward, 2011) Representation of hematopoiesis highlighting the cell-fate decisions influenced by Ikaros family members, Ikaros (Ik in red), Aiolos (Ai in green), Helios (He in blue) and Eos (Eo in brown). Abbreviations: HSC hematopoietic stem cell, CLP common lymphoid precursors, CMP common myeloid precursors, NK natural killer, GMP granulocyte/macrophage precursors, MEP megakaryocyte/erythoid precursors, Th T helper cell, Tc cytotoxic T cell, Treg regulatory T cells, Mem memory B cells, Osteo osteoclasts, Mono/macro monocyte/macrophages, Grano granulocytes, Ery erythroid and Mega megakaryocytes.

In addition, Ikaros plays an important role as a tumor suppressor. Ikaros targeted mouse lines develop T-lymphomas with high penetrance (65-100%, depending on the mutation) (Dumortier et at., 2006; Papathanasiou et al., 2003; Winandy et al., 1995). Furthermore, Ikaros gene mutations or over-expression of dominant negative Ikaros isoforms have been found in human B and T cell lymphomas and leukemias (Mullighan et al., 2008; Nakase et at., 2000; Olivero et al., 2000). Thus, Ikaros suppresses leukemogenesis and lymphomagenesis in mice and humans.

I.1.4. Ikaros, the transcription factor

Regulation of gene expression by Ikaros is complex as it can be involved in both the activation and repression of genes. However, Ikaros has generally been considered a transcriptional repressor. The molecular function of Ikaros remains unclear; however, there are at least four possible mechanisms how Ikaros may function.

1) Localizing genes to heterochromatin. The distribution analysis of Ikaros proteins in the B cell nucleus, demonstrated that Ikaros is located at discrete foci in association with centromeric heterochromatin and with transcriptionally inactive genes (Brown et al., 1997). This suggests that Ikaros may contribute to the pericentromeric repositioning and heritable inactivation of these genes (Brown et al., 1997). Ikaros and inactive genes migrate with similar kinetics toward centromeric foci when resting B cells are stimulated to enter the cell cycle (Brown et al., 1999). T cells, the Ikaros target gene TdT is also repositioned to centromeric foci upon activation (Brown et al., 1999), suggesting that Ikaros binding to TdT may lead to pericentromeric repositioning. Moreover, it was shown that the DNA binding domain of Ikaros is essential for its pericentromeric localization (Cobbs et al., 2000). These results suggest that Ikaros might repress the expression of its target genes by binding the promoter/enhancer of active genes and bringing them to the heterochromatin. However, this function has not been demonstrated.

2) Competing with transcriptional activators. Ikaros modulates the expression of the pre-B cell receptor component Igll1 (λ5) by competing with the transcription factor

early B cell factor 1 (EBF1) (Thompson et al., 2007). In addition, Ikaros represses the Notch1 target gene Hes1 by competing with the RBP-J/Notch1 complex (Kleinmann et al., 2008). This mechanism seems to be dependent on the developmental stage of a cell: Ikaros represses Hes1 at the DN4 stage during T cell development, but not in earlier stages, indicating that Ikaros target gene repertoire may vary depending on cell type and differentiation state.

3) Recruiting co-repressors. Ikaros interacts with the C terminal binding protein (CtBP) and CtBP interacting protein (CtIP) through the N- and C- terminal repression domains. Each of these may in turn repress transcription by interacting directly with the basal transcriptional machinery (TATA binding protein and transcription factor IIB) (Koipally and Georgopoulos, 2002). However, it is unclear if this mechanism is relevant *in vivo*, as all these data are derived from *in vitro* experiments.

4) Recruiting chromatin remodeling complexes. Ikaros can interact with components of various histone deacetylase complexes, like Sin3 and nucleosome-remodelling deacetylase (NuRD) complex (Koipally and Georgopoulos, 2002). It has been shown that Ikaros associates predominantly with the NuRD complex in primary thymocytes (Sridharan and Smale, 2007). Thus, Ikaros may repress transcription by promoting remodeling of chromatin to an inaccessible state, by the destruction of activating epigenetic chromatin marks (e.g. histone deacetylation), and/or by the deposition of repressive epigenetic marks (e.g. methylation). All these possible mechanism are mediated by Ikaros via the recruitment of chromatin remodeling complexes.

In addition, Ikaros may also function as a transcriptional activator. Ikaros appears to directly activate *cd8a* transcription in developing T cells. It was shown that Ikaros was part of chromatin complexes formed *in vivo* on regulatory elements of the *cd8a* locus in CD8^{+} cells (Harker et al., 2002). The analysis of Ik^{+/-} thymocytes displayed an apparent increase in CD4 populations with immature phenotype suggesting the fail to up-regulate CD8 expression (Harker et al., 2002). The Ikaros mediated *cd8a* regulation could be through the recruitment of the SWI/SNF chromatin remodeling complex, which has histone acetyltransferase and chromatin remodeling activities (Wang, 2003) and interacts with Ikaros in T cells (Kim et al., 1999). To support this, it has shown that Ikaros interact with SWI/SNF

components in erythrocytes, where this interaction is required for the activation of adult globin genes (Lopez et al., 2002). Thus, Ikaros can repress or activate transcription through a variety of mechanisms (not all of them totally demonstrated *in vivo*) depending on cell type, differentiation state, and target gene.

Ikaros function can be also regulated by post-translational modifications, such as SUMOylation and phosphorylation. Ikaros SUMOylation interferes with its ability to repress transcription by disrupting its interactions with HDAC-dependent and –independent corepressors like CtBP, Sin3, and Mi-2β of the NURD complex, but does not influence its nuclear localization into pericentromeric heterochromatin. (Gomez del Arco et al., 2005). The phosphorylation of Ikaros by CK2 regulates the subcellular localization of Ikaros to pericentromeric heterochromatin, and its DNA-binding affinity, such in cell cycle-specific phosphorylation (Gomez del Arco et al., 2004; Dovat et al., 2002).

I.1.5. Ikaros as a tumor suppressor: potential mechanisms

As mentioned above, section I contains an introduction about Ikaros and its functions including a description of the Ikaros tumor suppressor function. In section II, the implication of Ikaros mutations in B- and T-acute lymphoblastic leukemia (ALL) will be described more in detail.

The development of tumors in the different Ikaros targeted mouse models highlights the role of Ikaros as a tumor suppressor. Several studies with human ALL have shown Ikaros mutations resulting in haploinsufficiency and/or the expression of small dn Ikaros isoforms which also decrease the Ikaros activity. Nevertheless, the mechanism by which Ikaros suppresses malignant transformation and the development of ALL remains unclear. The discovery of several Ikaros target genes has provided potential clues to its mechanism. One of these proposed mechanisms is the Ikaros-mediated downregulation of the Notch pathway. The Notch pathway is necessary for T cell development. It has been shown that mutations in Notch1 are the most common mutation in human T-ALL (Weng et al., 2004) and that leukemias derived from Ikaros deficient mice have Notch pathway activation (Dumortier et al., 2006; Mantha et al., 2007). Beverly and Capobianco (2003) suggested the synergism

between Notch activation and the loss of Ikaros function in T cell leukemogenesis, as the consensus binding sequence of RBP-J, the Notch transcriptional activator, and Ikaros were highly similar. Ikaros competes with RBP-J for binding to the upstream regulator elements of the Notch target genes Hes-1 (Kleinmann et al., 2008). Ikaros mediated transcriptional repression of Notch target genes involves chromatin remodeling by decreasing histone H3 acetylation at the Hes-1 locus (Kathrein et al., 2008). Thus, the Notch activation is a common feature in T-ALL, and its regulation by Ikaros seems to be an important event for leukemogenesis. In the section II, I describe in more detail the Notch signaling pathway and the mutations found in human T-ALL.

Ikaros can also function as a tumor suppressor because of its involvement in the negative regulation of cellular proliferation. Ikaros binds to the c-Myc gene promoter and suppresses its expression in pre-B cells. Repression of c-Myc by Ikaros in pre-B cells leads to induction of p27 expression and the downregulation of Cyclin D3, resulting in the inhibition of pre-B cell proliferation (Ma et al., 2010). In addition, Ikaros might have a role in the regulation of the G1/S checkpoint. During the G1/S transition, Ikaros is phosphorylated in a serine/threonine-rich conserved region (p1) in exon 7.   Mutations that prevent phosphorylation in p1 increase Ikaros' ability to impede cell cycle progression and its affinity for DNA (Gomez del Arco et al., 2004). Further, Ikaros could regulate apoptosis. Loss of Ikaros function is associated with the up-regulation of the anti-apoptotic factor Bcl-x$_L$ in human pituitary tumors (Ezzat et al., 2006). This leads to the hypothesis that Ikaros regulates apoptosis and that decreased Ikaros activity in leukemia cells would increase resistance to chemotherapy (Payne and Dovat, 2012). However this remains speculative due to a lack of supporting, mechanistic data. Thus, Ikaros deficiency could regulate cell proliferation and protect the cells against apoptosis.

More recently, Ikaros defects have been linked to myeloproliferative neoplasm (Jager et al., 2008; Tefferi 2010) and childhood acute myelogenous leukemia (AML) (Yagi et al, 2002), where Ikaros activity is lost due to a deletion of the Ikaros gene or expression of dn Ikaros isoforms, respectively. These studies provide evidence that Ikaros tumor suppressor activity extends also to the myeloid lineage. In conclusion, Ikaros may function as a tumor

suppressor by the regulation of genes or pathways involved in the normal development of lymphocytes, as the Notch pathway, and by the regulation of genes involved in proliferation and cell survival.

I.1.6. Ikaros as a key regulator for B cell development

I.1.6.1. B cell development

B cell development begins in the fetal liver and continues in the bone marrow after birth by sequential steps that are characterized by gene expression programs, cell surface markers and developmental checkpoints centered on antigen receptor rearrangement. To track these developmental stages in murine BM, two methods have been proposed based on phenotypic markers. 1) Rolink et al. (1994) used cell size and the expression of c-kit, CD25 and the surrogate light chains (λ5 and VpreB) and 2) Hardy et al. (1991) used CD43, CD24 and BP1 on $B220^+$ BM cells to divide developing B cells into 7 fractions (Fr), labeled A-F (Fig. I.4). Here, I used the Hardy classification. $CD43^+B220^+$ cells represent the most immature B lineage cells and can be subdivided using the expression of BP1 and CD24. Fr. A, or pre-pro-B cells, is negative for CD24 and BP1 and includes the earliest B cell progenitor, although these cells are not committed to the B cell lineage. Fr. A cells mature into Fr. B cells where they express CD24 and begin immunoglobulin heavy chain (*Igh*) rearrangements (D_H to J_H gene segments). In Fr. C, the cells express BP1 in addition to CD24, and have initiated V_H-DJ_H rearrangements. Together, fractions B and C are referred to as pro-B cells. Fr. C' contains cells with slightly higher expression of CD24. These early pre-B cells undergo several rounds of division if they express functional Ig heavy chains. Early pre-B cells then down-regulate CD43 and become Fr. D or late pre-B cells, and begin rearrangement of the Ig light chain (V_L-J_L). The cells that express functional B cell receptors (BCR), consisting of Ig heavy and light chains, are then selected to become immature B cells (Fr. E). These cells migrate to the spleen where they undergo further maturation and selection into the peripheral B cell pool. Each of these steps includes important developmental events and checkpoints, which will be described below.

	Pro-B			Pre-B		Immature	Mature B
Cell size	large				small		
	pre-pro-B	pro-B	pro-B	early pre-B	late pre-B		
Fraction	A	B	C	C'	D	E	F
IgH	germline	D-J	V-DJ	V-DJ	V-DJ		
IgL	germline	germline	germline	germline	V-J		
CD43	+	+	+	+	-	-	-
CD24	-	+	+	++	++	+	+
BP1	-	-	+	+	+	-	-
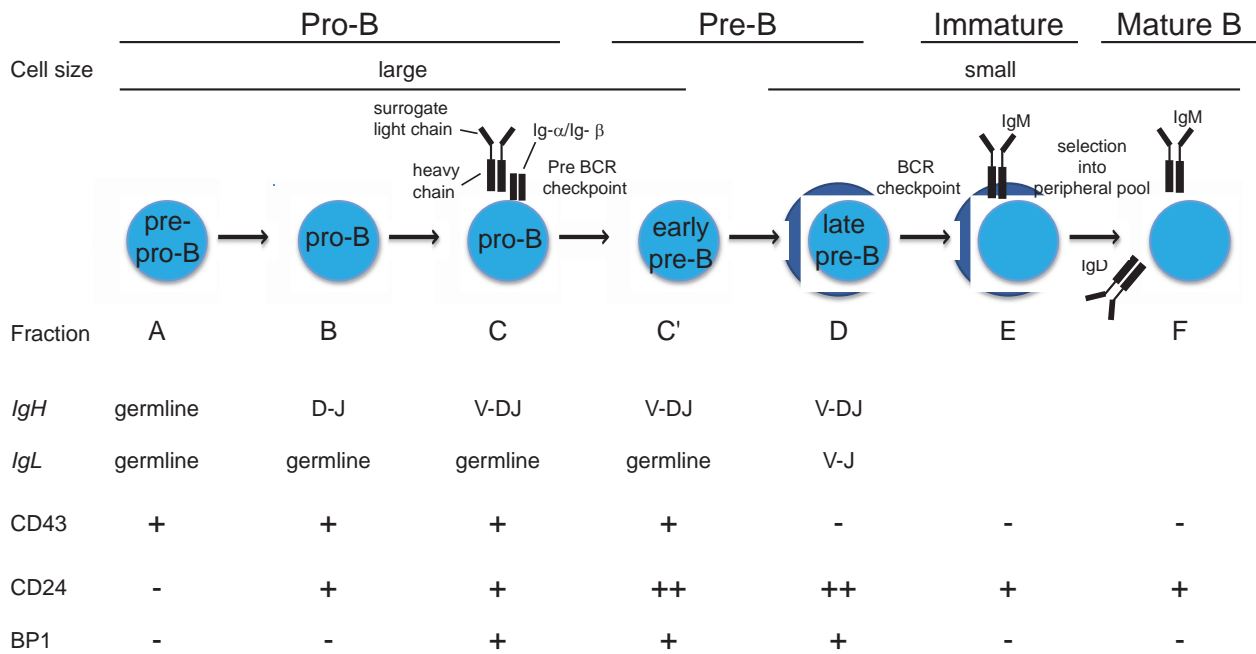
Figure I.4. B cell development according to Hardy nomenclature. B cell development in the BM is characterized by the cell surface expression of B220, CD43, CD24 and BP-1, as well as the status of antigen receptor rearrangements (Hardy et al., 1991). All the cells above express B220. Adapted from Miosge and Goodnow, 2005.

HSC differentiate into lymphoid primed multi-potent progenitors (LMPP) and then into common lymphoid progenitors (CLP) (Nutt and Kee, 2007). Signaling through Flt3 and IL-7R induces CLPs to differentiate into pre-pro B cells. IL-7R signaling, in combination with the E2A transcription factor, initiates B cell lineage specification by upregulating EBF1 (Sitnicka et al., 2003). EBF1 allows further progression to the pro-B stage and induces the expression of B cell lineage genes, acting as a lineage commitment factor by repressing alternative lineage fates (Pongubala et al., 2008). One of the crucial roles of EBF1 in B lymphopoiesis is to activate the expression of Pax5, a B cell lineage commitment factor, which shuts off alternative cell fates (Nutt and Kee, 2007; Cobaleda et al., 2007). Pax5 plays important lineage specification roles, as it reinforces *Ebf1* transcription and contributes to the expression of components of the pre-BCR and BCR signaling pathways (e.g. CD19, λ5, CD79a (Igα)) (Busslinger, 2004) and important B cell transcription factors (e.g. Aiolos, IRF4, IRF8, Lef1, SpiB) (Nutt and Kee, 2007). At the pro-B stage, cells undergo *Igh* rearrangements with the expression of recombination activating genes (Rag1 and Rag2). The pro-B cells that

correctly rearranged the heavy chain are able to pair them with the surrogate light chain (SLC) proteins λ5 and VpreB1/2, and thereafter, with the Igα/Igβ signaling heterodimer to form the pre-BCR (Kitamura et al., 1992 and Mundt et al., 2001, Miosge and Goodnow 2005). The pre-BCR signals down-regulate the expression of Rag1/Rag2 to prevent rearrangements of the other heavy chain locus (allelic exclusion) (Grawunder et al., 1995). The pro-B cells that passed the pre-BCR checkpoint undergo several rounds of division and finally differentiate to pre-B cells. The pre-B cells proceed with the rearrangement of the light chain gene loci (Miosge and Goodnow 2005). Because of allelic exclusion, only one light chain isotype, λ or κ is expressed on each B cell (Corcoran 2005). Those cells that express functional BCR, consisting of Ig heavy and Ig light chains will become immature B cells (Hardy and Hayakawa, 2001) and migrate to the spleen to undergo final maturation steps.
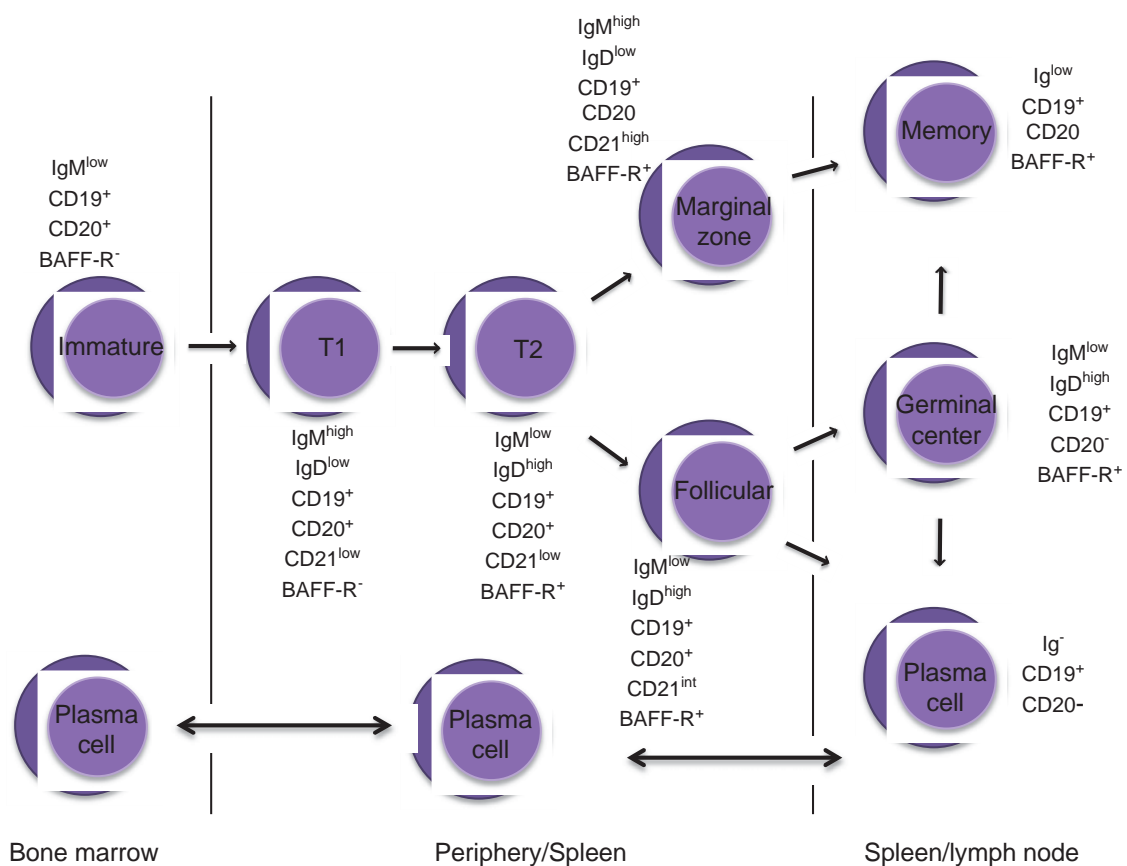

Figure I.5 B cell development in the periphery. Cell surface markers for B cell subsets during differentiation are indicated. Adapted from Cope and Feldmann, 2004.

In the spleen, the immature B cells are called transitional (T) B cells (Fig. I.5). A subset of splenic B cells expresses low levels of CD21 and CD93/AA4, suggesting immaturity (Allman et al., 2001). These cells can be further subdivided into three transitional subpopulations based on IgM and CD23 expression (Allman et al., 2001). T1 B cells (IgM^{hi}CD23$^-$) start to express a second class of BCR, the IgD, to later become T2 B cells (IgM^{hi}CD23$^+$) which express both CD21 and CD23. T3 B cells (IgM^{low}CD23$^+$) down-regulate IgM and eventually recirculate as mature B cells in the periphery (Chung et al., 2003). These cells have a short half-lives. The mature B cells can differentiate into plasma cells (secreting antibodies cells) or into memory cells after antigen BCR activation.

I.1.6.2. Ikaros in immature B cells

Ikaros contributes to nearly every level of B cell differentiation and function. It is required for the development of the earliest B cell progenitors and at later stages for VDJ recombination and B cell receptor expression. The activation threshold for various stimuli (Kirstetter et al., 2002) and the correct antibody isotype during class switch recombination is also influenced by Ikaros in mature B cells (Fig. I.6) (Sellars et al., 2009).

Ikaros plays crucial roles in B lineage specification and commitment. Specification involves the activation of lineage specific genes, and commitment consists of suppressing alternative cell fates though the repression of alternative lineage genes. Ik$^{-/-}$ mice lack CLPs and pre-pro-B cells and exhibit a complete block in B lymphopoiesis (Wang et al., 1996), suggesting that Ikaros is crucial for B lineage lymphopoiesis. This might be due to a role for Ikaros in promoting Flt3 and/or IL-7R expression on early hematopoietic progenitors. Indeed Ik$^{-/-}$ LSK cells lack *Flt3* mRNA expression and Ik$^{-/-}$ LMPPs express reduced levels of *Il7r* mRNA (Nichogiannopoulou et al., 1999 and Yoshida et al., 2006). However, independent retroviral expression of Flt3 and IL-7R in Ik$^{-/-}$ LSKs, did not rescue B cell development, indicating that it is the reduced expression of both receptors together which blocks Ik$^{-/-}$ B lymphopoiesis, and/or that Ikaros has other important functions in B lineage specification such as the promotion of EBF expression (Reynaud et al., 2008). The EBF-induced Ik$^{-/-}$ pro-B cell lines exhibit promiscuous myeloid gene expression and even latent myeloid

differentiation capacity. In addition, like Pax-5$^{-/-}$ pro-B lines, Ik$^{-/-}$ pro-B lines can be differentiated into macrophages when cultured with M-CSF (Reynaud et al., 2008). Thus, Ikaros plays an important role for the commitment of B cells by shutting off alternative cell fates.

Ikaros performs important roles in B cell development. Ik$^{L/L}$ mice exhibit a partial block in B cell development between the pro-B and pre-B states (Kirstetter et al., 2002). In accordance, EBF induced Ik$^{-/-}$ pro-B cells do not mature into pre-B cells, further demonstrating that Ikaros contributes to developmental checkpoints in pro-B cells (Reynaud et al., 2008). Ik$^{L/L}$ pro-B cells express low levels of *Rag1/2* and *Igll1* (λ5), indicating that Ikaros could be important for *Igh* rearrangement (Kirstetter et al., 2002). In support of this, Ik$^{-/-}$ pro B cells lack *Rag1* and *Rag2* expression and Ikaros was shown to bind directly to their promoters in these cells, indicating that Ikaros is required for Rag1/2 expression (Reynaud et al., 2008). In addition to Rag gene expression, Ikaros also contributes to *Igh* locus condensation, a critical step required for V-DJ recombination (Reynaud et al., 2008). Thus, Ikaros is required for differentiation beyond the pro-B cell stage, because it controls multiple aspects of *Igh* locus rearrangement.

I.1.6.3. Ikaros in mature B cells

Activation of mature B cells produces high-affinity antibodies with various constant domains that provide unique effector functions. Ikaros controls both the threshold at which B cells respond, as well as the choice of antibody isotype they will express.

Ikaros regulates the activation threshold in response to BCR stimulation. Ik$^{L/L}$ B cells exhibit lower activation thresholds to stimulation than WT cells (e.g. proliferate in response to lower concentrations of anti-IgM stimulation) (Kirstetter et al., 2002) and similar data were obtained from mice bearing a B cell specific transgene encoding the dn Ikaros 7 isoform (hyper-responsive to stimulation by mitogens) (Wojcik et al., 2007). Thus, Ikaros sets B cell activation thresholds for antigen and mitogen stimuli. However, the mechanism of how Ikaros contributes to B cell activation thresholds remains unclear. Results section 3 addresses these questions.

Ikaros is a central regulator of immunoglobulin isotype specification during class switch recombination. $Ik^{L/L}$ mice exhibit skewed serum isotype titers, characterized by a reduction in IgG_3 (90%) and IgG_1 (50%) and increases in IgG_{2b} (50%) and IgG_{2a} (90%) (Kirstetter et al., 2002). Sellars et al. (2009) showed that Ikaros deficiency results in increased and ectopic class switch recombination (CSR) to IgG_{2b} and IgG_{2a} and reduced CSR to all other isotypes, regardless of stimulation. Ikaros by binding directly to the *Igh* locus regulates isotype gene transcription and suppresses active chromatin marks (Sellars et al., 2009). Also, Ikaros–mediated repression of γ2b and γ2a transcription promotes switching to other isotypes genes by allowing them to compete for activation-induced cytidine deaminase (AID)-mediated recombination. Thus, Ikaros is a central regulator of *Igh* locus transcription and a regulator of isotype specification during CSR.
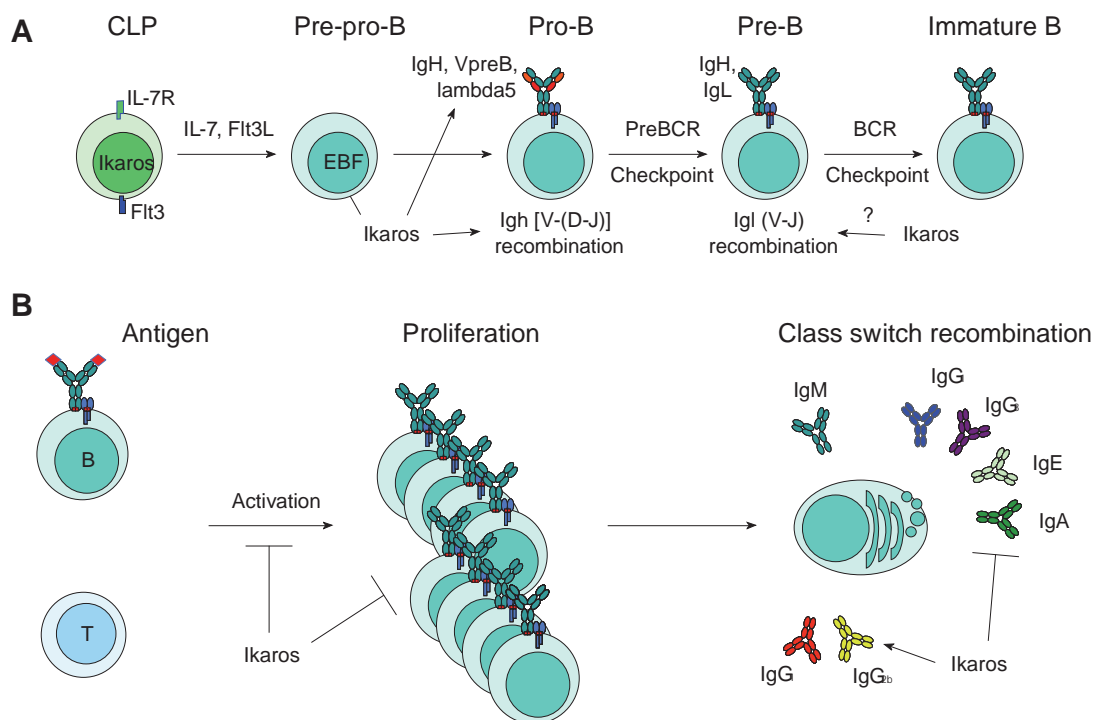
Figure I.6. Ikaros functions in B cells. (Sellars et al., 2011) A. Ikaros promotes the B cell lineage by inducing the expression of the IL-7R and Flt3 in common lymphoid progenitors (CLPs) and the expression of the EBF transcription factor in pre-pro-B cells. In pro-B cells, Ikaros regulates Igh recombination by activating Rag gene expression. After the preBCR checkpoint, Ikaros also downregulates the expression of the preBCR component λ5. B. In mature B cells, Ikaros sets the B cell activation threshold to antigen and inhibits the hyper-proliferation of activated B cells. Finally during class switch recombination, Ikaros controls isotype choice by inhibiting switching to IgG2b and IgG2a and promoting switching to all other isotypes.

Section II. **THE DEVELOPMENT OF THE IKAROS-DEFICIENT TUMOR IS NOTCH DEPENDENT**

INTRODUCTION

II.1. Acute lymphoblastic leukemia

ALL is a malignant heterogeneous disease of lymphoid precursor cells arrested at different stages of T- and B-cell development. It is characterized by recurring chromosomal abnormalities including translocations, trisomies and deletions. Clinically, it is described by high white blood cell counts, increased numbers of blast cells and enlarged mediastinal lymph nodes. ALL affects people of every age. In the case of T-cell ALL (T-ALL), it represents 15% of pediatric and 25% of adult ALL cases. Prognosis is variable, highlighting the heterogeneity of this disease and the potentially different molecular mechanisms involved in tumor initiation and progression. Treatment involves long-term and intensive combination of chemotherapy associated with severe side effects. Relapse is still frequent with very poor outcome. Hence, it is important to understand the initiation and progression of leukemia, the mechanism of how normal cells can be transformed, as well as the identification of the cells that are able to re-initiate the disease, to provide tools for the development of better treatments that target these mechanisms or cells, respectively.

II.1.1. Ikaros in human B-ALL

The Ikaros gene is mutated in 20-30% of B-ALL, mostly by genomic deletions (Mullighan et al., 2008; Kuiper et al., 2010) that lead to the production of dn Ikaros isoforms or haploinsuficient mutations. One B-ALL subtype with an especially poor prognosis is characterized by the Philadelphia chromosome (Ph) arising from the t(9;22) (q34;q12) translocation which encodes the constitutively activated BCR/ABL1 tyrosine kinase. Ph positive B-ALLs represent 5% of pediatric B-progenitor ALL and 40% of adult ALL. Expression of BCR/ABL1 is also the major pathological lesion underlying chronic myelogenous leukemia (CML).

IKZF1 mutations occur frequently in human leukemias that express the BCR/ABL1. Mullighan et al. (2008) have found that the most frequent somatic copy number alteration present in BCR/ABL1 B cell-progenitor ALLs was deletion of *IKZF1*. This was the case in 80% of BCR/ABL1 ALL cases (76% of pediatric and 90% of adults). These deletions were confined to a subset of internal *IKZF1* exons, most commonly exons 3-6, generating a dn Ikaros isoform. This study demonstrated that the expression of dn Ikaros isoforms was due to *IKZF1* genomic abnormalities, and not aberrant post-transcriptional splicing induced by BCR/ABL1 fusion protein. Finally, the lack of dn Ikaros isoforms in CML samples suggests that this is an exclusive event for BCR/ABL1 B cell-progenitor ALLs (Mullighan et al, 2008). In addition to the BCR/ABL1 B-ALL studies, it was shown that 15% of pediatric B-ALLs have a deletion of single *IKZF1* allele or mutation of a single copy of *IKZF1* (Mullighan et al., 2007).

In addition, Ikaros deletions are significantly associated with poor relapse-free and overall survival rates (Kuiper et al., 2010). Relapsing B-ALL harbor twice more genomic abnormalities at diagnosis as compared with non-relapsing ALL. The deletion or mutations in *IKZF1* were highly enriched in relapse-prone diagnosis samples. In contrast to other lesions, like *CDKN2A*, *IKZF1* lesions were found to be preserved at relapse in all paired samples (Kuiper et al., 2010). Recently, it was shown that about 20% of B-ALL patients with *IKZF1* mutations present two distinct deletions: biallelic and biclonal deletions. The biallelic deletions lead a complete loss of Ikaros function by the loss of the second *IKZF1* allele and thus, providing a selective oncogenic advantage to leukemic cells that had already lost one allele. The biclonal deletions were found in patients displaying exons deletions and haploinsuficient mutations but that still exhibited Ikaros mRNA and protein suggesting that these mutations occurred in different clones as secondary events during leukemogenesis. (Dupuis et al., 2012) Thus, Ikaros loss-of-function mutations are a common and complex event in B-ALL particularly in high risk B-ALL. These genomic deletions could result in the production of dn Ikaros isoforms or haploinsufficiency, where the initiating codon was deleted. Importantly, these mutations can be secondary events during leukemogenesis.

II.1.2. Ikaros in human T-ALL

Although, Ikaros is strongly associated with B-ALL leukemias expressing the BCR/ABL1 fusion protein, it still remains unclear if Ikaros functions as tumor suppressor in human T-ALL. Sun et al. (1999) reported a high prevalence of aberrant, dominant-negative Ikaros isoforms in all 18 pediatric T-ALL cases in which Ikaros proteins were localized in the cytoplasm of the leukemic cells. Later studies, however, have not confirmed these initial results and failed to detect dominant-negative Ikaros (Nakase et al., 2000; Ruiz et al., 2004). Recently, using more sensitive techniques such as high resolution comparative genomic hybridization (CGH) arrays, low frequencies of genomic Ikaros deletions were demonstrated (6 out of 120 reported cases) (Maser et al., 2007; Kuiper et al., 2007; Meleshko et al., 2008; Mullighan et al., 2008; Marçais et al., 2010). Besides direct genetic inactivation, Ikaros can also be inactivated at the functional level as suggested by the localization of Ikaros proteins in the cytoplasm (Sun et at., 1995; Marçais et al., 2010). In a study of 25 cases of human T-ALL, only one sample had inactivation of Ikaros. One allele was lost by genomic deletion. The intact allele produced an Ikaros protein that was delocalized. It exhibited an association with an abnormal cytoplasmic structure and a loss of nuclear localization. These results suggest that Ikaros is inactivated via two mechanisms: genomic deletion of one allele and cytoplasmic retention of the protein synthesized from the second allele (Marçais et al., 2010). Recently, the study of early T cell precursor (ETP) ALL, have shown that 58% of the samples have alterations in genes with roles in hematopoietic and lymphoid development, including *RUNX1, IKZF1, ETV6, GATA3*, and *EP300*. The *IKZF1* gene was deleted or mutated in its sequence in 15% of the ETP-ALL samples. Furthermore, reconstruction of the transcriptional network of ETP-ALL using the algorithm for the reconstruction of accurate cellular networks (ARACNE), identified *IKZF1* and *RUNX1* as the hub genes for 30 gene networks, suggesting that these transcription factors are key determinants of the transcriptional profile of ETP-ALL (Zhang et al., 2012). Thus, Ikaros loss-of-function mutations seem to be a recurrent anormaly in human T-ALL principally in the ETP-ALL subtype.

II.1.3. Ikaros in mouse T-ALL

The studies of Ikaros targeted mouse models show that Ikaros play a role in the development and function of almost all hematopoietic cell types and that it is a tumor suppressor in T cells. The $Ik^{+/dn}$, $Ik^{plastic\ /+}$, $Ik^{-/-}$ and $Ik^{L/L}$ mice develop T-ALL with a rapid onset. Thus, all mice carrying mutations in Ikaros develop T-cell leukemias with high incidence demonstrating a strong tumor suppressor function for Ikaros in murine T cells.

Importantly, the implication of Ikaros in T-ALL was not only seen in the genetically modified Ikaros mice. Frequent loss-of-function Ikaros mutations can been found in murine thymic lymphomas induced by irradiation, mutagens or deficiency in DNA repair pathways (Shimada et al, 2000; Kakinuma et al., 2002; Beverly and Capobianco, 2003; Kakinuma et al., 2007; Uren et al., 2008). These mutations, present in 20-85% of the tumors, show two types of defects: 1) focal genomic deletion in the proximal part of chromosome 11 where Ikaros is located or 2) point mutations in the coding regions (missense mutations) or mutations leading to premature stop codons which probably behave as null allele mutations. Thus, the inactivation of Ikaros function as tumor suppressor gene could be generated by several mechanisms such as genomic deletions or loss-of-function mutations which result in the development of murine T-ALL.

II.1.3.1. $Ik^{L/L}$ tumors

The deficiency of Ikaros in T cells leads to the development of aggressive T-lymphoma. All homozygote $Ik^{L/L}$ mice develop thymic lymphomas between 12-20 weeks of age and rapidly die from an enlarged thymus or general organ failure due to metastasis in the bone marrow, spleen, kidneys or liver (Fig. II.1A) (Dumortier et al.,2006). "Early" thymic tumors, 10-12 weeks of age, were defined as slightly enlarged thymus, exhibiting a heterogeneous CD4, CD8 expression profile and no detectable metastasis. "Late" thymic tumors, 18-22 weeks of age, exhibit a varied phenotype where most were $CD4^+CD8^+$ double positive (DP) with some CD8+ single positive (SP) cells (Fig. II.1B and data not shown). Most tumors appear to be monoclonal, although some showed two or more TCR β rearrangements (Dumortier et al., 2006).
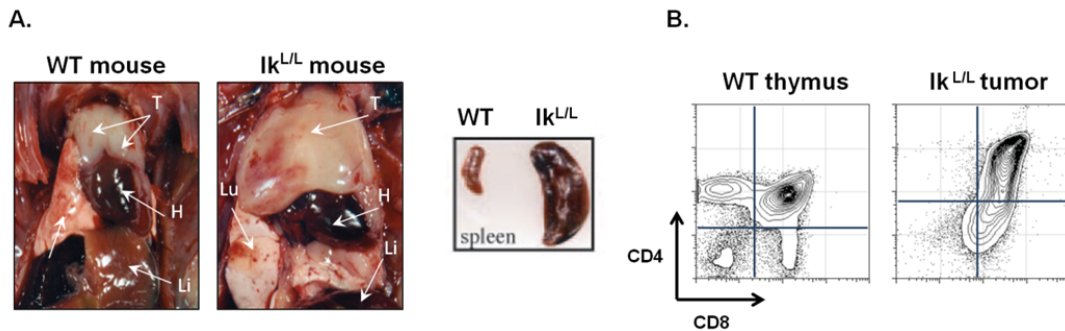
Figure II.1. Ikaros$^{L/L}$ thymic lymphoma. A. Photography of WT thymus (4 weeks old) and Ik$^{L/L}$ tumor (22 weeks old) with metastases in the spleen. Th, thymus; Lu, lung; H, heart; Li, liver. B. Flow cytometry analysis of CD4 and CD8 expression on thymocytes from WT and Ik$^{L/L}$ thymi.

Ik$^{L/L}$ tumors appear to start in the thymus. Thymectomized Ik$^{L/L}$ mice (surgery at 5 weeks of age) remain healthy and tumor free 1.5 years after the surgery (Dumortier et al., 2006). Thus, the Ik$^{L/L}$ tumor development seems to have a strong dependence on signals received from the thymus environment. The transcriptome analysis of Ik$^{L/L}$ tumors (18-20 weeks old) compared with WT thymic (3 weeks old) and premalignant Ik$^{L/L}$ thymus (3 weeks old) revealed the over-expression of a group of genes, that included Notch1 and the Notch target genes Deltex-1, Hes-1 and pTα, as well as Notch3. These genes were also over-expressed in "early" Ik$^{L/L}$ tumors (Dumortier et al., 2006). Thus, an activated Notch pathway is a prominent and early feature in Ik$^{L/L}$ tumors.
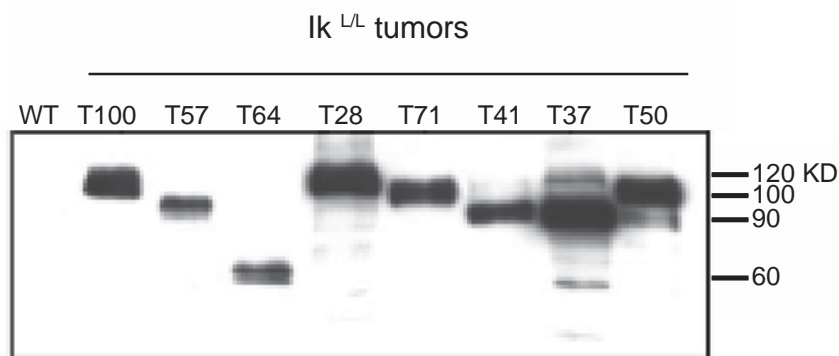
Figure II.2. Ik$^{L/L}$ tumors over-express Notch1 protein of variable size. (Dumortier et al., 2006) Nuclear extracts from WT and Ik$^{L/L}$ tumors were analyzed with an anti-cleaved Notch1 antibody. 75% the Ik$^{L/L}$ tumors showed variability in size of cleaved intracellular Notch1 proteins.

The majority of the Ik$^{L/L}$ tumors express Notch1 proteins with deletions in the PEST domain. The analysis of the intracellular Notch1 protein (the active form) revealed that the

majority of Ik$^{L/L}$ tumors tested expressed high amount of intracellular Notch1 protein with smaller size than expected (120kDa) (Fig. II.2). The sequencing of these Notch1 transcripts showed frameshift mutations leading to the PEST domain deletions (Dumortier et al.,2006). Thus, Notch1 mutations are a common feature in Ik$^{L/L}$ tumors.

Notch activation is required for tumor cell proliferation *in vitro*. Cell lines derived from Ik$^{L/L}$ tumors were cultured in presence of a γ-secretase inhibitor (GSI), which blocks the cleavage of surface Notch and the subsequent translocation of the active Notch into the nucleus. The GSI treatment stopped the proliferation of the Ik$^{L/L}$ cell lines. However, the proliferation can be restored with the ectopically expression of intracellular Notch1. Thus, Ik$^{L/L}$ cell line proliferation is dependent on Notch activation.

In summary, the Ik$^{L/L}$ mice develop a thymus-dependent aggressive leukemia with strong Notch signaling activation. These tumors harbor Notch1 mutations in the PEST domain and their proliferation *in vitro* depends on Notch activation. However it remained unclear how Notch signaling contributes to T-cell transformation *in vivo.* Results in section II address the Notch dependence for the Ik$^{L/L}$ tumor development.

II.2. Notch signaling pathway

The Notch signaling pathway is a highly conserved cell-cell communication mechanism though the interaction of Notch receptors and their ligands (Fig. II.3). This pathway is implicated in cell differentiation processes during embryonic and adult life. Mammals have four Notch receptors (Notch1-Notch4), and five ligands (Jagged 1 and Jagged 2 and Delta-like 1(Dll1), Dll3 and Dll4). During transport to the cell surface, Notch receptors are modified by Fringe-type glycosylases and are cleaved by a furin-like protease at the S1 site, a site just external to the transmembrane subunit, resulting in mature heterodimeric receptors consisting of non-covalently-associated extracellular (EC) and transmembrane (TM) domains. Ligand-receptor engagement results in two successive proteolytic cleavages of Notch. The first cleavage mediated by the metalloprotease tumor necrosis factor-α-converting enzyme (TACE) occurs at the S2 site in the EC domain and creates a

short-lived membrane bound form of the TM domain. The second cleavage occurs at the
S3 site in the TM domain, and is catalyzed by a multiprotein protease complex commonly
known as γ-secretase that consists of presenilin, nicastrin, APH1 and PEN2 proteins. γ-
secretase cleavage releases the intracellular domain of Notch (ICN), and allows its
translocation to the nucleus where it binds to its downstream transcription factor RBP-J.
ICN also binds Mastermind-like-1-3 that recruit coactivators with histone acetyl transferase
activity. ICN is short-lived and is targeted for proteasome-mediated degradation (Radtke et
al., 2005).
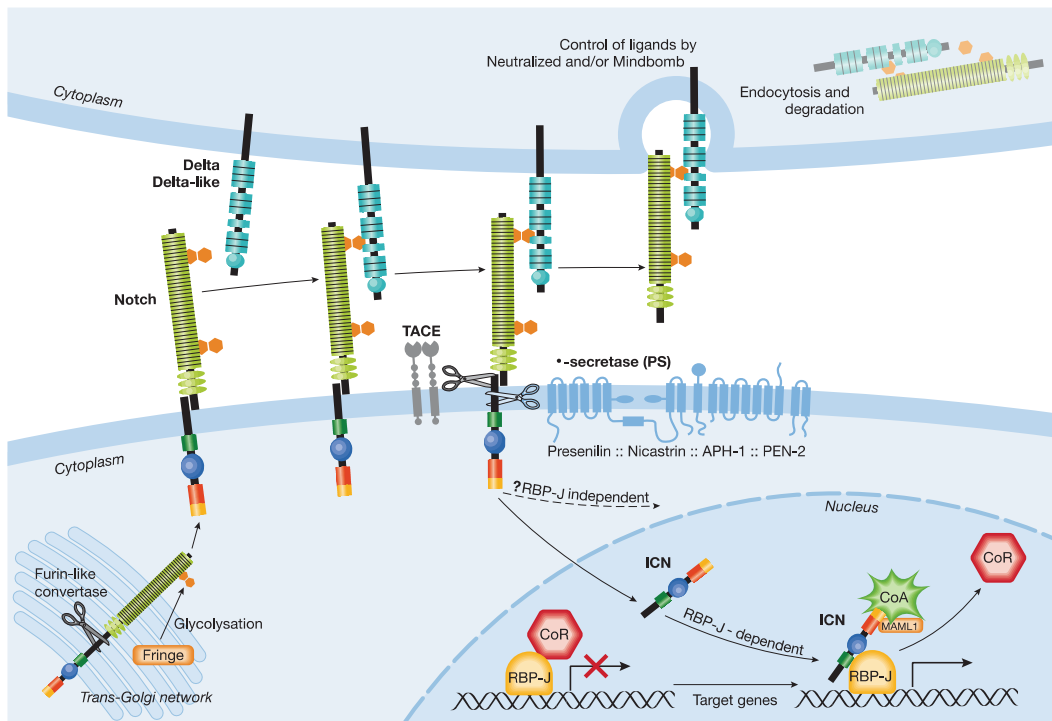
Figure II.3. The Notch signaling pathway. (Radtke et al., 2005). Notch receptors are synthesized as single
precursor proteins that are cleaved at S1 in the Golgi by a Furin-like convertase during their transport to the
cell surface where they are expressed as heterodimers. Ligand-receptor interaction induces two sequential
proteolytic cleavages. The first one at S2 mediated by the metalloprotease TACE. The cleaved extracellular
(EC) domain of the receptor is trans-endocytosed by the neighboring ligand-expressing cell. The second
cleavage occurs at S3 mediated by the γ-secretase complex. The liberated intracellular domain of Notch
(ICN) translocates into the nucleus and binds to the transcription factor RBP-J. This interaction leads to
transcriptional activation by displacement of corepressors (CoR) and simultaneous recruitment of
coactivators (CoA), including mastermind-like proteins (MAML1).

II.2.1. Structure of Notch receptor

The Notch receptors are heterodimeric transmembrane proteins composed of EC and TM domains. The EC domain of Notch1-4 contains 29-36 tandem EGF-like repeats that bind their ligands, followed by 3 Notch/Lin-12 repeats (LNR), and a conserved heterodimerization domain (~100 amino acid region) that maintains stable EC-TM association. The TM domain, contains a RAM domain, 7 tandem ankyrin repeats and a C-terminal PEST domain. Between the ankyrin repeats and PEST domain lays a region with considerable sequence variation between Notch1 and Notch 4 (Fig. II.4).
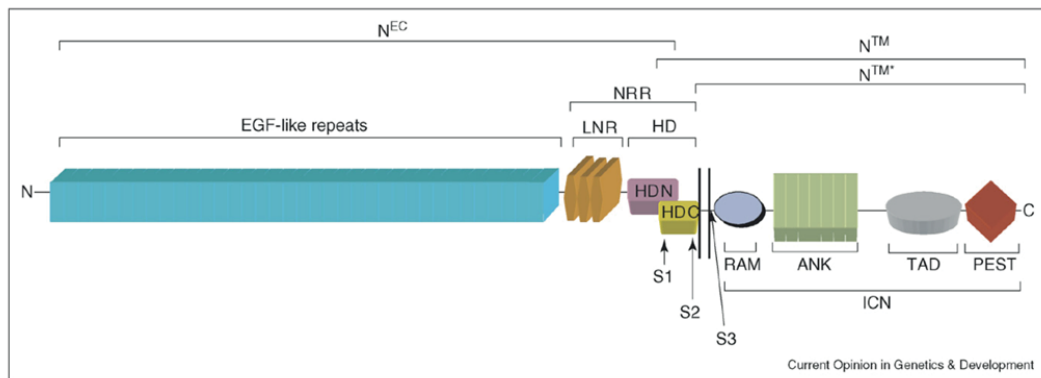
Figure II.4. Structure of the Notch receptor. (Roy et al., 2007). Cleavage at S1 by furin-like protease creates two non-covalently associated subunits (N^{EC} and N^{TM}). The negative regulatory region (NRR) that prevent Notch proteolytic cleavage and activation in the absence of ligands, is composed of three LIN12-Notch repeats (LNRs) and the heterodimerization (HD) domain with the N- (DN) and C-terminal (HDC) regions. Ligand-receptor interaction through the EGF-like repeats induces the cleavage at site S2 by metalloproteases, creating a short-lived intermediate N^{TM*}. The γ-secretase cleavage at S3 releases the intracellular domain of Notch (ICN). Abbreviations: ANK, ankyrin-like repeats; PEST, degron sequence rich in the amino acids proline, glutamate, serine and threonine; RAM, RAM domain; TAD, transcriptional activation domain.

II.2.2. Notch in T cell development

T cells originate from pluripotent precursors in the BM or fetal liver, which migrate to the thymus (Fig. II.5). The earliest T cell progenitors (ETP) in the thymus are found in the CD4$^-$ CD8$^-$ double-negative 1 (DN1) population and display a lack of lineage markers (CD2, CD3, CD4, CD5, CD8, NK1.1, B220, Ter-119, Gr-1) (Lin$^-$) and a Sca1$^+$c-kit$^+$CD24$^{lo/+}$CD25$^-$ CD44$^+$IL-Rα$^{-/lo}$ surface phenotype. DN1 cells differentiate to the DN2 (CD25$^+$CD44$^+$) stage. ETPs and DN2 cells proliferate extensively while acquiring their first T cell characteristics

and initiate the TCR rearrangements (Allman et al., 2003). After the T cell reaches the DN3 (CD25$^+$CD44$^-$) stage, they stop proliferating, greatly increase the TCR gene rearrangement and generate the first fully rearranged TCR loci (TCRβ, TCRγ and/or TCRδ) (Taghon et al., 2006). DN3 cells are blocked at this stage until they correctly rearrange their locus, then they re-start the proliferation. The DN3 cells that successfully rearrange TCRγ and δ-chains are selected as γδT cells. Otherwise, the expression of TCRβ qualifies the cells to undergo β-selection. The β-chains in DN3 cells bind with an auxiliary chain called pTα (pre-T-cell α). The pre-TCR is expressed at the surface in complex with CD3 molecules. The pre-TCR:CD3 complex induce proliferation, stop the β chains rearrangements, and promote the expression of CD4 and CD8 to continue with the T cell maturation. During the transition DN-DP, the DN3 evolve to DN4 due to the loss of CD25 expression and go through an immature simple positive stage (ISP) that expresses initially CD8 and then CD4 to become DP cells. The DN4 cells initiate the rearrangement of the α-chain locus which culminates at DP. The DP cells represent the majority (75-80%) of the thymocytes and are not proliferating cells. The formation of the TCRαβ complexes allows them to undergo positive and negative selection to generate mature CD4$^+$ or CD8$^+$ TCRαβ$^+$ T cells (CD4+SP or CD8$^+$SP, respectively) (Rothenberg et al., 2008).

Notch signaling is essential for the early steps of T-cell development. The thymic epithelium provides a combination of receptor ligands and growth factors to trigger and support T cell differentiation, proliferation and survival. The most important of these receptor ligands are ligands for the Notch cell-surface receptors, delta-like ligand 1 (DLL1) and DLL4 (Maillard et al., 2005). Loss-of-function experiments have shown that Notch plays a crucial role in determining T versus B lymphoid lineage decision. Deletion of Notch1 prior to T cell commitment ablates T cell development and causes the accumulation of ectopic immature B cells in the thymus (Han et al., 2002; Radtke et al., 1999; Wilson et al., 2001). Conversely, gain-of-function analysis involving over-expression of constitutively active Notch1 in BM lineage negative progenitors indicate that activated Notch1 results in thymic-independent T cell development at the expense of B cell development in the BM (Pui et al., 1999). Transplantation experiments have shown that Notch activity is important for T or B cell lineage commitment. Low Notch activity is sufficient to inhibit ectopic B cell

differentiation, whereas ETP generation requires higher Notch activity (Schmitt et al., 2004; Tan et al., 2005). It remains unclear in which organ the commitment takes place. However, Varnum-Finney et al. (2008) have demonstrated the importance of the thymic environment for the expression of Notch target genes like Hes5 to commit for the T lineage. Thus, the Notch signaling plays an important role for the commitment of lymphoid precursors to the T lineage.
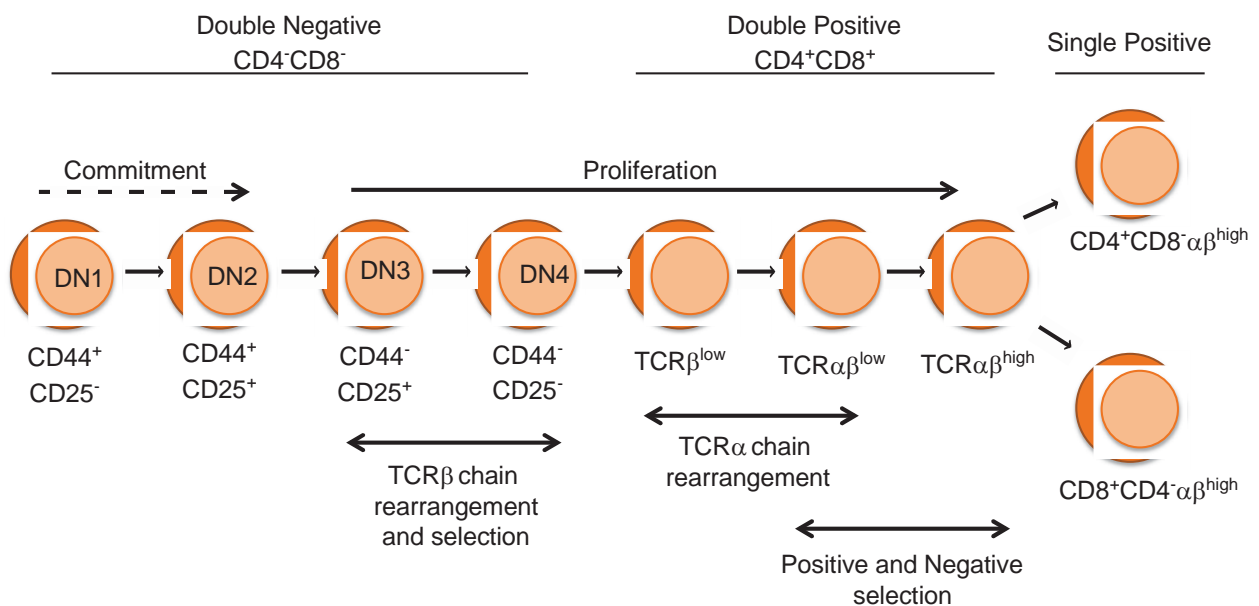
Figure II.5. T cell development. Early T cell progenitors (ETP) migrate and differentiate in the thymus from double negative to double positive and then to single positives. Surface markers for the classification of the DN1-DN4 population are indicated. The stages where the TCR rearrangements take place are also indicated.

Notch signaling is not only required for the generation of the earliest intrathymic ETP. It is also necessary for the generation and maintenance of DN1 cells, where Hes-1 expression is induced (Tan et al., 2005). At DN2 and DN3 stages, Notch activation induces the expression of characteristic markers for these stages like *Ptcra* (pTα) and the DN2-DN3 stage specific marker *Cd25* in addition to *Deltex-1*, *Notch1*, *Notch3* expression (Taghon et al., 2005) DN3 cells need the Notch signaling for the transition to DN4. Notch and E2A induce the expression of pTα to form the pre-TCR. Then Notch signaling collaborates with the pre-TCR and suppresses E2A activity, which induces the proliferation of the TCRβ-selected

DN4 cells (Engel and Murre, 2002; Nie et al., 2003; Talora et al., 2003). Also, Notch supports the DN3-DN4 transition by the induction of *Tcrb* expression (Hoflinger et al., 2004) and promoting survival of DN3 by Akt activation (Ciofani and Zuniga-Pflucker, 2005). However, the DN4 cells appear less dependent on Notch signaling for maturation into the DP population (Kleinmann et al., 2008). Notch signaling might influence αβ versus γδ T cell lineage commitment. Lethally irradiated mice reconstituted with Notch1$^{+/+}$ and Notch1$^{+/-}$ BM cells showed that Notch $^{+/-}$ cells develop more efficiently into γδ T cells than Notch $^{+/+}$ BM cells (Washburn et al., 1997). However, the mice lacking the Notch ligand Jagged2 show fewer γδ T cells (Jiang et al., 1998). By using the OP9-DL1 stromal cell culture system, Ciofani et al. (2006) demonstrated a complex Notch regulation for γδ T cell development. The absence of Notch signaling impairs γδ T cell development from DN2 cells, but leaves a normal γδ T cell development from DN3 cells. These results provide unclear data about the real Notch function in αβ versus γδ T cell lineage commitment. Taken together, these findings demonstrate the essential role of Notch1 signaling to induce and promote survival and proliferation throughout the early stages of intrathymic T cell development.

Notch activation is also important for the peripheral T cell differentiation. Notch signaling enhances T cell proliferation in the presence of antigen presenting cells and induces polarization toward the T helper type 2 (T$_H$2) lineage (Amsen D, et al., 2004). To support this, it was shown that a sequence called the conserved noncoding sequence 2 (CNS2) in the 3' enhancer of the *interleukin-4* (IL-4) gene promoter, contains RBP-J binding sites, suggesting that the regulation of *IL-4* expression by Notch signaling may influence T$_H$1 versus T$_H$2 differentiation (Tanaka S, et al., 2006). Thus, Notch signaling might influence the T cell mediated immune responses.

II.2.3. Notch implication in human T-ALL

The Notch signaling pathway was first implicated in a rare case of T-ALL exhibiting a t(7;9) (q34;34.3) translocation present in 1% of T-ALL cases. This fusion protein is composed of the TCRβ promoter/enhancer region and the C-terminal region of EGF repeat 34 of the human Notch1 gene, resulting in the expression of an N-terminal truncated, dominant

active, and ligand-independent human Notch1 receptor (Ellisen et al., 1991; Reynolds at al., 1987). The oncogenic potential of this fusion protein was shown with mice transplanted with BM progenitors expressing this fusion protein. These mice developed T cell neoplasms as early as 2 weeks after BM transplantation (Pear et al., 1996). Later, other truncated Notch isoforms as well as Notch2 and Notch3 were shown to induce T cell leukemias when over-expressed in BM progenitors or immature thymocytes (Bellavia et al., 2000; Rohn et al., 1996). Originally, it was thought that Notch played a minor role in the molecular pathogenesis of human T-ALL due to the rare frequency of this translocation. This changed after Aster and colleagues (Weng et al., 2004) showed that Notch1 mutations are the most common mutation in T-ALL. A functional screening of human T-ALL cell lines showed two set of mutations either in the heterodomain (HD) or in the PEST domain. In addition, the analysis of 96 pediatric T-ALL samples revealed that 55% of these T-ALLs had at least one mutation in the HD domain or the PEST domain of the Notch1 gene, with 17% of the tumors having mutations in both domains (Fig. II.6) (Weng et al., 2004). Mutations in the HD domain (around S2 and S3 sites) favor the generation of intracellular, constitutively active Notch1 proteins (ligand-independent S2 cleavage). In other hand, the mutations in the PEST domain were predicted to preserve the Notch1 protein stability, because essential recognition sequences for ubiquitin ligases that ensure a rapid turnover of the protein are lost.

Moreover, Notch1 mutations can indirectly lead to the development of leukemia by the oncogenic effect of its downstream effectors. One of these effectors is MYC. The analysis of Notch dependent murine T-ALL cell lines revealed MYC as a direct target of Notch1 (Weng et al., 2006; Palomero et al., 2006). Bonnet et al. (2011) have shown that T-ALL patients with Notch1 mutations are associated with high MYC and low PTEN protein levels, even in absence of *PTEN* mutations. The Notch mutations in these patients contribute to leukemogenesis by activating MYC transcription and stabilizing MYC protein via PTEN repression (Bonnet et al., 2011). Thus, Notch1 mutations are an important feature for T-ALL in different ways.
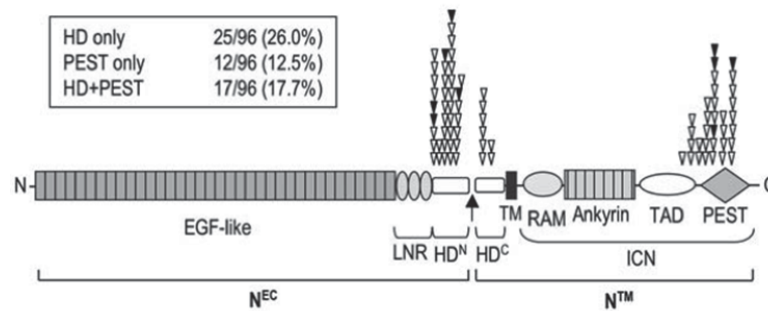
Figure II.6. Distribution of Notch1 mutations in human T-ALL.(Weng et al. 2004) The positions of mutations in Notch T-ALL cell lines (filled triangles) and primary human T-ALL samples (empty triangles).

Thus, the most common Notch1 mutations found in human T-ALL are located in the HD domain, allowing for ligand-independent cleavage. In contrast, within the murine T-ALL models (T-ALL murine models deficient for E2A, p53 or Ikaros), the most common mutations are truncations of the PEST domain that enhance the stability of the truncated protein (Reschly et al., 2006; O'Neil et al., 2006; Dumortier et al., 2006), not mutations in the HD domain. Due to the different mutations between human T-ALL and murine T-ALL, the question of how ligand-independent Notch1 activation is initiated in the T-ALL tumors remained unclear. The following results provide an answer to this question.

Section II. THE DEVELOPMENT OF THE IKAROS-DEFICIENT TUMOR IS NOTCH DEPENDENT

RESULTS

After I arrived to the IGBMC I began to study the $Ik^{L/L}$ leukemias. It had already been shown that the proliferation of $Ik^{L/L}$ tumor-derived cell lines were Notch dependent but it remained unclear if the Notch pathway was required for the development of the tumor.

To investigate the Notch dependence in the development of $Ik^{L/L}$ tumors, we crossed $Ik^{L/L}$ mice with mice carrying a null mutation of Notch3, or floxed alleles for RBP-J (the transcription factor of the Notch pathway) or Notch1. The deletion of the floxed alleles was driven by the CD4-Cre transgene. The deletion of RBP-J delayed the onset of leukemia from 18 weeks in $Ik^{L/L}$ mice to 30 weeks in double mutant mice. The absence of Notch3 had no effect on the development of the $Ik^{L/L}$ tumor; the mice died with similar kinetics and the tumors displayed similar CD4/CD8 profiles. Surprisingly the T-cell specific deletion of floxed Notch1 promoter/exon1 sequences accelerated leukemogenesis. The $Ik^{L/L}$ Notch1$^{f/f}$ CD4-Cre$^+$ (INC+) tumors exhibited a similar CD4/CD8/CD3 profile as the $Ik^{L/L}$ tumors but they lacked Notch1 expression as measured by flow cytometry. We also found that Notch target genes were strongly up-regulated in INC+ tumors. These results and the high expression of CD25, a Notch target gene, suggested the activation of the Notch pathway. We found that the deletion of the Notch1 promoter is oncogenic in T cells, since it leads to the activation of a cryptic intragenic promoter in the 3' region that generates transcripts encoding a constitutively active Notch1 protein.

The results of this work were published in Blood as a Plenary paper, **"Oncogenic activation of the Notch1 gene by deletion of its promoter in Ikaros–deficient T-ALL."**

My principal contribution to this work was the analysis of tumor-derived cell lines and primary tumors from the different mouse lines. I demonstrated that full-length RBP-J protein and the intracellular Notch1 protein of variable sizes were expressed in the RBP-J-

deleted tumors, suggesting that the tumor cells escaped the RBP-J deletion mediated by the CD4-Cre transgene (Fig. 1C). The analysis of the INC+ primary tumors that I performed by surface marker staining, had shown the lack of extracellular Notch1 but high CD25 expression. The expression of CD25, which is a Notch target gene, supports the idea that Notch pathway remains active in these tumors. Using western blot, I demonstrated that the INC+ tumors expressed intracellular Notch1 proteins with variable molecular weights indicating mutations in the Notch1 gene (Fig. 3D, G). I characterized the INC+ and INC-tumor-derived cell lines in terms of CD4/CD8 surface expression and the intracellular Notch1 expression. In addition, my results showed that the inhibition of the γ-secretase cleavage by GSI decreased the amount of intracellular Notch1 protein (supplementary Fig. 2). Since the sequencing of INC+ 5'RACE products predicted the lack of the extracellular domain but the presence of the γ-secretase cleavage site, I analyzed the Notch1 proteins from INC+ and INC- tumor-derived cell lines treated or not with GSI and showed that the INC+ proteins contain the γ-secretase cleavage site (Fig. 5F). To validate if the 5'promoter deletion could induce transcription initiation from 3'sites, we established an inducible cell line to delete the floxed Notch1 sequences by Cre-ERT2. I treated the cells with 4-OH tamoxifen for 24hrs and showed the deletion of the floxed allele by PCR (Fig. 6E). Finally, I analyzed the spontaneous deletions of 5' genomic sequences in several Ik$^{L/L}$ tumors (Fig. 7).

Oncogenic activation of the Notch1 gene by deletion of its promoter in Ikaros-deficient T-ALL

Robin Jeannet, Jérôme Mastio, Alejandra Macias-Garcia, Attila Oravecz, Todd Ashworth, Anne-Solen Geimer Le Lay, Bernard Jost, Stéphanie Le Gras, Jacques Ghysdael, Thomas Gridley, Tasuku Honjo, Freddy Radtke, Jon C. Aster, Susan Chan and Philippe Kastner

---

Updated information and services can be found at:
http://bloodjournal.hematologylibrary.org/cgi/content/full/116/25/5443

Articles on similar topics may be found in the following *Blood* collections:
Plenary Papers (283 articles)
Lymphoid Neoplasia (624 articles)

Information about reproducing this article in parts or in its entirety may be found online at:
http://bloodjournal.hematologylibrary.org/misc/rights.dtl#repub_requests

Information about ordering reprints may be found online at:
http://bloodjournal.hematologylibrary.org/misc/rights.dtl#reprints

Information about subscriptions and ASH membership may be found online at:
http://bloodjournal.hematologylibrary.org/subscriptions/index.dtl

Plenary paper

Oncogenic activation of the *Notch1* gene by deletion of its promoter in Ikaros-deficient T-ALL

*Robin Jeannet,[1] *Jérôme Mastio,[1] *Alejandra Macias-Garcia,[1] Attila Oravecz,[1] Todd Ashworth,[2] Anne-Solen Geimer Le Lay,[1] Bernard Jost,[3] Stéphanie Le Gras,[3] Jacques Ghysdael,[4] Thomas Gridley,[5] Tasuku Honjo,[6] Freddy Radtke,[7] Jon C. Aster,[2] Susan Chan,[1] and Philippe Kastner[1,8]

[1]Institut de Génétique et de Biologie Moléculaire et Cellulaire (IGBMC), Illkirch, France; [2]Department of Pathology, Brigham and Women's Hospital and Harvard Medical School, Boston, MA; [3]IGBMC Microarray and Sequencing Platform, Illkirch, France; [4]Institut Curie, Centre de Recherche, Orsay, France; [5]The Jackson Laboratory, Bar Harbor, ME; [6]Department of Immunology and Genomic Medicine, Graduate School of Medicine, Kyoto University, Kyoto, Japan; [7]Ecole Polytechnique Féderale de Lausanne (EPFL), SV/ISREC, Lausanne, Switzerland; and [8]Université de Strasbourg, Faculté de Médecine, Strasbourg, France

The Notch pathway is frequently activated in T-cell acute lymphoblastic leukemias (T-ALLs). Of the Notch receptors, Notch1 is a recurrent target of gain-of-function mutations and Notch3 is expressed in all T-ALLs, but it is currently unclear how these receptors contribute to T-cell transformation in vivo. We investigated the role of Notch1 and Notch3 in T-ALL progression by a genetic approach, in mice bearing a knockdown mutation in the Ikaros gene that spontaneously develop Notch-dependent T-ALL. While deletion of *Notch3* has little effect, T cell–specific deletion of floxed Notch1 promoter/exon 1 sequences significantly accelerates leukemogenesis. Notch1-deleted tumors lack surface Notch1 but express γ-secretase–cleaved intracellular Notch1 proteins. In addition, these tumors accumulate high levels of truncated Notch1 transcripts that are caused by aberrant transcription from cryptic initiation sites in the 3′ part of the gene. Deletion of the floxed sequences directly reprograms the *Notch1* locus to begin transcription from these 3′ promoters and is accompanied by an epigenetic reorganization of the *Notch1* locus that is consistent with transcriptional activation. Further, spontaneous deletion of 5′ Notch1 sequences occurs in approximately 75% of Ikaros-deficient T-ALLs. These results reveal a novel mechanism for the oncogenic activation of the *Notch1* gene after deletion of its main promoter. (*Blood*. 2010;116(25):5443-5454)

Introduction

T-cell acute lymphoblastic leukemia (T-ALL) is a heterogeneous disease that is characterized by multiple subtypes. T-ALL affects both children and adults and results from the accumulation of blasts blocked at specific stages of T-cell differentiation. Treatment involves long-term and intensive combination chemotherapy, which are associated with severe side effects. Relapse is frequent in adult T-ALL with very unfavorable outcome. Less than 60% of patients survive longer than 5 years.[1]

T-ALL is associated with recurrent genetic and epigenetic abnormalities. Chief among them is the activation of the Notch pathway.[2] The oncogenic effects of the Notch pathway are probably linked to its pleiotropic influence on T lymphocytes. Notch receptors are expressed on the surface of T cells, and upon binding to ligands expressed by neighboring cells, the heterodimeric receptor is cleaved by metalloproteases (at the S2 site) and γ-secretase (at the S3 site) to release an activated, intracellular form of Notch (ICN). Cleaved Notch then translocates to the nucleus where it binds to its downstream transcriptional mediator, recombination signal binding protein for immunoglobulin kappa J region (RBP-J), and coactivators to activate the transcription of Notch-dependent target genes.[3-6]

Of the 4 Notch receptors (Notch1-4), Notch1 appears to be the most important in human T-ALL. This was first demonstrated by the finding of a rare translocation in approximately 1% of T-ALL that fuses the sequences encoding the C-terminal portion of Notch1 downstream of the promoter of the β chain of the T-cell receptor (TCR), resulting in the expression of a constitutively active intracellular Notch1 protein that acts as a powerful oncogene.[7] More recently, Aster and colleagues[8] found that the *Notch1* gene contains point mutations or deletions in approximately 70% of T-ALL cases, which are situated in the heterodimerization domain and the 3′ PEST domain. These mutations lead to increased cleavage of Notch1 as well as stabilization of the intracellular protein. Collectively, these studies suggest that Notch1 is the crucial receptor for oncogenic mutations. On the other hand, Notch3 mRNA expression is up-regulated in all T-ALL cases studied, also suggesting a role for this receptor in T-ALL development.[9,10]

A variety of murine T-ALL models have addressed the oncogenic role of Notch proteins carrying different mutations or deletions, usually by overexpressing them in retroviral systems or by transgenesis.[11-15] These have provided valuable information about the potential of activated proteins to induce transformation, but they also come with caveats, as overexpression studies do not always resemble the physiologic disease. For example, overexpression of intracellular Notch1-3 are equally capable of inducing leukemia in the retroviral bone marrow transfer model,[16] yet Notch2 does not appear to be affected in human T-ALL. Thus, the

The publication costs of this article were defrayed in part by page charge payment. Therefore, and solely to indicate this fact, this article is hereby marked "advertisement" in accordance with 18 USC section 1734.

individual roles played by the specific Notch receptors in T-ALL progression remain poorly understood.

We recently described a spontaneous model of T-ALL in mice bearing a knockdown mutation of the Ikaros gene (Ik$^{L/L}$).[17] These mice develop clonal T-cell lymphomas in the thymus with an early and reproducible time of onset, between 10-12 weeks of age, and they die at a median age of 18 weeks. Disease incidence is 100%. The tumor phenotype is predictable and shows an accumulation of blasts at the CD4$^+$CD8$^+$ (DP) and CD4$^-$CD8$^+$ (CD8 SP) stage of differentiation; αβ TCR/CD3 expression levels vary from low to intermediate. Interestingly, all tumors show high up-regulation of Notch target gene expression at the mRNA level. This is accompanied by the accumulation of intracellular Notch1 proteins that show point mutations or deletions in the PEST domain of the *Notch1* gene. Tumor cell proliferation is strictly dependent on Notch signaling. Ik$^{L/L}$ mice therefore develop a Notch-dependent T-ALL that is highly reminiscent of the human disease. Importantly, the Notch pathway genes were unmanipulated in this system.

Thus, the Ik$^{L/L}$ mouse line is a relevant model for studying the role of Notch activation and the function of specific Notch receptors in the pathogenesis of T-ALL. Here, we deleted *RBP-J*, *Notch3*, and *Notch1* in Ik$^{L/L}$ mice and evaluated their genetic contribution to T-ALL initiation and progression. We show that Notch1 is the critical receptor in T-ALL and uncover a novel mechanism for the generation of oncogenic Notch1 proteins that involves deletion of its 5′ promoter.

Methods

Methods are available on the *Blood* Web site (see the Supplemental Materials link at the top of the online article). Research on mice at the IGBMC was approved by the Direction des Services Vétérinaires du Bas-Rhin. All microarray data are available on the Gene Expression Omnibus (National Center for Biotechnology Information) public database under accession number GSE23972.

Results

Genetic contribution of RBP-J, Notch3, and Notch1 to tumor progression in a spontaneous model of T-ALL

To determine the significance of Notch activation and to define the role of Notch receptors in T-ALL progression, we crossed Ikaros$^{L/L}$ mice with animals carrying null mutations or floxed alleles for *RBP-J*, *Notch3*, and *Notch1*.[18-20] To delete the floxed alleles, the CD4-Cre tg,[21] which excises floxed sequences at the DN4 (CD4$^-$CD8$^-$CD44$^-$CD25$^-$) to DP stage of thymocyte differentiation, was chosen for 3 reasons: (1) because the constitutive null mutation is embryonic-lethal (eg, with *RBP-J* and *Notch1*), (2) because deletion at an earlier time point (eg, using lck-Cre) impairs T-cell differentiation and might introduce unnecessary side effects to our interpretation of the results,[22] and (3) because the Ik$^{L/L}$ tumors consistently express a αβ TCR and display a DP to CD8 SP cell-surface phenotype, suggesting that most tumor cells undergo some differentiation and will activate the CD4 promoter.

The effect of *RBP-J* inactivation was therefore studied in RBP-J–expressing Ik$^{L/L}$RBP-J$^{f/f}$CD4-Cre$^-$ (IRC$^-$) and RBP-J–deleted Ik$^{L/L}$RBP-J$^{f/f}$CD4-Cre$^+$ (IRC$^+$) mice. In agreement with published results,[23] CD4-Cre–mediated deletion of *RBP-J* in Ik$^{L/L}$ mice did not affect T-cell differentiation and thymic cellularity (data not shown). In contrast, loss of RBP-J significantly pushed

T-ALL–related death from a median of 18 weeks to 30 weeks (Figure 1A; $P = 2 \times 10^{-10}$). To determine whether this was due to a delay in tumor initiation or tumor growth, we analyzed the thymus of IRC$^+$ and IRC$^-$ mice at 18 weeks of age. At this age, IRC$^-$ mice were either dead or showed pronounced thymic lymphomas with an abnormal CD4/CD8 phenotype (Figure 1B). In contrast, IRC$^+$ mice were healthy and exhibited a normal thymic phenotype, similar to wild-type (WT). Nevertheless, IRC$^+$ mice eventually died from T-ALL. IRC$^+$ tumors expressed full-length RBP-J and intracellular, γ-secretase–cleaved Notch1 polypeptides (ICN1) of variable size (Figure 1C), suggesting a selection of PEST mutations in the *Notch1* gene. These tumors showed low levels of deletion of the floxed sequences (Figure 1D), indicating that the CD4-Cre transgene had not been activated in most of the cells. Indeed, some IRC$^+$ tumors were composed mostly of CD4$^-$CD8$^-$ or CD4$^-$CD8$^+$ cells (see T99 and T96 in Figure 1E). Other tumors expressed CD4 but may have acquired resistance to the Cre-mediated deletion through another mechanism. Collectively, these results demonstrate that Notch activation is required for T-ALL initiation in Ik$^{L/L}$ mice.

Notch3 is highly expressed in human T-ALL and in Ik$^{L/L}$ tumors.[9,10,17] We therefore evaluated the role of Notch3 in tumor progression by crossing Ik$^{L/L}$ mice with Notch3-null animals. Ik$^{L/L}$ mice died from T-ALL with similar kinetics and similar tumor profiles (DP/CD8 phenotype, low levels of αβ TCR) in the presence or absence of Notch3 (Figure 2 and not shown), indicating that Notch3 has minimal impact on T-ALL induced by Ikaros deficiency.

To investigate the role of Notch1, Ik$^{L/L}$ mice were crossed with animals expressing floxed *Notch1* alleles and CD4-Cre to generate Ik$^{L/L}$Notch1$^{f/f}$CD4-Cre$^+$ (IN1C$^+$) and Ik$^{L/L}$Notch1$^{f/f}$CD4-Cre$^-$ (IN1C$^-$) mice. Unexpectedly, Notch1-deleted IN1C$^+$ mice died significantly faster and developed T-ALL earlier than their IN1C$^-$ littermates (11 weeks for IN1C$^+$ vs 20 weeks for IN1C$^-$; Figure 3A,C). Furthermore, there was no detectable difference in tumor phenotype: both IN1C$^+$ and IN1C$^-$ tumors exhibited similar CD4/CD8/CD3 profiles, showed biased TCR β chain rearrangement, and could transfer disease with similar kinetics in irradiated primary and secondary recipients (supplemental Figure 1 and not shown). In addition, the acceleration in tumor development was strictly dependent on the presence of both the floxed *Notch1* alleles and the CD4-Cre tg, as Ik$^{L/L}$Notch1$^{+/+}$CD4-Cre$^+$ mice also died near 20 weeks of age (Figure 3A blue curve). These results suggest that deletion of the *Notch1* floxed alleles is an oncogenic event.

Notch1 activation in Notch1-deleted tumors

Tumor development in IN1C$^+$ mice could mean that the *Notch1* alleles of the tumor cells had escaped deletion by the CD4-Cre tg. We evaluated the deletion efficiency of the floxed alleles in a panel of primary tumors from Ik$^{L/L}$, IN1C$^-$, and IN1C$^+$ mice by polymerase chain reaction (PCR) analysis (Figure 3B) and found that the IN1C$^+$ tumors showed high levels of deletion, suggesting that most IN1C$^+$ tumor cells had efficiently deleted both *Notch1* alleles. We also evaluated the cell-surface expression of Notch1 on primary IN1C$^+$ tumors by flow cytometry. In these experiments, IN1C$^-$ tumors uniformly expressed high levels of CD25, a putative Notch target gene, and surface Notch1 (Figure 3D). In contrast, IN1C$^+$ tumors still expressed CD25 but not Notch1 (Figure 3D), indicating that Notch1 was no longer expressed on the surface of IN1C$^+$ tumor cells.

That IN1C$^+$ tumor cells expressed CD25 suggested that the Notch pathway was still active in these tumors. To test this
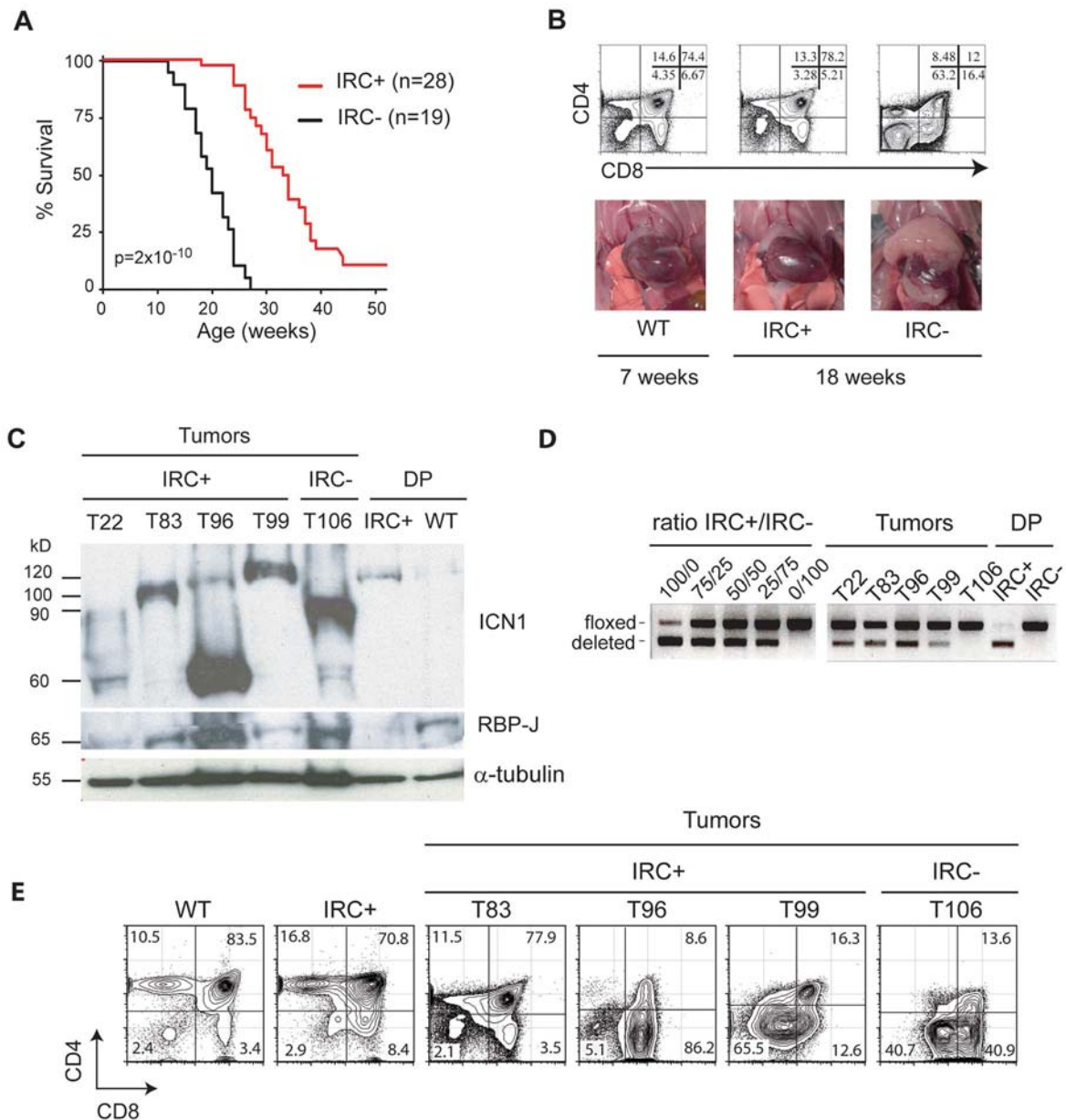
Figure 1. RBP-J deletion delays T-ALL development. (A) Survival curves of $Ik^{L/L}RBP-J^{f/f}CD4-Cre^+$ (IRC^+) mice and $Ik^{L/L}RBP-J^{f/f}CD4-Cre^-$ (IRC^-) mice. The statistical significance was calculated by log-rank test. Note that the 2 IRC^+ mice killed at 52 weeks did not show signs of disease. (B) Thymocyte CD4/CD8 profiles as determined by flow cytometry (top) and photos of the thoracic cavity (bottom) from 18-week-old IRC^+ and IRC^- mice and a 7-week-old WT mouse. (C) Western blot of RBP-J and ICN1 (Val1744 antibody) expression in a panel of thymic tumors from IRC^+ mice. Control samples are an IRC^- tumor and sorted $CD4^+CD8^+$ (DP) cells from 4-week-old IRC^+ and WT mice. α-Tubulin was used as a loading control. The variable sizes of the ICN1 proteins are likely due to C-terminal truncations. Note that the deletion of the RBP-J floxed sequences effectively leads to loss of RBP-J proteins in nontransformed IRC^+ DP cells. (D) PCR analysis of the deletion of the floxed sequences in the samples shown in C. The left panel shows amplification of control samples consisting of mixes of DNA from IRC^+ and IRC^- thymocytes, at the indicated ratio. (E) CD4/CD8 profiles of samples shown in panel C, except for T22 where the FACS profile was not available.

possibility and to determine whether additional cooperative oncogenic pathways were activated in $IN1C^+$ tumors, we analyzed the transcriptome profiles of 3 $IN1C^+$ and 3 $IN1C^-$ tumors, and compared them with those of Tel-Jak2–induced T-cell tumors (that exhibit low levels of Notch target gene expression[17]), as well as with WT DN3 ($CD4^-CD8^-CD44^-CD25^+$), DN4, and DP thymocytes. Notch target genes were strongly up-regulated in both $IN1C^+$ and $IN1C^-$ tumors (Figure 3E), suggesting Notch activation in both cases. In addition, $IN1C^+$ tumors did not show a deregulation of genes associated with other known oncogenic pathways (data not shown). To determine whether $IN1C^+$ tumors were dependent on Notch signaling for proliferation, cell lines

generated from $IN1C^+$ and $IN1C^-$ tumors were cultured in the presence of a γ-secretase inhibitor (GSI) (see supplemental Figure 2 for characterization of the cell lines). In all cases, GSI treatment arrested cell proliferation (Figure 3F). Together, these results indicate that the Notch pathway remains a dominant oncogenic pathway in Notch1-deleted T cells.

Finally, we asked whether activated Notch1 proteins were still expressed in $IN1C^+$ tumors, using an antibody specific for γ-secretase–cleaved Notch1 (Val1744). Strikingly, all $IN1C^+$ tumors expressed ICN1 (Figure 3G). These proteins varied in size, were shorter than the expected 120 kDa in 60%-70% of the cases, and were similar to the truncated ICN1 proteins in $Ik^{L/L}$ tumors,[17]
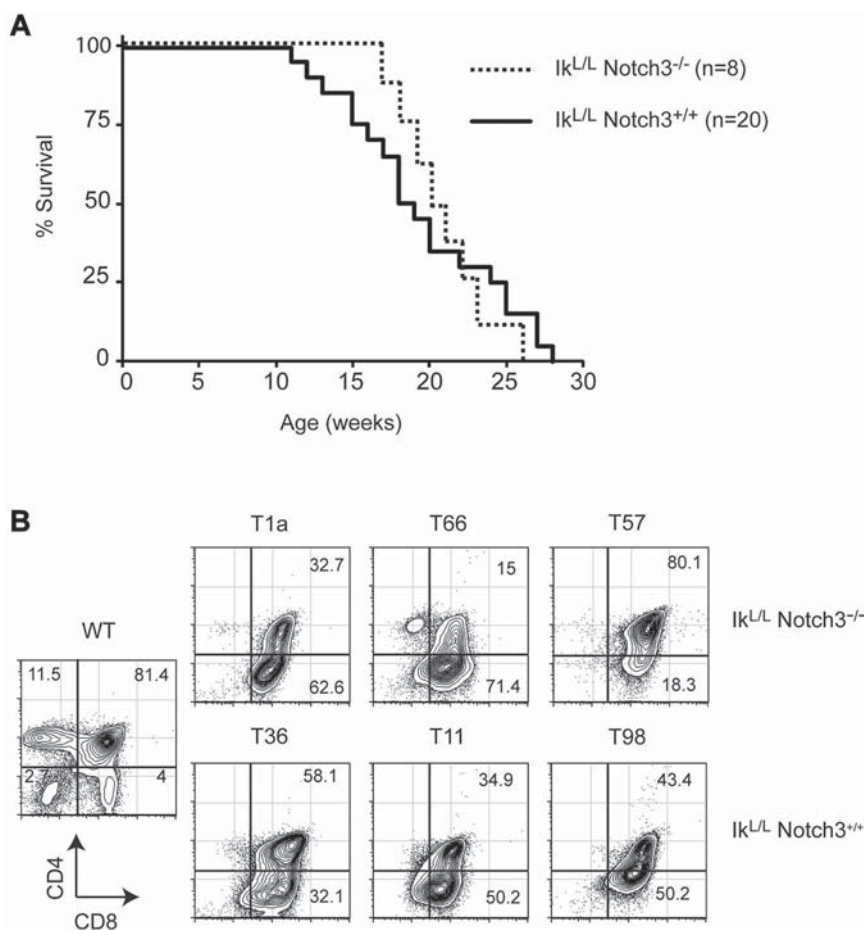
Figure 2. Notch3 is dispensable for leukemogenesis in Ik[L/L] mice. (A) Survival curves of Ik[L/L]Notch3^{+/+} and Ik[L/L]Notch3^{−/−} mice. (B) Representative CD4/CD8 profiles of thymic lymphomas from Ik[L/L]Notch3^{+/+} and Ik[L/L]Notch3^{−/−} mice.

suggesting the presence of PEST domain mutations at the DNA level. This was confirmed by sequencing the Notch1 transcripts in 8 IN1C^{+} tumors, which revealed heterozygous frame-shift mutations in the 3′ Notch1 sequence that would result in the production of truncated Notch1 proteins lacking the PEST domain in 5 cases (Figure 3H). Thus, the *Notch1* gene is still a target of oncogenic mutations despite the deletion of floxed sequences and the absence of surface Notch1 in IN1C^{+} T cells.

Deletion of the *Notch1* promoter/exon 1 is oncogenic in Ikaros-deficient T cells

In the course of this study, we came across intriguing results from Aster and colleagues, who discovered a panel of murine T-cell lines that did not express surface Notch1, were sensitive to GSI for growth, and exhibited 5′ deletions in the *Notch1* gene (see companion paper by Ashworth et al[25]). Their results, as well as those from Tsuji et al,[26] suggested that Notch1 could be transcribed from cryptic intragenic promoters if the conserved 5′ promoter is lost and that the resulting proteins may be oncogenic. We therefore revisited the *Notch1* floxed mutation. In this mutation, the loxP sites were placed around a 3.5-kb sequence encompassing the conserved promoter and exon 1, which encodes the leader peptide responsable for surface Notch1 expression.[20] Previous analyses have shown that Cre-mediated deletion of the floxed sequence leads to the loss of Notch1 proteins in thymocytes,[21] indicating that the floxed mutation is null.

To determine whether deletion of the Notch1 floxed sequences leads to a null allele or an oncogenic allele on an Ikaros-deficient background, we generated Ik[L/L] mice heterozygote for the floxed allele. Floxed *Notch1* mice were bred with cytomegalovirus-Cre tg mice to delete the floxed sequences in the germline (the germline-deleted allele was designated N1[Δf]). Notch1[+/Δf] mice were then crossed with Ik[L/L] animals to obtain Ik[L/L]Notch1[+/Δf] (IN1[+/Δf]) mice. Strikingly, IN1[+/Δf] mice died from T-ALL at a median age of 11 weeks, while Ik[L/L]Notch1^{+/+} littermates died near 20 weeks (Figure 4A). Thus, deletion of the *Notch1* promoter/exon 1 on a single allele significantly accelerates tumorigenesis.

Like IN1C^{+} tumors, IN1[+/Δf] tumors expressed truncated ICN1 proteins (Figure 4B), suggesting a selection of oncogenic PEST mutations. To determine whether the PEST mutations occurred on the WT allele, or the deleted one, we exploited the observation that these alleles differed by a single nucleotide polymorphism at position 5179 in exon 26 (numbering according to the Notch1 reference sequence NM_008714). The deleted allele, derived from the 129/Sv strain (the parental strain of the GS-1 embryonic stem cell line used to engineer the mutation), had an "A" at this position, while the WT allele (derived from the C57Bl/6 strain; see "Methods") had a "G" (Figure 4C). We amplified cDNA fragments spanning exons 26-34 (that comprises both the single nucleotide polymorphism and the PEST domain sequences) from 3 IN1[+/Δf] tumors, subcloned, and sequenced the amplification products. All 3 tumors showed PEST mutations in the 129/Sv allele, while the C57Bl/6 allele showed no mutations (Figure 4D). These data suggest that the PEST mutations are strongly selected for on the N1[Δf] allele compared with the WT allele. Thus, our results indicate that loss of the Notch1 promoter/exon 1 is oncogenic on an
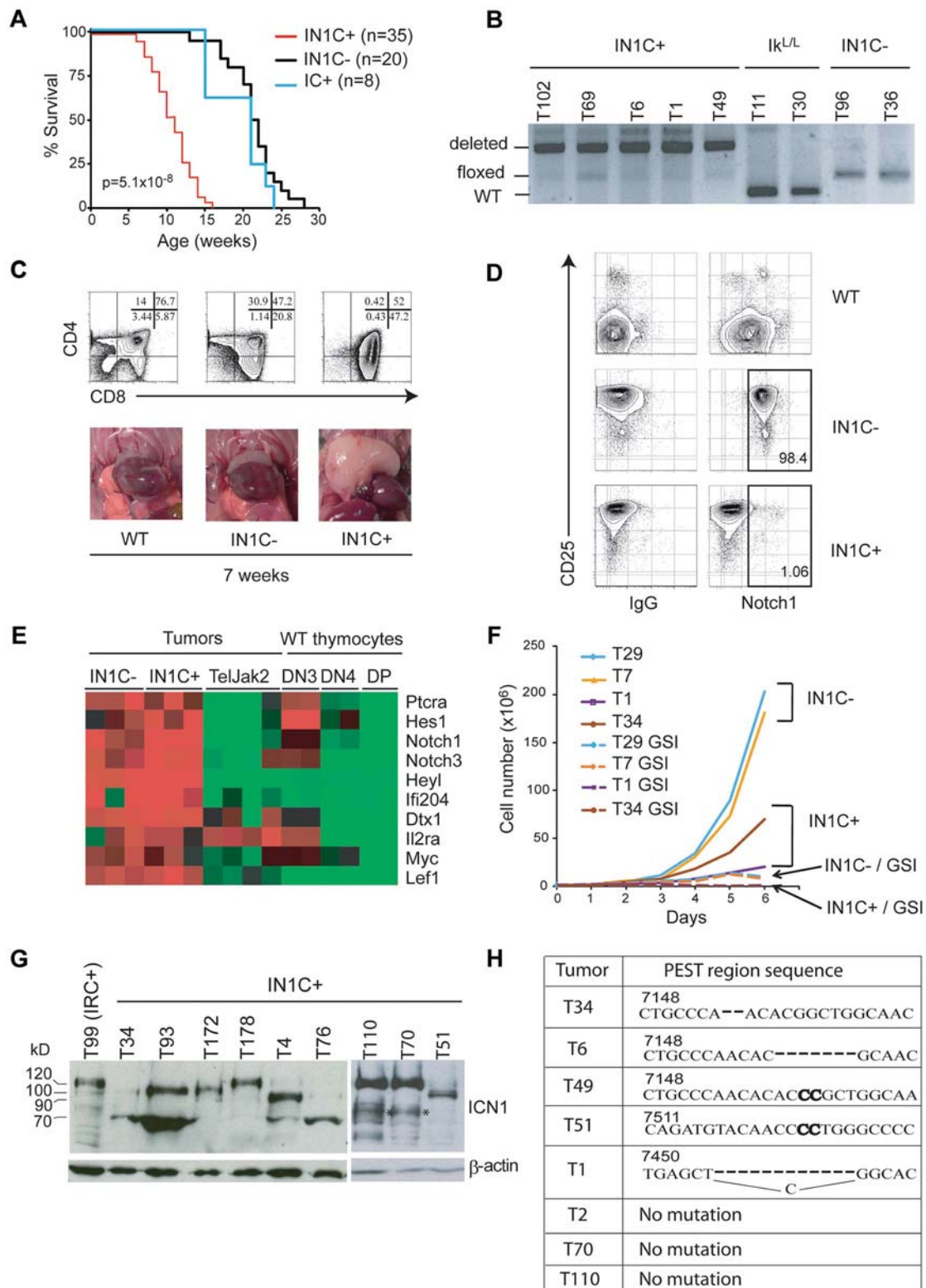
Figure 3. Deletion of Notch1 accelerates T-ALL development. (A) Survival curves of Ik$^{L/L}$Notch1$^{f/f}$CD4-Cre$^+$ (IN1C+), Ik$^{L/L}$Notch1$^{f/f}$CD4-Cre$^-$ (IN1C−), and Ik$^{L/L}$Notch1$^{+/+}$CD4-Cre$^+$ (IC+) mice. The *P* value corresponds to the statistical difference between the survival of IN1C$^+$ and IN1C$^-$ mice by log-rank test. (B) PCR analysis of the deletion of the floxed sequences in a panel of IN1C$^+$ tumors. (C) Thymocyte CD4/CD8 profiles (top) and photos of the thoracic cavity (bottom) from 7-week-old WT, IN1C$^-$, and IN1C$^+$ mice. (D) Surface Notch1 and CD25 expression of IN1C$^+$ and IN1C$^-$ tumor cells and WT thymocytes. The immunoglobulin G isotype control is shown in the left panels. Similar results were observed in all Ik$^{L/L}$/IN1C$^-$ and IN1C$^+$ mice analyzed (n > 10). (E) Transcriptome profiling of Notch target genes in 3 IN1C$^+$ and 3 IN1C$^-$ tumors using Affymetrix 430 2.0 arrays. The data were normalized with those from leukemic T cells of Tel-Jak2 tg mice[24] and from WT DN3, DN4, and DP thymocytes using the Robust Microarray Analysis algorithm. Red and green colors indicate high and low expression, respectively. (F) Proliferation of IN1C$^+$ and IN1C$^-$ cell lines in the absence or presence of γ-secretase inhibitor over 6 days. Representative of 3 independent experiments. (G) Western blot of ICN1 expression in IN1C$^+$ tumors using the Val1744 antibody. β-actin was used as a loading control. T99 is a IRC$^+$ tumor that expresses ICN1 proteins of the normal 120 kDa size. The asterisk in the right panel points to likely degradation products. (H) PEST region sequences of IN1C$^+$ tumors. The bold nucleotides correspond to insertions in the WT sequence. ICN1 proteins from samples T34, T6, and T49 are shown in supplemental Figure 1C; T51, T70 and T110 are shown in Figure 3G; T1 and T2 correspond to IN1C$^+$ cell lines described in supplemental Figure 2. Numbering according to the Notch1 reference sequence NM_008714.
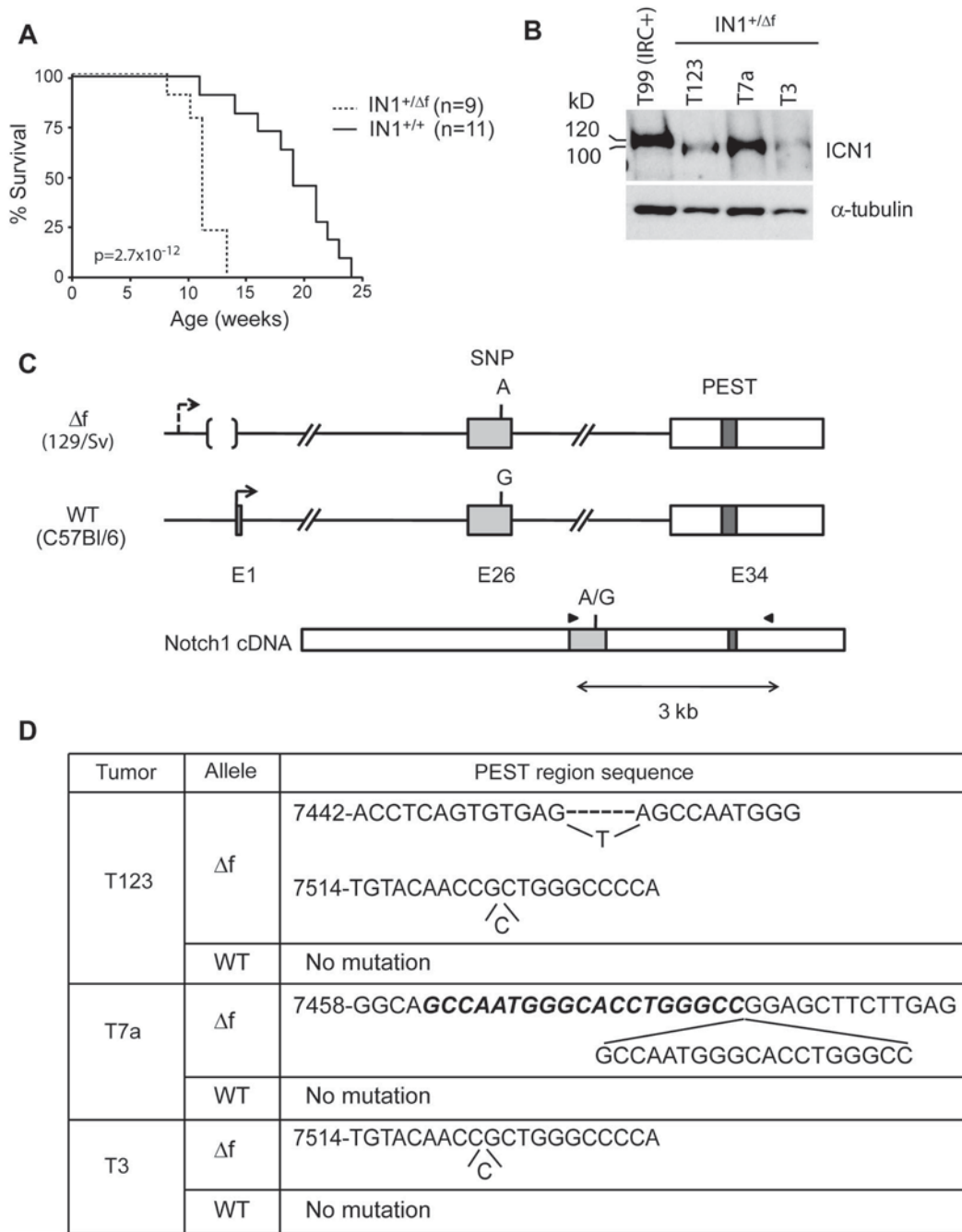
Figure 4. Oncogenic effect of deleting floxed Notch1 sequences from a single allele. (A) Survival curves of Ik$^{L/L}$Notch1$^{+/\Delta f}$ (IN1$^{+/\Delta f}$) and Ik$^{L/L}$Notch1$^{+/+}$ (IN1$^{+/+}$) mice. The statistical significance was calculated by log-rank test. (B) Western blot of ICN1 expression in IN1$^{+/\Delta f}$ tumors. The control sample is the IRC$^+$ T99 tumor shown in Figure 1C, which expresses ICN1 proteins of normal size. α-Tubulin was used as a loading control. (C) Strategy to identify the allele harboring the PEST domain mutation. A single nucleotide polymorphism in exon 26 (rs27201809; Mouse Genome Informatics database) distinguishes the WT and deleted alleles, which are derived from the C57Bl/6 and 129/Sv strains, respectively. RT-PCR amplification and sequencing of exon 26 and the PEST region in exon 34 identifies the allele carrying the mutation. (D) Association of PEST region mutations with the N1$^{\Delta f}$ allele in the 3 tumors shown in B. T3 had a single nt insertion. T7a had a duplication of 19 nt (in bold and italic). T123 had 2 separate mutations, both in the N1$^{\Delta f}$ allele: a deletion of 6 nt, which were replaced by a single T, and a single nt insertion. Numbering according to the Notch1 reference sequence NM_008714.

Ikaros-deficient background and that the deleted allele is sensitive to subsequent PEST mutations.

Truncated transcripts encoding constitutively active Notch1 proteins are expressed in IN1C$^+$ tumors

To investigate how oncogenic Notch1 proteins are generated after deletion of the main promoter, we compared the Notch1 transcripts in IN1C$^+$ tumors with those in IN1C$^-$ or Ik$^{L/L}$ tumors and WT thymocytes by Northern blot using a probe corresponding to exon 34. As expected, this probe revealed full-length approximately 9-kb transcripts in WT thymocytes, Ik$^{L/L}$, and IN1C$^-$ tumor cells (Figure 5A). In contrast, the majority of the transcripts in the IN1C$^+$ tumors were between 4-6 kb. Some 9-kb transcripts were still detected in IN1C$^+$ tumors; these may have initiated from the cryptic 5′ 1a and 1b promoters upstream of the main promoter,[26] with subsequent splicing to 5′ exons, as detected by reverse-transcription (RT)–PCR

Figure 5. Truncated Notch1 transcripts and proteins in IN1C+ tumors. (A) Northern blot of total RNA (10 μg) from primary tumors and cell lines of the indicated genotypes using a probe for exon 34 (top). Methylene blue staining of 18S and 28S ribosomal RNA was used as a loading control (bottom). (B) RT-quantitative PCR of Notch1 transcripts, using primers to amplify exons 23-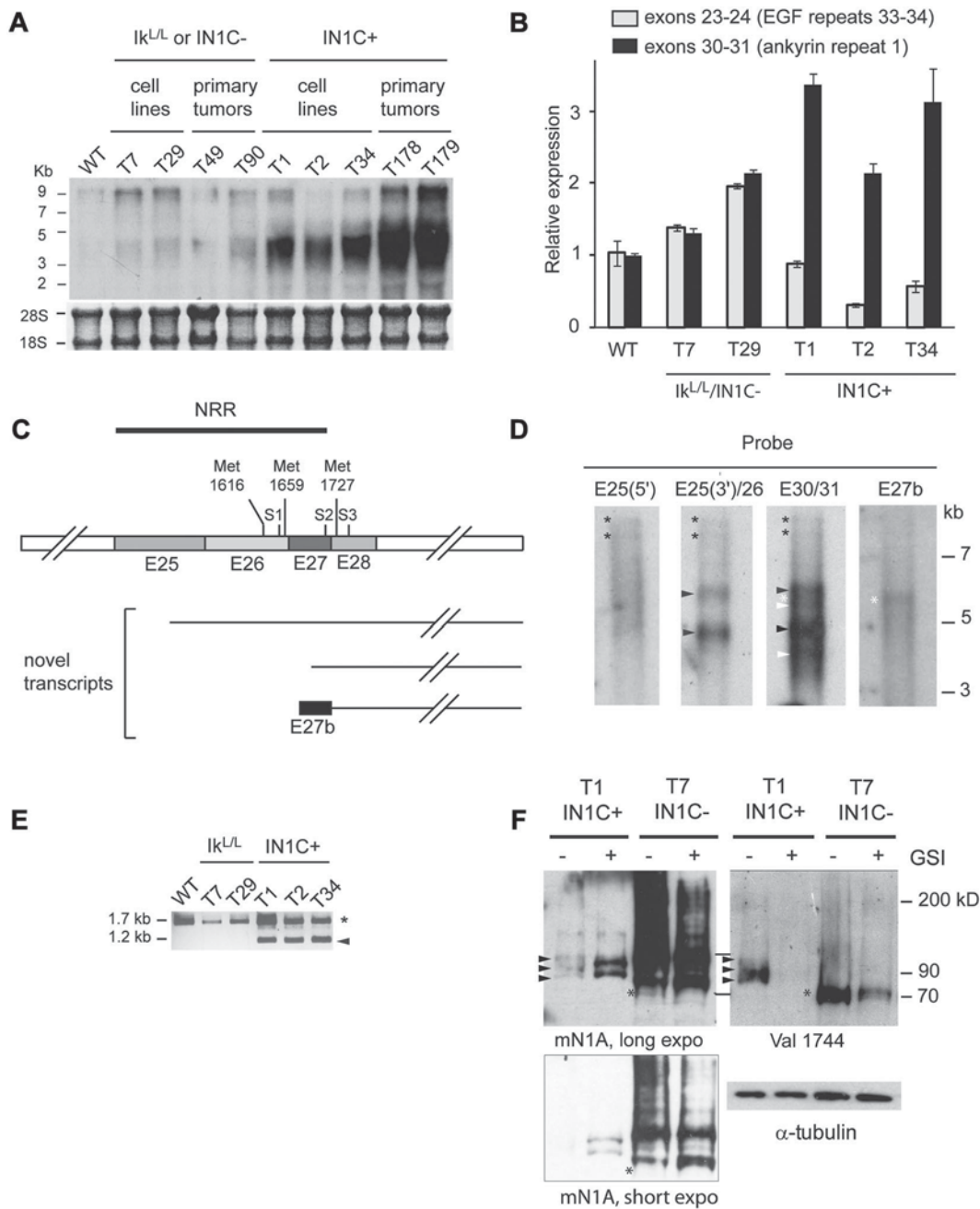24 (encoding the extracellular EGF repeats 33/34) and exons 30-31 (encoding the first intracellular ankyrin repeat). Results were normalized to hypoxanthine-guanine phosphoribosyltransferase levels and to those of WT thymocytes, for which the exon 23-24 mRNA level was arbitrarily fixed at 1. Data represent the mean of 2 experiments. (C) Scheme summarizing the results of the 5′-RACE experiments performed on the T1 and T34 IN1C+ cell lines. The organization of the Notch1 transcript in the region of interest is shown, with the position of the S1, S2, and S3 cleavage sites, and the putative methionines that could be used for translation initiation. cDNAs identified by 5′-RACE are shown (see supplemental Figure 5 for sequence details). (D) Northern blot of Notch1 transcripts in poly(A)+ RNA (1.5 μg each) from the T1 cell line, hybridized with probes from the indicated exons/introns. E25(5′) corresponds to nt 4279-4741; E25(3′)/26 corresponds to nt 4758-5246; E30/31 corresponds to nt 5715-6179 (reference sequence NM_008714). E27b corresponds to a 628 nt region from intron 27 that includes the 113 nt sequence of exon 27b (see supplemental Figure 5). Autoradiograms for E25(3′)/26 and E30/31 were exposed for 18 hours; those for E25(5′) and E27b were exposed for 44 hours. Asterisks indicate transcripts initiating from 5′ promoters; black arrowheads indicate transcripts initiating from exon 25; white arrowheads indicate transcripts initiating downstream of exon 26 (likely in exon 27); white asterisks indicate transcripts containing exon 27b. (E) RT-PCR of exon 27b–containing transcripts in the indicated samples. cDNA was amplified using a forward primer located within exon 27b and a reverse primer from exon 31. The arrowhead indicates the correctly spliced transcripts; the asterisk indicates likely splicing intermediates that had not excised intron 27. (F) Western blot of Notch1 expression in total cell extracts from the T1 IN1C+ and T7 IN1C− cell lines, cultured in the presence or absence of GSI for 3 days. The membrane was first analyzed with the Val1744 antibody, and then with the mN1A Ab. α-tubulin was used as a loading control. Long (10 minutes) and short (30 seconds) exposures are shown for the mN1A Ab. The lines between the top 2 panels indicate the positions of the molecular weight markers used to align the blots. Asterisks indicate the γ-secretase–cleaved proteins from the T7 cell line; arrowheads indicate the γ-secretase–cleaved proteins from the T1 cell line. Note that the ICN1 proteins in the T7 line do not completely disappear after GSI treatment, probably due to the increased stability of the truncated proteins in this cell line. All data are representative of > 2 independent experiments.

(supplemental Figure 3). We further analyzed the relative levels of Notch1 transcripts containing 5′ and/or 3′ sequences in a ratiometric RT-quantitative PCR assay, using primers to amplify exons 23-24 (which encodes part of the extracellular domain) or exons

30-31 (which encodes part of the cytoplasmic domain). These assays showed that the ratio of 5′ to 3′ transcripts were similar in the Ik[L/L] or IN1C^{−} cell lines (Figure 5B). In contrast, there was a clear bias toward the 3′ transcripts in the IN1C^{+} cell lines. Thus, deletion of the proximal promoter results in the transcription of truncated 3′ Notch1 transcripts in IN1C^{+} cells.

To map the 5′ ends of the truncated transcripts, we performed 5′-RACE on IN1C^{+} tumor cells, using an assay that specifically detects full-length capped mRNA. A sequence in exon 31 was used as the 3′ anchor. Distinct 5′-RACE products were amplified from 2 IN1C^{+} cell lines ranging from 700-1200 bp (supplemental Figure 4 and data not shown). Sequencing of the subclones revealed a variety of 5′ ends that started from the end of exon 25 all the way to exon 29 (Figure 5C and see supplemental Figure 5 for sequence information). Several clones began in intron 27 and contained a 113 bp segment of this intron (hereafter named exon 27b) spliced to exon 28 and downstream exons (Figure 5C and supplemental Figure 5). To determine whether these sequences corresponded to the truncated transcripts identified in the Northern blot, we performed further Northern blots on poly(A)[+] RNA from a IN1C^{+} cell line and used a series of probes covering exons 25-31 (Figure 5D). No transcripts were detected with a probe from the 5′ end of exon 25. Two major transcripts (approximately 4.5 and 6 kb) were detected with a probe from the 3′ end of exon 25 and exon 26 (black arrowheads). Three additional transcripts (approximately 4, 5.5, and 5.7 kb) were detected with a probe from exons 30-31 (white arrowhead and asterisk). Finally, a weak transcript was detected with an exon 27b probe (white asterisk). These results suggest that IN1C^{+} tumors predominantly express transcripts that start in exons 25-27, with a minor transcript starting in exon 27b. Interestingly, transcripts of different sizes were detected with 2 of the probes, suggesting that they also use different polyadenylation signals (see companion paper by Ashworth et al[25]).

The exon 27b–containing transcript was intriguing in that it includes intronic sequences not found in the normal full-length Notch1 mRNA. RT-PCR analyses readily amplified this product from all IN1C^{+} cell lines tested but not from lines with intact Notch1 5′ sequences (Figure 5E arrowhead). In addition, screening of > 40 RNA samples from a wide range of normal tissues, as well as from embryos and embryonic stem cell lines, did not reveal the presence of this transcript (data not shown). These results suggest that the exon 27b–containing transcripts may be specific to leukemic cells with 5′ promoter deletions.

We next evaluated the Notch1 proteins synthesized from the truncated transcripts. Three methionines (aa 1616, 1659, 1727) are present between exons 26-28 (Figure 5C). Proteins initiating from these methionines would be predicted to lack the extracellular domain and the negative regulatory region but retain the S3 cleavage site, thereby creating a protein susceptible to γ-secretase cleavage in the absence of ligand. To test this hypothesis, we analyzed the Notch1 proteins from T1 IN1C^{+} and T7 IN1C^{−} cells, treated or not with GSI, by Western blot (Figure 5F). Two anti-Notch1 antibodies were sequentially used: the Val1744 antibody that specifically detects γ-secretase–cleaved Notch1 and the mN1A antibody that detects the cdc10/ankyrin repeat domain of all Notch1 proteins before and after cleavage but which appears to detect γ-secretase–cleaved Notch1 with lower intensity in our hands. As expected, the untreated IN1C^{−} sample contained mainly uncleaved Notch1 proteins (left panel, the larger size bands above the asterisk; see lower panel for a short exposure of the same membrane) and some γ-secretase–cleaved proteins (right panel, asterisk). Interestingly, less proteins were detected by the mN1A

antibody from IN1C^{+} cells compared with IN1C^{−} samples (left panel), suggesting that the truncated Notch1 transcripts are not efficiently translated. Nevertheless, cleaved Notch1 proteins were readily detected by the Val1744 antibody in the untreated IN1C^{+} sample (right panel, arrowheads), and similar size proteins were detected by both antibodies (left and right panels, arrowheads), suggesting that most of the truncated Notch1 proteins are rapidly cleaved. Proteins of slightly larger size were detected by the mN1A antibody in GSI-treated IN1C^{+} cells, indicating that these proteins contain the γ-secretase cleavage site. Together, our analyses at the RNA and protein levels indicate that IN1C^{+} tumors express novel transcripts that encode proteins constitutively activated by γ-secretase cleavage.

Loss of the Notch1 promoter induces transcription initiation in the 3′ region of the Notch1 locus and chromatin remodeling

Our results suggest that transcription of the *Notch1* gene is reorganized in Ikaros-deficient cells after deletion of the 5′ promoter. To map these changes, we evaluated the distribution of acetylated histone H3 (H3ac), a chromatin mark associated with active promoters, in the *Notch1* locus of IN1C^{+} versus IN1C^{−} tumor cells, by chromatin immunoprecipitation-sequence analysis (Figure 6A top 2 histograms). In IN1C^{−} cells, where the main promoter is intact, we detected a broad approximately 15-kb region of H3 acetylation in the 5′ end of the *Notch1* gene. In IN1C^{+} cells, this region of H3 acetylation was still present, indicating that the deleted floxed sequences are not required to target active epigenetic marks to the proximal *Notch1* region. Strikingly, IN1C^{+} cells showed a novel domain of high H3 acetylation over a 10-kb region in the 3′ portion of the gene between exons 25-34. These results indicate a major reorganization of the epigenetic landscape in the *Notch1* gene of IN1C^{+} tumor cells after deletion of the 5′ promoter, where de novo marks of transcriptional activation accumulate in the 3′ part of the gene.

We then asked whether H3 acetylation was specific to tumor cells, and whether Ikaros deficiency was required for the transcriptional reorganization. To address these questions, we analyzed the H3ac distribution in the *Notch1* locus between WT and Ikaros-expressing Ik^{+/+}Notch1[f/f]CD4-Cre[+] (N1C[+]) thymocytes (Figure 6A bottom 2 histograms). N1C^{+} cells showed low but distinct enrichment of H3ac between exons 25-34 compared with WT (Figure 6A, see arrowheads and inset). Using the "statistical model for identification of chip-enriched regions" algorithm,[27] which predicts islands of enriched tag frequency, we identified 2 islands of H3ac enrichment in the 3′ region of the *Notch1* gene in N1C[+] thymocytes that were not present in WT cells (labeled I1 and I2 in Figure 6A; see Table 1 for relevant parameters). Although H3 acetylation in these regions was reduced compared with IN1C^{+} leukemic cells, the enrichment over WT or input was significant ($P < 10^{-10}$; Table 1) and was confirmed by real-time PCR for island I1 (Figure 6B; enrichment was not confirmed for I2, which probably reflects the smaller increase of H3 acetylation at this island). Thus, deletion of the 5′ promoter appears to initiate chromatin reorganization in the Notch1 locus and promote the acquisition of activation marks in the 3′ region of the gene. Importantly, this occurs in the presence of WT levels of Ikaros and in the absence of transformation.

Chromatin reorganization in the 3′ region of the *Notch1* gene in N1C[+] thymocytes was accompanied by low levels of transcription from that region. Transcripts of 4.5 and 6 kb, similar to the major transcripts in IN1C^{+} tumor cells, were detected by Northern blot in N1C^{+} cells (Figure 6C). In addition, exon 27b–containing transcripts were detected by RT-PCR in N1C[+] and nontransformed
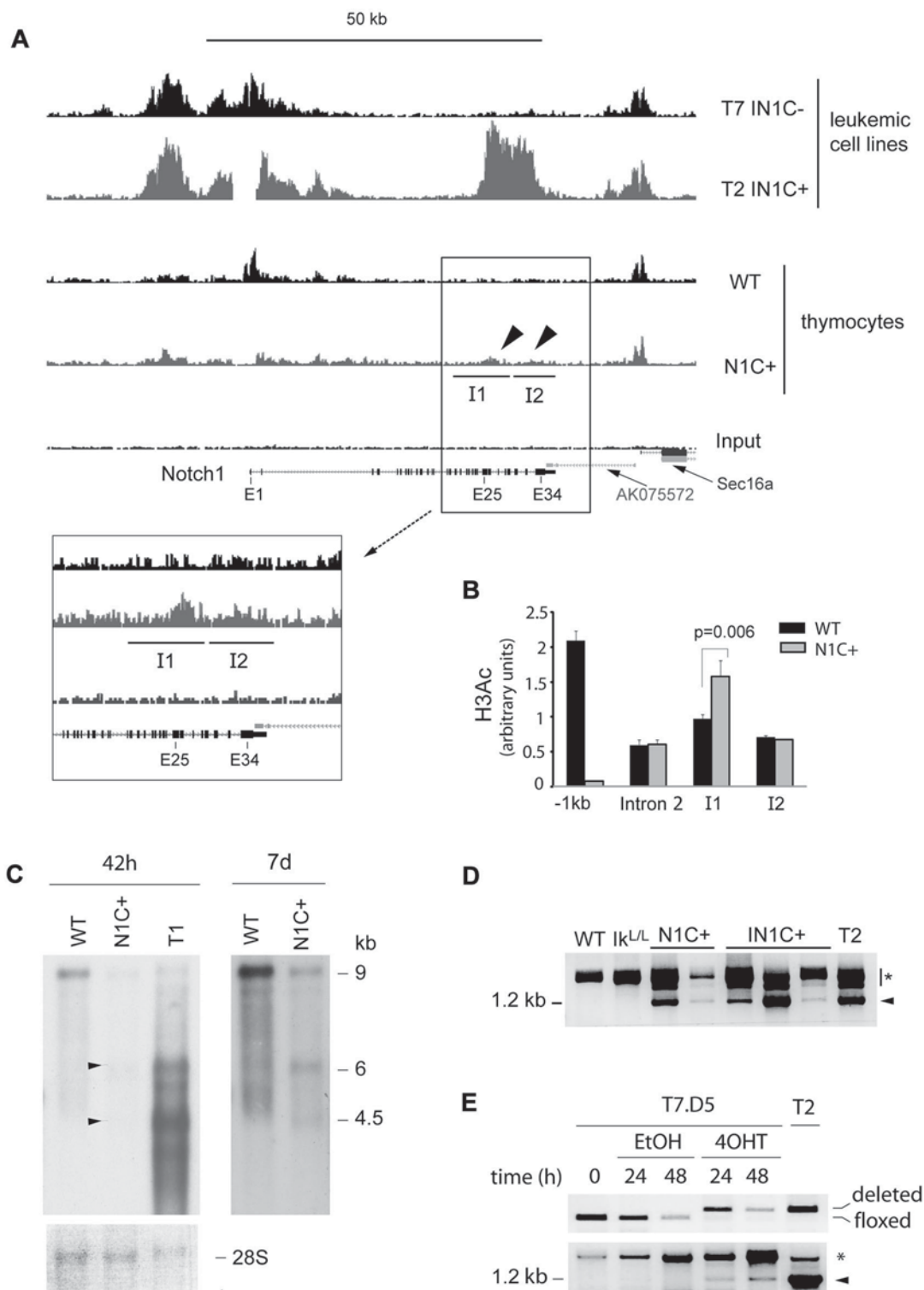
Figure 6. Transcriptional reprogramming of the Notch1 locus after deletion of proximal promoter sequences. (A) Chromatin immunoprecipitation-sequence analysis of histone H3 acetylation in the *Notch1* locus of T7 IN1C⁻ and the T2 IN1C⁺ cells and WT and Notch1^{f/f}CD4-Cre⁺ (N1C⁺) thymocytes. Top 4 histograms have a vertical scale of 150. The enlarged histograms in the inset have a vertical scale of 50. The regions identified as I1 and I2 correspond to islands of enriched tag density in the IN1C⁺ thymocytes, which were predicted by the "statistical model for identification of chip-enriched regions" algorithm in the N1C⁺, but not in the WT or input samples (see also Table 1).[27] The gap in the T2 IN1C⁺ sample corresponds to the location of the floxed deletion. (B) Real-time PCR measurement of H3 acetylation in the WT and N1C⁺ samples shown in panel A at several positions along the Notch1 locus. Amplicons in intron 2 and islands I1 and I2 were located, respectively, at 29.3, 36.5, and 41.7 kb downstream of the transcription start site. (C) Northern blot of Notch1 transcripts in WT and N1C⁺ thymocytes and in the T1 IN1C⁺ cell line. An amount of 2 μg of poly(A)⁺ RNA was loaded for each sample, and the blots were hybridized with the E30/31 probe (see Figure 6D). The left panel shows a 42-hour exposure; the right panel shows a 7-day exposure of the WT and N1C⁺ lanes. Arrowheads indicate transcripts likely to have initiated from 3′ promoters in the N1C⁺ sample. A photo of the methylene blue staining of the membrane is shown as a loading control in the bottom panel. (D) RT-PCR of exon 27b–containing transcripts in nontransformed thymocytes from 3- to 4-week-old mice with the indicated genotypes. See Figure 5E for details. Samples were defined as nontransformed according to their CD4/CD8 profile and normal CD25 expression. (E) RT-PCR of exon 27b–containing transcripts in the T7.D5 Cre-ERT2⁺ clone cultured in the presence of 4OHT or vehicle for the indicated times (bottom). Cells were also analyzed for the deletion of floxed Notch1 sequences by PCR (top). T2 corresponds to a IN1C⁺ leukemic cell line. Similar results were obtained in 4 independent experiments. In panels D and E, the arrowhead indicates the specific product from a correctly spliced transcript; the asterisk indicates products that may correspond to splicing intermediates of transcripts initiated at upstream locations.

Table 1. Detection of enriched histone H3 acetylation islands in the 3′ region of the *Notch1* gene in N1C⁺ thymocytes

	Island 1 (I1)	Island 2 (I2)
Coordinates (chromosome 2)	26320200-26328599	26313600-26319199
Island score (range, 30-15 000)	245	138
Input tag number	66	46
WT tag number	80	83
N1C⁺ tag number	231	145
P (vs input)	9.8×10^{-57}	3.7×10^{-31}
P (vs wild-type)	9.9×10^{-43}	1.6×10^{-11}

Chromatin immunoprecipitation sequence data were analyzed with the "statistical model for identification of chip-enriched regions" algorithm to detect islands of enriched H3ac. Two islands (I1 and I2, see Figure 6A for positions) were predicted in the *Notch1* gene in N1C⁺ cells but not in wild-type thymocytes or input. Tag numbers were calculated by multiplying the raw data with a correction factor that corresponds to the total sequence tags in the N1C⁺ sample divided by the combined total sequenced tags in all samples (9.3×10^6, 14.8×10^6, and 12.8×10^6 for input, wild-type, and N1C⁺, respectively). The coordinates were obtained from the Mm9 build of the mouse genome.

IN1C⁺ cells but not in WT or Ik^{L/L} thymocytes (Figure 6D). As N1C⁺ animals do not develop T-ALL, these results suggest that transcription from 3′ cryptic promoters is initiated in nontransformed T cells. Transcription from 3′ promoters appears to be T-cell specific, as analysis of Notch1-expressing tissues from N1^{+/Δf} mice (with a heterozygous germline deletion of the floxed sequences) revealed exon 27b–containing transcripts only in the thymus (supplemental Figure 6).

To determine whether deletion of the 5′ promoter could directly induce transcription initiation from 3′ sites, we established an inducible system to delete the floxed Notch1 sequences in vitro. The IN1C⁻ cell line, T7, in which the Notch1 promoter/exon 1 sequences are floxed but not deleted, was transduced with a retroviral vector encoding green fluorescent protein and Cre-ERT2, a tamoxifen-inducible fusion protein between the Cre recombinase and the ligand binding domain of the estrogen receptor. Green fluorescent protein–positive cells were cloned and expanded. The T7.D5 clone, which did not show detectable levels of deletion before tamoxifen (4-hydroxytamoxifen [4OHT]) treatment but showed efficient deletion after 24 hours in 4OHT-supplemented medium (> 90% deletion; Figure 6E), was chosen for further study. T7.D5 cells were cultured in the presence of 4OHT, or vehicle, for 24 or 48 hours. We analyzed exon 27b–containing transcripts by RT-PCR, the ratio of 5′ to 3′ Notch1 transcripts by RT-quantitative PCR, and H3 acetylation by chromatin immunoprecipitation. Although the 5′ to 3′ transcript ratio and the H3 acetylation levels did not vary significantly in 4OHT-treated cells (not shown), exon 27b–containing transcripts were detected as early as 24 hours after

4OHT treatment. Thus, deletion of the 5′ promoter directly reprograms the *Notch1* locus to begin transcription from 3′ promoters.

Spontaneous deletions of 5′ genomic sequences in Ikaros-deficient primary tumors

Intriguingly, our analysis of primary Ik^{L/L} or IN1C⁻ tumors revealed low levels of approximately 4-kb transcripts (Figure 5A). To determine whether transcription from 3′ sites was common in Ikaros-deficient T-ALL, we analyzed 8 primary Ik^{L/L} or IN1C⁻ tumors using the exon 27b–specific RT-PCR assay. Strikingly, exon 27b–containing transcripts were detected in 7 of the tumors (Figure 7). As RAG-mediated deletion of the sequences between the 2 cryptic recombination signal sequences at −8191 and +3575 bp of the transcription initiation site is always associated with transcription from 3′ sites (see companion paper by Ashworth et al[25]), we tested if similar deletions occurred in the endogenous *Notch1* locus of Ik^{L/L} tumors by PCR (P1 and P2 in Figure 7). An approximately 500-bp fragment was amplified from 6 of 7 tumors that expressed the exon 27b–containing transcripts but not from premalignant Ik^{L/L} thymocytes, the T135 primary T-ALL, or the T29 and T7 cell lines (Figure 7). These results indicate that 5′ deletions and 3′ Notch1 transcripts occur spontaneously in approximately 75% of Ikaros-deficient T-ALL.

Discussion

Ikaros-deficient Ik^{L/L} mice represent an important model to study the natural evolution of Notch-dependent T-ALL, as they develop a disease highly reminiscent of the human condition. Although induced Notch-dependent models have been described, based on the overexpression of activated Notch1 or Notch3, their capacity to recapitulate the progressive activation of this pathway is limited. Few spontaneous models have been reported or studied extensively. In this study, we demonstrate by a genetic approach that activation of the Notch pathway is key to tumor initiation in Ik^{L/L} mice. Our results show that Notch activation is dependent on RBP-J, thereby implicating the transcription of Notch target genes in the leukemic process.

Our results also reveal that novel Notch1 transcripts are transcribed upon deletion of the 5′ main promoter to generate truncated proteins lacking the extracellular domain. Importantly, the truncated Notch proteins are predicted to lack the negative regulatory region but retain the S3 γ-secretase cleavage site, suggesting that they are membrane bound and γ-secretase sensitive. Indeed, IN1C⁺ tumor cells require γ-secretase activity for
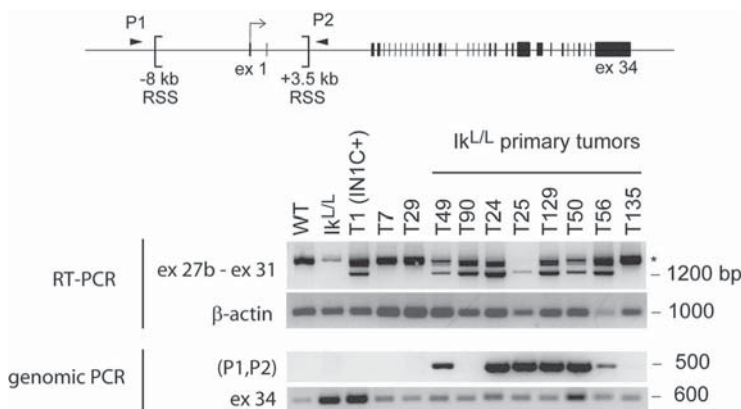
Figure 7. Presence of 3′ Notch1 transcripts and 5′ genomic deletions in primary Ik^{L/L} tumors. The indicated RNA or DNA samples were analyzed for the presence of exon 27b–containing transcripts by RT-PCR (top) and genomic deletion of sequences between 2 recombination signal sequences (RSS) present in the 5′ region of the *Notch1* locus by PCR (bottom). RAG-mediated deletion of the sequences between the RSS sites moves the sequences of the PCR primers P1 and P2 closer together, allowing amplification of a 500-bp fragment. The Ik^{L/L} sample was extracted from premalignant thymocytes of a 7-week-old mouse; T7 and T29 are cell lines derived from IN1C⁻ and Ik^{L/L} tumors, respectively; T49 and T90 are the primary tumors from Figure 5A. β-Actin and exon 34 of Notch1 served as control RT-PCR and PCR reactions, respectively. *Products that may correspond to splicing intermediates of transcripts initiated upstream.

proliferation. The oncogenic effect of the promoter deletion is therefore similar to that of mutations targeting the negative regulatory region (which decreases ligand dependency) or chromosomal translocations where the breakpoint occurs in intron 24.[7] All lead to the synthesis of constitutively active, γ-secretase–sensitive Notch1 proteins.

Surprisingly, Notch3 is not required for tumorigenesis in Ik[L/L] mice. The role of this receptor in T-ALL is controversial, and it is currently unclear how Notch3 contributes in leukemogenesis. Our results suggest that Notch3 is dispensable for the initiation and progression of Ik[L/L] tumors. Notch3 is expressed in all cases of human T-ALL and has been shown to modulate the splicing of Ikaros transcripts to favor those encoding dominant-negative Ikaros isoforms.[9,28] However, we were unable to detect dominant-negative Ikaros isoforms in a group of human T-ALL samples, suggesting that Notch3 may be not sufficiently active in these leukemias to influence Ikaros splicing.[29]

We demonstrate that deletion of the main Notch1 promoter is an oncogenic event that accelerates T-ALL. Our data also indicate that 5′ deletions of the Notch1 promoter occur spontaneously and are common in Ik[L/L] leukemias as well as in other murine T-ALL models (companion paper by Ashworth et al,[25] Tsuji et al[26]). Promoter deletion reprograms the epigenetic landscape around the Notch1 locus and leads to the accumulation of active chromatin marks in the 3′ part of the gene. Importantly, this occurs in nontransformed thymocytes. Thus, transcriptional reprogramming predates leukemia initiation. Although deletion of the Notch1 promoter strongly promotes tumorigenesis, it is not sufficient for tumor initiation, as N1C[+] mice or animals carrying one deleted allele in the germline do not develop T-ALL. Other events, such as PEST mutations, are likely to synergize with the promoter deletion to increase Notch1 activation. It is also likely that Ikaros deficiency facilitates Notch1 transcription, as Ikaros silences Notch target gene transcription at the molecular level.[17,30,31] Thus, strong activation of Notch1 appears to require multiple hits.

How 3′ cryptic promoters are activated remains to be elucidated. In yeast, aberrant transcription from cryptic initiation sites within the coding region has been linked to defects in reforming the nucleosome structure during transcription elongation. Moreover, histone deacetylation during transcription appears to be important for correct nucleosome positioning and prevention of cryptic initiation.[32-37] Our results show that aberrant transcription from the Notch1 coding region is accompanied by a significant increase in H3 acetylation along the 3′ part of the gene, suggesting a loss of deacetylation dynamics in the absence of the 5′ promoter. Interestingly, Ikaros binds to a region of exon 25 in the *Notch1* gene of WT thymocytes (supplemental Figure 8). Ikaros has been shown to associate with Sin3 and the NuRD histone deacetylase complex and specifically with histone deacetylase complex 1 and 2.[38,39] Thus, Ikaros may function to recruit deacetylase complexes to the Notch1 coding region during transcription to prevent intragenic initiation.

Why does deletion of the Notch1 promoter stimulate 3′ transcription if initiation from cryptic sites is linked to ongoing transcription? Transcription may still occur from the alternative 5′ promoters 1a or 1b, both of which are active in IN1C^{+} tumor cells (supplemental Figure 3). Deletion of the main promoter may also change the topology of the Notch1 locus and facilitate the nucleation of new transcription initiation complexes at the 3′ sites. It will be important to determine whether the complexes normally involved in Notch1 transcription are required for 3′ promoter activation. Indeed, the −5-kb and +1.4-kb ICN1 binding sites are not deleted

in IN1C^{+} cells.[40] Thus, stimulation by RBP-J/ICN1 complexes at these sites could establish a forward feeding mechanism that leads to high levels of 3′ transcription in IN1C^{+} cells. The deletion of the 5′ ICN1 binding sites in some Ik[L/L] primary tumors might explain why 3′ transcription is lower in these tumors (Figure 5A). Other events, as yet undefined, may also contribute. Indeed, chromatin acetylation and 3′ transcriptional activity are higher in IN1C^{+} leukemic cells than in premalignant IN1C^{+} thymocytes or in nontransformed N1C^{+} cells. Further, 4OHT-induced deletion of the 5′ Notch1 promoter triggers the expression of exon 27b–containing transcripts but not robust chromatin reorganization. Identification of the mechanism behind the strong activation of the 3′ Notch1 promoter will be important for understanding T-ALL progression.

In conclusion, the Notch pathway appears to be subject to multiple checkpoints in developing T cells. In the WT situation, Notch is activated after ligand interaction, cleaved Notch proteins are rapidly degraded by the proteasome, and transcriptional repressors such as Ikaros can silence Notch target gene transcription, even in the presence of Notch signals (Kleinmann et al[30] and our unpublished data). In the scenario described here, the Notch pathway is subject to multiple hits. First, when Ikaros function is diminished, Notch target genes are less efficiently silenced. In addition, when the 5′ promoter is deleted, truncated proteins are generated that do not require ligand interaction for cleavage, resulting in constitutive Notch activation. Finally, somatic mutations in the PEST domain prevent the rapid degradation of these oncogenic proteins in the cytoplasm. The end result is that the Notch pathway becomes the driver of the transformation process during T-ALL.

Authorship

Contribution: R.J., J.M., A.M.-G., A.O., S.C., and P.K. designed and performed experiments, analyzed data, and wrote the paper;

B.J. and S.L.G. performed high-throughput sequencing; A.-S.G.L.L., J.G., T.A., and J.C.A. shared data and protocols; T.H., T.G., and F.R. provided key reagents; and J.C.A. contributed to scientific discussions.

References

1. Pui CH, Robison LL, Look AT. Acute lymphoblastic leukaemia. *Lancet.* 2008;371(9617):1030-1043.

2. Aifantis I, Raetz E, Buonamici S. Molecular pathogenesis of T-cell leukaemia and lymphoma. *Nat Rev Immunol.* 2008;8(5):380-390.

3. Deftos ML, Huang E, Ojala EW, Forbush KA, Bevan MJ. Notch1 signaling promotes the maturation of CD4 and CD8 SP thymocytes. *Immunity.* 2000;13(1):73-84.

4. Huang YH, Li D, Winoto A, Robey EA. Distinct transcriptional programs in thymocytes responding to T cell receptor, Notch, and positive selection signals. *Proc Natl Acad Sci U S A.* 2004;101(14):4936-4941.

5. Jarriault S, Brou C, Logeat F, Schroeter EH, Kopan R, Israel A. Signalling downstream of activated mammalian Notch. *Nature.* 1995;377(6547):355-358.

6. Reizis B, Leder P. Direct induction of T lymphocyte-specific gene expression by the mammalian Notch signaling pathway. *Genes Dev.* 2002;16(3):295-300.

7. Ellisen LW, Bird J, West DC, et al. TAN-1, the human homolog of the Drosophila notch gene, is broken by chromosomal translocations in T lymphoblastic neoplasms. *Cell.* 1991;66(4):649-661.

8. Weng AP, Ferrando AA, Lee W, et al. Activating mutations of NOTCH1 in human T cell acute lymphoblastic leukemia. *Science.* 2004;306(5694):269-271.

9. Bellavia D, Campese AF, Checquolo S, et al. Combined expression of pTalpha and Notch3 in T cell leukemia identifies the requirement of preTCR for leukemogenesis. *Proc Natl Acad Sci U S A.* 2002;99(6):3788-3793.

10. Soulier J, Clappier E, Cayuela JM, et al. HOXA genes are included in genetic and biologic networks defining human acute T-cell leukemia (T-ALL). *Blood.* 2005;106(1):274-286.

11. Pear WS, Aster JC, Scott ML, et al. Exclusive development of T cell neoplasms in mice transplanted with bone marrow expressing activated Notch alleles. *J Exp Med.* 1996;183(5):2283-2291.

12. Capobianco AJ, Zagouras P, Blaumueller CM, Artavanis-Tsakonas S, Bishop JM. Neoplastic transformation by truncated alleles of human NOTCH1/TAN1 and NOTCH2. *Mol Cell Biol.* 1997;17(11):6265-6273.

13. Hoemann CD, Beaulieu N, Girard L, Rebai N, Jolicoeur P. Two distinct Notch1 mutant alleles are involved in the induction of T-cell leukemia in c-myc transgenic mice. *Mol Cell Biol.* 2000;20(11):3831-3842.

14. Bellavia D, Campese AF, Alesse E, et al. Constitutive activation of NF-kappaB and T-cell leukemia/lymphoma in Notch3 transgenic mice. *EMBO J.* 2000;19(13):3337-3348.

15. Chiang MY, Xu L, Shestova O, et al. Leukemia-associated NOTCH1 alleles are weak tumor initiators but accelerate K-ras-initiated leukemia. *J Clin Invest.* 2008;118(9):3181-3194.

16. Zweidler-McKay PA, Pear WS. Notch and T cell malignancy. *Semin Cancer Biol.* 2004;14(5):329-340.

17. Dumortier A, Jeannet R, Kirstetter P, et al. Notch activation is an early and critical event during T-cell leukemogenesis in Ikaros-deficient mice. *Mol Cell Biol.* 2006;26(1):209-220.

18. Han H, Tanigaki K, Yamamoto N, et al. Inducible gene knockout of transcription factor recombination signal binding protein-J reveals its essential role in T versus B lineage decision. *Int Immunol.* 2002;14(6):637-645.

19. Krebs LT, Xue Y, Norton CR, et al. Characterization of Notch3-deficient mice: normal embryonic development and absence of genetic interactions with a Notch1 mutation. *Genesis.* 2003;37(3):139-143.

20. Radtke F, Wilson A, Stark G, et al. Deficient T cell fate specification in mice with an induced inactivation of Notch1. *Immunity.* 1999;10(5):547-558.

21. Wolfer A, Bakker T, Wilson A, et al. Inactivation of Notch 1 in immature thymocytes does not perturb CD4 or CD8T cell development. *Nat Immunol.* 2001;2(3):235-241.

22. Wolfer A, Wilson A, Nemir M, MacDonald HR, Radtke F. Inactivation of Notch1 impairs VDJbeta rearrangement and allows pre-TCR-independent survival of early alpha beta Lineage Thymocytes. *Immunity.* 2002;16(6):869-879.

23. Tanigaki K, Tsuji M, Yamamoto N, et al. Regulation of alphabeta/gammadelta T cell lineage commitment and peripheral T cell responses by Notch/RBP-J signaling. *Immunity.* 2004;20(5):611-622.

24. Carron C, Cormier F, Janin A, et al. TEL-JAK2 transgenic mice develop T-cell leukemia. *Blood.* 2000;95(12):3891-3899.

25. Ashworth TD, Pear WS, Chiang MY, et al. Deletion-based mechanisms of Notch1 activation in T-ALL: key roles for RAG recombinase and a conserved internal translational start site in Notch1. *Blood.* 2010;116(25):5455-5464.

26. Tsuji H, Ishii-Ohba H, Ukai H, Katsube T, Ogiu T. Radiation-induced deletions in the 5′ end region of Notch1 lead to the formation of truncated proteins and are involved in the development of mouse thymic lymphomas. *Carcinogenesis.* 2003;24(7):1257-1268.

27. Zang C, Schones DE, Zeng C, Cui K, Zhao K, Peng W. A clustering approach for identification of enriched domains from histone modification ChIP-Seq data. *Bioinformatics.* 2009;25(15):1952-1958.

28. Bellavia D, Mecarozzi M, Campese AF, et al. Notch3 and the Notch3-upregulated RNA-binding protein HuD regulate Ikaros alternative splicing. *EMBO J.* 2007;26(6):1670-1680.

29. Marçais A, Jeannet R, Hernandez L, et al. Genetic inactivation of Ikaros is a rare event in human T-ALL. *Leuk Res.* 2010;34(4):426-429.

30. Kleinmann E, Geimer Le Lay AS, Sellars M, Kastner P, Chan S. Ikaros represses the transcriptional response to Notch signaling in T-cell development. *Mol Cell Biol.* 2008;28(24):7465-7475.

31. Kathrein KL, Chari S, Winandy S. Ikaros directly represses the notch target gene Hes1 in a leukemia T cell line: implications for CD4 regulation. *J Biol Chem.* 2008;283(16):10476-10484.

32. Kaplan CD, Laprade L, Winston F. Transcription elongation factors repress transcription initiation from cryptic sites. *Science.* 2003;301(5636):1096-1099.

33. Reid JL, Moqtaderi Z, Struhl K. Eaf3 regulates the global pattern of histone acetylation in Saccharomyces cerevisiae. *Mol Cell Biol.* 2004;24(2):757-764.

34. Govind CK, Zhang F, Qiu H, Hofmeyer K, Hinnebusch AG. Gcn5 promotes acetylation, eviction, and methylation of nucleosomes in transcribed coding regions. *Mol Cell.* 2007;25(1):31-42.

35. Carrozza MJ, Li B, Florens L, et al. Histone H3 methylation by Set2 directs deacetylation of coding regions by Rpd3S to suppress spurious intragenic transcription. *Cell.* 2005;123(4):581-592.

36. Keogh MC, Kurdistani SK, Morris SA, et al. Cotranscriptional set2 methylation of histone H3 lysine 36 recruits a repressive Rpd3 complex. *Cell.* 2005;123(4):593-605.

37. Joshi AA, Struhl K. Eaf3 chromodomain interaction with methylated H3-K36 links histone deacetylation to Pol II elongation. *Mol Cell.* 2005;20(6):971-978.

38. Kim J, Sif S, Jones B, et al. Ikaros DNA-binding proteins direct formation of chromatin remodeling complexes in lymphocytes. *Immunity.* 1999;10(3):345-355.

39. Sridharan R, Smale ST. Predominant interaction of both Ikaros and Helios with the NuRD complex in immature thymocytes. *J Biol Chem.* 2007;282(41):30227-30238.

40. Yashiro-Ohtani Y, He Y, Ohtani T, et al. Pre-TCR signaling inactivates Notch1 transcription by antagonizing E2A. *Genes Dev.* 2009;23(14):1665-1676.

Mice

The lines used in this study were described previously: $Ik^{L/L}$ (1); $Notch3^{-/-}$ (2); $Notch1^{f/f}$ (3); $RBP-J^{f/f}$ (4); $CD4-Cre^+$ (5). To generate the $Notch1^{\Delta f}$ allele, $Notch1^{f/f}$ mice were bred with a $CMV-Cre^+$ deleter strain, and the resulting germline $Notch1^{\Delta f}$ allele was subsequently segregated from the CMV-Cre tg. $Ik^{L/L}Notch1^{+/\Delta f}$ mice were obtained by mating with $Ik^{+/L}$ mice which were on a C57Bl/6 background (>10th generation backcross; see Fig. 4C).

Cell lines and culture

Cell lines derived from primary tumors were grown in RPMI 1640, 10% FCS, 1 mM sodium pyruvate, 2 mM L-glutamine and 1% antibiotics. Cells were frozen at an early passage (usually after 2 or 3 weeks of amplification), and were thawed and used for a 1-month period. The γ-secretase inhibitor XVIII (Compound E; Calbiochem) was used at a final concentration of 5 μM; 4OHT (Sigma-Aldrich) was used at a final concentration of 100 nM. For these experiments, the cells were plated at 1×10^6/ml and the medium was changed every day. To generate Cre-ERT2-expressing T7 cells, we first cloned the Cre-ERT2 cDNA (provided by D.

Metzger (6)) into the MigR1 retroviral vector (provided by W. Pear) and produced high titer retroviral supernatant after transfecion in the Eco-Phoenix packaging cell line (provided by G. Nolan). T7 cells were transduced according to standard protocols. After 24 h, the GFP+ cells were cloned and expanded.

Antibodies and flow cytometry

The following reagents were used: anti-CD8α conjugated to FITC, PerCP, Cy5.5 or biotin (BD Biosciences); anti-CD4 conjugated to FITC, PE or APC (BD Biosciences or Caltag), anti-CD25-PE or -APC (BD Biosciences), anti-CD3-FITC or -Cy5 (clone KT3; conjugated in-house), Streptavidin-PerCP (BD Biosciences) or -PE (Jackson ImmunoResearch), surface anti-Notch1 (provided by A. Gurney, OncoMed Pharmaceuticals Inc.), anti-human IgG biotin (Jackson ImmunoResearch), mouse IgG1 isotype control PE (eBioscience) and purified CD16/CD32 (Fc block; eBioscience). To detect surface Notch1, the cells were first incubated with anti-Notch1, then with anti-human IgG biotin, and finally with Streptavidin-PE. Cells were analyzed on a FACSCalibur (BD BioSciences) or sorted on a FACSVantage SE option DiVa (BD Biosciences). Sort purity was >98%. Results were analyzed using the FlowJo software (TreeStar).

Western blot

Total extracts from 1×10^6 cells were separated on a 6% SDS-PAGE gel, transferred to nitrocellulose, and blotted overnight with antibodies specific for γ-secretase-cleaved Notch1 (Val1744; Cell Signaling), total Notch1 (mN1A; eBioscience), RPB-J (T6719; Institute of Immunology, Japan) and α-tubulin (in-house preparation). All secondary antibodies were horse-radish conjugated (Santa Cruz, Jackson ImmunoResearch). The blots were revealed with the Enhanced Chemiluminescence SuperSignal Substrate (Pierce) and exposed to film.

Total and poly(A)$^+$ RNA isolation

Total RNA was isolated using the RNeasy Midi Kit (Qiagen) according the manufacturer's instructions (including on-column DNase digestion). Poly(A)$^+$ mRNA was subsequently selected using Dynabeads oligo(dT)$_{25}$ (Invitrogen).

RT-PCR, PCR and qPCR

Reverse transcription was performed on 500 ng of total RNA using oligo(dT)$_{18}$ and Superscript II (Invitrogen) in a total volume of 20 μl. To amplify the fragment used for the

combined detection of the exon 26 SNP and PEST domain sequences, PFU DNA polymerase (in-house) was used with the following primers: 5'-AACAGTGCCGAATGTGAGTG and 5'-TTAAAAGGCTCCTTTGGTCG. PCR conditions were: 94°C for 5 min, followed by 35 cycles of 94°C for 30 s, 60°C for 30 s and 68°C for 6 min, with a final step at 68°C for 7 min. PCR products were cloned with the Zero Blunt PCR Cloning Kit (Invitrogen). For detection of exon 27b-, exon 1a- or exon 1b-containing transcripts, Taq DNA polymerase (Roche) was used with the following conditions: 94°C for 5 min, followed by 35-40 cycles of 94°C for 30 s, 60°C for 30 s and 72°C for 45 s, with a final step of 72°C for 5 min. The primers for exon 27b were: 5'-CTCTTCAGGGATGGGTTCAT (exon 27b; Figs. 6E and 7C), 5'-TGTGGCTAGTGGGAGCCGTG (exon 27b, with a 3 nt overhang at the 3' end which corresponds to the first 3 nt of exon 28; Fig. 7D) and 5'-TGTTCTGCATGTCCTTGTTG (exon 31). Primers used to amplify sequences between exon 32 and exon 34 were: 5'-GATGGCACAACTCCACTGAT (forward, exon 32) and 5'-TTAAAAGGCTCCTTTGGTCG (reverse, exon 34). The primers for exon 1a and 1b were: 5'-CTCAGTCCTGGCCTCTTCC (forward, exon 1a), 5'-CAAATACACTGACCAACAAATGG (forward, exon 1b) and 5'-TCACAGTTCTGTCCAGCAAA (reverse, exon 5). Analysis of TCRb rearrangement was performed with the following primers: 5'-GTAGGCACCTGTGGGGAAGAAACT (Dβ2.1) and 5'-TGAGAGCTGTCTCCTACTATCGATT (Jβ2.7). The PCR conditions were: 94°C for 5 min, followed by 35 cycles of 94°C for 1 min, 63°C for 2 min and 72°C for 2 min, with a final step of 72°C for 10 min. The primers to analyze the deletion of the Notch1 floxed alleles were: 5'-CTGACTTAGTAGGGGGAAAAC, 5'-AGTGGTCCAGGGTGTGAGTGT and 5'-TAAAAAGCGACAGCTGCGGAG. The PCR conditions were: 5 min at 94°C, followed by 40 cycles of 94°C for 15 s, 60°C for 30 s and 72°C for 30 s, with a final step of 72°C for 5 min. The primers to analyze the deletion of the RBP-J floxed alleles were: 5'-CTTGATAATTCTGTAAAGAGA (forward); 5'-ACATTGCATTTTCACATAAAAAAGC (reverse); 5'-CCACAGCAGGCAACAATTGAG (reverse). The PCR conditions were: 5 min at 94°C, followed by 33 cycles of 94°C for 30 s, 55°C for 30 s and 72°C for 45 s. Primers used to analyze the occurrence of spontaneous 5' genomic deletions in $Ik^{L/L}$ tumors were: 5'-ATGGTGGAATGCCTACTTGTA (forward, nucleotide -8388 to -8366 from exon 1) and 5'-CGTTTGGGTAGAAGAGATGCTTTAC (reverse, nucleotide 3929 to 3942). PCR conditions were 94°C for 5 min, followed by 35 cycles of 94°C for 30 s, 58°C for 30 s and 72°C for 45 s.

Real-time qPCR was performed in duplicate with the SYBR Green JumpStart Taq ReadyMix (Sigma-Aldrich) and the LightCycler 480 Real-time PCR System (Roche). PCRs were analyzed with the LightCycler 480 basic software and the concentration of amplified cDNA was calculated relative to a standard curve obtained with serial dilutions of a control cDNA from WT thymocytes. PCR conditions were 95°C for 10 s, 60°C for 30 s and 72°C for 15 s. The primers were: 5'-TGTGCAGCGTGTTAATGACT (exon 23) and 5'-CAGGGCACCTACAGATGAAT (exon 24); 5'-GGATGTCAATGTTCGAGGAC (exon 30) and 5'-CAGCAGGTGCATCTTCTTCT (exon 31); 5'-GTTGGATACAGGCCAGACTTTGTTG and 5'-GATTCAACTTGCGCTCATCTTAGGC for hypoxanthine phosphoribosyltransferase (HPRT). PCR analysis of H3Ac was carried out with the following primers: Notch1 -1kb: 5'-AGCATGAGAGGCTGTGTTGA and 5'-AGGGAACTCCCCAAGGACTA; Notch1 intron 2: 5'-CCTCTAAATGCCCATAACCC and 5'-GTAAGAGTGTATGCAGAAGGAG; Notch1 island I1: 5'-ACCAGCTACGGAACAACTC and 5'-GTACCAGGAAGCAGTGAAG; Notch1 island I2: 5'-GAGGTTTAAGAGTGTCTGGG and 5'-AGGCTCAAGTAACCGTGAC. Data were normalized to H3Ac levels at the CD8α gene (+1kb relative to the TSS) within the same samples, as H3 acetylation was similar between the WT and N1C+ samples in the ChIP-seq data. CD8α sequences were amplified with the primers 5'-CTTCTTGGGTAAAGGCTAAGTGG and 5'-CGACAATCTTCTGGTCTCTGG.

Northern blot

Total RNA (10 μg) or poly(A)$^+$ RNA (1.5-2 μg) were separated on 1% agarose/formaldehyde gels. After electrophoresis, alkaline-treated (0.05 M NaOH, 15 min) gels were blotted with Hybond-N membrane (Amersham Biosciences). For total RNA, the membrane was then stained with a sodium acetate 0.5M methylene blue solution after a 15 min pre-treatment with 5% acetic acid. Hybridizations were performed using standard conditions (7). The exon 34 probe was purified from a plasmid containing sequences of this exon, while other probes were amplified by PCR from a plasmid containing the full-length Notch1 cDNA, or from genomic DNA (for exon 27b). 50 ng of probe were radiolabeled with ^{32}P α-dCTP by random priming and purified.

Rapid amplification of cDNA ends (5'-RACE)

250 ng of poly(A)$^+$ RNA from the T1 and T34 cell lines were used. 5'-RACE was performed with the FirstChoice RLM-RACE Kit (Ambion). The exon 31-derived nested 3' primers were

5'-TGTTCTGCATGTCCTTGTTG for the first step and 5'-CAGCAGGTGCATCTTCTTCT for the second step. The PCRs were performed using PFU DNA polymerase: 94°C for 5 min, followed by 35 cycles of 94°C for 30 s, 60°C for 30 s, 68°C for 4 min, with a final step of 68°C for 7 min. The PCR products were cloned with the Zero Blunt PCR Cloning Kit.

Microarray analysis

RNA from IN1C+ and IN1C- tumors were extracted with the RNeasy kit (Qiagen), and used for transcriptome analysis with Affymetrix 430 2.0 arrays, according to standard procedures.

ChIP-sequencing

For the H3ac ChIP-seq, 45×10^6 T2 or T7 cells, or 12×10^6 N1C+ or N1C- (labeled as WT in Fig. 7A) total thymocytes, were used. For the Ikaros ChIP-seq, 160×10^6 thymocytes enriched for $CD4^+CD8^+$ cells (~95% purity) were isolated using the MACS Column Technology (Miltenyi Biotech). Briefly, total thymocytes were labeled with a biotinylated anti-CD8α antibody (Caltag), and streptavidin-coupled microbeads (Miltenyi Biotech). Labeled cells were isolated on LS columns (Miltenyi Biotech). The ChIP protocol was adapted from Millipore (http://www.millipore.com/techpublications/tech1/mcproto407), as described previously (25). Cells were cross-linked with 1% ultra-pure formaldehyde (Electron Microscopy Sciences) in PBS/0.5% BSA at 37°C for 10 min, and quenched with 125 mM Glycine. After 2 washes with ice-cold PBS containing protease inhibitor cocktail (PIC; Roche), cells were lysed on ice for 10 min in 0.5 ml 1% SDS in 50 mM Tris pH 8.1 and 10 mM EDTA containing PIC, and sonicated using a Bioruptor 200 sonicator (Diagenode) to obtain 200-500 bp fragmented genomic DNA. Chromatin samples were diluted 10x in ChIP buffer (0.01% SDS, 1.1% Triton X-100, 1.2 mM EDTA, 16.7 mM Tris-HCl pH 8.1, 167 mM NaCl) and pre-cleared by rotating for 1 h at 4°C with 100 µl of a 50% protein A slurry (0.5 mg/ml BSA, 50% protein A Sepharose; Sigma). 1% of the pre-cleared samples was saved as input, the rest was incubated overnight at 4°C with anti-AcH3 (06-599; Millipore) (10 µg for T2 and T7 cells, 5 µg for total thymocytes) or 2 µg anti-Ikaros (rabbit anti-mouse produced in-house) antibodies. ChIPs were recovered with 100 µl of a 50% protein A slurry overnight, beads were washed once each with low-salt buffer (20 mM Tris-HCl pH 8.1, 150 mM NaCl, 2 mM EDTA, 1% Triton X-100, 0.1% SDS), high-salt buffer (same as low salt buffer but with 500 mM NaCl), LiCl buffer (10 mM Tris-HCl pH 8.1, 1 mM EDTA, 1% deoxycholate, 1% NP40, 0.25 M LiCl), and twice with Tris-EDTA (TE). Protein-DNA complexes were eluted in 200 µl of 1% SDS, 0.1 M NaHCO$_3$ for 30 min, and cross-linking was reversed by adding

NaCl to 0.2 M for 4-6 h at 65°C. After adding 10 µl 0.2 M EDTA, 8 µl 1 M Tris-HCl pH 6.5 and 1 µl proteinase K (10 mg/ml) for 30 min at 45°C, DNA was extracted with 200 µl ultra-pure phenol/chloroform/isoamyl alcohol (25:24:1; Invitrogen) and subsequently purified with the QIAquick PCR Purification Kit (Qiagen). Recovered DNA was subjected to high-throughput sequencing.

ChIP-seq libraries were prepared following Illumina's protocol with some modifications. The precipitated DNA was blunted, phosphorylated and ligated to single-end adapter dimers, and then amplified by PCR [30 s at 98°C; (10 s at 98°C, 30 s at 65°C, 30 s at 72°C) x 14 cycles; 5 min at 72°C]. Excess PCR primers and adapter dimers were removed using AMPure beads (Agencourt Biosciences Corporation). Size selection was performed on a 2% agarose gel and DNA fragments in the range of 250-350 bp were excised and purified using QIAquick Gel Extraction Kit (Qiagen). DNA libraries were checked for quality and quantified using the 2100 Bioanalyzer (Agilent). The libraries were loaded in the flowcell at 8 pM concentration and clusters were generated following Illumina's instructions. Libraries were sequenced on the Illumina Genome Analyzer II as single-end 36 base reads. Image analysis and base calling were performed using the Illumina Pipeline v1.6. Sequence reads were mapped to a reference genome (Mm 9). For data visualization, tag counts in non-overlapping 200 bp genomic segments were determined, and after quantile normalization, bedGraph tracks were uploaded to the USCS Genome Browser (http://genome.ucsc.edu/).

The SICER spatial clustering approach described by Zang et al (8) was used for the identification of H3 acetylation-enriched genomic regions. SICER was run with the following parameters: p-value threshold=0.08; window size=200; fragment size=300; gap size=800; E=10; FDR=0.001. Other parameters were left as default. The analysis was performed on sequence tag libraries that contained the following numbers of unique tags aligned to the Mm9 mouse genome assembly: WT=14809113, N1C+=12866720, input control=9357967.

REFERENCES

1. Kirstetter, P., M. Thomas, A. Dierich, P. Kastner, and S. Chan. 2002. Ikaros is critical for B cell differentiation and function. *Eur J Immunol* 32:720-730.
2. Krebs, L.T., Y. Xue, C.R. Norton, J.P. Sundberg, P. Beatus, U. Lendahl, A. Joutel, and T. Gridley. 2003. Characterization of Notch3-deficient mice: normal embryonic development and absence of genetic interactions with a Notch1 mutation. *Genesis* 37:139-143.

3.   Radtke, F., A. Wilson, G. Stark, M. Bauer, J. van Meerwijk, H.R. MacDonald, and M. Aguet. 1999. Deficient T cell fate specification in mice with an induced inactivation of Notch1. *Immunity* 10:547-558.

4.   Han, H., K. Tanigaki, N. Yamamoto, K. Kuroda, M. Yoshimoto, T. Nakahata, K. Ikuta, and T. Honjo. 2002. Inducible gene knockout of transcription factor recombination signal binding protein-J reveals its essential role in T versus B lineage decision. *Int Immunol* 14:637-645.

5.   Wolfer, A., T. Bakker, A. Wilson, M. Nicolas, V. Ioannidis, D.R. Littman, P.P. Lee, C.B. Wilson, W. Held, H.R. MacDonald, and F. Radtke. 2001. Inactivation of Notch 1 in immature thymocytes does not perturb CD4 or CD8T cell development. *Nat Immunol* 2:235-241.

6.   Metzger, D., J. Clifford, H. Chiba, and P. Chambon. 1995. Conditional site-specific recombination in mammalian cells using a ligand-dependent chimeric Cre recombinase. *Proc Natl Acad Sci U S A* 92:6991-6995.

7.   Tomasetto, C., C. Regnier, C. Moog-Lutz, M.G. Mattei, M.P. Chenard, R. Lidereau, P. Basset, and M.C. Rio. 1995. Identification of four novel human genes amplified and overexpressed in breast carcinoma and localized to the q11-q21.3 region of chromosome 17. *Genomics* 28:367-376.

8.   Zang, C., D.E. Schones, C. Zeng, K. Cui, K. Zhao, and W. Peng. 2009. A clustering approach for identification of enriched domains from histone modification ChIP-Seq data. *Bioinformatics* 25:1952-1958.

9.   Yashiro-Ohtani, Y., Y. He, T. Ohtani, M.E. Jones, O. Shestova, L. Xu, T.C. Fang, M.Y. Chiang, A.M. Intlekofer, S.C. Blacklow, Y. Zhuang, and W.S. Pear. 2009. Pre-TCR signaling inactivates Notch1 transcription by antagonizing E2A. *Genes Dev.* 23:1665-76.

Figure S1. Characterization of IN1C+ tumors

(**A**) CD4/CD8 profiles of IN1C+ and IN1C- tumors. (**B**) PCR of Vβ2-Jβ2 rearrangements in IN1C+ tumor cells. (**C**) Western blot analysis of IN1C+ and IN1C- tumors with the Val7144 antibody. Samples indicated by arrows were analyzed for PEST region mutations (see Fig. 3H).

Figure S2. Characterization of tumor-derived cell lines

(**A**) CD4/CD8 profiles of the indicated cell lines. (**B**) Western blot of ICN1 expression in IN1C+ and control cell lines. T99 is a IRC+ sample that expresses ICN1 proteins of WT size. (**C**) PCR analysis to determine the efficiency of Notch1 deletion in IN1C+ cell lines. The Hes1 gene was used as a control. The right panel shows a similar PCR on indicated mixes of T2 (IN1C+) and T7 (IN1C-) DNA, indicating that the limit of detection is <1% of floxed sequences. Thus residual floxed sequences in IN1C+ cell lines are <1%. (**D**) GSI sensitivity of IN1C+ cell lines. The indicated cell lines were cultured in the presence or absence of GSI (72 hrs), and ICN1 levels were analyzed by Western blot with the Val1744 antibody.

Figure S3. Presence of Notch1 transcripts that initiate from the upstream promoters 1a and 1b

RT-PCR for Notch1 transcripts from the indicated cell lines, using primers in exons 1a or 1b and in exon 5. The expected PCR products are 737 and 721 bp. The minor bands may correspond to partially or alternatively spliced transcripts. No PCR products were detected when primers from exon 1c were used on the same samples (not shown).

Figure S4. 5'-RACE of Notch1 transcripts in the T1 cell line

The control lane is a positive control provided with the RLM-RACE kit.

Figure S5. Sequences of the 5'-RACE products.

The genomic sequence of the Notch1 gene is shown for the region of interest. Nucleotides in red correspond to 5' ends of the 5'-RACE clones. The number of individual 5'-RACE clones obtained for each 5' end are respectively: exon 25: 4 clones; exon 27, 5': 2 clones; exon 27, 3': 3 clones; exon 27b: 5 clones; exon 29: 1 clone. The sequence of exon 27b is highlighted in blue.

Figure S6. Analysis of exon 27b-containing transcripts in tissues from N1$^{+/_\Delta f}$ mice

RNA was extracted from the indicated tissues of a N1$^{+/_\Delta f}$ mouse (5-week-old) and expression of canonical Notch1 transcripts (exon 32-34) or exon 27b-containing transcripts were analyzed by RT-PCR, as indicated. β-actin was amplified as a control. Note that the exon 27b-specific RT-PCR products for the N1$^{+/_\Delta f}$ tissues correspond to a stronger exposure than those for the control WT and IN1C+ samples.

Figure S7. Ikaros binds to the Notch1 gene

ChIP-seq results of Ikaros binding in the Notch1 locus in WT thymocytes. Note that a peak of Ikaros binding is detected in exon 25. The position of the binding sites for E2A and ICN1 in DN thymocytes, as characterized by Yashiro-Ohtani et al (9), have also been indicated.
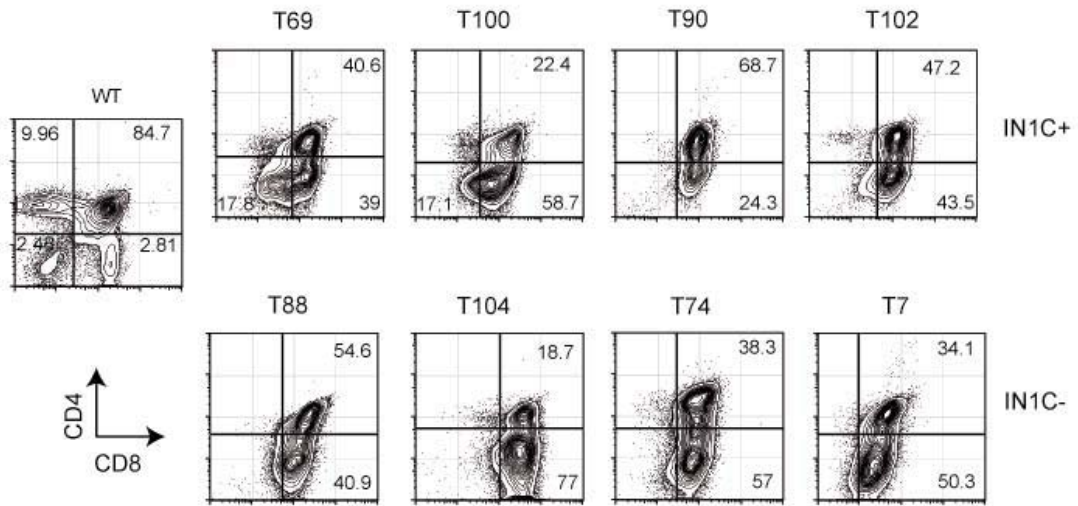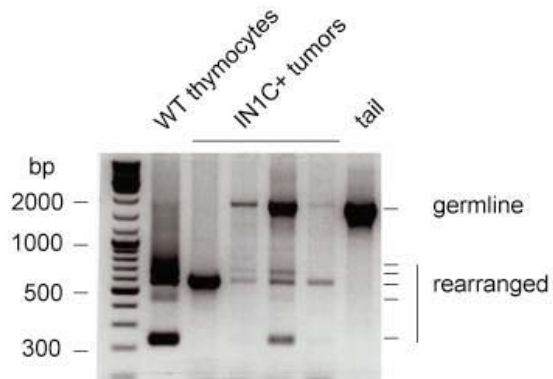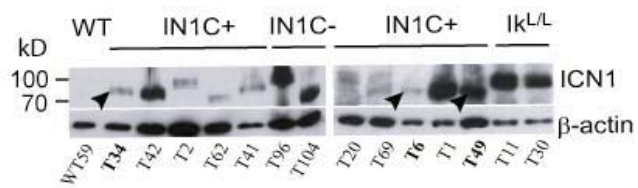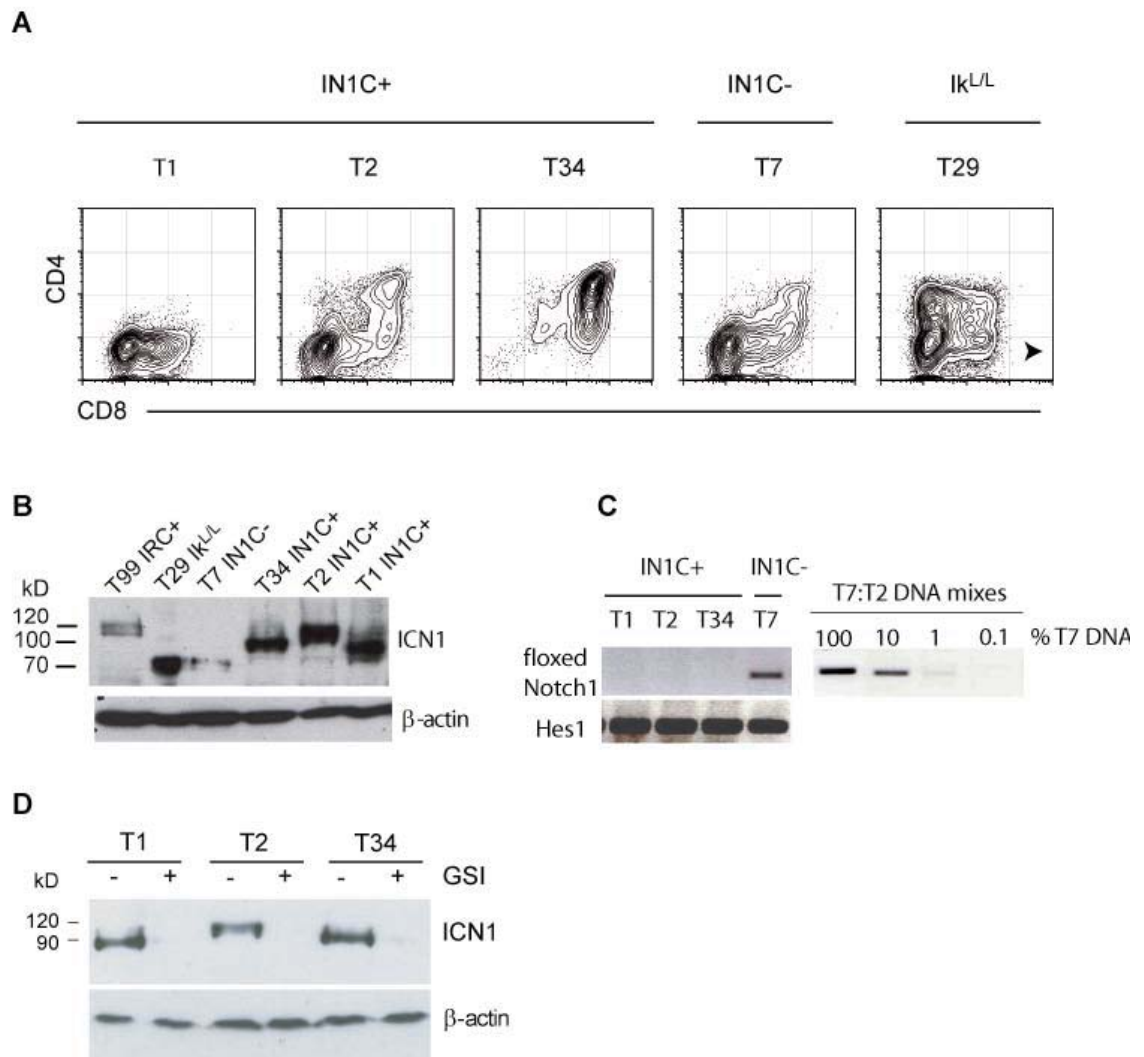
Figure S1

Figure S2

Figure S3

Figure S4

Figure S5

Figure S6

Figure S7

Section II. **THE DEVELOPMENT OF THE IKAROS-DEFICIENT TUMOR IS NOTCH DEPENDENT**

DISCUSSION

We demonstrated the importance of Notch activation for the development of the Ik$^{L/L}$ leukemia and that this is due to the oncogenic up-regulation of an alternative promoter in the 3' part of the Notch1 gene. First, our results showed that T-cell specific deletion of RBP-J, the transcription factor of the Notch pathway, delays the onset of the leukemia, highlighting the importance of Notch target genes for the initiation of these leukemias. However, the deletion of the exon1-promoter region of Notch1 accelerates the emergence of the disease. We revealed the generation of Notch1 transcripts from cryptic initiation sites in the 3' part of the gene, between exon 25-29, after the T-cell specific deletion of the 5' promoter. These transcripts produced a truncated, ligand-independent Notch1 protein. Finally, the analysis of several Ik$^{L/L}$ tumors reveals that the spontaneous deletion of the 5' promoter is observed in 75% of the Ik$^{L/L}$ T-ALL. The discussion below is related to recent data as a complement to the discussion that is in the paper.

Is the canonical RBP-J-mediated Notch activation required for T-ALL development? We showed that the RBP-J mediated Notch activation is required for T-ALL initiation in the Ikaros deficient Ik$^{L/L}$ mice. The deletion of RBP-J mediated by CD4-Cre in the Ik$^{L/L}$ (IRC$^+$) background delays the appearance of leukemia from 18 weeks to 30 weeks, and even some IRC$^+$ mice did not develop tumor throughout their life. Indeed, IRC$^+$ tumor cells analysis revealed a non complete deletion and tumor cells expressing full length RBP-J protein, suggesting a selection of cells that escaped the deletion. Supporting our results, Gomez del Arco et al. (2010) illustrated the decrease in leukemia incidence after the CD2-Cre mediated deletion of RBP-J at ETP stage in the Ik$^{-/-}$ and Ik$^{+/dn}$ mice. The lack of RBP-J mediated Notch activation delays the onset of leukemia in Ikaros deficient mice. In contrast, Chari et al (2010) have shown that the CD4-Cre-mediated deletion of RBP-J in Ik$^{-/-}$ mice results in no difference for the development of clonal T cell population compared to the non deleted RBP-J Ik$^{-/-}$ mice. However, RBP-J levels were not measured in the clonal

population and it is possible that the no difference phenotype may be due to partial or defective deletion. It is also possible that the stage of development is important for RBP-J deletion. The clonal expansion in Ik$^{-/-}$ mice starts at 4 weeks after birth in contrast to the 8-10 weeks seen in Ik$^{L/L}$ mice. The development of leukemia in the Ik$^{-/-}$ mice may therefore start earlier than in the Ik$^{L/L}$ mice, due to low levels of Ikaros proteins produced in the Ik$^{L/L}$ mice. Thus, an early deletion of RBP-J like with the CD2-Cre (which is expressed at the ETP stage) and not the CD4-Cre (which is expressed at theDN4-DP stage), may be required to see an effect of RBP-J deletion in tumor development. Although, the CD4-Cre mediated RBP-J deletion in the Ik$^{L/L}$ mice is sufficient to delay the appearance of Ik$^{L/L}$ tumors, it would be interesting to test if an early deletion would avoid the selection of cells that escape deletion. Thus, the Notch activation is required for the transition of Ikaros deficient thymocytes to a leukemic state and this event is RBP-J mediated.

After the deletion of the 5' Notch1 promoter, which are the necessary translation initiating sites to generate a constitutive active, ligand-independent Notch1 protein? In human T-ALL the most frequent Notch1 mutations are localized in the negative regulatory region (NRR) leading to the expression of a ligand-independent Notch1 protein. In T-ALL mouse models, the majority of the Notch1 mutations are described in the PEST domain. However, we demonstrated here that the deletion of the exon1/promoter region of Notch1 results in the expression of a truncated ligand-independent Notch1 protein from a cryptic 3' promoter. The sequence analysis these truncated Notch1 transcripts revealed the presence of three methionines, M1116, M1659 and M1727, as possible initiating sites for translation. The initiation site from these methionines seems to be conserved between murine leukemias. It was found that the conditional deletion of Notch1 in Ik$^{-/-}$ and Ik$^{+/dn}$ mice under the control of the Lck-Cre transgene generated shorter Notch transcript initiated in exon25 (Gomez-del-Arco et al., 2010). The analysis of the exon 25 transcripts displays six putative translation initiation methionines, M1615, M1659, M1727, M1796, M1845 and M1848. By *in vitro* mutagenesis, it was shown that mutation of M1727 abolished the major isoform and in addition, that mutations in downstream methionines increased the translation from M1727 (Gomez-del-Arco et al., 2010). This suggests a competition between alternative initiation sites for the translation of exon 25 transcripts. Finally, it was described that 2 somatic deletions in the 5'

end of Notch1 in murine T-ALL cell lines can cause ligand-independent Notch1 activation. Type 1 deletions remove exon1 and the proximal promoter and are Rag-mediated. Type 2 deletions remove sequences between exon1 and exon 26 to 28 of Notch1 and are Rag-independent (Ashworth et al., 2010). The virtual translation of these transcripts showed the presence of 3 possible initiating sites, M1616, M1659 and M1727. The analysis of transient expression of the type 1 and type 2 transcripts in U2OS cells showed that only the mutations of M1727 decreases the Notch1 activation in both types of deletions (Ashworth et al., 2010). Moreover, M1727 is conserved in human Notch1 (encoded by codon 1738). The analysis of the CUTLL1 cell line derived from a human T-ALL with a t(7;9) translocation (TCRB-NOTCH1 fusion gene), demonstrated that the Notch1 transcript contains the M1738 as the only possible translational start site (Ashworth et al., 2010). Thus, the M1727 appears to be the initiation site of the aberrant Notch1 proteins after the deletion of the 5'promoter in murine T-ALL. Importantly, all these truncated Notch1 proteins are sensitive to γ-secretase and the translation initiation from M1727 allows the expression of Notch1 proteins just upstream of the γ-secretase cleavage site.

Is the activation of the cryptic Notch1 promoter a common event? Is the Ikaros deficiency required for this activation? Although the deletion of the Notch1 promoter strongly promotes tumorigenesis, it is not sufficient for tumor initiation. We have shown that the deletion of the Notch1 5' promoter in $Ik^{+/+}$ Notch1$^{f/f}$ CD4-Cre$^+$ (N1C$^+$) thymocytes leads to enhanced acetylation of histone H3 (H3ac) between exons 25-34 of the gene compared with WT thymocytes though at lower levels than in the $Ik^{L/L}$ Notch1$^{f/f}$ CD4-Cre$^+$ (IN1C$^+$) tumors cells. However, the N1C$^+$ mice do not develop T-ALL. These results suggest that the oncogenic Notch1 activation is not sufficient to induce tumorigenesis, and requires multiple hits such as the Ikaros deficiency and the deletion of the 5' promoter. However, truncated Notch1 proteins have been seen in other murine leukemias without an Ikaros deficient origin. Similar truncated Notch1 proteins have been demonstrated in murine T-ALL cell lines from Kras-G12D, SCID, BCR/ABL1 and Tal1 transgenic background. The analysis of Ikaros mutations showed dn Ikaros isoforms or point mutations in some of these cell lines but not in all of them (Ashworth et al., 2010) pointing out that Ikaros mutations leading to loss of Ikaros function are common but not general.

E2A deficiency generates leukemic tumors with strong Notch activation mediated by 3' Notch1 transcripts (Gomez del Arco et al., 2010). It was demonstrated that E2A, as Ikaros, have multiple binding sites throughout the Notch1 gene and therefore E2A may repress Notch1 activation (Gomez del Arco et al., 2010). These observations suggest that Ikaros and E2A could participate in a common mechanism of transformation associated with the generation of aberrant Notch1 transcripts. Nonetheless, mutations in Ikaros were not analyzed in those E2A deficient tumors to exclude the Ikaros deficiency-mediated Notch1 activation, as was done in a recent study (Wang et al., 2012). The decrease of E2A function by expression of the DNA-binding protein inhibitor Id1 leads to T cell lymphomas. The majority of these Id1 tumors had elevated Notch1 activity (Wang et al., 2012). Analysis of Notch1 transcripts containing 5' or 3' sequences by a radiometric RT-PCR showed that 40% of the Id1 tumors generated the truncated Notch1 transcripts. Further analysis by RT-PCR determines reduced Ikaros expression in Id1 tumors to less than 70% of the wild type level. However, not all the Id1 tumors with reduced Ikaros expression showed the usage of 3' Notch1 promoters (Wang et al., 2012). Thus, these results suggest that diminution of Ikaros expression in Id1 tumors offers selective advantage to the usage of 3' Notch1 promoters. In addition, the truncated Notch1 proteins were also present in other types of leukemia. It was shown that the mouse model for stem cell leukemia-lymphoma syndrome (SCLL), the ZMYM2-FGFR1 mouse develop leukemia with strong ligand-independent Notch activation. The analysis of ZMYM2-FGFR1 lymphoma cells showed exon1b/exon2 Notch1 deletions identical to those seen in Ik$^{L/L}$ T-ALL cells (Ren and Cowell, 2011). Unfortunately, Ikaros expression and/or mutations were not investigated in these lymphomas.

The truncated Notch1 transcripts were also described in human T-ALL. A recent report by Haydu et al. (2012) showed the intragenic deletion encompassing the 5' region of the Notch1 gene in a T-ALL patient sample. The emerging Notch1 protein (started in exon 26) was constitutively active and γ-secretase sensitive, resembling the truncated Notch1 proteins found in the murine T-ALL models. Nevertheless, this seems to be a rare event in human T-ALL as additional samples did not show 5' truncated forms of Notch1. In conclusion, these studies demonstrated that the truncated Notch1 transcript from the 3'

cryptic promoter is a common event in murine leukemias and a rare albeit existing event in human T-ALL. The studies also suggest that Notch1 activation could be enhanced by Ikaros deficiency as mutations or reduce expression of Ikaros was seen in high percentage in these samples. However, the analysis of Ikaros function cannot be measured only by expression levels and/or the presence of mutations. Indeed, Ikaros function is also modulated by post-transcriptional modifications such as SUMOylation and phosphorylation. Ikaros SUMOylation interferes with its ability to repress transcription (Gomez-del-Arco et al., 2005) and phosphorylation of Ikaros regulates the subcellular localization and its DNA binding affinity (Gomez-del-Arco et al., 2004; Dovat et al., 2002). Thus, further analysis of Ikaros function should be performed to understand the contribution of Ikaros loss of function to the activation of the alternative 3' Notch1 promoters.

HD domain mutations in human T-ALL versus promoter deletion in murine T-ALL. The majority of the Notch1 mutations found in human T-ALL are in the HD domain (Weng et al., 2004). These mutations destabilize the interaction between the intracellular and extracellular subunits, and induce or facilitate ligand-independent Notch1 signaling. In contrast, in murine T-ALL, the most common mutations lead to truncations of the PEST domain that enhance the stability of the truncated proteins (Dumortier et al., 2006; Aster et al., 2008). Here we show that T specific deletion of the promoter/exon1 of the murine Notch1 gene results in the generation of a truncated, ligand-independent Notch1 protein resembling the proteins seen in human T-ALL with mutations in the HD domain. However, the mechanism to generate ligand-independent Notch1 proteins seems to be different. Ashworth et al. (2010) found that murine T-ALL cell lines have deletions that remove the promoter and exon1. These deletions appear to be RAG-mediated as the deletions occurred adjacent to sequences resembling RAG signal sequences (RSS). In addition it was shown that RAG2 protein can bind to the Notch1 gene in thymocytes near the ectopic TSSs that give rise to these deletions (Ashworth et al., 2010). We found that these RAG mediated deletions occurs in 75% of the Ik$^{L/L}$ tumors, allowing a spontaneous deletion of the 5' promoter. Our results and those of Ashworth et al (2010) suggest that the RAG-mediated deletion of Notch1 promoter is a common feature in murine T-ALL. However, in humans the deletion of the 5' Notch1 promoter is not common. This difference can be due

to the divergence in the ectopic RSS. Thus, ligand-independent Notch1 proteins are found in human and murine T-ALL, but the mutations that lead to the production of these proteins are different.

In conclusion, the activation of the Notch pathway is an important event for the development of $Ik^{L/L}$ tumors. However, the activation of Notch1 by itself seems to be not sufficient for tumor initiation, as it needs multiple hits such as Ikaros deficiency and/or 5' promoter deletion. While 5' promoter deletions appear to be common in murine leukemias, in human it is a rare event. This suggests that the 5' promoter deletion can be an event for a specific subtype of human T-ALL, like T-ALL bearing the t(7;9), and more studies should be performed to clarify this point. Moreover, the specific targeting of Notch1 at specific sites that target the constitutively activated, ligand-independent Notch1 protein could be a useful therapeutic strategy.

Section III. **ANALYSIS OF LEUKEMIA INITIATING CELLS IN A MOUSE MODEL OF T-ALL DEFICIENT FOR IKAROS**

INTRODUCTION

III.1. Leukemia initiating cells

III. 1.1. The heterogeneity of the tumors

The definition of cancer as a group of cells with uncontrolled proliferation formed the basis of the cancer research for more than 7 decades. Therefore, the development of drugs was directed to target the enhanced rate of neoplastic proliferation. After, the better understanding of the molecular basis of cancer, the therapeutic strategies focused on the inhibition of the molecular drivers of the disease. These strategies considered cancer as a homogeneous, abnormal entity. Now, it is known that tumors, whether leukemic or solid, exhibit significant heterogeneity in terms of morphology, cell surface markers, genetic lesions, kinetics of cell proliferation, and response to therapy (Dick, 2008). Individual cancer cells share common genetic aberrations reflective of their clonal origin. However, single-cell analysis has shown the existence of variation in genetic and epigenetic abnormalities between different cells within a tumor.

Tumor heterogeneity was first described in 1937, when Furth and Kahn established that a single cell from a mouse tumor, and not a transmissible agent such as bacteria, could initiate a new tumor in a recipient mouse (Furth and Kahan, 1937). Subsequent studies have demonstrated that the frequency of these tumor initiating cells in solid tumors and leukemias was variable but low and that the resulting tumors showed the morphologic heterogeneity of the original tumor (Makino, 1956; Hewitt, 1958; Bruce and Van Der Gaag, 1963). Pierce et al. (1960) showed that malignant teratocarcinoma cells can spontaneously differentiate into multiple differentiated, nontumorigenic cells. Using radiolabeling and auto-radiography techniques to measure cell proliferation, lifespan and hierarchical

organizations within normal and neoplastic tissues, Pierce showed that in mouse squamous cell carcinoma, the early labeling occurred almost exclusively in the undifferentiated cells. At later time points, the well-differentiated cells display the labeling, suggesting that they derived from the undifferentiated cells. These well-differentiated cells were not able to initiate tumors when transplanted into recipient mice (Pierce and Wallace, 1971). With these results, Pierce and Speers proposed the early definition of the cancer stem cell (CSC) concept: "a concept of neoplasms, based upon developmental and oncological principles, states that carcinomas are caricatures of tissue renewal, in that they are composed of a mixture of malignant stem cells, which have a marked capacity for proliferation and a limited capacity for differentiation under normal homeostatic conditions, and of the differentiated, possibly benign, progeny of these malignant cells" (Pierce and Speers, 1988).

Additional studies supported the heterogeneity in the hematological tumors. These studies showed that the majority of leukemia blast cells from human AML and ALL were postmitotic and needed to be continuously replenished form a relatively small proliferative fraction (Clarkson, 1969; Killmann et al., 1963; Clarkson et al., 1971). Later analysis demonstrated two proliferative fractions in patients: a larger, fast cycling and a smaller, slow cycling fraction in a dormancy state. Clarkson and colleagues inferred that the slowly cycling fraction was generating the fast cycling fraction and suggested that these represented a leukemic stem cell population as they had similar cytokinetic properties to those observed for normal HSC (Clarkson, 1974).

III.1.2. Models of tumor heterogeneity

The studies described above established that tumors are functionally heterogeneous in terms of cell proliferation or even in tumor initiation based on transplantation assays. The heterogeneity among cancer cells could be explained by two mutually exclusive models, the stochastic or clonal and the hierarchy or CSC models (Fig. III.1).
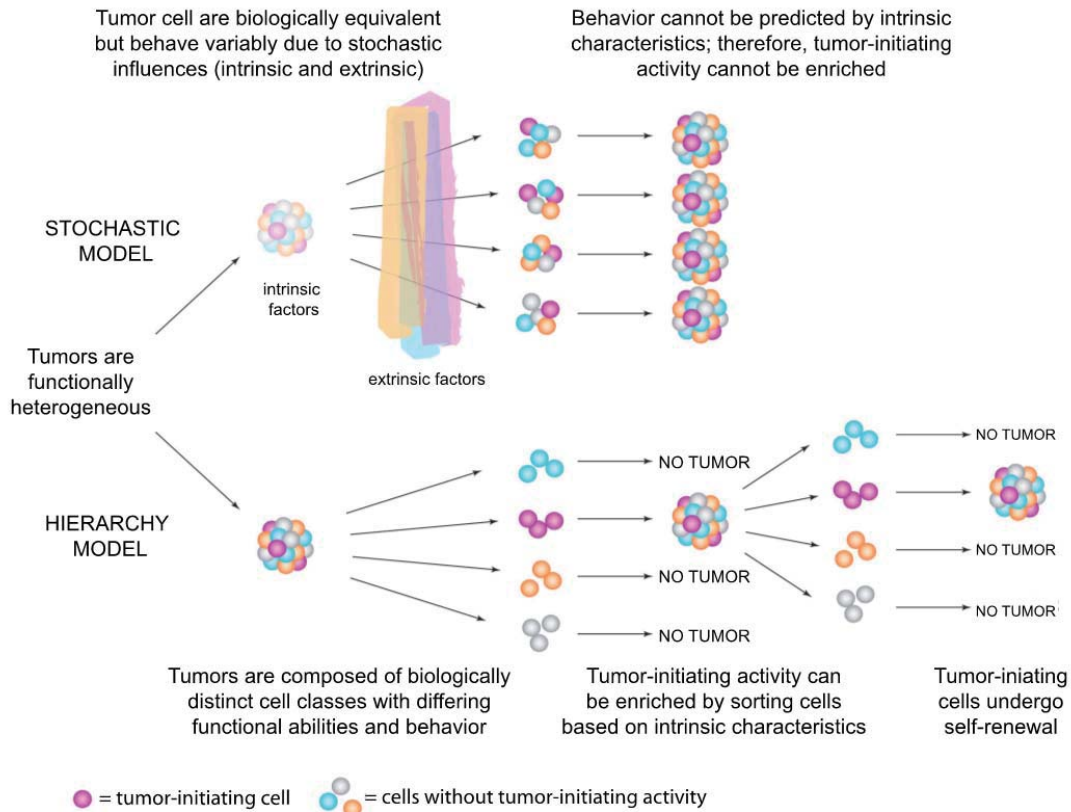
Fig.III.1. Tumor heterogeneity models. (Dick, 2008). Tumors are composed of phenotypically and functionally heterogeneous cells. There are two models to explain how the heterogeneity arises. The stochastic model describes tumor cells as biologically equivalent, however, intrinsic and extrinsic factors can influence their behavior to generate tumor initiating cells. The hierarchy model postulates the existence of biologically distinct classes of cells with differing functional abilities and behavior. Only small subsets of cells are tumor initiating cells.

The stochastic or clonal model predicts that a tumor is biologically homogeneous and the behavior of the cancer cells is influenced by intrinsic genetic (Nowell, 1976) or epigenetic (Baylin and Jones, 2011) changes, or extrinsic factors, such as different microenvironments within a tumor which may confer phenotypic and functional differences on the cancer cells in different locations (Polyak et al., 2009). These influences occur randomly and result in heterogeneity in the expression of cell surface markers, in the entry to cell cycle or in the tumor initiation capacity. All tumor cells are equally sensitive to such stochastic influences and the cells can revert from one to another because these influences are not permanent (Wang and Dick, 2005). Thus, in the stochastic model, every tumor cell has equal probability to

behave as a stem cell. The hierarchy or CSC model describes the tumor as a caricature of normal tissue development. It proposes the existence of distinct classes of cells within a tumor, each one with a different capacity for self-renewal and proliferation. The leukemic stem cells are biologically distinct. They maintain themselves and their clones by self-renewal, and they mature to generate progeny that lack stem cell properties. Thus, in the hierarchy model, only a small subset of cells will consistently have the capacity to initiate a tumor and reproduce the hierarchy of cell types that comprise the tumor (Wang and Dick, 2005). Both models describe the existence of functional leukemic stem cells, namely, cells that have the capacity to initiate leukemia. Therefore, they are called Leukemia Initiating Cells (LICs). For the development of new cancer therapies that either targets the bulk tumor or only the LICs, it is essential to determine which model corresponds to each type of cancer.

Recently, the branching multi-clonal evolution model has been proposed (Notta et al., 2011). This model links the two previous ones. The hierarchical model focuses on the functional heterogeneity but does not take into account tumor evolution or the existence of genetically distinct subclones. The stochastic model focuses on genetic heterogeneity without considering the functional variation. The branching multi-clonal evolution model proposes that genetic diversity occurs in functionally defined LICs and that many diagnostic patient samples contain multiple genetically distinct LIC subclones (Notta et al., 2011). This model originated from the analyses of leukemia in twins and from DNA copy number alteration (CNA) profiling of paired diagnostic and relapse ALL samples. The analyses of ETV6-RUNX1-positive ALL in twins by chromosomal translocation breakpoints and CNA profiling showed that pre-leukemic clones are initiated *in utero*. These clones are present in both twins but they evolve with different kinetics and CNA acquisition in each twin (Bateman et al., 2010; Hong et al. 2008). Analyses of paired diagnostic and relapse ALL samples indicated that in most cases the relapse clone contains different genetic identity compared to the predominant diagnostic clone. In other cases, the relapse clone is the same or a direct evolutionary product of the diagnostic clone (Mullighan et al, 2008). This suggests the existence of a pre-diagnostic clone that give rise to at least two clonal lineages by independently acquisition of different genetic aberrations. Thus, this model proposes that

tumor evolution may occur by a branching pattern that gives rise to genetically distinct subclones and exalts the importance of therapies that eradicate all intratumor subclones.

III.1.3. LIC definition and identification

LICs can be characterized either by their function and/or by the stem cell-related phenotype. LIC function includes self-renewal capacity, extensive proliferative potential and generation of progeny of more differentiated cells. The stem cell-related phenotype could be described by surface marker expression, by their quiescence or by the ability to efflux Hoechst dye (Deng and Zhang, 2010). However these cells can only be identified as LICs after they are shown experimentally to recapitulate the generation of a continuously growing tumor (Clarke et al., 2006).

III.1.3.1. LIC functionality assays

Self renewal and lineage capacity are the hallmarks of normal stem cell, thus, the LICs need to be evaluated for these criteria. To date, the best available assay to demonstrate these criteria is serial transplantation, in which tumor cells from a mouse, injected previously with primary tumor cells, should be able to re-initiate the tumor in a second recipient mouse. The self-renewal can be symmetrical or asymmetrical. Thus, if a LIC undergoes self-renewal, it would generate either two LICs, or one LIC and one bulk tumor cell. Several *in vitro* assays have been used to identify stem cells or LICs, including sphere assays, serial colony-forming unit assays and label retention assays. However, the interpretation of these results is complicated and LIC activity must be confirmed *in vivo*. Thus, the functional analysis of potential LICs should be done by serial transplantation assay to show their self-renewal capacity. In addition to test the functionality of the LIC, it is necessary to quantify their frequency with a limiting dilution transplantation assay. To perform this assay, decreasing numbers of cells are injected in groups of mice to find the minimal amount of tumor cells that are able to generate a new tumor.

One important tool to study some aspects of leukemia biology is the xenotransplantation, which is the human leukemia cell transplantation in immunodeficient mice recipients. This assay allows the identification of distinct clinical risk groups and the possibility to amplify

the human leukemia cells *in vivo* (Meyer and Debatin, 2011). In the beginning, the severe combined immunodeficiency (SCID) mice (Bosma et al., 1983) were used as recipient, but the residual immunity of these mice limits the xenograft. Later, the non-obese (NOD)-SCID mice (Shultz et al., 1995) and strains with impaired innate immunity and absent NK cell activity, such as NOD/Lt-SCID/IL-2Rγ^{null} (NSG) (Shultz et al., 2005) and NOD/SCID/cnull (NOG) (Ito et al., 2002) provide recipient mice with up to 100% engraftment and *in vivo* differentiation of transplanted normal hematopoietic stem cells and increased xenograft of leukemia cells. However, the progressive use of more permissive recipient mice generates controversy as a distinct engraftment phenotype upon leukemia xenotransplantation is observed (Meyer and Debatin, 2011).

III.1.3.2. LIC phenotypic assays

The characterization of tumor cells by their immunophenotype is important to distinguish different subpopulations of cells that may exist in tumors. The identification of potential LICs can be done on the basis of the expression of stem cell surface markers like CD34 and CD38 or immature stage-related surface markers such as CD19 and CD133 in B-ALL and CD7 and CD4 for T-ALL in human leukemia. In murine leukemias, markers such as c-kit, Sca-1, CD44 and Thy1, or the expression of CSC-related surface markers like CD133 are used. However, the immunophenotyping of tumor cells is not sufficient to define LICs; all putative LICs should be analyzed by a functional assay. It is important to note that the markers used to isolate stem cells in normal or cancer samples are not expressed exclusively by stem cells. In addition, the markers used to identify stem cells in one type of cancer might not be useful to identify stem cells in other cancers (Clarke et al., 2006). However, the use of different surface markers to identify a specific subpopulation within the tumor is a helpful strategy to characterize the tumor and to identify a potential and/or rare subpopulation to analyze for LIC activity.

Another phenotype used to identify potential LICs is their presence within the "side population". The side population assay is based on the differential potential of cells to efflux the Hoechst dye via the ATP-binding cassette (ABC) family of transporter proteins expressed within the cell membrane (Goodell et al., 1996). Hoechst is a fluorescent dye that

binds all nucleic acids with preference for the AT-rich regions of the minor groove of DNA (Lalande and Miller, 1979). Hoechst 33342 can traverse the intact plasma membrane of living cells. While uptake of the dye occurs uniformly in all cells through passive diffusion, the efflux is an active energy-driven process. Only cells expressing a sufficient number of ABC transporters are able to actively efflux the dye of the cell. The optimal side population resolution is given by the visualization of the Hoechst profile simultaneously in two distinct channels in a flow cytometer equipped with an ultraviolet (UV) laser. Hoechst 33342 is excited by UV light and emits fluorescence that can be detected in both, the "Hoechst Blue" (450/50nm band-pass filter) and the "Hoechst Red" (675/20 nm long-pass filter) channels (Goodell et al., 1996). As the "Hoechst Red" channel is more sensitive to small changes in dye concentration, the side population cells emerge as a distinct tail extending first on the side of the main population toward the lower "Hoechst Blue" signal. Appropriate side population discrimination is due to the use of controls treated with ABC transporter inhibitors such as Verapamil (Goodell et al., 1996). The side population assay has recently been used to assess the presence of putative CSCs in a variety of cancer cell lines and primary tumors. Side population cells have been identified in cancers where they have been shown to possess self-renewing capacity and tumorigenicity when transplanted into mice (Chiba et al., 2006; Haraguchi et al., 2006; Wu et al., 2007; Chua et al., 2008). The side population phenotype might explain the resistance of specific subpopulations of tumor cells to chemotherapy (Chua et al., 2008; Dean et al., 2005; Hirshmann-Jax et al., 2004; Wu et al., 2007). Though not every cancer contains side population cells, the analysis of side population cells within a tumor can help with the identification of subpopulations with potential LIC function.

The assumption that normal stem cells or CSCs spend long periods in a non-cycling state, or quiescence, led to the idea that a label retention (bromodeoxyuridine incorporation) assay might be used to identify LICs. While bulk tumor cells proliferate fast, LICs divide slowly (Ho and Wanger, 2006) and therefore preserve the labeled state for an extended period. However, it is known that not all stem cells are able to retain the dye and not all label-retaining cells are stem cells (Clarke et al., 2006). This quiescent status is associated with resistance to conventional chemotherapy strategies that target rapidly dividing cells. Thus, the label retention assay could help to identify non/slowly dividing cells, as potential LICs.

In addition, genome-wide analyses such as DNA microarrays to obtain the CNA profiles provide tools to identify the genetic diversity found in the heterogeneous leukemia cells and to recognize the diverse LICs or subclones that may exist in the leukemia. These techniques were used to show the clonal heterogeneity of the BCR/ABL1 positive B-ALL and the cortical/mature T-ALL (Notta et al., 2011; Clappier et al., 2011). However, these techniques required high numbers of cells hindering their use.

III.1.4. The first evidence for the existence of LICs

The first evidence for the existence of CSCs was found in hematological malignancies where only a small subset of slowly dividing cells were able to induce transplantable AML. Dick and colleagues demonstrated that most subtypes of AML, except acute promyelocytic leukemia (APL), could be engrafted reliably in SCID mice (Lapidot et al., 1994). Limiting dilution analysis showed that the frequency of the initiating cells was variable by more than 1000-fold between donors and it was exceedingly rare with an average of 1 per 10^6 cells. They showed that leukemic engraftment could only be initiated from the $CD34^+CD38^-$ cell fraction. The $CD34^+CD38^-$ cells could produce large numbers of colony-forming progenitors, $CD34^+CD38^+$ cells and mature blasts (Lapidot et al., 1994). Later, it was demonstrated that the $CD34^+CD38^-$ cells have the differentiative and proliferative capacities and the potential for self-renewal characteristics of a typical leukemia initiating cell (Bonnet and Dick, 1997). Thus, these studies demonstrated the existence of specific cells that can reinitiate a tumor, the LICs, and provided evidence for the hierarchy model in AML.

Subsequent studies demonstrated the existence of CSC in solid tumors. Al-Hajj et al. (2003) showed that breast tumors comprise a minor, phenotypically distinct tumor cell population that was able to form mammary tumors in non-obese diabetic (NOD)/SCID mice. As few as 100 $CD44^+CD24^{-/low}$ cells were sufficient to develop a tumor in immunodeficient mice, whereas 10^4 cells with different phenotypes were not able to re-initiate the tumor. The tumorigenic cells could be serially transplanted, demonstrating their self-renewal capacity. They were also able to generate tumor heterogeneity to produce differentiated, nontumorigenic progeny (Al-Hajj et al., 2003). In addition, it was demonstrated

that CD133$^+$ cells in human brain cancers have differentiative and self-renewal capacities to initiate tumor growth *in vivo*, whereas CD133$^-$ cells could not (Singh et al., 2004). In these studies, small numbers of cells defined by specific markers were able to transfer the disease into immunodeficient mice and the frequencies of tumorigenic cells were variable and low. Thus, there is evidence for the existence of CSC (in the case of solid tumors) or LICs (in the case of hematological tumors) in different types of cancers. In both cases, they are compatible with the hierarchy model.

III.1.4.1. The controversy

Despite these and other studies, there are reports that questioned the universality of the CSC or hierarchy model. Kelly et al. (2007) showed that primary pre-B/B lymphoma cells from Eμ-*myc* transgenic mice were able to reinitiate tumor development in non-irradiated congenic animals regardless of the number of injected cells, from 10 to 10^5 cells. The demonstration that the LIC frequency in some induced murine leukemia models can be as low as 1 in every 10 cells, makes the LICs a fairly common population (Kelly et al., 2007). To explain the difference in frequency obtained between mouse and human tumors, the authors suggested that the xenotransplantation may underestimate the percentage of LICs due to host resistance factors and to the absence of cross-species reactivity of cytokines and other microenvironmental factors. However, Dick and colleagues showed that when human and murine leukemia models were both induced with the same mixed-lineage-leukemia (MLL) fusion protein, the LIC frequency was the same (Kennedy et al., 2007). They generated a genetically induced model of human B-ALL by transplanting human umbilical cord blood stem/progenitor cells expressing the oncogene MLL-ENL into immunodeficient mice. The frequency of LICs in this model was comparable to the frequency obtained with a murine retroviral transduction model of MLL-AF9-induced AML (Krivtsov et al., 2006; Kennedy et al., 2007). Thus, Kennedy et al. (2007) emphasized that the fundamental concept of the CSC model is not directly related to the frequency of the LICs, but rather to the functional evidence of tumor heterogeneity and a hierarchical organization. In addition, there are studies that have been reported phenotypically different LICs in the same type of cancer. In 2009, Cox et al. showed that CD19$^-$CD133$^+$ ALL blast were the only cells able to propagate human leukemia in immune deficient NOD/SCID mice. However, one year

before, le Viseur et al., have shown that a wide variety of blast at different stages of maturation (CD34$^+$ and CD34$^-$, CD19$^-$ and CD19$^+$, CD20$^-$ and CD20$^+$) were able to propagate leukemia in NK cell depleted NOD/SCID and NSG mice after intrafemoral injection. It is important to note that this difference can be due to the use of different recipient mice: the identification of LICs with an immature immunophenotype used more conventional NOD/SCID mice (Cox et al., 2009), whereas the wide variety of blast with LIC potential was found after xenotransplants in NK cell-depleted NOD/SCID mice and with a more invasive inoculation (intrafemoral injection) (Le Viseur et al., 2008). Both groups suggest that the discrepancy in the ALL LICs can be due to the use of different methodology (strains of recipient mice and inoculation techniques) and a standardization of xenotransplantation should be necessary (Heidenreich and Vormoor, 2009; Diamanti and Blair, 2009). But methodology includes more than immunodeficient mice recipients and inoculation techniques. The controversy about the LIC existence also touches the antibodies that are used to select the cell population. Studies in AML have shown that LICs are not only present in the CD34$^+$CD38$^-$ cells (Lapidot et al., 1994) but also in the CD34$^+$CD38$^+$ (Taussig et al., 2008) or CD34$^-$ (Taussig et al., 2010) cells. Taussig et al. (2008) found that some antibodies reduced the engraftment of hematopoietic cells in NOD/SCID mice such as anti-CD33. The analysis of a range of antibodies to human antigens reported that anti-CD38 antibody has an inhibitory effect on the engraftment of normal and leukemic repopulating cells. The CD38-coated human cells were clearanced by the innate immune cells through a process that is dependent of the Fc portion of the antibody (Taussig et al., 2008). These results suggest that the clearance of the CD38-coated cells influence the enrichment of LICs in the CD34$^+$CD38$^-$ population that was observed before and highlight the importance of the antibodies used to sort the leukemic cells. Nonetheless, it seems that AML follows the hierarchy model. The debate continues but not only for LICs. Quintana et al (2008) demonstrated how xenotransplantation assay can be modified to increase the frequency of cells with tumorigenic potential from the same sample. Melanoma cells from the same patient were transplanted either in NOD-SCID or NSG recipient mice and with or without matrigel to enhance the engraftment of the tumor cells. The results obtained showed an important increase of xenograft in the more immunecompetent NSG recipient with matrigel (Quintana et al., 2008). Thus, the frequency of

LICs and CSCs can vary among different cancers as demonstrated by xeno- or syngeneic transplantation assays and all these variations can be due to the immunodeficiency of the recipient mice, the methodology used like the inoculation techniques (intrafemoral against intravenous injection), the sex (higher engraftment in female than male) and age (young age is associated with superior engraftment) of the recipient mice and the antibodies used to select the cells (Notta et al., 2010; Ballen et al., 2001; Taussig et al., 2008). Moreover, it is necessary to determine the existence of LIC and the model of heterogeneity in different types of tumors as this may have an impact on the therapeutic strategies.

III.1.5. LICs in ALL
III.1.5.1. LICs in B-ALL

The first demonstration of LICs in B-ALL was provided by Cabaleda et al. (2000) who showed that only the primitive $CD34^+CD38^-$ blast cells were able to transfer BCR/ABL1 positive B-ALL in NOD/SCID mice. Another study proposed that $CD34^+CD38^-CD19^+$ cells could represent a candidate for LICs in B-ALL (Castor et al., 2005). However, subsequent studies raised the question about the B-ALL LIC description as $CD34^+CD38^{-/low}CD19^+$ cells and suggested a non hierarchical model of heterogeneity. It was shown that in pediatric B-ALL there are less than 1% of $CD133^+CD19^-$ cells that are capable of initiating and maintaining long-term cultures of B-ALL cells and of initiating tumors by serial transplantation in NOD/SCID mice (Cox et al., 2009). In contrast, Le Viseur et al. (2008) showed that $CD34^+CD19^-$, $CD34^+CD19^+$ and $CD34^-CD19^+$ cells contain LICs, although with different frequencies. This suggests that the LICs in B-ALL can switch between different populations. In addition, the xenotransplant of unfractionated leukemic blasts from BM of childhood B cell precursor-ALL into NSG mice revealed a very high LIC frequency, suggesting a stochastic but not hierarchical model for this leukemia (Morisot et al., 2010). Finally, using xenografting and CNA profiling of human BCR/ABL1 positive B-ALL, it was demonstrated that B-ALL is composed of genetically distinct subclones (predominant and/or minor subclones) that are present with varying proportions at diagnosis and have different functional capacities in xenografts (Notta et al., 2011). Here, the propagation of genetic abnormalities found in the diagnostic sample was tracked by comparing the CNA profiles of the diagnosis sample with paired primary and secondary xenografts. This

analysis showed that the majority of the xenografts exhibited the same distribution of CNA as the diagnostic patient sample. However, multiple xenografts, derived from the same patient, harbored distinct genetic changes compared to the predominant diagnostic clone even if they shared the major CNA such as for *IKZF1* and *CDKN2A/B*. Moreover, the ability of different subclones in xenotransplantation assays to engraft seems to correlate with the clinical outcome. The patients whose xenografts derived from the predominant clone have a worse outcome compared to those in which the engraftment originates from a minor subclone. These results suggest the existence of subclones that are present at low levels in the diagnostic samples and further suggest that these clones undergo divergent evolution from the diagnostic clone. Thus, these data support the branching clonal-evolution model in BCR/ABL1 B-ALL.

III.1.5.2. LICs in T-ALL

When we started the analysis of LICs in the Ik$^{L/L}$ mice, there were limited and contradictory information concerning the potential existence and the immunophenotype of the LICs in T-ALL. Cox et al. (2007) had demonstrated that CD34$^+$CD7$^-$ cells were able to grow *in vitro* and *in vivo*. Limiting dilution assays with unfractionated leukemia cells had shown that 5x10^5 to 10^7 cells were required for engraftment, indicating that LICs are rare in human T-ALL (Cox et al., 2007). Later, Gerby et al, (2011) showed that in mature/cortical T-ALL, the CD34$^+$CD7$^-$ population, previously described as LICs in T-ALL (Cox et al., 2007), contained normal human progenitor and HCSs. Moreover, these cells did not have the original genetic abnormality identified at diagnosis, such as gene rearrangement or microdeletion. Instead, by limiting dilution xenotransplantations, the authors showed that the LIC activity was enriched in CD34$^+$CD7$^+$ cells (Gerby et al., 2011). In addition, it was demonstrated that the combination of dexamethasone and inhibitors of Notch signaling prevented proliferation and LIC activity in the CD34$^+$CD7$^+$ cell population (Gerby et al., 2011). Moreover, it was recently described that a CD7$^+$CD1a$^-$ T-ALL subpopulation was enriched with LICs when xenotransplanted in NSG mice. This is contrary to previous results, showing that CD34 was not a universal marker for T-ALL LICs (Chiu et al., 2010). Treatment with glucocorticoid showed that CD1a$^-$ cells are resistant and suggest that CD1a$^-$ LICs may possess unique

biological and molecular properties (Chiu et al., 2010). Thus, the immunophenotype of LICs in T-ALL remains unclear.

Regardless the unclear LIC immunophenotype in T-ALL, increasing number of studies highlight the importance of Notch as a major player in the LIC activity. The development of a long-term co-culture assay of primary human T-ALL cells with a murine stromal cell line expressing the human Notch ligand DL-1 (MS5-DL1) has allowed the first study of how Notch activation influences T-ALL maintenance and growth (Armstrong et al., 2009). This assay demonstrated that most T-ALLs with or without Notch mutations require activation of the Notch pathway for proliferation. T-ALL cells cultured with MS5-DL1 showed 100% engraftment in NOD/SCID mice. However, cells co-cultured with MS5-GFP were not able to engraft. Moreover, the transplantation of T-ALL cells that were cultured with GSI for 30 days resulted in only 1 out of 12 mice with T-ALL development (Armstrong et al., 2009). These results demonstrate a major role for Notch signaling in regulating the LIC activity in T-ALL. Subsequent studies support the role of Notch in LIC activity. For example, as described before, T-ALL LICs CD34$^+$CD7$^+$ proliferate more upon Notch activation than other subpopulation such as CD34$^-$CD7$^+$ and were sensitive to dexamethasone and Notch inhibitors (Gerby et al., 2011). Recently, it was also shown that CD34$^+$ cells from Notch1^{mutated} pediatric T-ALL samples had higher leukemic engraftment and serial transplantation capacity than the CD34+ Notch1^{WT} cells (Wenxue et al., 2012). The use of Notch1 monoclonal antibody reduced LIC survival and self-renewal in the engrafted mice (Wenxue et al., 2012). Thus, the Notch1 signaling plays an important role in LICs activity.

Similar to the BCR/ABL1 positive B-ALL, T-ALLs appear to have clonal heterogeneity at diagnosis and clonal evolution at relapse. The comparison between the CNA profiles of diagnosis, relapse and xenograft samples showed that xenograft and relapse samples clustered together and harbored a range of new genetic lesions compared with diagnosis cells (Clappier et al., 2011). The additional genomic lesions in xenograft leukemic cells increased the expression of cell cycle and mitosis genes and caused a diminished sensitivity to drugs, reminiscent of relapse leukemias. Thus, this study highlights the relevance of the xenograft assays as a model of patient relapse as it favors the emergence

of leukemic subclones and increases other relapse features such as enhanced LIC activity, increased proliferation and drug resistance.

In murine leukemia, also the existence of LIC was unclear. Li et al. (2008) characterized various stages of tumor development in a murine model of T-ALL initiated by retrovirus-mediated overexpression of intracellular Notch1 in lineage negative BM cells. The over-expression of intracellular Notch1 led to the generation of polyclonal non-tumorigenic $CD4^+CD8^+TCR$-$\alpha\beta^-$ cells that were not qualified as LICs as they did not generate tumors upon transfer into nude mice (Li et al., 2008). The authors concluded that even though the tumors consisted of phenotypically heterogeneous cells, no evidence for LICs was found in that model.   Recent studies in the Tax transgenic mouse model for adult T-cell leukemia/lymphoma (ATL) and the Tal1/Lmo2 mouse model for T-ALL suggest the existence of LICs. Yamazaki et al. (2009) have estimated the LIC frequency by limiting dilution transplantation assays as 1 per 10^4 splenic lymphomatous cells in the Tax transgenic mouse. The subsequent LIC identification by side population assay and the $CD38^-CD71^-CD117^+$ phenotype showed that 10^2 cells were sufficient to re-initiate the original lymphoma. Thus, LICs exist in the ATL mouse model. Finally, with the Tal1/Lmo2 mouse model, it was demonstrated that murine T-ALLs are phenotypically and functionally heterogeneous with a LIC frequency of 1 per 10^5 cells (Tatarek et al., 2011). Transplantation assays showed that the LICs were present in a subset of DN3 cells (Tatarek et al., 2011). Tal1/Lmo2 mice develop a heterogeneous tumor with spontaneous mutations in Notch1. Therefore, the consequences of Notch1 inhibition on LIC activity were analyzed. T-ALL cells *in vitro* were incubated with GSI or vehicle for 48 hr and then transplanted into syngeneic mice where treatment was maintained for 3 weeks (Tatarek et al., 2011). Notch inhibition significantly reduced or eliminated LICs. Thus, these results supported the LIC activity dependence on Notch signaling.

Regardless of the not well defined presence of LIC population in all types of T-ALL, evidence is emerging that relapse (30% of T-ALL cases) may result from a failure to eliminate LICs. In the CSC model of tumor biology is suggested that treatments eliminating bulk tumor cells without eradicating CSCs will result in relapse as CSC reemerge (Wang,

2007). In conclusion, CSCs or LICs are cells able to generate and maintain tumors by their special capacity to self-renew. The goal of identify LIC lies not only in the better understanding of tumor initiation and progression but also in the development of effective anticancer therapies that target tumor cells that initiate and maintain the tumor.

Section III. **ANALYSIS OF LEUKEMIA INITIATING CELLS IN A MOUSE MODEL OF T-ALL DEFICIENT FOR IKAROS**

RESULTS

In this part of my work I analyzed Ik$^{L/L}$ tumors to determine the occurrence of LICs. I performed transplantation assays to test the ability of Ik$^{L/L}$ tumor cells to re-initiate leukemia in recipient mice and used limiting dilution assays to find the minimum number of cells required to initiate the tumors. I characterized the Ik$^{L/L}$ tumors by staining for different surface markers to define subpopulations present in the tumor and to test their capacity to initiate tumors. Finally, I sought stem-cell like characteristics in the Ik$^{L/L}$ tumors.

III.2. Leukemia initiating cell analysis

For the transplantations shown here, we used lethally irradiated (9Gy) C57BL/6J WT mice (CD45.2^{+}). By intravenous injection (in tail vein), we transplanted tumor cells from leukemic Ik$^{L/L}$ mice (around 18-20 weeks old) that expressed the leukocyte common antigen CD45.2. To support the reconstitution of the hematopoietic system, we also transplanted 2.5x10^{5} WT BM cells from a mouse that expressed CD45.1 (B6Ly5.1) or CD45.1/CD45.2 (B6Ly5.1/5.2) (Fig. III.2). With the differential expression of CD45 we can follow the tumor or the supporting cells in the recipient mouse. The proliferation of the Ik$^{L/L}$ tumor cells into the recipient mice is high and the tumor phenotype is clear. Therefore, regardless of the fact that the tumor and the host cells express CD45.2, we can distinguish, by CD4/CD8 surface staining, if the cells are tumor or host cells. For some transplantation, B6Ly5.1 or B6Ly5.1/5.2 mice were also used as recipient mice. Topro3, a dye that cannot penetrate the intact membrane of live cells, was added to the cell suspensions before sorting in order to discard the dead cells.
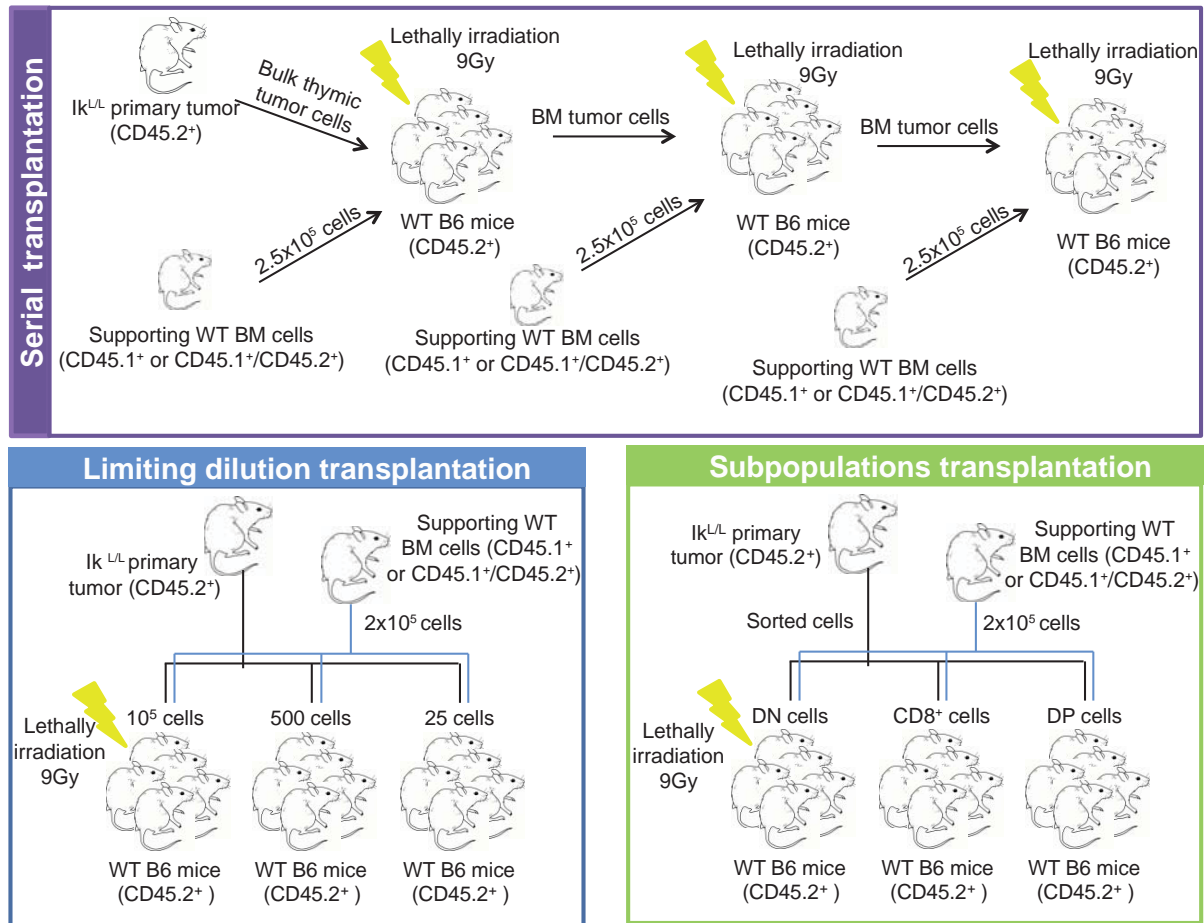
Figure III.2. Strategy of transplantation experiments. The transplantation experiments performed here were made by injection of Ik$^{L/L}$ primary tumor cells into lethally irradiated (9Gy) recipient mice. To support the reconstitution of the hematopoietic system, 2.5x10^5 WT BM cells were also co-injected. In the serial transplantation, the generated tumor cells from the first recipient mice were used to inject the second recipient mice and so on (top). For the limiting dilution transplantation, decreasing numbers of cells were injected into recipient mice. Subpopulation transplantations were performed by injecting sorted Ik$^{L/L}$ tumor subpopulations.

III.2.1. Functional Assay

III.2.1.1. Self-renewal capacity by serial transplantation

To investigate the self-renewal capacity of the Ik$^{L/L}$ tumor cells, we performed serial transplantation assays. The first recipients received Ik$^{L/L}$ primary tumor cells. For the second round of transplantations we used tumor cells derived from the BM of the first recipient mice. In the recipient mice the tumor appears first in the BM with later metastasis in the spleen and thymus.

We performed a transplantation experiment using 10^5 tumor cells and 2.5×10^5 supporting WT BM cells. Two weeks after the transplantation, the recipient mice showed disease symptoms. The Ik$^{L/L}$ tumor cells were able to initiate tumor in both the 1st and the 2nd round recipient mice, and all the tumors showed similar CD4/CD8 staining phenotype. In both serial transplantations the tumors developed about 2 weeks after transplantation (data not shown).

After the limiting dilution assays (see section III.2.2.1) we noticed that 10^5 tumor cells were an excessive number. Therefore, we performed another serial transplantation assay using 500 primary tumor cells (the limiting number that developed tumors in recipient mice). We followed the capacity of self-renewal until the 5th round of transplantation. The 1st recipient group developed the tumor faster than the subsequent rounds (41 days vs. 64 days on average for the other groups) but between the 2nd and 5th round the kinetics of tumor development was similar (Fig. III.3A). We noticed that in the 4th and 5th round of transplantation, only 2 out of 4 mice from each group got sick. This suggests that either the tumor cells started to lose their self-renewal capacity or that the LIC numbers started to decrease. All the tumors, regardless of the round of serial transplantation, showed similar CD4/CD8 but not CD3/CD25 phenotype (Fig. III.3B). This phenotype was seen in all of the experiments. The expression of CD4/CD8 was similar between the recipient tumors, and all of the tumors displayed a DP/CD8+SP phenotype. However, it was common to see a decrease in CD3 and an increase in CD25 expression compared to the original tumor.

Thus, the Ik$^{L/L}$ tumors cells showed an important stem cell characteristic. They have the capacity to self-renew, as it is possible to perform serial transplantations for at least 5 rounds.

A.   **Serial transplantation**

B.
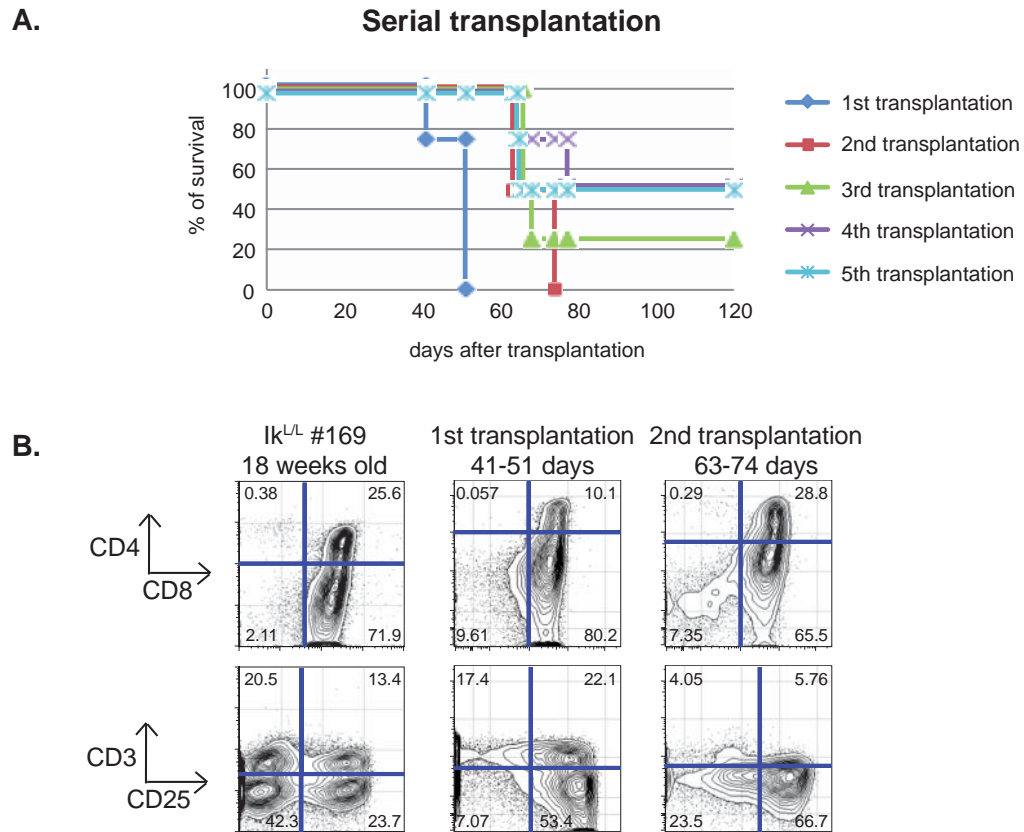
Figure III.3. Ik$^{L/L}$ tumor cells have self-renewal capacity. Lethally irradiated recipient mice were injected with 500 Ik$^{L/L}$ tumor cells derived from a primary tumor or BM tumor cells from recipient mice for the serial transplantation. A. Survival curve of the recipient mice groups (n=4 mice) in each of the 5 rounds of transplantation. B. CD4/CD8 and CD3/CD25 phenotype of the original tumor and one recipient mouse from the 1st and 2nd round of transplantation. The data shown here represent a serial transplantation assay with the Ik$^{L/L}$ #169 primary tumor. A second serial transplantation assay was performed with an amplified Ik$^{L/L}$ tumor and similar results were obtained (data not shown).

III.2.2. Frequency Assay

III.2.2.1. Determining the number of leukemia initiating cells by limiting dilution transplantation

To establish the frequency of leukemia initiating cells in the Ik$^{L/L}$ tumors, we performed limiting dilution assays. We injected decreasing numbers of Ik$^{L/L}$ tumor cells into lethally irradiated recipient mice. With the minimal number of cells necessary to start new tumor, it is possible to estimate the frequency of LICs present in the tumor.

The limiting dilution assays were performed with 10^5 to 25 tumor cells. The mice were sacrificed when they showed disease symptoms or 150 days after injection. The results shown in table III.1 represent 4 independent transplantation experiments, each one from a different $Ik^{L/L}$ primary tumor. Each transplantation tested different cell dilutions, however, some dilutions were repeated to better validate our data.

	1st assay	2nd assay	3rd assay	4th assay
10^5 cells	n=3 mean 27 days (24d 2x, 41d 1x)	n=3 mean 31 days (31d 3x)		
10^4 cells	n=3 mean 41 days (41d 3x)	n=3 mean 31 days (31d 3x)		
$5x10^3$ cells			n=5 mean 42 days (41d 2x, 44d 3x)	
10^3 cells		n=3 mean 60 days (60d 3x)	n=4 mean 51 days (50d 2x, 52d 2x)	
500 cells			n=6 mean 61 days (56d 3x, 57d 1x, 80d 1x, survive 150d 1x)	n=3 mean 45 days (45d 3x)
250 cells				n=5 (47d 1x, survive 150d 4x)
100 cells			n=6 no tumor	n=5 no tumor
50 cells				n=5 no tumor
25 cells				n=5 no tumor

Table III.1. Limiting dilution transplantations data obtained from 4 assays. Each experiment tested different dilution. The description of how many mice were injected with each dilution is indicated as well as the mean days after transplantation that takes for every group to develop tumors. It is also indicated the days required for single mouse to develop tumors.

Transplanting 10^5 or 10^4 $Ik^{L/L}$ tumor cells led to similar kinetics of tumor growth. However, when fewer cells were used, the number of injected cells was inversely correlated with the time required for tumor generation. The survival curve representing one of the experiments shows that the last group of mice which developed tumors was injected with 500 tumor cells. All of these tumors showed a DP/CD8+SP phenotype similar to the donor cells. When 250 tumor cells were injected, only one out of 5 mice developed a tumor and none of the mice injected with 100, 50 or 25 $Ik^{L/L}$ tumor cells displayed any disease after 150 days. The analysis of thymus and BM from these mice revealed a normal phenotype. Thus, to develop new tumor in lethally irradiated recipient mice it is necessary to inject at least 500

tumor cells. The frequency of LICs was calculated by Poisson statistics and the method of maximum likelihood provided in L-Calc software (StemCell Technologies) with all the data obtained from the limiting dilution assays. It was estimated to be 1/531 cells (95% confidence interval, with a ±1 SE range of 1/384 to 1/724).
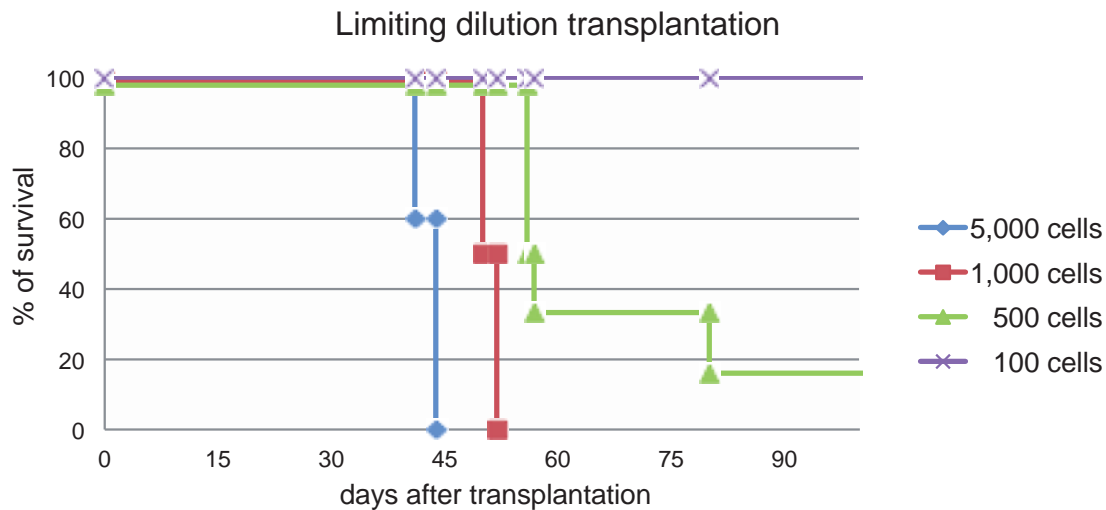
Figure III.4. 500 Ik$^{L/L}$ tumor cells are sufficient to develop tumors in lethally irradiated recipient mice. The survival curve representing a limiting dilution assay for groups of recipient mice injected with 5,000 (n=5), 1,000 (n=4), 500 (n=6), 100 (n=6) Ik$^{L/L}$ tumor cells.

III. 2.3. Identification of LIC phenotype

III.2.3.1. Ik$^{L/L}$ tumor characterization by surface marker staining

III.2.3.1.1. Ik$^{L/L}$ thymus phenotype

Based on the results above, we suspected the existence of a specific tumor cell subpopulation that has properties of LICs within the Ik$^{L/L}$ tumors. Therefore we sought to identify the phenotype of these cells. Ik$^{L/L}$ thymocytes display an unusual pattern of T cell markers as early as 8 weeks of age. We can observe a decreased CD4+SP and an increased CD8+SP and CD25$^+$ cells compared to WT thymus (Fig. III.5). After 13 weeks of age, the CD4/CD8 phenotype already resembled the final Ik$^{L/L}$ tumor but the percentage of CD4+SP cells was still high and there was no metastasis in the spleen or the BM (Fig. III.5D and data no shown). The CD4/CD8 phenotype displayed at 16 to 20 weeks was essentially

the same, but the expression of other markers like CD25 was higher at older age (Fig. III.5E, F). We also found higher numbers of cells in the thymus and in the metastatic organs. In order to characterize specific subpopulations of the Ik$^{L/L}$ tumors, we looked for up regulated genes in the Ik$^{L/L}$ tumors compared to WT thymocytes by transcriptome analysis. After, we analyzed their expression by FACS. We also stained tumor cells with stem cell-related markers. This analysis revealed that markers like CD138 and Sca-1 are also increased during tumor progression (Fig. III.5).
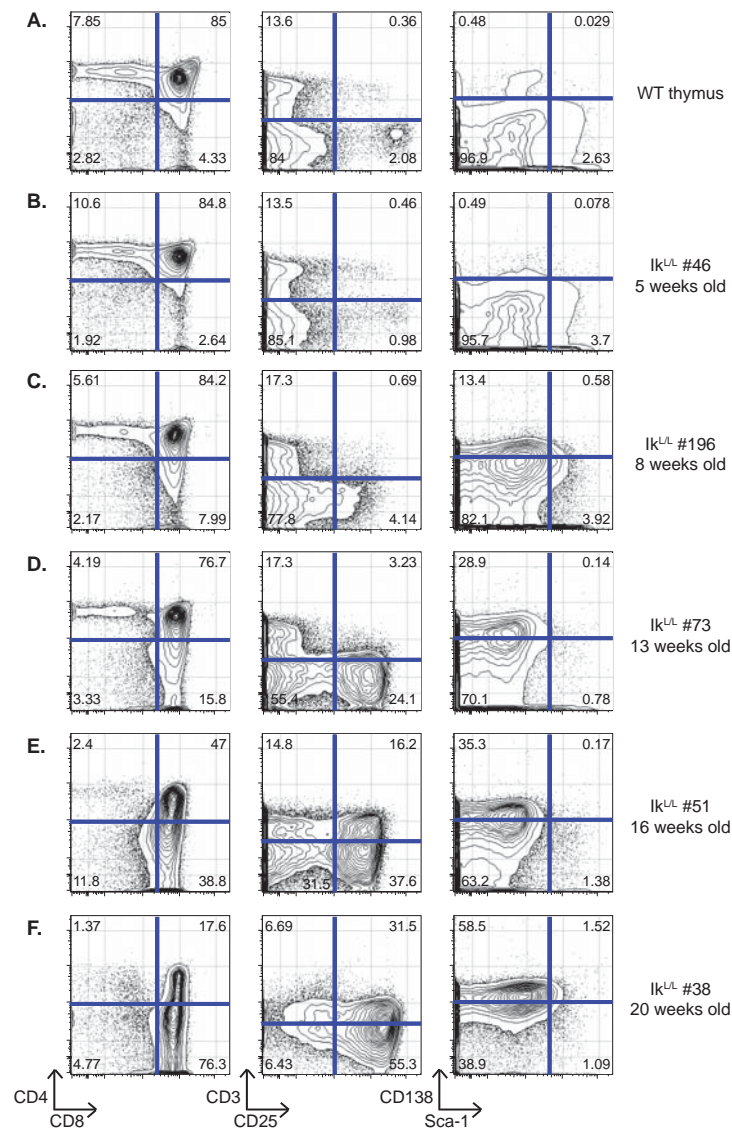
Figure III.5. Variable expression of surface markers in thymi of Ik$^{L/L}$ mice throughout life. The thymocytes from Ik$^{L/L}$ mice at different ages were stained to analyze the CD4/C8, CD3/CD25 and CD138/Sca-1 profiles. A. WT thymus, B. Ik$^{L/L}$ thymus 5 weeks old, C. Ik$^{L/L}$ thymus 8 weeks old, D. Ik$^{L/L}$ thymus 13 weeks old, E. Ik$^{L/L}$ thymus 16 weeks old and F. Ik$^{L/L}$ thymus 20 weeks old.

Thus, the majority of the Ik$^{L/L}$ tumors (75-80%) displayed the DP/CD8+SP phenotype such as Ik$^{L/L}$ #51 (Fig. III.5E) or Ik$^{L/L}$ #38 (Fig. III.5F), and the accumulation of these subpopulations started at an early age. The expression of the other markers (CD3, CD25, CD138 and Sca-1) was variable between the tumors. However, they had a tendency to increase in the tumors, the expression of CD25 and CD138 were increased with age. We commonly saw a high expression of CD25 and CD138 in the Ik$^{L/L}$ tumors.

III.2.3.1.2. Ik$^{L/L}$ tumor phenotype

We studied a large number of tumors by staining the following surface markers: CD4, CD8, CD3, CD25, Sca-1, CD138, CD24, CD44, CD69, CD133, IL-7Rα, γδ-TCR, CD150, CD90, c-kit, CD34, CD71, FLT-3, CD16, Ter119, CD48, CD43 and CD135. Most of the tumors showed a DP/CD8+ phenotype (76%) with high CD25 expression but sometimes they also displayed a DP/CD4+SP phenotype (4 cases in 17 tumors analyzed) (Fig. III.6A). The expression of the other markers was either highly heterogeneous between the tumors (Fig. III.6B) or they were not expressed.

Thus, the most common Ik$^{L/L}$ tumor phenotype is DP/CD8+SP with low CD3 and high CD25 expression. However the heterogeneous expression of the other markers hindered their use in identifying subpopulations of cells in the Ik$^{L/L}$ tumors.
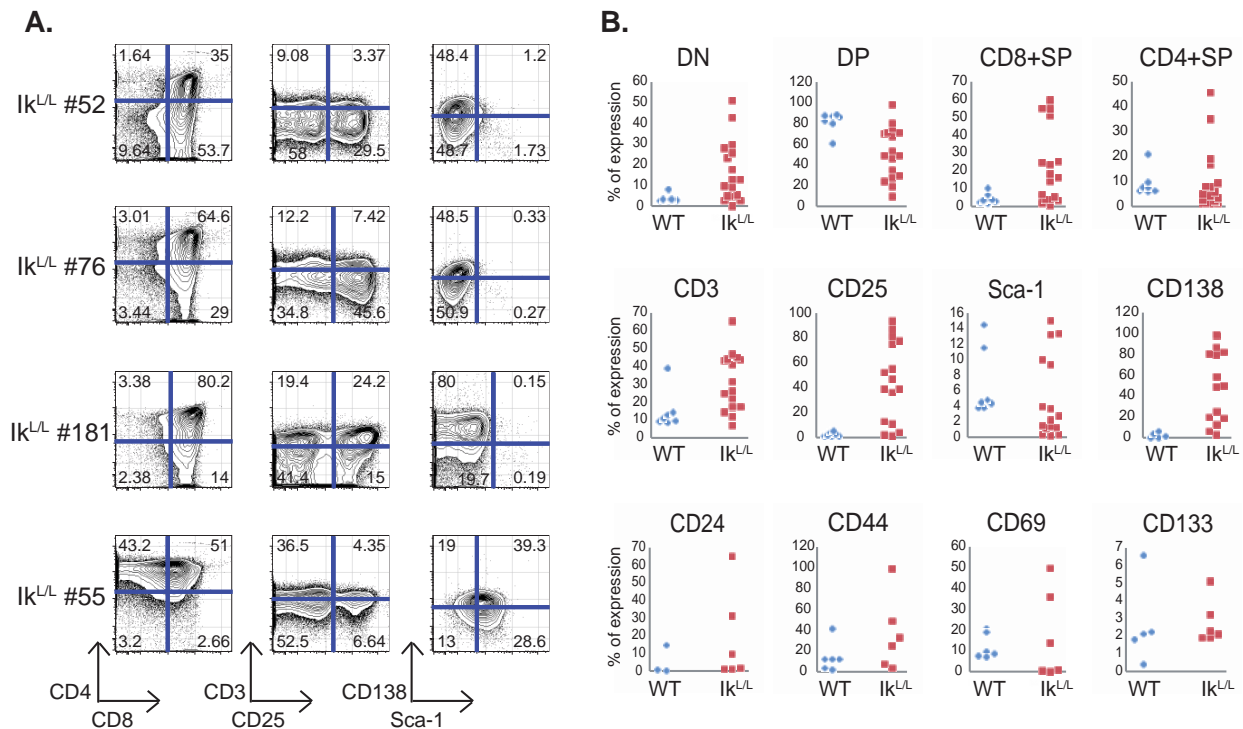
Figure III.6. Heterogeneous phenotype of Ik$^{L/L}$ tumors. Several Ik$^{L/L}$ tumors were analyzed by surface staining to identify the most common phenotype. A. Examples of the most frequent phenotypes in terms of CD4/CD8, CD3/CD25 and Sca-1/CD138 markers. B. Graphs showing the percentages of subpopulations (DN, DP, CD8+SP and CD4+SP) or the expression of different markers used for the phenotype analysis of the tumors.

III.2.3.1.3. Tumor amplification.

It is important to analyze the characteristics of the same tumor by different tests. However it was not possible to perform all of the analyses with primary tumor cells or to have enough cells to do it. To be able to study the same Ik$^{L/L}$ tumor in different experiments (transplantations), we performed tumor amplification in vivo. First, the primary Ik$^{L/L}$ tumors were analyzed by surface staining and then frozen in 90%FCS/10% DMSO. Then, the selected tumor was amplified by injecting 10x10^6 Ik$^{L/L}$ tumor cells into lethally irradiated recipient mice. 12-15 days after the injection, the tumor obtained in the recipient mouse showed the same phenotype as the primary tumor in terms of CD4/CD8 and CD3/CD25 surface staining (Fig. III.7). Thus, it was possible to work with the same tumor by amplifying the primary tumor in a recipient mouse. In addition, we hypothesized that the high number

of injected cells and the fast development of the tumor in recipient mice might avoid the selection of different clones in the tumor.
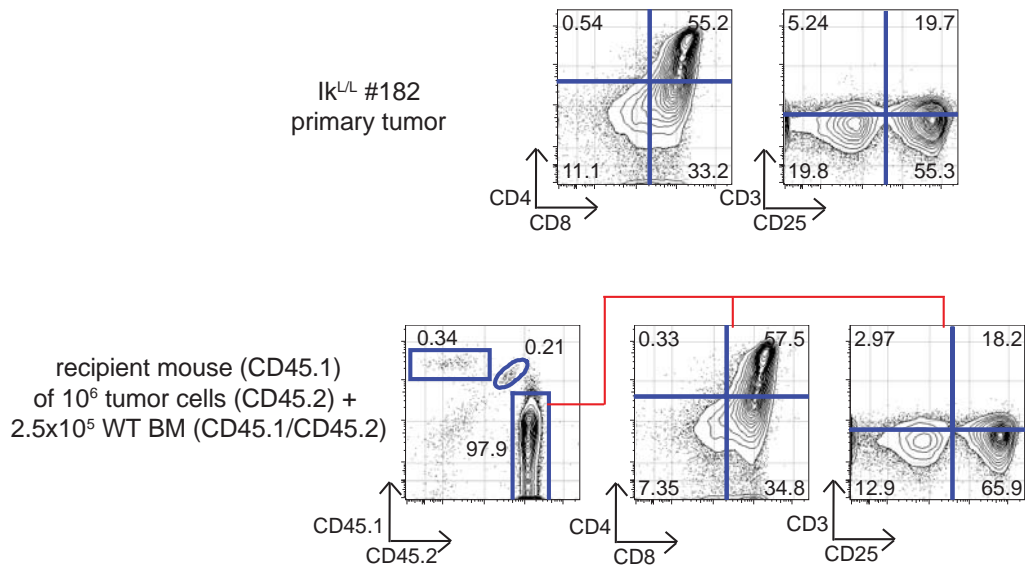
Figure III.7. Tumor amplification by injection of 10x10^6 Ik$^{L/L}$ tumor cells generates an "identical" tumor in the recipient mice. Description of the primary tumor phenotype on top and the tumor phenotype (gated on CD45.2$^+$ cells) of the recipient mouse at bottom. CD45.1/CD45.2 staining allows to follow the host cells (CD45.1), the supporting cells (CD45.1/CD45.2) and the Ik$^{L/L}$ tumor cells (CD45.2).

III.2.3.2. Subpopulation transplantation

To identify the phenotype of cells that can initiate the leukemia, we performed subpopulation transplantations in which purified Ik$^{L/L}$ tumor subpopulations were injected in recipient mice. As shown before, the majority of Ik$^{L/L}$ tumors display a DP/CD8+SP cell surface phenotype with variable expression of CD3 and CD25 and high heterogenic expression of other surface markers. We decided to test the ability of the major subpopulations present in the tumors to re-initiate tumor. DP and CD8+SP tumor cells were tested and the influence of CD3 and CD25 was observed.

At the beginning, large numbers of cells were injected. In the first experiment, we injected 2x10^4 bulk tumor cells, CD8+SP CD3$^-$, DP CD3$^-$ and CD8+SP CD3$^+$ cells. In the second experiment, we injected 10^4 bulk tumor cells, DN CD3$^-$CD25$^-$, CD8+SP CD3$^-$CD25$^+$, DP CD3^{low}CD25$^+$ and DP CD3$^+$CD25$^+$ cells. All of the subpopulations gave rise to tumors in

recipient mice. Moreover, all recipient tumors displayed similar DP/CD8+SP cell surface phenotypes regardless of the initial subpopulation (data not shown). Thus, all Ik$^{L/L}$ tumor cells with the capacity to develop a tumor in recipient mice give rise to tumors with the same complexity as the original. Regarding the kinetics of development the CD8+SP CD3$^-$ population in the first transplantation (17 days versus 19-21 days for the other populations) and the DN CD3$^-$CD25$^-$ population in the second transplantation (28 days versus 39-54 days for the other populations) developed earlier, suggesting that LICs might arise in the early stages of T cell maturation.

As limiting dilution assays showed that 500 tumor cells were sufficient to develop a tumor we repeated the assay (bulk tumor, DN CD3$^-$CD25$^-$, CD8+SP CD3$^-$CD25$^+$, DP CD3^{low}CD25$^+$ and DP CD3$^+$CD25$^+$ subpopulations) by injecting only 500 tumor cells. Unfortunately, all the mice from the DP CD3$^+$CD25$^+$ group died before 12 days due to radiation problems. The DN CD3$^-$CD25$^-$ injected mice were again the first to get sick (52-54 days after transplantation). The bulk tumor and the CD8$^+$CD3$^-$CD25$^+$ injected mice were next to become sick (88 days after transplantation). Only one out of three mice injected with the DP CD3$^-$CD25$^+$ population become sick as early as the DN CD3$^-$CD25$^-$ injected mice but the other two remained healthy (Fig. III.8). The BM cells of the latter group showed a normal phenotype when analyzed 120 days after transplantation. Thus, the use of 500 tumor cells allows a better analysis of the capacity to re-initiate tumors from subpopulations.

As the DN CD3-CD25- group developed tumors the faster, we tested if the lack of CD25 gives some advantage to tumor development. We added the CD8+SP CD3$^-$CD25$^-$ subpopulation in the next assay. The CD4+SP subpopulation was also added as we found that these cells were increased after 5'FU treatment (see III.2.3.3.2. Enrichment of side population cells), suggesting that these cells were in a quiescent state and could therefore comprise LICs. Thus, bulk tumor cells, DN CD3$^-$CD25$^-$, CD8$^+$CD3$^-$CD25$^-$, CD8$^+$CD3$^-$CD25$^+$, DP CD3$^+$CD25$^+$ and CD4+SP subpopulations were tested. This time, the CD8+SP CD3$^-$CD25$^+$ injected mice were the first to get sick, followed by the DN CD3$^-$CD25$^-$ and the bulk tumor groups, suggesting that the lack of CD25 expression is not important for re-initiating

a tumor. In fact, the CD8$^+$CD3$^-$CD25$^-$ injected mice needed more time than the CD8$^+$CD3$^-$CD25$^+$ ones. The subpopulations that expressed CD4, namely DP CD3$^-$CD25$^+$ and CD4$^+$SP, did not develop tumors (Fig. III.9).

A.

B.
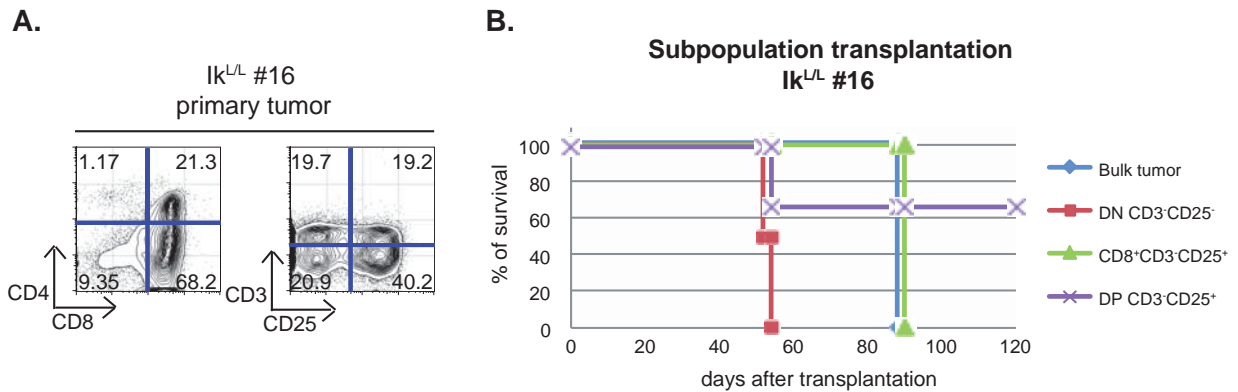
Figure III.8. The DN CD3$^-$CD25$^-$ subpopulation from the primary tumor Ik$^{L/L}$ #16 was the first one to re-initiate tumors in recipient mice. To test the capacity of different subpopulations to develop tumors, 500 sorted cells were injected. A. CD4/CD8 and CD3/CD25 phenotype of the primary tumor Ik$^{L/L}$ #16. B. Survival curve of the mice injected with bulk tumor (n=3), DN CD3$^-$CD25$^-$ (n=3), CD8$^+$CD3$^-$CD25$^+$ (n=3) and DP CD3$^-$CD25$^+$ (n=3) subpopulations.

A.

B.
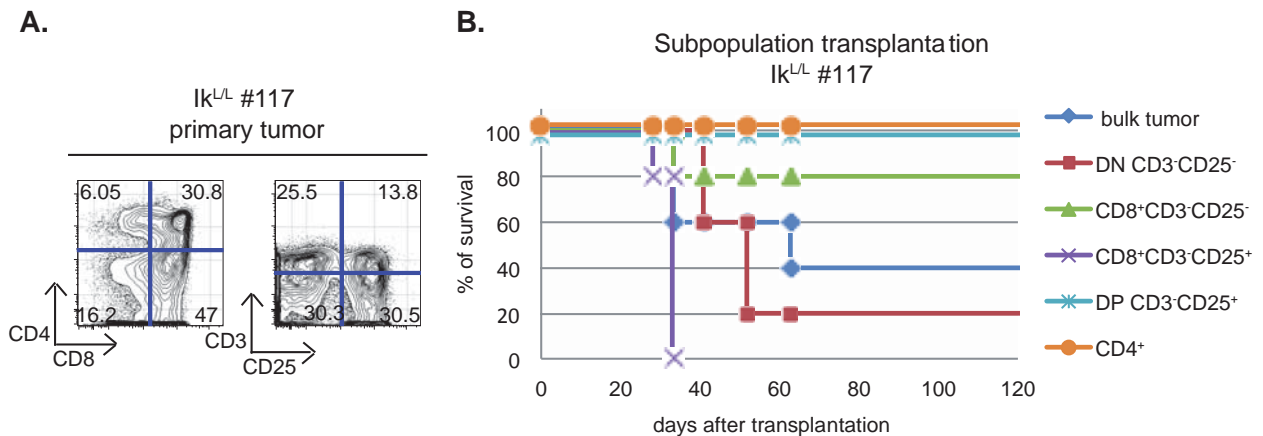
Figure III.9. The subpopulations that expressed CD4 in the primary tumor Ik$^{L/L}$ #117 did not develop tumors in recipient mice. Different subpopulations were injected at the limiting cell number (500) to test their ability to re-initiate tumors in recipient mice. A. CD4/CD8 and CD3/CD25 phenotype of tumor Ik$^{L/L}$ #117. B. Survival curve of the mice injected with bulk tumor (n=5), DN CD3$^-$CD25$^-$ (n=5), CD8$^+$CD3$^-$CD25$^-$ (n=5), CD8$^+$CD3$^-$CD25$^+$ (n=5), DP CD3$^-$CD25$^+$ (n=5) and CD4$^+$SP (n=5) subpopulations.

To have more repetitive results, we used the same tumor in different assays. The tumor Ik$^{L/L}$ #52 was amplified in recipient mice by injection of 10x10^6 cells. 13 days later, the bulk tumor cells, DN CD3$^-$, CD8+SP CD3$^-$, CD8+SP CD3$^+$, DP CD3$^-$ and DP CD3$^+$ subpopulations were sorted from the BM of the recipient mouse. This time, the requirement for CD3 expression was tested. CD3 expression seems to give some advantage, as the first mouse to develop a tumor came from the CD8+SP CD3$^+$ group, followed by one mouse each from the bulk tumor and the CD8+SP CD3$^-$ groups. However, the first group where all the mice became sick was the DN CD3$^-$ group. In this experiment, as in the previous ones with 500 tumor cells, the DP subpopulations did not develop tumors (Fig.III.10).
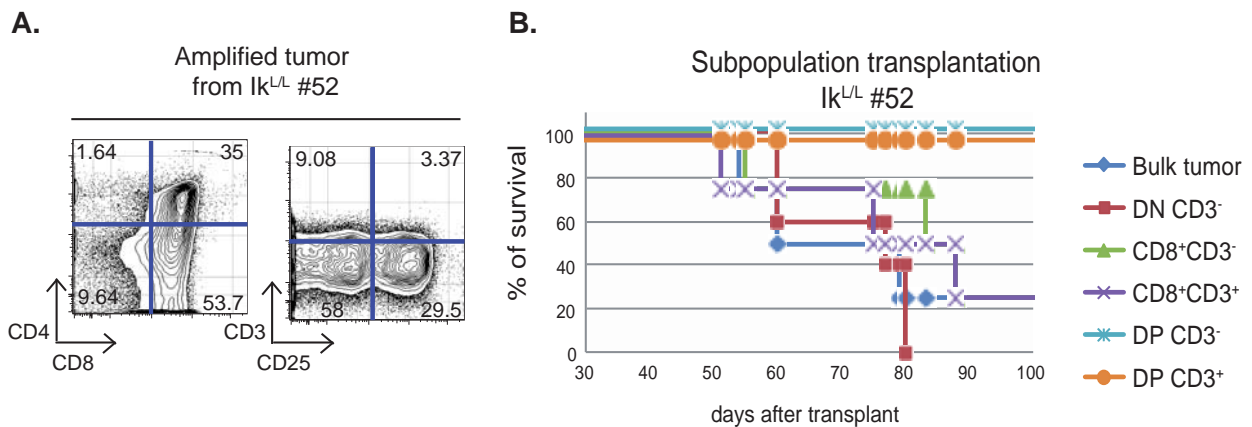
Figure III.10. Subpopulation transplantation with an amplified tumor from Ik$^{L/L}$ # 52. Different subpopulations were tested for their capacity to re-initiate a tumor in recipient mice. A. CD4/CD8 and CD3/CD25 surface staining phenotype of the amplified tumor. B. Survival curve of the mice injected with bulk tumor (n=4), DN CD3$^-$ (n=5), CD8$^+$CD3$^-$ (n=4), CD8$^+$CD3$^+$ (n=5), DP CD3$^-$ (n=4) and DP CD3$^+$ (n=5) subpopulations.

Thus, in Ik$^{L/L}$ tumors that display a DP/CD8+SP phenotype, a subpopulation of cells in the DN and CD8$^+$SP cell compartments, are more potent in re-initiating a tumor with the same complexity as the original, in lethally irradiated recipient mice. These subpopulations seem to be immature as the groups expressing CD4, DP and CD4+SP cells, did not give rise to tumors when using 500 sorted tumor cells. Although, all the subpopulations gave rise to a tumors in the transplantations of 2x10^4 or 10^4 cells this could be due to the use of high numbers of cells, where the possibility of cell contamination is higher.

III.2.3.3. Side population cells

III.2.3.3.1. Side population assay

We looked for the existence of side population cells within the Ik$^{L/L}$ tumors. Hoechst staining showed that 0.18-2% of the Ik$^{L/L}$ tumor cells are side population cells. To discriminate the side population from the bulk tumor cells, the cells were incubated with Verapamil, a specific ABC transporter inhibitor against dye efflux. These cells are specific to the tumor as we did not find side population cells in the thymus of young Ik$^{L/L}$ mouse (5 weeks old) or in the WT thymus (Fig. III.11). The side population cells of the tumor seem to have the same ability to efflux the Hoechst dye compared to the HSC present in the WT BM cells. The presence of side population cells within the Ik$^{L/L}$ tumor therefore shows a specific cell population able to efflux Hoechst dye.
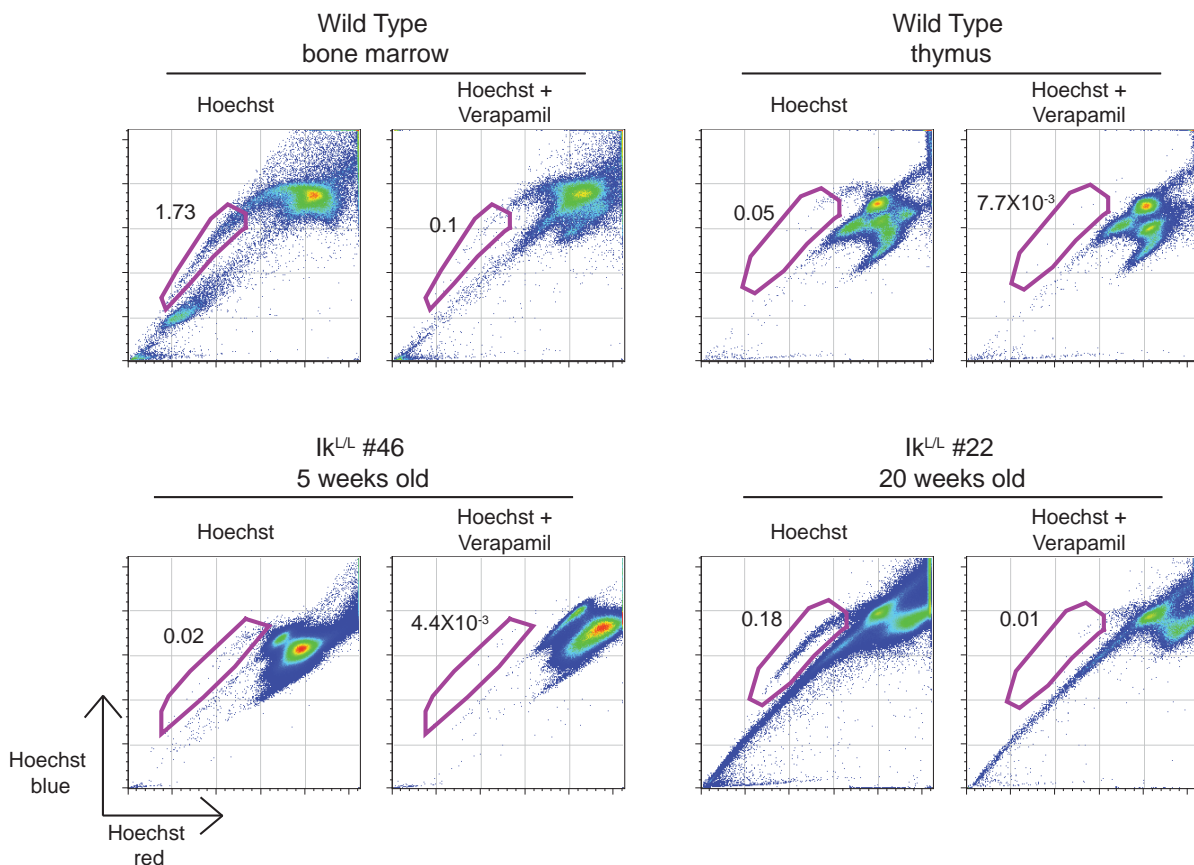
Figure III.11. The Ik$^{L/L}$ tumors contain side population cells. Analysis of side population cells by the ability to efflux the Hoechst 33258 dye (5ug/ml) with or without Verapamil (25ug/ml). The gate for side population cells was set according to their typical profiles in Hoechst red versus Hoechst blue bivariate dot plot. The side population cells were present in the HSC in the WT BM and in the Ik$^{L/L}$ tumor. However the WT thymocytes and the thymus of young Ik$^{L/L}$ mice did not contain side population cells.

III.2.3.3.2. Enrichment of side population cells

To determine if the side population cells in the Ik$^{L/L}$ tumor contain leukemia initiating cells, we needed to study their ability to generate a new tumor in recipient mice. The low frequency of these cells prevented us from to performing the transplantation. However, it was shown that the frequency of side population cells in leukemic cell lines can be increased after incubation with 5'Fluorouracil (5'FU) (Zhang et al., 2010). 5'FU is a pyrimidine analogue, with similar shape as uracil, which works through an irreversible inhibition of thymidylate synthase, thereby inducing cell cycle arrest and apoptosis in proliferating cells. This enrichment of side population cells by 5'FU treatment is based on the observation that stem cells are in a quiescent state and are resistant to chemotherapy which act on cycling cells.

To test the effect of 5'FU on the frequency of side population cells in the Ik$^{L/L}$ tumors, we injected 150mg/kg 5'FU into leukemic Ik$^{L/L}$ mice. 24 hours after 5'FU injection, the frequency of side population cells increased greatly from 0.72% in the non-injected mouse to 6.07% in the 5'FU-injected mouse (Fig. III.12B). The majority of the tumor cells died. The number of cells in the thymus decreased from 300-900x10^6 to less than 20 x10^6. Mice treated with 5'FU lost 5% of their body weight. Metastasis also decreased. The size of the spleen and the number of splenocytes was reduced compared to the untreated Ik$^{L/L}$ mice. The effect of 5'FU on WT mice was different, as it increased the percentage of side population cells in the BM (data not shown) but had no effect in the thymus (Fig. III.12A).

Beside the increase of the side population cells in the tumors, we also found an altered CD4/CD8 profile after the 5'FU treatment (Fig. III.12B). 5'FU injected tumors showed an increase of the CD4+SP and/or DN subpopulations and sometimes the phenotype resembled that of WT thymus. However, when gated on the side population cells, the CD4/CD8 profile was similar between the 5'FU treated or untreated Ik$^{L/L}$ tumors showing CD4+SP and DN subpopulations and a low percentage of DP cells (Fig. III.12B).
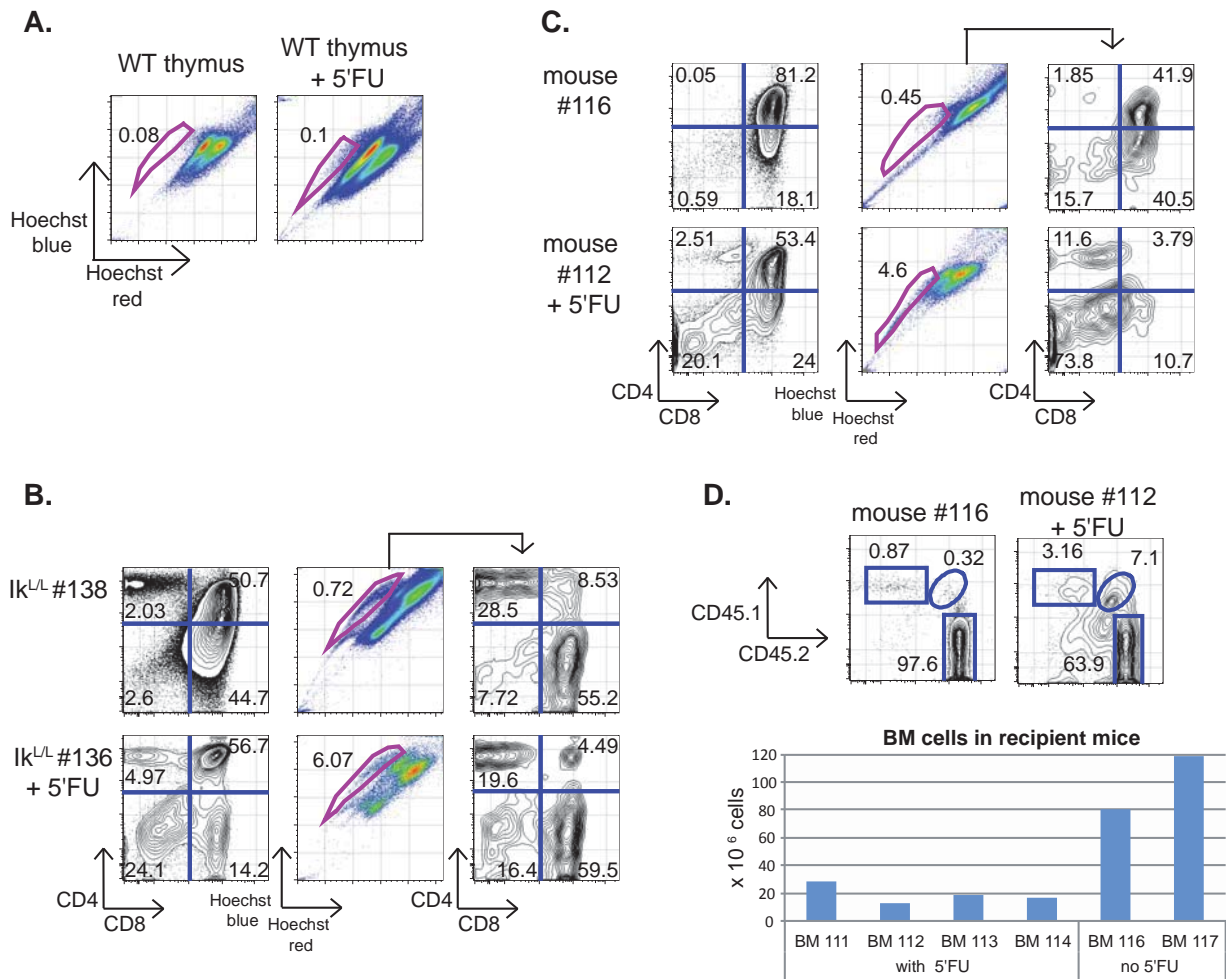
Figure III.12. The 5'FU treatment increases the frequency of side population cells in Ik$^{L/L}$ tumors. A. Side population cells present in WT thymus with or without 5'FU treatment for 24 hours. B. CD4/CD8 profile and frequency of side population cells in primary tumors treated or not with 5'FU (Ik$^{L/L}$ #136 and Ik$^{L/L}$ #138 respectively), the CD4/CD8 profile on the right was gated on side population cells present in each tumor. C. Side population analysis from amplified tumors in recipient mice treated or not with 5'FU (mouse #112 and mouse #116 respectively). The CD4/CD8 and the side population analysis were gated on live cells (Topro3 negative cells). At right, the CD4/CD8 profile from the side population cell. D. CD45.1/CD45.2 plot to discriminate between tumor cells (CD45.2), supporting cells (CD45.1/CD45.2) and host cells (CD45.1) in the amplified tumor from recipient mice injected or not with 5'FU 10 days after transplantation. The bar graph represents the number of BM cells obtained from femur and tibia from each recipient mouse injected or not with 5'FU.

As the DP/CD8+SP profile of the tumor in 5'FU injected Ik$^{L/L}$ mice were abnormal, we tested if this change was due to the 5'FU treatment, using amplified tumors. We transplanted 10^7 previously frozen tumor cells into lethally irradiated recipient mice and then treated them with 150mg/kg 5'FU at day 10 after transplantation when they started to

show disease. As we expected, the side population cells increased after the 5'FU treatment (Fig. III.12C and table III.2) from 0.45% to 4.6% in the 5'FU injected mice. The tumor phenotype changed from 80% DP/18% CD8+SP to 53%DP/24% CD8+SP with 20% of DN and 2.5% CD4+SP. In addition, analysis of BM cells of the recipient mice showed a decrease in the percentage of cells derived from the tumor cells (CD45.2) and an increase in the number of supporting cells (CD45.1/CD45.2) (Fig. III.12D). The number of BM cells of 5'FU-injected recipient was lower than that of the control recipient, suggesting that 5'FU treatment was killing both the BM supporting cells and the bulk tumor. The results indicate that tumor amplification followed with 5'FU treatment is not a good strategy to increase the frequency of side population cells.

$Ik^{L/L}$ leukemic mice				recipient mice from tumor amplification			
non-injected	% of side population	injected with 150mg/kg 5'FU	% of side population	non-injected	% of side population	injected with 150mg/kg 5'FU	% of side population
$Ik^{L/L}$ #186	0.5	$Ik^{L/L}$ #22 24h	4.3	# 116	0.45	# 111 24h	1.02
$Ik^{L/L}$ #25	0.027	$Ik^{L/L}$ #135 24h	2.4	# 117	0.22	# 112 24h	4.6
$Ik^{L/L}$ #138	0.72	$Ik^{L/L}$ #177 24h	3.15			# 113 24h	2.13
$Ik^{L/L}$ #38	0.11	$Ik^{L/L}$ #136 24h	6.07			# 114 24h	1.47
$Ik^{L/L}$ #51	0.77	$Ik^{L/L}$ #151 1w	2.81				
$Ik^{L/L}$ #22	0.15	$Ik^{L/L}$ #143 2w	3.77				

Table III.2. Percentages of side population cells obtained from different experiments where $Ik^{L/L}$ mice with tumor and recipient mice were injected or not with 5'FU. The mice were analyzed at the indicated times after 5'FU injection.

III.2.3.3.3. Side population transplantations

To test the ability of this specific subpopulation to generate new tumors, we performed 3 experiments where the recipient mice received sorted cells from $Ik^{L/L}$ leukemic mice injected with 5'FU 24hrs before. We tested different dilutions (1,000, 500 and 100 cells) of side population and non-side population cells (Hoechst retaining cells) co-injected with

$2.5x10^5$ WT BM supporting cells. As a control, one group of mice was injected with bulk tumor cells, stained with Hoechst dye and sorted for live cells (Topro3 negative cells). Unfortunately these experiments did not provide conclusive results. None of the mice become sick, even those injected with total tumor cells. We considered two possible explanations: 1) Hoechst dye toxicity (high percentage of dead cells after the staining) or 2) the 5'FU resistant cells do not proliferate anymore.

To test the first possibility we transplanted WT BM cells stained or not with Hoechst 33258. We transplanted either 10^6 or $2.5x10^5$ BM cells and followed their recovery. Two out of 3 mice injected with $2.5x10^5$ Hoechst stained BM cells died at day 10, the same time as the control mouse (irradiated but not injected), suggesting a radiation problem. The other mice injected with Hoechst stained BM cells survived and showed the same percentage of transplanted cells versus host cells as the mice injected with non-stained BM cells. These results showed that the cells stained with Hoechst can reconstitute lethally irradiated mice and that the protocol is not toxic.

To analyze the effect of 5'FU, we first assessed the ability of 5'FU resistant cells, obtained from the tumor of 5'FU injected Ik$^{L/L}$ mice, to proliferate in culture. After 20 days in non-enriched medium, the cells started to expand and showed the same CD4/CD8 profile as the primary tumor, in this case only CD4$^+$SP cells. We also tested the ability of the 5'FU resistant cells to proliferate in vivo. We transplanted 10^5 and 10^4 5'FU resistant cells into lethally irradiated recipient mice. Here we expected a fast tumor development. We followed the mice until day 100 but they did not show disease. Thus, the 5'FU resistant cells of the IK$^{L/L}$ tumors can grow in long term cultures, but they do not give rise to new tumors.

III.2.3.3.4. Analysis of the 5'FU resistant cells in the Ik$^{L/L}$ tumor

We then analyzed the 5'FU resistant cells from the primary tumors to determine if they were tumor cells. The CD4/CD8 phenotype of the 5'FU resistant Ik$^{L/L}$ tumor cells showed subpopulations that were not usually present, or at least not in that percentage. We looked at their clonality by TCR rearrangement. We performed PCR to see the Dβ2-Jβ2 TCR rearrangement from sorted DN, DP, CD8+SP and CD4+SP thymic populations of an Ik$^{L/L}$

79

mouse injected with 5'FU. The PCR showed that the DN and CD4+SP subpopulations had more than one rearrangement (Fig. III.13) and that the rearrangement detected in bulk tumor, DP and CD8+SP cells was weakly detected in these cells. Thus, 5'FU resistant cells may not all be tumor cells.
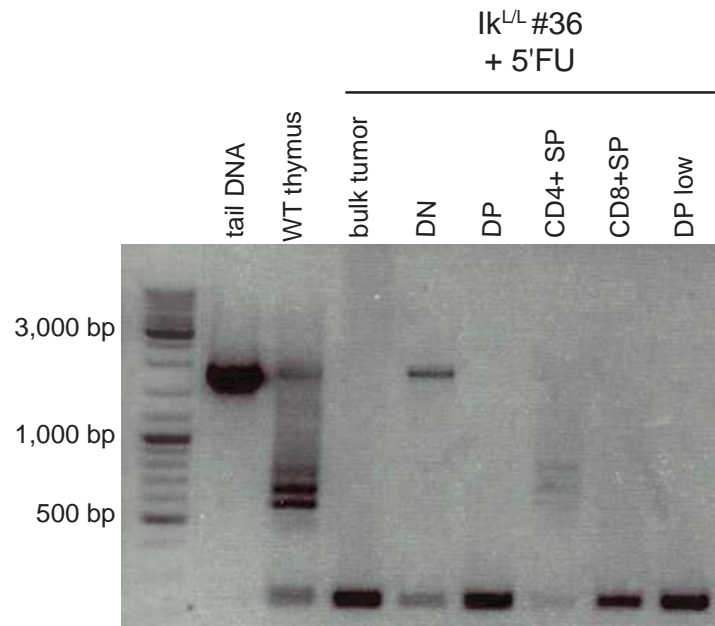
Figure III.13. The DN and CD4+SP 5'FU resistant populations are not monoclonal like the other subpopulations in the tumor. After sorting the indicated subpopulations genomic PCR was performed to check the Dβ2-Jβ2 TCR rearrangement.

III.3. Technical problems

It is important to clarify that not all the experiments were successful. At some point during this work, we started to have technical problems that affected the variability and the reproducibility of the results. During the first two years, the transplantation assays showed results with small variability between mice from the same group; the injected mice displayed symptoms of disease with a difference of +/- 2 days. Suddenly, some experiments were lost because all or the majority of the recipient mice died 10-12 days after transplantation. Those experiments were performed after the irradiator was broken, suggesting that these problems could be due to an over-dose of radiation. In fact, the mice that died did not show disease symptoms before death and the analysis of moribund mice

revealed very low numbers of cells in the BM or the spleen (these mice had no thymus). For the subsequent transplantations, we decreased the radiation dose from 9 to 8 Gy. However, we noted more variability in the kinetics of tumor development, or in the time of latency. Some mice did not get sick at all. In addition, the control mice, irradiated but not injected, did not die, demonstrating that the lethal irradiation was, in fact, not lethal. It was at this time that we performed the side population experiments, and unfortunately, the results were not conclusive.

We performed some tests on the radiation dose, as well as the age and sex of the recipient mice, but the variability continued. Therefore, the project was stopped. Thus, the functional analysis of LIC activity in the $Ik^{L/L}$ tumors was not successful as the technical problems affected the interpretation of the transplantation assays.

Section III. **Analysis of leukemia initiating cells in a mouse model of T-ALL deficient for Ikaros**

DISCUSSION

Here, we described the analysis of LICs in the Ikaros deficient mouse model of T-ALL. We demonstrated that Ik$^{L/L}$ tumors contain cells with self-renewal capacity that are present in 1 in 500 cells. These cells are able to re-initiate the tumor with the same characteristics as the original tumor. Various subpopulations of tumor cells exhibited different capacities to initiate the tumor in transplantation assays. Although they exhibit a heterogeneous expression of stem cell-related surface markers, Ik$^{L/L}$ tumor cells display characteristics associated with stem cells such as quiescence and the ability to efflux the Hoechst dye. Thus, these results strongly suggest the existence of LICs in the Ik$^{L/L}$ tumors although their phenotype remains unclear.

The 1/500 frequency in the Ik$^{L/L}$ tumors is higher than the $1/5 \times 10^5$ to $1/10^7$ frequency required for the xenograft of human CD34$^+$CD7$^-$ T-ALL cells (Cox et al., 2007). Yet, it is lower than the 1/10 cells necessary to develop a Notch1 dependent tumor in a murine model of T-ALL (Li et al., 1008). Here we showed that the Ik$^{L/L}$ self-renewing cells are able to generate the heterogeneity of the original tumor in the recipient mice a function that is expected of LICs. In addition, the potential Ik$^{L/L}$ LICs were found in different subpopulations. Thus, Ik$^{L/L}$ tumors have a subset of cells that can be described as LICs by the functional characteristics of self-renewal and by their ability to regenerate tumors with the same complexity or heterogeneity as the original tumor.

Do the Ik$^{L/L}$ tumor cells have characteristics of normal stem cells? The analysis of the Ik$^{L/L}$ tumors revealed a population of cells with the ability to pump out the Hoechst dye, the so called side population cells. These cells are present at low frequencies, but they are tumor specific, as they are absent in WT or in 5-week-old Ik$^{L/L}$ thymi. 5'FU treatment also increased the percentage of side population cells in the Ik$^{L/L}$ tumors. In addition, the 5'FU treatment showed that there are non proliferative cells within the tumors. Thus, Ik$^{L/L}$ tumors

contain cells that have stem cell-like characteristics such as the ability to efflux the Hoechst dye and quiescence. However, these results do not indicate the definitive presence of LICs. Though side population cells have been demonstrated to exist in different types of cancers and are associated with CSC activity (Chiba et al., 2006; Haraguchi et al., 2006; Wu et al., 2007; Chua et al., 2008), the expression of ABC transporters, is not exclusive to stem cells (Cooray et al., 2002; Tang et al. 2010). Additionally, the interpretation of the side population assay can be altered because Hoechst binds to DNA and tumor cells often exhibit aneuploid populations, leading to a more heterogeneous Hoechst profile (Golebiewska et al., 2011). Thus, the identification of cells with stem cell-like characteristics such as the efflux of Hoechst dye and quiescence within the Ik$^{L/L}$ tumors is an important finding. However, these cells cannot be called LICs until they are tested for their functional capacity to self-renew. Unfortunately, the transplantation assays performed to test their capacity were not conclusive and they have to be repeated.

Which model could explain the heterogeneity of the Ik$^{L/L}$ tumor cells? Is it possible to have functionally distinct LICs within a tumor? The 1/500 frequency of the LICs in the Ik$^{L/L}$ tumors indicates that LICs are not a rare event, which suggests that the stochastic model could explain the heterogeneity in the Ik$^{L/L}$ tumors. However, not all the subpopulations have the same capacity to reinitiate a tumor. In fact, the subpopulation transplantation performed with 500 tumor cells showed that the DP and CD4+SP subpopulations did not generate tumors in the recipient mice. This suggests that the cells within a Ik$^{L/L}$ tumor differ in terms of tumor initiation. The observation that various subpopulations give rise to tumors with distinct kinetics could suggest the existence of different functional LICs. It is possible that one subpopulation might have the ability to serially transplant the tumor, while others might not be able to establish long term due to a very low frequency of LIC. This was observed with CD34^{+}CD7^{+} and CD34^{-}CD7^{+} cells in human T-ALL where both populations have LIC activity but the percentage of engraftment in serial transplantation was lower with the CD34^{-}CD7^{+} cells (Gerby et al., 2011). Thus, the serial transplantation of the different subpopulations highlights the populations where LICs are enriched. This experiment should be done with the Ik$^{L/L}$ tumors. Another interesting experiment that could be done to clarify the existence of different LICs in the Ik$^{L/L}$ tumors is the comparison of the CNA profiles from

original and serial transplanted Ik$^{L/L}$ tumors, in order to detect the different genetic changes that might occur at transplantation and the comparison of these changes between the recipient tumors.

MATERIALS AND METHODS

1. Mice

The Ik$^{L/L}$ mouse line has been described previously (Kirstetter et al., 2002). The tumor formation was checked weekly by the apparition of disease (lethargy, hunched back, palpable spleen growth, anemia (by discoloration of the footpad), and hair loss). The recipient mice were C57BL/6J female mice from Charles River at 6-7 weeks of age. Supporting BM cells come from B6/Ly5.1 (CD45.1$^+$ CD45.2$^-$) and mice from crossing B6/Ly5.1 with C57BL/6J (CD45.1$^+$CD45.2 $^+$) mice. These mice were occasionally used as recipient mice. The Ik$^{L/L}$, B6/Ly5.1 and t B6/Ly5.1-C57BL/6J mice were bred in the specific pathogen free (SPF) animal rooms in this institute.

2. PCR

10^7 cells were digested in 500µl tail digestion buffer (100 mM Tris-HCl, pH8.5, 5mM EDTA, 0.2% SDS, 200mM NaCl, 100µg/ml proteinase K) at 50°C overnight and spun down at 13,000 rpm for 5 min. DNA was precipitated by adding 1 volume of isopropanol, washed with 70% ethanol and resuspended in 200µl TE (10mM Tris-HCl, 0.1 mM EDTA). For genotyping, the mouse tails were cut when mice were at 1-2 weeks age and then digested in the same way. 2 µl of the DNA dilution were used as PCR templates.

The PCR was done with the following conditions:

Ik$^{L/L}$ genotyping. One cycle of 5 min at 94°C, 40 cycles of 15 sec at 94°C/30 sec at 60°C /30 sec at 72°C and 1 cycle of 5 min at 72°C.

Dβ2-Jβ2 rearrangements. One cycle of 5 min at 94°C, 30 cycles of 30 sec at 94°C/45 sec at 60°C /1 min at 72°C and 1 cycle of 5 min at 72°C.

The primers were:

Genotyping	ABG209	GAAGCCCAGGCAGTGAGGTTTTTCC
	ABG301	GGCAAAGCGCCATTCGCCATTCAG
	ABG304	CATGCCTCGATCACTCTTGGAGTTC
Dβ2-Jβ2 rearrangements	Dβ2.1	GTAGGCACCTGTGGGGAAGAAACT
	Jβ2.7	TGAGAGCTGTCTCCTACTATCCATT

3. Flow cytometry

To stain surface markers, up to 5×10^6 cells were put in round-bottom 96 well plates. Cells were spun down at 1200 rpm for 2 min. Cells were incubated with biotin-labeled or purified primary antibody diluents in 25 µl of staining buffer for 10 min on ice in dark. Cells were washed and stained with fluorochrome-conjugated antibodies (primary and secondary) as the previous steps. Stained cells were resuspended in staining buffer and analyzed directly by FACSCalibur or FACS LSR II (BD BioScience) and FlowJo software (TreeStar). Tumor cells were sorted on FACSAria II SORP (BD BioSciences).

The following antibodies were used:

Anti-	Clone	Conjugated	Company
CD3	500A2	V500	BD Pharmingen
CD4	RM4-5	PE	BD Pharmingen
		AlexaFluor-647	
		APC	
	GK1.5	AlexaFluor-700	eBioscience
CD8	53-6.7	PerCP-Cy5.5	BD Pharmingen
		Biotin	
		FITC	
		PE-Cy5	Biolegend
CD16/CD32	93	unconjugated	eBioscience
		PE-Cy7	
CD24	30F1	PE	eBioscience
CD25	PC61	PE	BD Pharmingen
		APC	
CD34	RAM34	FITC	BD Pharmingen
CD43	S7	FITC	BD Pharmingen
CD44	1M7.8.1	PE-Cy7	Biolegend
		PE-Cy5.5	eBioscience
CD45.1	A20	APC-eFluor 780	eBioscience
		PE	
		PE-Cy7	
CD45.2	104	PE-Cy7	Biolegend
	104.2	FITC	BD Pharmingen
CD48	BCM1	APC	eBioscience
CD69	H1.2F3	FITC	BD Pharmingen

CD71	C2	Biotin	BD Pharmingen
CD90.2	5a-8	PE	Invitrogen
CD133	13A4	Biotin	eBioscience
CD138	281-2	Biotin	BD Pharmingen
CD150	TC15-12F12.2	PerCP-Cy5.5	Biolegend
		PE-Cy7	
c-kit	2B8	APC-Cy7	Biolegend
		Pacific Blue	
		Biotin	Invitrogen
FLT-3 (CD135)	A2F10.1	PE	BD Pharmingen
γδ-TCR	GL3	Biotin	BD Pharmingen
IL-7R	A7-R34	PE-Cy7	eBioscience
		APC-eFluor 780	
Sca-1	D7	FITC	BD Pharmingen
		PE	
		PE-Cy5	Biolegend
Streptavidin		Pacific Blue	Invitrogen
		APC-Cy7	
		AlexaFluor 405	
Ter119	Ter-119	APC	BD Pharmingen

Staining buffer: PBS 0 + .5% BSA + 2mM EDTA

4. Cell transplantation

The recipient mice were lethally irradiated one day before transplantation 2 times at 4.5Gy with around 4 hr interval. Tumor cells obtained from primary/recipient or thawed cells were resuspended with BM supporting cells in IMDM media +10% FCS and injected into recipient mice at 400 µl volume through tail vein

5. Cell freezing and thawing

To freeze cells, after centrifuging at 1200 rpm for 5min, cells were resuspended in 90% FCS,10% DMSO at 10^6 to 10^7 cells/ml. Aliquots of cells in cryogenic vials were kept at -80°C. To thaw cells, cells stocks were quickly thawed in 37°C water-bath. Thawed cells were transferred to 10 ml medium and centrifuged at 1200 rpm for 5 min. Cells were washed again, counted and resuspend in adequate volume to injected into mice

6. 5'FU treatment

5'FU was administered at dose of 150mg/kg by intraperitoneal injection. 5'FU (Fluorouracile Dakota, Sanofi-Aventis France) was stocked at 50 mg/ml at room temperature. 1:5 dilution was done with PBS before use.

7. Side population Assay

Up to $5x10^6$ cells were resuspended in 900 µl staining media (DMEM + 2% FCS + 10mM HEPES). Hoechst 33342 (Sigma) stock (5 mg/ml in H2O) was diluted in medium to obtain the working dilution (5µg/ml). Both, cells and dye were incubated for 20-30 min at 37^oC in a water bath to warm them up. 100 µl of Hoechst working dilution were added to the cells and incubated for 90 min at 37^oC. For control, one aliquot of cells were also incubated in presence of Verapamil at 25µg/ml. The cells were mixed every 15-20 min by tube inversion. After incubation the reaction was stopped by putting the cell tube in ice. The cells were spun down at 1200rpm for 5min in a pre-cooled centrifuge. Cells were washed with cold PBS with 2% FCS and 10mM HEPES. Cells were stained for surface markers as describe before always keeping the cells cold. Topro3 was added before acquiring to exclude dead cells. The side population cells were analyzed in the FACSAria II cell sorter (BD BioScience).

The staining media was. Hoechst 33342 (Sigma) were stocked at 5mg/ml in H2O, and diluted in medium to obtain the working dilution 5µg/ml. Verapamil (Sigma) were stoked at 100mg/ml and diluted to obtain 25µg/ml before use.

Section IV. **B CELL ACTIVATION AND ITS RELATION WITH AUTO-IMMUNE SYMPTOMS IN THE IK$^{L/L}$ MOUSE**

INTRODUCTION

IV. 1. Mature B cells in the Ik$^{L/L}$ mice

In contrast to other Ikaros targeted models, Ik$^{L/L}$ mice exhibit less severe hematopoietic defects (see Table I.1) and develop relatively normal numbers (~50%) of splenic B cells postnatally (Kirstetter et al., 2002) making the Ik$^{L/L}$ mouse a useful genetic model to study Ikaros function in B cells.

Ik$^{L/L}$ mice exhibit a striking reduction in pre-pro-B cells (Fr. A) (see Fig.I.4) in comparison to WT mice. There are 5x fewer B cell progenitors in Ik$^{L/L}$ than in WT BM, as measured by *in vitro* colony formation in response to IL-7 (Kirstetter et al., 2002). Besides the block in pre-pro-B cells, Ik$^{L/L}$ mice also exhibit a partial block between the pro-B and pre-B (Fr. C to Fr. D) stages. The Ik$^{L/L}$ pro-B cells were found to express lower levels of *Rag1/2* and *Igll1* (λ5). This indicates that Ikaros promotes this transition by playing an important role for *Igh* rearrangement and/or the expression of the pre-BCR components (Kirstetter et al., 2002).

Despite the block in differentiation some Ik$^{L/L}$ B cells differentiate and establish a mature compartment. In contrast to the BM, splenic Ik$^{L/L}$ B cells express B220 at similar levels compared to WT and the proportion of immature versus mature B cells appear normal (Fig. IV.1) (Kirstetter et al., 2002). The Ik$^{L/L}$ B cells proliferate *in vitro* to lower concentrations of anti-IgM stimulation than WT B cells. However, they form less germinal centers than WT (Kirstetter et al., 2002). Thus, Ik$^{L/L}$ B cells are less able to respond to antigen even though they have a lower threshold of activation. However, it remains unclear how Ikaros contributes to the regulation of B cell activation. Furthermore, Ik$^{L/L}$ mice exhibit abnormal serum antibody levels, as characterized by reduced IgG$_3$, IgG$_1$ and increased IgG$_{2b}$ and IgG$_{2a}$ (Kirstetter et al., 2002). Until now, it is unknown if Ikaros deficient B cells are predisposed to produce autoantibodies as has been found for B cells from other mouse lines with reduced B cell

activation thresholds (Gauld et al., 2006). The results shown in section IV provides answers to these questions.
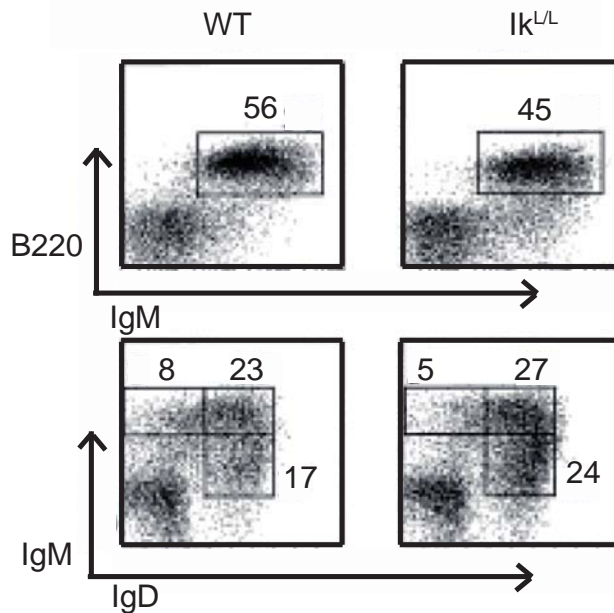
Figure IV.1. Analysis of splenic Ik$^{L/L}$ B cells. (Kirstetter et al., 2002) Splenocytes from WT and Ik$^{L/L}$ mice were stained with anti-B220, anti-IgM and anti-IgD antibodies. Ik$^{L/L}$ splenocytes express B220 at levels comparable to WT and the proportion of immature (IgM$^+$IgD$^-$) versus mature (IgM$^+$IgD$^+$ and IgM^{lo}IgD$^+$) B cells appear normal.

IV.2. B cell receptor signaling

IV.2.1. BCR structure

The BCR is a multiprotein structure consisting of an antigen-binding, membrane-bound immunoglobulin (mIg) component and two signal transduction molecules: Igα and Igβ (Dal Porto et al., 2004). The mIg consists of two identical Ig light chains (IgL) and two identical Ig heavy chains (Igh). Each of them has a variable and constant region. The complementary-determining regions (CDR) present in the variable region of each Ig chain are responsible for the variability of the antigen-binding, creating a ligand-binding site unique for every BCR. The constant region of the Igh directs the expression of different isotypes. Moreover, after the constant region of the Igh, there is a transmembrane region to anchor the mIg into the cell membrane. mIgM molecules have only a very short cytoplasmic tail and they cannot transduce signals into the cytosol (DeFranco, 1993). The Igα and Igβ heterodimer,

representing the signaling–transduction subunit of the BCR, is noncovalently associated with the mIg (Reth, 1992). The cytoplasmic tails of Igα and Igβ contain one immunoreceptor tyrosine-based activation motif (ITAM) that enables the transmission of extracellular signals (Flaswinkel and Reth, 1994). The ITAM is a conserved motif including two tyrosine residues that endow the antigen receptors with specific binding sites for Src homology 2 (SH2) domain containing proteins (Reth, 1989).

IV.2.2. BCR activation

B cells are a critical component of the adaptive immune system. B cell activation is initiated following the recognition of an antigen by the BCR which results in a wide range of biological responses such as differentiation, activation, proliferation, anergy and apoptosis. The BCR stimulation initiates multiple signaling cascades, which are integrated into the nucleus to affect gene transcription. BCR signaling can be divided in three steps: initiation, propagation and integration (Fig. IV.2).

IV.2.2.1 Initiation

BCR signals are initiated by antigen binding, which leads to the aggregation and activation of protein tyrosine kinases. Antigen engagement leads to BCR cross-linking and phosphorylation of ITAMs by Src-family protein tyrosine kinases (PTK) such as Lyn, Fyn, BLK and Lck (Kurosaki, 1999). The Scr-family PTK are already located in the proximity of the BCR via acylation (myristoylation and palmitoylation), which anchors the kinases to the plasma membrane (Clark et al., 1992; Pleiman et al., 1994a; Resh, 1999). The highly expressed Lyn is considered as the initiator of the BCR signaling. Igα and Igβ ITAM domains are eventually phosphorylated on both tyrosine residues, which allows the recruitment of the spleen tyrosine kinase (Syk) through its tandem SH2 domains (Rowley et al., 1995). Recruitment of Syk to Igα and Igβ results in activation of the kinase, which facilitates the initiation of several different signaling pathways (Pao et al., 1998) via the phosphorylation and interaction with the adaptor molecule B cell linker protein (BLNK). Thus, the initiation of the BCR signaling is crucial for the phosphorylation of ITAMs to provide a platform for the activation of PTKs.
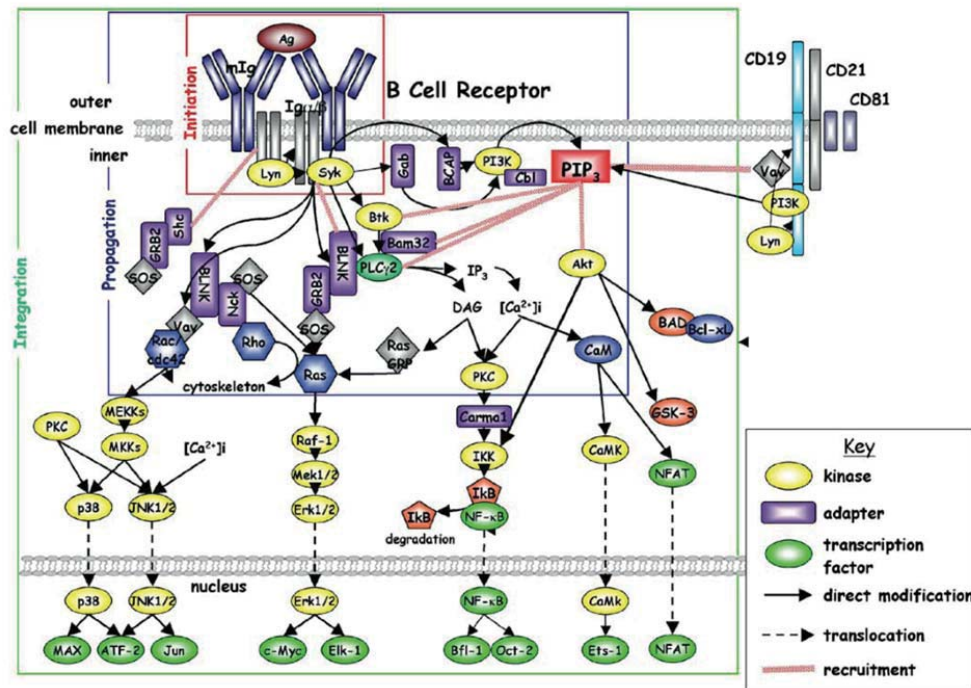
Figure IV.2. B cell receptor signaling. (Dal Porto et al., 2004). (1) Initiation: BCR aggregation triggers Igα and Igβ phosphorylation, which provides an initial platform to activate Lyn and Syk kinases for further signaling. (2) Propagation: through protein-protein and protein-lipid interactions, important scaffolding molecules and major signaling pathways, including PI-3K and PLCγ2, are recruited and activated, respectively. (3) Integration: signaling pathways that end in the nucleus and directly affect transcription factors are activated. This leads to a transcriptional response, which is a major determinant of cell fate.

IV.2.2.2. Propagation

The phosphorylation of ITAMs initiates the formation of the signalosome formed by Syk, Btk, BLNK and PLCγ2. This is an intracellular signaling complex which is mediated through protein-protein and protein-lipid interactions. Upon BCR ligation, phosphatidylinositol-3-kinase (PI-3K) is activated by its recruitment to the plasma membrane (Gold et al., 2000). It then, phosphorylates the plasma membrane lipid phosphatidylinositol-4,5-bisphosphate (PIP$_2$) to make phosphatidylinositol-3,4,5-trisphosphate (PIP$_3$) (Gold et al., 1992). This step is essential for the recruitment of the Bruton's tyrosine kinase (Btk). Once Syk and Btk are activated, progression of signaling requires the tyrosine phosphorylation-dependent activation of effector molecules such as phospholipase-Cγ2 (PLCγ2) (Dal Porto et al., 2004). It was described that the adaptor molecule BLNK (also known as SLP-65 or BASH) was

92

essential for PLCγ2 recruitment from the cytosol to the plasma membrane and for coupling BCR aggregation to Ca^{2+} influx (Fu et al., 1998; Goitsuka et al., 1998; Wienands et al., 1998). BLNK is phosphorylated and activated by Syk leading to the recruitment of PLCγ2, as well as other molecules such as the guanine exchange factor Vav, and the adaptor complex Grb2/SOS to activate Rac and Ras MAP kinase pathways (Dal Porto et al., 2004). Further, BLNK interacts with Btk and the phosphorylation of PLCγ2 by both Btk and Syk is responsible for PLCγ2 activity (Chiu et al., 2002; Hashimoto et al., 1999; Ishiai et al., 1999). PLCγ2 cleaves membrane-associated phosphoinositide PIP$_2$ into the I(1,4,5)P$_3$ (IP$_3$) and diacylglycerol (DAG) second messengers (Dal Porto et al., 2004). IP$_3$ diffuses to the endoplasmic reticulum (ER) and binds to the IP$_3$ receptors to mediate Ca^{2+} release from the ER into the cytosol (Fruman et al., 1999). Depletion of the ER Ca^{2+} store induces the opening of Calcium release activated calcium (CRAC) channels in the plasma membrane. The opening of Ca^{2+} permeable ion channels allows the influx of extracellular Ca^{2+} (Suzuki et al., 1999). The increased cytoplasmic Ca^{2+} concentration leads to activation of several Ca^{2+} dependent enzymes such as Calmodulin-dependent kinase and the transcription factors NF-AT and NF-κB (Bellacosa et al., 1991). DAG activates multiple Protein Kinase C (PKC) isoforms, which can in turn activate the p38, ERK and JNK MAP kinase pathways.

IV.2.2.3. Integration

BCR signaling must be integrated into a transcriptional program in the nucleus by the activation of various pathways to directly target the transcription factors.

IV.2.2.3.1. Mitogen activated protein kinases (MAP kinase pathway)

Three MAP kinases participate in BCR signaling: the extracellular signal-regulated kinase (ERK) 1/2, the c-Jun NH2-terminal kinase/Stress activated protein kinase (JNK/SAPK) and the p38 MAP kinase (Dong et al., 2002; Johnson and Lapadat, 2002) (Fig. IV.3). Each MAP kinase is activated by well defined kinase cascades and in turn phosphorylates and activates unique sets of transcription factors. The JNK and p38 pathways appear to be largely downstream of PLCγ2 signaling with the involvement of IP$_3$ and Ca^{2+} in JNK activation and DAG involvement in p38 activation (Dal Porto et al., 2004; Hashimoto et al., 1998). In contrast, the events upstream of the ERK1/2 pathway appear to be more complex. It has been shown

that ERK has both positive (survival/proliferation) and negative (apoptosis/deletion) roles depending on the maturation state and activation status of the B cell (Gauld et al., 2002; Norvell et al., 1995; Richards et al., 2001; Rui et al., 2003).

ERK1/2 can be activated as a consequence of the Ras/Raf/MEKK cascade. BCR ITAM phosphorylation recruits Shc that forms a complex with Grb2 and SOS resulting in Ras activation (D'Ambrosio et al., 1996; Nagai et al., 1995). In addition, Raf, and thereby ERK1/2, can be activated via a DAG-dependent PKC (Hashimoto et al., 1998). Moreover, PI-3K pathway may also be upstream of ERK1/2, as a dominant negative form of PI-3K or PI-3K inhibitors can interfere with ERK1/2 (Jacob et al., 2002). Finally, it was described by Guo et al. (2007) that IL-4 exposure induces an alternate pathway in which BCR mediated ERK phosphorylation become independent of PI-3K and PLCγ2 signalosome mediators but dependent on Lyn. This alternate pathway leads to the production of the autoimmunity-associated cytokine, osteopontin (Opn) by B cells, making a link between ERK activation and autoimmunity (Guo et al., 2009; Rothstein and Guo, 2009).
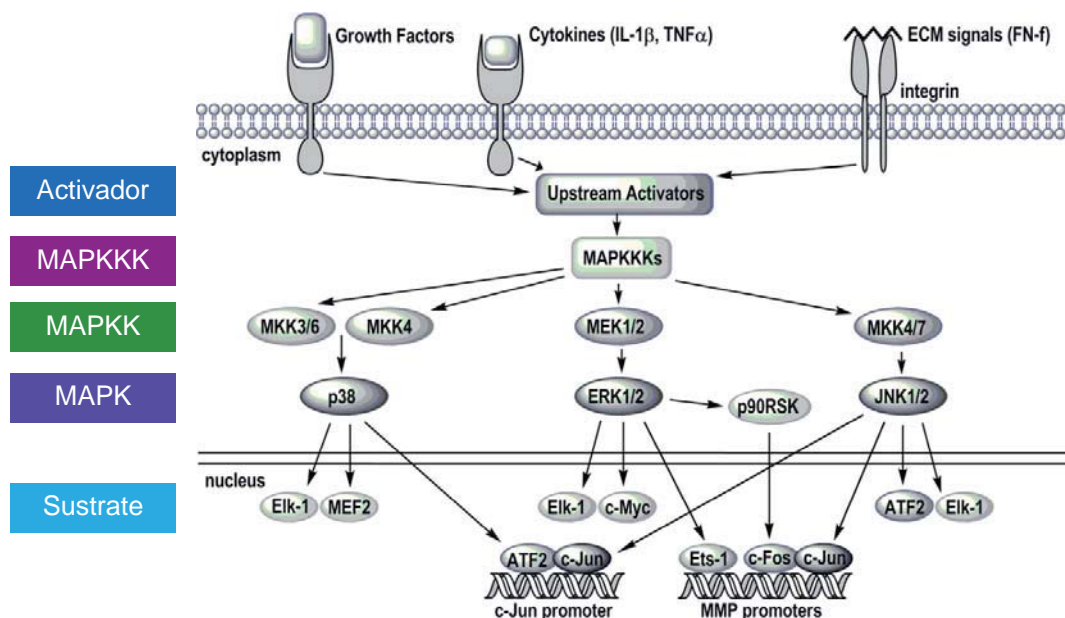
Figure IV.3. MAP kinase signaling. (Adapted from Loeser et al., 2008) A diverse array of receptors, including growth factor, cytokine, and integrin receptors, activate signaling pathways which lead to the activation of the MAP kinase pathways. MAP kinase kinase kinases (MAPKKKs) activate MAP kinase kinases (MKKs; MAP and ERK kinase or MEK), which in turn activate the MAP kinases (p38, ERK1/2, and JNK). The MAP kinases activate other kinases, such as p90RSK, and transcription factors that regulate gene transcription including Elk-1, MEF2, ATF2, c-Myc, Ets-1, and c-Jun.

IV. 2.2.3.2. Akt

Akt is a serine/threonine kinase that phosphorylates cellular targets involved in apoptosis, glycogen metabolism, and cell growth (Jastrzebski et al., 2007; Niiro and Clark, 2002). Akt lies downstream of PI-3K in BCR signaling, as the generation of PIP$_3$ results in the recruitment of Akt to the plasma membrane. Indeed, the binding of its PH domain to PIP$_3$ leads to the activation of Akt by phosphorylation at key threonine and serine sites (Bellacosa et al., 1998; Dal Porto et al., 2004). Activated Akt can then migrate to the cytoplasm and the nucleus to interact with numerous substrates and transcription factors (Jastrzebski et al., 2007; Meier et al., 1997). One substrate is Bad, a pro-apoptotic member of the Bcl-2 family, which promotes apoptosis by neutralizing Bcl-x$_L$. Akt-mediated Bad phosphorylation results in the dissociation of Bad from Bcl-x$_L$, thereby suppressing apoptosis and promoting cell survival (Datta et al., 1997; del Peso et al., 1997). Another substrate is the glycogen synthase kinase-3 (GSK-3), a multifunctional kinase involved in the regulation of cell cycle and proliferation. GSK-3 is inhibited by Akt mediated phosphorylation (Cross et al., 1995).

IV.2.2.3.3. Nuclear factor κB (NF-κB) and nuclear factor of activated T cells (NF-AT)

NF-κB consists of hetero- or homo-dimers of the subunits NF-κB1 (p50), NF-κB2 (p52), c-Rel, RelA (p65) and RelB, and is important for B cell development, proliferation and immunoglobulin class switching (Ruland and Mak, 2003). The activation of NF-κB occurs mainly via Btk/PI-3Kdependent manner, primarily through Akt but is also influenced by PLCγ2 activity, which allows their translocation to the nucleus (Petro and Khan, 2001; Dal Porto et al., 2004). The NF-AT transcription factor is also activated downstream of BCR signaling and its activation appears to be dependent on PI-3K and Ca^{2+} (Garcia-Cozar et al., 1998; Gold et al., 2000). Both, NF-κB and NF-AT are influenced by the Ca^{2+} signal. While the magnitude of the calcium response controls NF-κB activity, it is the duration of elevated Ca^{2+} that influences NF-AT and ERK activation (Dolmetsch et al., 1997).

IV.2.3. BCR mediated proliferation

BCR stimulation can induce proliferation in mature B cells through ERK, PI-3K/Akt and NF-κB pathways (Niiro and Clark, 2002). The inhibition of ERK antagonizes anti-IgM mediated proliferation, indicating that it plays an important role during this process (Richards et al., 2001). BCR signaling also induces the expression of multiple cell cycle regulatory proteins, which are likely to guide B cells through the cell cycle (Solvason et al., 1996). Indeed, one of these proteins, Cyclin D2, is crucial for BCR induced cell cycle progression (Solvason et al., 2000). Interestingly, ERK, PI-3K and NF-κB all contribute to BCR mediated Cyclin D2 induction, with PI-3K possibly being upstream of ERK (Piatelli et al., 2002; Piatelli et al., 2004). Thus ERK contributes to cell cycle progression and proliferation following BCR stimulation.

IV.2.4. BCR mediated apoptosis

Beside the BCR mediated proliferation, BCR signals can also induce apoptosis. mIgM ligation in transitional (BM and spleen) and mature B cells results in apoptosis (Allman et al., 2001; Carsetti et al., 1993). It is thought that BCR mediated apoptosis depends on the Bcl-2 family which are crucial regulators of the mitochondrial pathway for apoptosis within the mitochondrial pathway (Tsujimoto, 2003; Chao et al., 1998; Eeva and Pelkonen, 2004). While the anti-apoptotic members, Bcl-2 and Bcl-x$_L$, blocks BCR-mediated apoptosis in both B cell lines and mouse B cells, the pro-apoptotic member Bim (Enders et al., 2003) and Bad (Malissein et al., 2003) induce apoptosis. Bim induces apoptosis when it is translocated to the mitochondria, which occurs during BCR-mediated apoptosis (Enders et al., 2003). MAP kinase signaling is also involved in BCR mediated apoptosis where it plays positive and negative regulatory roles. p38 can promote BCR mediated apoptosis. p38 inhibition blocks apoptosis in response to anti-IgM stimulation, in human (Graves et al., 1996) and murine cells (Craxton et al., 1998). On the other hand, ERK can protect against or induce apoptosis depending on the maturation stage of the cells and the length of the ERK activation. In immature B cell lines, ERK may activate mitochondrial apoptosis pathways via phospholipase A2 (Katz et al., 2004). In contrast, in primary murine cells, ERK activation has been shown to be transient in transitional B cells (which all die), and more prolonged in mature cells (at least some of which survive) (Koncz et al., 2002), suggesting that temporally short ERK signals may contribute to apoptosis, while longer ERK activation could protect

cells from BCR induced apoptosis. In summary, BCR signals can induce apoptosis with different efficiency depending on B cell maturation state, and MAP kinases may act both positively and negatively in this process.

IV.2.5. BCR co-stimulators

Although Igα and Igβ are the primary signal transducers of BCR complexes, the signal can be influenced by co-receptors, which can synergize and modulate the fate of BCR signaling. Co-stimulation through CD19, CD22 or CD40 can reduce activation thresholds (e.g. the number of BCRs that must transduce a signal to induce a B cell response) (Batista et al., 2007). BCR-associated CD19 molecules positively influence the BCR signal by enhancing the recruitment and activation of Lyn, PI-3K, Btk and Vav (Bulh and Cambier, 1999; Fujimoto et al., 2000). In addition, co-stimulation mimicking T cell help (with anti-CD40) can prevent BCR induced apoptosis (Tsubata et al., 1993). Certainly, signals through CD40, IL-4R and Notch promote survival and synergize with the BCR to induce robust B cell proliferation and class switch recombination (Donjerkovic and Scott, 2000; Thomas et al., 2007). Interestingly, some co-stimulatory molecules induce signaling cascades that include MAP kinase pathways. CD40 leads to sustained ERK phosphorylation and activation (Mizuno and Rothstein, 2005). In addition, p38 is important for CD40 mediated B cell proliferation, as shown using p38 kinase specific inhibitors (Craxton et al., 1998). Indeed, synergistic promotion of B cell proliferation by Notch and the BCR is dependent on ERK activity (Thomas et al., 2007). Finally, it should be noted that some surface receptors such as CD22 and CD72 can negatively regulate BCR signaling. Both CD22 and CD72 contain immunoreceptor tyrosine-based inhibition motifs (ITIMs) in the cytoplasmic region. The phosphorylation of ITIMs mediated by Lyn activates the protein tyrosine phosphatase SHP-1, which negatively regulates BCR signal by dephosphorylating various signaling molecules (Adachi et al., 1998; Sato et al., 1996; Adachi et al., 2001; Dal Porto et al., 2004; Tsubata 2005). Thus, co-receptors play important roles in survival and proliferation and this can be mediated by the MAP kinase pathways.

IV.3. B cell tolerance

The random assembly of the BCR leads to the development of a high proportion of auto-reactive clones (up to 55-75% of immature B cells in humans) (Wardemann et al. 2003). These autoantibodies are removed by two major checkpoints, one in the BM and the second one in the periphery (Wardemann et al. 2003). The BM checkpoint consists of two distinct mechanisms: receptor editing and clonal deletion. Immature BM B cells with auto-reactive specificity can undergo receptor editing, in which they continue to rearrange their Ig genes (most often the IgL). The additional rearrangement for the LC loci replaces the auto-reactive Ig with a non-auto-reactive BCR (usually Igκ, then Igλ) (Nemazee 2006). However, receptor editing can lead to the expression of a second IgL (allelic inclusion) which dilutes the auto-reactive receptor enough to continue with normal B cell maturation (Liu et al., 2005). Clonal deletion is a negative selection for the auto-reactive BM B cells that fail to undergo receptor editing by inducing apoptosis (Carsetti et al., 1995; Halverson et al., 2004). Thus, receptor editing is the major mechanism for central tolerance and clonal deletion acts as a fail-safe mechanism.

The second checkpoint in the periphery appears to occur at the transitional B cell stage (Wardemann et al., 2003). It has been shown that T1 B cells in the spleen rapidly undergo apoptosis in response to BCR stimulation (Allman et al., 2001; Norvell et al., 1995; Su and Rawlings, 2002). This suggests that T1 B cells can be negatively selected before developing into mature B cells. It was shown that systemic lupus erythematosus (SLE) patients display an expansion in transitional B cells and plasma blasts, and a reduction in the memory B cells. Chang et al. (2008) showed that SLE patients have altered proportions of several B cell subsets and that this occurs at an early developmental stage. The T2 B cell compartment is larger than that seen in controls, a stage when B cells first acquire the capacity to proliferate in response to BCR stimuli (Chang et al., 2008). Moreover, the elevated B cell activation factor (BAFF) expression in the peripheral B cell populations in patients with SLE supports the expansion of the T2 B cell compartment which contributes to a break in the B cell tolerance (Landolt-Marticorena et al., 2011). Thus, the checkpoint at the transitional B cell

stage is important to remove self-reactive B cells before the T2 B cell stage and to avoid their accumulation, a feature seen in autoimmune disease.

In addition to these major checkpoints, other mechanisms may prevent the activation of auto-reactive cells. These cells can become anergic or ignorant. Auto-reactive B cells exposed to low levels of self antigen are subject to anergy (Shlomchik 2008). They become refractory to BCR stimulation (Cooke et al., 1994) and may also exhibit low surface IgM expression (Shlomchik, 2008).   Anergic B cells show active SHIP-2, suggesting a constitutively active inhibitory feedback loop for the BCR (Gauld et al., 2006). On the other hand, ignorant cells express BCRs that are weakly reactive to self antigens and can emerge from the BM as normal, non-self-reactive B cells. However, they respond to anti-IgM stimulation and participate in immune responses (Shlomchik, 2008). Thus, auto-reactive B cells that escape the major checkpoints can become anergic or ignorant.

Loss of B cell tolerance plays a key role in autoimmune disease. Burnet had described in 1972 his hypothesis of the forbidden clone, and proposed that autoimmune disease develops as a result of the persistence of self-reactive lymphocyte clones that should have been deleted via immune tolerance. These auto-reactive clones multiply and effect immune-mediated end-organ damage via peripheral self-antigen recognition (Burnet, 1972). Actually, the success of B cell depletion as a therapy of autoimmune disease supports the key role of B cells in the contribution to autoimmune disease (McQueen, 2012).

B cell tolerance can be affected by alterations in the activation threshold (Gauld et al., 2006; Kil et al., 2012). The unresponsiveness of the auto-reactive cells that undergo anergy is due to an active inhibition of BCR signaling (Gauld et al., 2006). On the other hand, murine B cells over-expressing Btk are hyperresponsive to BCR stimulation, show defective elimination of self-reactive B cells in vivo and exhibit antinuclear autoantibody production (Kil et al., 2012). Moreover, Wojcik et al. (2007) have suggested a possible role for Ikaros in the maintenance of B cell tolerance. Over-expression of dn Ikaros isoforms in B cells results in the accumulation of activated B cells and the production of autoantibodies (Wojcik et al., 2007). Thus, there is evidence to demonstrate a connection between activation threshold

and autoimmunity. The fact that Ik$^{L/L}$ mature B cells have a low threshold of activation (Kirstetter at el., 2002) suggests possible consequences on B cell tolerance and autoantibody production. Results in section IV address the autoantibody production in Ik$^{L/L}$ mice and its relation with SLE.

IV. 4. Systemic lupus erythematosus

SLE is a complex disease caused by an aberrant autoimmune response. It is characterized by the production of autoantibodies and clinical involvement of multiple organs. The clinical heterogeneity of the disease forced the establishment of 11 criteria with 4 needed for the formal diagnosis of SLE. These criteria include malar and discoid rash, photosensitivity, oral ulcers, arthritis, serositis, kidney (proteinuria), neurologic and blood disorders (anemia, leucopenia, lymphopenia and thrombocytopenia), immunologic disorder (anti double stranded (ds) DNA) and antinuclear antibody production. It is more frequent in females than males with a ratio of 9:1. The highest prevalence is reported in Brazil. In the USA, people of African, Hispanic or Asian ancestry tend to show an increased prevalence compared with other racial or ethnic groups. The 10-year survival rate is about 70% (Tsokos, 2011). The pathogenesis of SLE is not clearly understood and different factors (environmental and genetic) can contribute to a loss of self tolerance and organ dysfunction. The disease activity can be measured by the SLE Disease activity index (SLEDAI), where a score from 0-8 indicate low disease activity and the high disease activity is defined by a score higher than 8. The patients can be in a quiescent state, with a low SLEDAI score ($\leq$5).

The preferential susceptibility of females to SLE suggests a hormonal influence for the development of this disease. However, studies using castrated female and male mice, genetically modified to express XX or XO in females and XY or XXY in males, suggest that the cause is not hormonal but the presence of two X chromosomes that increases the severity of SLE (Smith-Bouvier et al., 2008). Epigenetic changes such as DNA methylation and histone modifications have also been described as an influential factor. Drugs such as hydralazine and procainamide inhibit DNA methylation and induce SLE in healthy persons

(Ballestart et al., 2006). In addition, the treatment of lupus-prone mice with Trichostatin A, an inhibitor of histone deacetylase, results in disease improvement (Mishra et al., 2003).

Genome-wide association studies have identified more than 30 risk genes associated with SLE. Within these loci, are genes involved in the innate immune response (IRF5), in T and B cell signaling (STAT4, TNFSF4 and Blk), in autophagy/apoptosis (ATG5), ubiquitinylation (UBE2L3, TNFAIP3, TNIP1) and phagocytosis (ITGAM, FCGR3A and FCGR3B) (Han et al., 2009; Cunninghame Graham et al., 2011). Recently, new susceptible genes, which influence the regulation of type-I and type-II interferon production were described. These loci include NCF2, IKZF1, IRF8, IFIH1 and TYK2 (Cunninghame Graham et al., 2011). A genotype-phenotype analysis to explore the relationships of some susceptibility genes with the clinical features of SLE showed that the SNP rs4917014 *IKZF1* is associated with renal nephritis and malar rash (He et al., 2010). This genotype-phenotype analysis was done by a case-only analyses (e.g. presence of malar rash versus no malar rash) to identify which subphenotypes were associated with the specific SNPs and by a subphenotype-control analyses (e.g. presence of malar rash versus healthy controls) to examine the risk conferred by the SNPs (He et al., 2010). Thus, the existence of SNPs in the Ikaros gene contributes to SLE risk. Moreover, Hu et al. (2011) have reported that the expression levels of *IKZF1* mRNA in the peripheral blood mononuclear cells from patients with SLE are significantly decreased compared to healthy controls. However, they did not find any association between the variant of the SNP rs491714 and the *IKZF1* mRNA expression levels (Hu et al., 2011). These studies suggest a role for Ikaros in the development of SLE.

The immunological events surrounding the onset of SLE highlight the central role of B cells. B cells deserve attention in the study of SLE as they produce autoantibodies, are activated during the disease, are responsible for hypergammaglobulinemia and could present some intrinsic defects (Garaud et al., 2011). Three categories of B cell defects can lead to a lupus-like phenotype: 1) B cell activation threshold, 2) B cell defects in apoptosis and 3) autoantigen processing (Anolik, 2007). It was reported that FcγRIIb deficiency leads to a lupus-like phenotype in mice by reducing the threshold of auto-reactive B cell activation (Fukuyama et al., 2005), and that its restoration prevents the expansion and accumulation of

autoantibody-producing plasma cells (McGaha et al., 2005). Moreover, polymorphisms in FcγRIIb are associated with human SLE (Floto et al., 2005).

The effects of the B cell defects in apoptosis for the development of SLE can be seen in mice transgenic for BAFF, which promotes B cell survival by blocking BCR-mediated apoptosis. Mice over-expressing BAFF develop a lupus-like phenotype with excessive numbers of mature B cells, spontaneous germinal center reactions, autoantibody production, high plasma cell numbers and Ig deposition in the kidney (Mackay et al., 1999). In addition, lupus-prone mice display alterations in BCR-mediated apoptosis. In New Zealand Black (NZB) x New Zealand White (NZW) F1 mice, defects in BCR-mediated apoptosis of B cells can be observed even in young mice, suggesting that this defect is B cell intrinsic and not a result of the disease (Tsubata et al., 1994). MRL/lpr mice carry a loss-of-function mutation in the Fas gene (Watanabe-Fukunoga et al., 1992). The Fas receptor induces apoptosis upon interaction with its ligands but it is not involved in BCR-mediated apoptosis. B cells from MRL/+ mice, which do not contain the lpr mutation, are defective in BCR-mediated apoptosis, whereas this defect is not observed in B cells from C57BL/6-lpr mice carrying the lpr mutation (Yoshida et al., 2000). Indeed, the MRL/lpr mice develop much severe disease compared to C57BL/6-lpr mice, suggesting that defects in the BCR-mediated apoptosis from the MRL background contribute to the sever disease in MRL/lpr mice. Thus, defects in BCR-mediated apoptosis contribute to the development of SLE in the lupus-prone mice.

The major characteristic of SLE is the generation of large amounts of autoantibodies directed against chromatin and other self-antigens. Thus, the loss of B cell tolerance is a key factor in the development of this disease. It was shown that the loss of B cell tolerance occurs very early, as SLE patients express antinuclear antibodies (ANA) several years before the onset of clinical disease (Arbuckle et al., 2003). Moreover, in a small number of SLE patients, peripheral checkpoints were found to be defective, leading to a further increase in auto-reactivity within the mature naïve B cell compartment (Yurasow et al., 2005). Increased autoantibody production causes the formation of immune complexes in the tissue and the further activation of complement. In the kidney, immune complexes accumulate in the

subendothelial and mesanginal areas first, followed by deposition in the basement membrane and subepithelial areas. In addition, immune complexes may accumulate in the skin and the central nervous system (Tsokos, 2011).

Thus, the onset of SLE can be influenced by the loss of B cell tolerance, to alterations in the activation threshold and autoantibody production. The results in section IV address how Ikaros, whose gene is a susceptibility locus for SLE, negatively regulates B cell activation and how Ikaros deficiency leads to the production of autoantibodies.

Ikaros deficiency promotes autoantibody production and activation of the MAPK pathway in B cells

Alejandra Macias-Garcia[1], MacLean Sellars[1,2], Sylviane Muller[3], Philippe Kastner[1,4] and Susan Chan[1]

[1]Institut de Génétique et de Biologie Moléculaire et Cellulaire (IGBMC), INSERM U964, CNRS UMR 7104, Université de Strasbourg, 67404 Illkirch, France; [3]Institut de Biologie Moléculaire et Cellulaire (IBMC), UPR9021, CNRS, 67000 Strasbourg, France; [4]Faculté de Médecine, Université de Strasbourg, Strasbourg, France

[2]Present address: New York University School of Medicine, New York, NY 10016, USA

*Correspondence: Susan Chan and Philippe Kastner
                    IGBMC
                    1 rue Laurent Fries
                    67404 Illkirch Cedex, France
                    Tel: 33-3-88 65 34 61
                    Fax: 33-3-88 65 32 01
                    Email: scpk@igbmc.fr

ABSTRACT

Systemic lupus erythematosus (SLE) is a complex autoimmune disease characterized by autoantibody production and a diverse set of clinical phenotypes. It is influenced by multiple genetic factors. The IKZF1 gene which encodes the Ikaros transcription factor was recently identified as a susceptibility locus for SLE. How Ikaros may play a role in SLE development is unclear. We show here that freshly isolated B cells deficient for Ikaros are poised for activation, and show dysregulation of multiple gene networks that regulate the mitogen activated protein kinases. Ikaros deficient B cells show enhanced ERK-1/2 and p38 phosphorylation and hyper-proliferation upon B cell receptor stimulation. Further, Ikaros deficient mice produce significant levels of SLE-associated autoantibodies. Our results suggest that Ikaros is a negative regulator of B cell activation, and protects against autoantibody production by repressing the MAPK pathway in these cells.

INTRODUCTION

Systemic lupus erythematosus (SLE) is a chronic autoimmune disorder that affects mostly women with a ratio of 9:1 females to males (1). It is characterized by the production of antinuclear autoantibodies (ANA) against double-stranded (ds) DNA, chromatin/nucleosome, histones and RNA-binding proteins (2). The clinical symptoms include skin rash, neurological and muscular manifestations, hematological and immunological disorders, and renal nephritis, which may be partly mediated by the extensive deposition of immune complexes. The etiopathology of SLE is not clearly understood and both environmental and genetic factors have been implicated.

Although the pathogenesis of SLE is complex and involves multiple cell types, B lymphocyte abnormalities have been recognized to play a major role in this disease (3, 4). Under WT conditions, engagement of the B cell receptor (BCR) is critical for the survival, differentiation and immune function of B cells (5). Co-stimulatory signals are also important, as CD40 and the IL-4 receptor signaling rescue B cells from BCR induced apoptosis, and induce and sustain B cell responses to antigen. These diverse functions are mediated by a myriad of intracellular signaling cascades that include the activation of kinases and phosphatases, the clustering of these components with the BCR in lipid rafts and intracellular Ca++ mobilization. MAP kinases such as ERK-1/2 and p38 are critical downstream mediators of BCR and CD40 signaling. ERK phosphorylation is important for B cell proliferation in response to these signals and promotes the expression of cyclin D2, required for BCR mediated cell cycle progression (6-9). ERK activity may also protect B cells against BCR induced apoptosis (10). In contrast, p38 can promote BCR mediated apoptosis, but it is required for CD40 induced gene expression and proliferation (11, 12). Thus p38 and ERK are crucial to a B cell's choice to die, or to survive and proliferate following BCR and/or CD40 stimulation.

The IKZF1 gene, which encodes the Ikaros transcription factor, was recently identified as a susceptibility locus for SLE in chinese and european populations (13, 14), suggesting that it may play a role in SLE development. Ikaros is highly expressed in hematopoietic cells, and mouse models have shown that it is essential for lymphocyte development and function. In B cells, Ikaros is required for lineage specification and differentiation (15-18), as well as for allelic exclusion at the Igk light chain locus (19, 20). In addition, transgenic mice overexpressing a dominant negative form of Ikaros in B cells exhibit some autoantibody production in their serum (21).

We have studied Ikaros function in B cells using mice bearing a knock-down mutation in the Ikzf1 locus (Ik$^{L/L}$) by homologous recombination. Ik$^{L/L}$ mice carry a LacZ

reporter within exon 2 of the Ikzf1 gene, resulting in the production of low levels of functional but truncated Ikaros proteins (10-20% of WT) in the hematopoietic cells (16). Ik$^{L/L}$ mice display a variety of defects. They develop acute T cell leukemias that result in death by 16-20 weeks of age (22). They also show a partial block in B cell differentiation at the proB cell stage (B220^{+}CD43^{+}) in the bone marrow. Interestingly, near normal numbers (~50%) of splenic B cells are detected in Ik$^{L/L}$ mice, but these cells exhibit a lower threshold of activation upon B cell receptor (BCR) stimulation (16). In addition, Ik$^{L/L}$ B cells are biased towards IgG2a and IgG2b production during class switch recombination (23).

In this study, we find that Ikaros is a negative regulator of B cell activation. Ikaros deficient B cells show enhanced ERK-1/2 and p38 phosphorylation and hyper-proliferation upon B cell receptor stimulation. Further Ikaros deficient mice produce significant levels of SLE-associated autoantibodies. Our results provide evidence that Ikaros protects against autoantibody production by repressing the MAPK pathway in B cells.

RESULTS

Autoantibody production in Ikaros deficient mice

Given that the IKZF1 gene was identified as an SLE susceptibility locus, we tested the serum of Ik$^{L/L}$ mice for SLE-associated autoantibodies. These mice were analyzed before 10 weeks of age as Ik$^{L/L}$ mice develop T cell leukemias at later stages. As a positive control, serum from 20-week-old lupus-prone MRL/Fas^{lpr} mice were included. Ik$^{L/L}$ serum displayed higher antinuclear antibody (ANA) activity on HEp-2 cells when compared with WT, when evaluated by indirect immunofluorescence (Figs. 1a, S1). In addition, Ik$^{L/L}$ serum showed significantly higher levels of IgM antibodies to chromatin/nucleosome, double-stranded (ds)DNA and histones, as measured by ELISA (Fig. 1b). Higher levels of rheumatoid factor and anti-thyroglobulin antibodies were also detected (Fig. S2). The levels of IgM autoantibodies from Ik$^{L/L}$ mice reached the lower range of those detected in MRL/Fas^{lpr} mice and were sometimes level with those of MRL/Fas^{lpr} animals (eg. anti-chromatin/nucleosome, anti-H3). IgG autoantibody levels, however, were markedly lower in Ik$^{L/L}$ than in MRL/Fas^{lpr} samples, perhaps due to the younger age of the test animals, although they were still higher than those observed in WT serum (Fig. S1). These results indicate that Ik$^{L/L}$ mice produce antinuclear antibodies associated with SLE.

Ikaros deficient B cells hyper-proliferate to stimulation

An increase in BCR signal strength is linked to autoantibody production (24, 25), and we previously reported that Ik$^{L/L}$ B cells show increased DNA synthesis after anti-IgM stimulation (16). We therefore evaluated the capacity of WT and Ik$^{L/L}$ B cells to respond to different types of stimulation. Follicular (FO) B cells (B220$^+$CD23^{hi}CD21^{lo}) were studied in order to compare more homogeneous populations between genotypes. Freshly isolated Ik$^{L/L}$ FO B cells expressed higher levels of MHC class II, CD19, CD40 and CD43 than WT cells, similar levels of IgM and IL-4R, but lower levels of CD44, CD69 and CD86, suggesting that Ik$^{L/L}$ B cells are poised but not completely activated (Fig. S2). Indeed, after 72h of culture, Ik$^{L/L}$ and WT cells did not divide in the absence of stimulation, but Ik$^{L/L}$ cells divided more when stimulated with anti-IgM, anti-IgM + anti-CD40, or anti-CD40 + IL-4, as measured by CFSE dilution (Fig. 2A). Further, more Ik$^{L/L}$ cells proliferated than WT when the percentage of proliferating (CFSE low) vs. non-proliferating (CFSE high) cells were taken into account. However, Ik$^{L/L}$ and WT cells responded similarly when stimulated with anti-IgM + IL-4 (Fig. S3). Thus, Ik$^{L/L}$ cells proliferate more than WT cells in response to most types of stimulation in a cell-intrinsic manner.

Increased proliferation was accompanied by an early entry into cell cycle. While freshly isolated cells of both genotypes accumulated at G0/G1, Ik$^{L/L}$ cells stimulated with anti-IgM + anti-CD40 entered S/G2/M as early as 16h after stimulation, with a ~2-fold increase in the proportion of S/G2/M cells between 16-32h post-stimulation compared with WT, as shown by propidium iodide staining (Fig. 2b). In addition, Ik$^{L/L}$ B cells grew bigger with activation. We measured the protein content vs. the cell cycle state of WT and Ik$^{L/L}$ B cells stimulated with anti-IgM + anti-CD40 by staining with propidium iodide and free FITC, the latter of which forms covalent bonds with lysine residues and can be used to non-specifically stain cellular proteins (26). In this assay, G0 cells can be distinguished from G1 cells by the intensity of the FITC staining (Fig. 2c). Ik$^{L/L}$ B cells grow larger and enter G1 by 12h post-stimulation, when most WT cells were still phenotypically in G0. Ik$^{L/L}$ cells remain larger than WT cells throughout the 36h period, at all phases of the cell cycle (G1, S, G2/M). Thus Ikaros deficient B cells respond to stimulation through increased cell growth, early entry into cell cycle and hyper-proliferation.

To determine if the difference in proliferation was due to a difference in apoptosis, cell viability was measured after 18h in culture. Ik$^{L/L}$ and WT cells, stimulated with anti-IgM +/- anti-CD40, were evaluated with DiOC$_6$, a fluorescent dye that accumulates in mitochondria with intact membrane potential and distinguishes live from apoptotic cells (27, 28). Anti-IgM stimulated Ik$^{L/L}$ cells showed 12% more DiOC$_6$^{hi} cells than WT, suggesting less BCR-induced apoptosis in the mutant cultures (Fig. S3). However, in cultures stimulated with anti-IgM + anti-CD40, the percentage of viable cells was similar between genotypes. Thus Ikaros deficient B cells are more resistant to BCR-induced apoptosis, but reduced apoptosis does not fully explain the hyper-proliferative phenotype observed in the mutant cells.

The transcriptional program induced by BCR stimulation is unchanged in Ikaros deficient B cells

Ikaros has been proposed to set the activation threshold in T cells by altering the transcriptional response to stimulation (29). We asked if this was also true in B cells by analyzing the global gene expression profiles of Ik$^{L/L}$ and WT B cells, stimulated with anti-IgM for 3 or 12h (Affymetrix 430 2.0 arrays). Approximately 10^4 probe sets with the greatest variance across all samples were selected, and fuzzy C-means (FCM) partitional clustering was used to identify those with similar expression patterns (Fig. S4) (30). These data revealed that most of the genes were similarly expressed between activated Ik$^{L/L}$ and WT cells (Fig. 3a), indicating that the transcriptional response to BCR signaling is largely

intact in Ikaros deficient cells. All major groups of activated and repressed genes were regulated correctly, and no ectopically induced genes were detected in Ik$^{L/L}$ cells. Surprisingly, >2000 probe sets were dysregulated between resting Ik$^{L/L}$ and WT cells; among them, 276 were increased or decreased >2-fold (Fig. 3b, Table S1). These results suggest that Ikaros deficiency changes B cells in their resting state, prior to stimulation.

To determine if the gene expression changes could affect the response of resting Ik$^{L/L}$ B cells to activation, we mined the transcriptome data for signal transduction associated genes using Ingenuity Pathway Analysis (IPA). Genes that were expressed in cells of at least one genotype, and which had a positive or negative log expression ratio (Ik$^{L/L}$ vs. WT) of ≥1.0, were fed into the IPA program. These analyses revealed an interconnected group of signal transduction genes that included IgM, as well as the MAP kinases ERK, p38 and JNK (Fig. 3c), suggesting that Ikaros deficiency modulates MAPK events downstream of the BCR and CD40.

ERK-1/2 and p38 phosphorylation is enhanced in Ikaros deficient B cells upon BCR stimulation

To determine if MAPK function was altered by loss of Ikaros, WT and Ik$^{L/L}$ B cells were stimulated with anti-IgM +/- anti-CD40, and the phosphorylation of a panel of kinases was measured by immunoblotting (Fig. 4a). These experiments showed that ERK-1/2 and p38 phosphorylation were increased in Ik$^{L/L}$ cells as early as 1 min after stimulation, and remained elevated 15 min after stimulation, compared with WT. In contrast, AKT, PKD/PKCμ, and p46/p54 JNK phosphorylation were similar or decreased in the mutant cells (Fig. 4a and data not shown). Little difference was detected in tyrosine phosphorylation between Ik$^{L/L}$ and WT cells (Fig. S5), suggesting that Ikaros deficiency does not affect the proximal elements associated with BCR signaling. ERK-1/2 and p38 phosphorylation were also examined by flow cytometry (Fig. 4b). Upon anti-IgM stimulation, all Ik$^{L/L}$ cells showed high P-ERK and P-p38 positivity compared with WT. Upon anti-IgM + anti-CD40 stimulation, cells from both genotypes showed strong P-ERK and P-p38 expression, although mutant cells continued to show higher phosphorylation levels. Akt phosphorylation levels, however, remained similar between WT and Ik$^{L/L}$ cells. Thus, Ikaros deficient cells respond to stimulation with increased ERK-1/2 and p38 phosphorylation.

Increased ERK-1/2 and p38 phosphorylation is required for hyper-proliferation in Ikaros deficient B cells

As ERK-1/2 and p38 are implicated in B cell proliferation and survival (6, 11, 31), we asked if increased phosphorylation of these kinases contributed to the hyper-proliferative phenotype in Ikaros deficient B cells. CFSE-labeled Ik$^{L/L}$ and WT B cells were stimulated after pre-treatment with U0126, to block MAP kinase/ERK kinase kinase (MEK) 1 and MEK2 signaling (which is upstream of ERK) (32), and/or SB203580, to block p38 activation (33). These inhibitors efficiently prevented ERK or p38 phosphorylation in WT B cells stimulated with anti-IgM + anti-CD40 (Fig. 4c). After 72h of stimulation, U0126 treatment reduced anti-IgM induced proliferation by ~1 division in both Ik$^{L/L}$ and WT B cells (Fig. 4d); anti-IgM + anti-CD40 stimulation was less affected. SB203580 treatment slightly increased the proliferation of both Ik$^{L/L}$ and WT cells, an effect that may be due to the inhibition of a p38-mediated apoptotic pathway downstream of the BCR (11, 12, 34). Neither inhibitor reduced the proliferation of Ik$^{L/L}$ cells to WT levels, indicating that a single MAPK pathway is not responsible for the hyper-proliferation phenotype. In contrast, when both SB203580 and U0126 were added, Ik$^{L/L}$ proliferation was reduced to WT levels, although the number of proliferating Ik$^{L/L}$ cells remained elevated. Importantly, the cells treated with both inhibitors completed up to two divisions with anti-IgM, and up to 3 divisions with anti-IgM + anti-CD40, indicating that they did not suffer from inhibitor toxicity. These results suggest that the combined increase in ERK-1/2 and p38 phosphorylation causes the hyper-proliferative phenotype of Ik$^{L/L}$ FO B cells.

As Ik$^{L/L}$ B cells enter cell cycle faster, we investigated if components of the G0/G1 to S transition were altered in mutant cells. Ik$^{L/L}$ and WT B cells were stimulated with anti-IgM +/- anti-CD40 for 0, 6, 9, 12 and 18h. The levels of CDK2, CDK4, CDK6, cyclin D2, cylin D3 and the inhibitors p19 and p27 were analyzed by Western blot (Fig. S6). These results suggest that both the positive and negative regulators of cell cycle entry were similarly expressed or induced between Ik$^{L/L}$ and WT B cells.

Ikaros deletion in mature B cells is sufficient to initiate the hyper-response to BCR stimulation and autoantibody production

As the Ik$^{L/L}$ mutation is germline, it was not possible to determine if the above changes were caused by Ikaros loss in B cells directly or indirectly via another cell type. We therefore inactivated Ikaros using a novel floxed Ikaros allele (Ik$^{f/f}$) in which the last exon encoding the dimerization domain was flanked by loxP sites. Deletion of the dimerization

domain by Cre recombinase results in a "null" allele similar to the one described by Wang et al (15).

Ik$^{f/f}$ mice were crossed with Rosa26-CreERT2 transgenic (tg) animals (35), which deletes the Ik$^{f/f}$ alleles in all tissues upon tamoxifen (TAM) injection. Ik$^{f/f}$ Rosa26-CreERT2^{+} and Ik$^{f/f}$ Rosa26-CreERT2^{-} mice were injected with TAM for 4 days and analyzed one day after that. At this timepoint, splenic FO B cells from TAM-treated Ik$^{f/f}$ Rosa26-CreERT2^{+} mice showed deletion of the floxed sequences and loss of Ikaros proteins (Fig. S7). No phenotypic differences were observed in the spleen between TAM-treated Ik$^{f/f}$ Rosa26-CreERT2^{+} or Ik$^{f/f}$ Rosa26-CreERT2^{-} mice (not shown). FO B cells from these mice were stimulated with anti-IgM and anti-CD40, and ERK-1/2 phosphorylation and proliferation were measured (Fig. 5a). TAM-treated Ik$^{f/f}$ Rosa26-CreERT2^{+} cells displayed increased ERK phosphorylation and proliferation compared with vehicle-treated cells. These results indicate that loss of Ikaros causes a rapid change in the capacity of FO B cells to respond to stimulation.

To delete Ikaros in splenic B cells, Ik$^{f/f}$ mice were crossed with CD21-Cre tg animals (36). Ik$^{f/f}$ CD21-Cre^{+} FO B cells showed deletion of the floxed sequences and loss of Ikaros proteins in splenic B cells but not in immature BM B cells or other cell types (Fig. S7). Ik$^{f/f}$ CD21-Cre^{+} and control Ik$^{f/f}$ CD21-Cre^{-} FO B cells were stimulated with anti-IgM, and ERK phosphorylation was measured (Fig. 5b). Ik$^{f/f}$ CD21-Cre^{+} cells displayed increased P-ERK compared with control cells. To determine if loss of Ikaros in B cells can initiate autoantibody production, we tested 10-week-old Ik$^{f/f}$ CD21-Cre^{+} and Ik$^{f/f}$ CD21-Cre^{-} mice for the presence of anti-chromatin/nucleosome and anti-dsDNA antibodies. Serum from Ik$^{f/f}$ CD21-Cre^{+} mice showed increased levels of IgM, but not IgG, autoantibodies compared to control animals (Fig. 5c). These results indicate that Ikaros deficiency in mature B cells is sufficient to dysregulate the MAPK response to BCR stimulation and initiate autoantibody production.

DISCUSSION

We show here that Ikaros negatively regulates B cell activation by controlling signaling cascades downstream of the BCR and CD40. Ikaros deficiency results in reduced apoptosis and increased proliferation and growth in response to stimulation. These phenotypes are due at least partly to enhanced and sustained phosphorylation of the MAP kinases ERK-1/2 and p38, as the hyper-proliferative response of Ik$^{L/L}$ B cells can be rescued through pharmacological inhibition of these kinases. Thus Ikaros controls the activation threshold in response to BCR and CD40 stimulation by repressing a regulatory network that antagonizes p38 and ERK activation. Loss of Ikaros results in the production of autoantibodies associated with SLE.

Our results are surprising in light of previous studies on Ikaros function during lymphocyte activation. In activated T cells, Ikaros has been shown to dynamically reorganize in the nucleus and enter into higher order chromatin structures where they colocalize with components of the DNA replication machinery (29). In addition, post-translational modifications of Ikaros have been reported to be important for changing the DNA binding ability of Ikaros during the G1-S transition in cell lines (37). Thus Ikaros was thought to regulate lymphocyte activation by controlling the transcriptional response downstream of antigen receptor signaling. We found that Ikaros is similarly reorganized into toroid-like structures in the nucleus of activated B cells (P. Kirstetter, PK and SC; unpublished). However, our gene expression analyses revealed that the transcriptional program downstream of BCR signaling is essentially normal in primary Ik$^{L/L}$ B cells. In contrast, we found significant gene deregulation in unstimulated Ik$^{L/L}$ B cells, indicating that Ikaros deficiency affects B cells before stimulation. Although we cannot rule out that Ikaros directly controls aspects of cell cycle progression and transcription, our data suggest that the most critical function for Ikaros during B cell activation is the modulation of p37 and ERK-1/2 MAPK signaling.

Our findings are at odds with those of Nera et al (38), who studied the effect of Ikaros on BCR signaling in the chicken DT40 cell line. Disruption of Ikzf1 in these cells leads to impaired Ca++ mobilization and reduced phospholipase Cγ2 (PLCγ2) phosphorylation after BCR cross-linking, leading the authors to conclude that Ikaros regulates B cell function by enhancing BCR signals. In our system, Ik$^{L/L}$ and WT B cells show similar Ca++ mobilization upon BCR stimulation (P. Kirstetter, PK and SC; unpublished observations), and although we did not investigate P-PLCγ2 levels here, ERK and p38 responses have been shown to be PLCγ2-dependent (39), suggesting that PLCγ2 phosphorylation is increased in Ik$^{L/L}$ cells. Further, our results on ERK and p38

phosphorylation as well as cell proliferation, using a germline knock-down mutation (Ik$^{L/L}$), a B cell specific mutation (Ik$^{f/f}$ CD21-Cre+) and an inducible mutation (Ik$^{f/f}$ Rosa26-CreERT2^{+}), clearly indicate that Ikaros functions to dampen BCR signals in primary murine B cells.

Ikaros also dampens antigen receptor signaling in T cells. Like T cells bearing dominant negative and null mutations (29), Ik$^{L/L}$ T cells hyper-proliferate to TCR stimulation (22). However, Ik$^{L/L}$ and WT T cells show similar levels of ERK-1/2 phosphorylation following anti-CD3 and/or anti-CD28 stimulation (unpublished observations). This could be due to differences in MAPK responsiveness downstream of the TCR vs. the BCR. Indeed, we have found that TCR stimulation alone leads to maximum ERK phosphorylation while CD40 co-stimulation enhances BCR-induced ERK phosphorylation in WT T and B cells, respectively. Alternatively, Ikaros may modulate MAPK signaling specifically in B cells. Further investigation will be needed to determine if a common mechanism mediated by Ikaros exists between B and T cells.

Our transcriptome analysis revealed a number of genes deregulated in freshly isolated Ik$^{L/L}$ B cells, among them potential regulators of signal transduction (see Table S1). T-plastin (Plastin-3) is the top upregulated gene in Ik$^{L/L}$ cells (up 38-fold). It is an actin filament cross-linking protein, and is homologous to L-plastin which is expressed in hematopoietic cells and has been shown to play a role in T cell activation (40). T-plastin is normally not expressed in leukocytes but is aberrantly expressed in malignant T cells (41, 42). Its role in B cell activation is currently unknown. In addition, Ptk2 (focal adhesion kinase) and its adaptor protein Grb7 are both upregulated in Ik$^{L/L}$ B cells (4.5- and 13-fold, respectively). These molecules are implicated in cell motility, proliferation and apoptosis; they are downstream targets of RapGTPases that regulate B cell morphology and spreading (43). Lastly, Rgs13, a member of the G protein signaling RGS family, has been shown to inhibit G protein-couple receptor signaling in B cells (44); it is down-regulated 11-fold in Ik$^{L/L}$ cells. It will therefore be important in the future to see if these genes are implicated in the hyper-responsive phenotype of Ikaros deficient B cells. In addition, Ik$^{L/L}$ B cells may represent a powerful tool to identify novel regulators of MAPK signaling downstream of the BCR and CD40.

Our results are in partial agreement with those of Wojcik at al who found that transgenic mice carrying a dominant negative (dn) Ikaros isoform in bone marrow B cells produce serum autoantibodies (21). This study identified a B cell intrinsic bias towards autoimmunity in the presence of dn Ikaros proteins, but it was unclear why the B cells were activated, or whether Ikaros was completely responsible for the phenotype observed, as

both Ikaros and Aiolos, a related family member, are expressed in bone marrow and splenic B cells , and the function of both can be inhibited by dn Ikaros expression. Indeed, Aiolos null B cells are hyper-responsive to stimulation and Aiolos null mice develop autoantibodies and immune complex-mediated glomerulonephritis (45, 46). In addition, IKZF3 which encodes Aiolos has recently been identified as a SLE susceptibility locus (47). Our combined results therefore indicate that Ikaros and Aiolos play unique roles in repressing autoimmunity. It remains to be determined if Aiolos also represses MAPK signaling in freshly isolated B cells, or whether its effects are directed towards cells post-stimulation.

Our results indicate that Ikaros is needed to attenuate the activation of IgM-expressing B cell clones that produce SLE-associated autoantibodies. Significant questions, however, remain unanswered. Do Ikaros deficient mice produce IgG autoantibodies, and do they show signs of physical disease such as elevated creatine levels, proteinuria and kidney destruction? These questions will require the continuing analyses of older mice bearing the B cell specific Ikaros loss-of-function mutation. If yes, then loss of Ikaros is sufficient to trigger SLE. If no, then Ikaros deficiency is important for the initiation of autoantibody production but other factors are required for disease progression.

Excessive response to antigen receptor signaling is strongly implicated in autoimmunity. It is noteworthy then that genome-wide studies have identified Ikaros polymorphisms in SLE and in Crohn's disease (13, 14, 48). Furthermore, reduced Ikaros expression was detected in peripheral blood mononuclear cells of SLE patients (49). Our data indicate that lower Ikaros levels in mice, for example in those bearing the knock-down $Ik^{L/L}$ mutation, also lead to autoantibody production. Together, these data suggest that lower Ikaros levels are associated with a predisposition to SLE. Our present results indicate that deregulation of BCR signaling may be a critical mechanism by which Ikaros deficiency promotes SLE progression. Finally, our results have implications for the potential treatment of SLE patients with Ikaros mutations or reduced Ikaros expression, and suggest that small molecule MEK inhibitors may be useful to reduce B cell hyper-activation in these patients.

MATERIALS AND METHODS

Mice

The Ik$^{L/L}$ mouse line was described previously (16). Mice were backcrossed 10 generations onto the C57Bl/6 background and were analyzed at 5-9 weeks of age. The Ik$^{f/f}$ mouse line was engineered by inserting loxP sites around exon 8 via homologous recombination in ES cells, similar to the mutation described by Wang et al (15). These mice were then crossed with CD21-Cre or Rosa26-CreERT2 tg animals (35, 36).

Cell culture

Follicular B cells were sorted on a FACSVantage SE option DiVa (BD BioSciences) or a FACSAria II SORP (BD BioSciences) (B220$^+$CD23^{hi}CD21^{lo}; >98% purity) or enriched by depletion of CD43$^+$ cells followed by positive selection of CD23$^+$ cells with MACS beads (CD43 beads and Streptavidin beads after CD23-biotin staining) (>90% purity, Miltenyi Biotech). Cells were labeled with CFSE (5μg/ml; Sigma) for 10 min at 37°C and 2.5-3x10^4 cells were cultured in flat bottom 96 well plates in 200ul complete medium (RPMI1640, 10% fetal calf serum, 25 mM HEPES, 1 mM sodium pyruvate, 2 mM L-glutamine, 1x non-essential amino acids, 5x10^{-5} M 2-mercaptoethanol and 1% antibiotics). Cells were stimulated with 10 µg/ml goat anti-mouse IgM F(ab')2 (Jackson Immunoresearch) and 2 or 10 µg/ml mouse anti-CD40 (clone 1C10; eBiosience). The following inhibitors were used: U0126 (1 µM, Cell Signaling), SB203580 (3 µM, Biotechnika). IL-4 (Peprotech) was used at 10 ng/ml. For immunoblotting (6x10^5 cells) and intracellular staining (1.5x10^5 cells), cells were stimulated at 1.5x10^5 cells/ml in 1.5ml tubes or round bottom 96 well plates, respectively, and lysed or fixed immediately after stimulation. For cell viability assays, DiOC$_6$ (Molecular Probes) was added to 50 nM and cells were incubated at 37°C for 10 min. For cell cycle and protein content staining, cells were fixed by adding ice cold EtOH to 70%, drop-wise while vortexing. After 3 PBS washes, cells were treated with RNase, and stained with 40 µg/ml propidium iodide (PI). For protein content analysis, cells were stained with 0.1 µg/mL FITC (Pierce) at RT, and washed 1x before PI staining.

Flow cytometery

The following reagents were used: anti-B220-PE-Cy7 (RA3-6B2), anti-CD19-PerCP-Cy5.5 (1D3), anti-CD21-APC (7G6), anti-CD43-FITC (S7), anti-CD44-PE-Cy7 (IM7.8.1), anti-CD69-FITC (H1.2F3) and anti-IL4R-PE (mIL-4R-M1) from BD Pharmingen, anti-CD16/32 Fc block (93), anti-CD23-biotin (B3B4), anti-CD40 unconjugated (1C10), anti-CD86-APC (GL1) and anti-MHC class II-PE (M5/114.15.2) from eBioscience, anti-IgM-PE and

13

streptavidin-PE from Jackson Immunoresearch, anti-rabbit IgG (H+L)-biotin from Vector Laboratories and anti-rat IgG-Qdot 605 from Invitrogen. Cells were analyzed with a FACSCalibur and FACS LSR II (BD BioSciences) and FlowJo software (TreeStar). For intracellular stainings for phospho-kinases, cells were fixed in 2% Ultra-pure Formaldahyde (Electron Microscopy Science) for 10 min at RT. Cells were pelleted and permeablized with 100% ice cold methanol and incubated for >30 min on ice or at -20˚C. Cells were then blocked in PBS supplemented with 10% FCS, 1% mouse serum, 1% rat serum and Fc Block (1:50). Samples were stained with the phospho-kinase specific antibodies listed below, at the manufacturer's recommended dilutions, followed by biotin conjugated anti-rabbit IgG and streptavidin-PE.

ELISA

The assays were performed according to Lacotte et al (50). Briefly, polystyrene plates (MaxiSorb, Nunc) were coated overnight at 37°C with the following antigens: individual histones H1, H2A, H2B, H3, H4 (50 ng/mm for H1 and 100 ng/ml for the core histones; Roche) in 0.05 M carbonate buffer (pH9.6), double-stranded (ds) DNA (Sigma; 100 ng/ml in 25 mM citrate buffer, pH5.4) and mouse chromatin extracted and purified from mouse lymphocytic leukemia cells L1210 [200 ng/ml expressed as dsDNA concentration in PBS, pH7.2]. Mouse sera [1:250 in PBS containing 0.05% Tween 20 (T) and 1% w/v BSA] were added for 1h, followed by goat anti-mouse IgG (1:2x104 in PBS-T; Fc gamma specific; Jackson ImmunoResearch) supplemented with goat anti-mouse IgG3 (1:7,500; Fc gamma specific; Nordic Immunology) or by goat anti-mouse IgM (1:2x10^4; mu-chain specific F(ab')2; Jackson ImmunoResearch) conjugated to horseradish peroxidase. After a 30 min incubation at 37°C, H_2O_2 and 3,3',5,5'-tetramethyl benzidine were added as substrate and chromogen, respectively, for 15 min. The reaction was stopped and the absorbance was measured at 450 nm.

Anti-nuclear antibodies (ANAs)

Assays for ANAs were performed by indirect immunofluorescence with Hep-2000 cells (Hep-2 substrate slides, Zeus Scientific INC., NJ, USA). In brief, Hep-2 cell coated slides were incubated for 30 min at room temperature with diluted sera, washed twice in PBS and visualized by fluorescence microscopy with FITC-labeled anti-mouse IgG or IgM (1:100). Controls included negative and positive sera form normal and MRL/lpr mice, respectively.

Western blot

Cells were lysed at 1.2×10^7 cells/ml with SDS lysis buffer [0.5% w/v SDS, 0.05 M Tris-Cl (pH8.0), 100 mM DTT, 100 mM Na_3VO_4, 1mM NaF, protease inhibitor cocktail (Roche)]. After 10 min on ice, lysates were sonicated and centrifuged (14K g at 4°C). Lysates were separated by SDS-PAGE and transferred to a PVDF membrane (Millipore). The following antibodies were used. Rabbit antibodies from Cell Signaling: Phospho-Akt (Ser473), Phospho-ERK (p44/42-Thr202/Tyr204), Phospho-p38 (Thr180/Tyr182), Phospho-JNK/SAPK (Thr283/Tyr185), Akt, ERK (p44/42), p38, JNK/SAPK (56G8), p27 (D37H1) and Cdk2 (78B2). Mouse antibodies from Cell Signaling: Cdk4 (DCS156) and Cdk6 (DCS83). Rabbit antibodies from Santa Cruz: p19 (M-167), Cyclin D2 (M-20), Cyclin D3(C-16) and Ikaros (H100). Other reagents included: anti-rabbit and anti-mouse horse radish peroxidase (HRP) (Jackson Immunoresearch), Immobilon Western Chemiluminescent HRP substrate (Millipore), anti-phosphotyrosine (PT66; Sigma), anti-mouse β-actin (AC-15; Sigma) and anti-mouse GADPH (Millipore).

Microarray analysis

Experiments were performed using the Affymetrix mouse 430 v2 microarray. Total RNA was isolated using the RNeasy micro kit (Qiagen). cRNA synthesis and hybridization of the array were performed according to the manufacturer's instructions (Affymetrix). Raw microarray data were analyzed using the Affymetrix MAS 5.0 software. We further selected the genes according to the following criteria: a "present call" in at least one of the samples and a coefficient of variation above 0.75 across the 12 samples, yielding a total of 10,747 genes. Fuzzy C-Means clustering was preformed as described (30), and analyzed using Cluster software (51). Data from unstimulated WT and $Ik^{L/L}$ FO B cells were further mined by Ingenuity Pathways Analysis (IPA) (Ingenuity Systems). Genes were selected based on a "present call" in either WT or $Ik^{L/L}$ samples and an average differential log ratio of ≥0.7. Log ratios of the selected genes were then submitted to the IPA application for mapping to the Ingenuity Pathways Knowledge Base.

PCR

10^6 cells were digested in 500 μl digestion buffer (100 mM Tris-HCl, pH8.5, 5 mM EDTA, 0.2% SDS, 200 mM NaCl, 100 μg/ml proteinase K) at 50°C. DNA was precipitated by adding 1 volume of isopropanol, washed with 70% ethanol and resuspended in 200 μl TE (10 mM Tris-HCl, 0.1 mM EDTA). To amplify the WT, floxed or deleted allele of Ikaros the following primers were used: 5'-GAGGACCAGATATAAGGCAGCTGGG, 5'-

15

GGCCATVAACGGCATGGAAACGATAA, 5'-AGCACAGGTTGGACAATACCTGAAA. The PCR conditions were: 94°C 5 min/ 94°C 30 s, 60°C 30 s, 72°C 45 s for 35 cycles/72°C 5 min.

ACKNOWLEDGEMENTS

REFERENCES

1. Hopkinson, N.D., Doherty, M., and Powell, R.J. 1994. Clinical features and race-specific incidence/prevalence rates of systemic lupus erythematosus in a geographically complete cohort of patients. *Annals Rheum Dis* 53:675-680.

2. Ippolito, A., Wallace, D.J., Gladman, D., Fortin, P.R., Urowitz, M., Werth, V., Costner, M., Gordon, C., Alarcon, G.S., Ramsey-Goldman, R., et al. 2011. Autoantibodies in systemic lupus erythematosus: comparison of historical and current assessment of seropositivity. *Lupus* 20:250-255.

3. Anolik, J.H. 2007. B cell biology and dysfunction in SLE. *Bulletin NYU Hos Joint Dis* 65:182-186.

4. Tsubata, T. 2005. B cell abnormality and autoimmune disorders. *Autoimmunity* 38:331-337.

5. Niiro, H., and Clark, E.A. 2002. Regulation of B-cell fate by antigen-receptor signals. *Nat Rev Immunol* 2:945-956.

6. Richards, J.D., Dave, S.H., Chou, C.H., Mamchak, A.A., and DeFranco, A.L. 2001. Inhibition of the MEK/ERK signaling pathway blocks a subset of B cell responses to antigen. *J Immunol* 166:3855-3864.

7. Solvason, N., Wu, W.W., Parry, D., Mahony, D., Lam, E.W., Glassford, J., Klaus, G.G., Sicinski, P., Weinberg, R., Liu, Y.J., et al. 2000. Cyclin D2 is essential for BCR-mediated proliferation and CD5 B cell development. *Int Immunol* 12:631-638.

8. Piatelli, M.J., Doughty, C., and Chiles, T.C. 2002. Requirement for a hsp90 chaperone-dependent MEK1/2-ERK pathway for B cell antigen receptor-induced cyclin D2 expression in mature B lymphocytes. *J Biol Chem* 277:12144-12150.

9. Piatelli, M.J., Wardle, C., Blois, J., Doughty, C., Schram, B.R., Rothstein, T.L., and Chiles, T.C. 2004. Phosphatidylinositol 3-kinase-dependent mitogen-activated protein/extracellular signal-regulated kinase kinase 1/2 and NF-kappa B signaling pathways are required for B cell antigen receptor-mediated cyclin D2 induction in mature B cells. *J Immunol* 172:2753-2762.

10. Koncz, G., Bodor, C., Kovesdi, D., Gati, R., and Sarmay, G. 2002. BCR mediated signal transduction in immature and mature B cells. *Immunol Lett* 82:41-49.

11. Craxton, A., Shu, G., Graves, J.D., Saklatvala, J., Krebs, E.G., and Clark, E.A. 1998. p38 MAPK is required for CD40-induced gene expression and proliferation in B lymphocytes. *J Immunol* 161:3225-3236.

12. Graves, J.D., Draves, K.E., Craxton, A., Saklatvala, J., Krebs, E.G., and Clark, E.A. 1996. Involvement of stress-activated protein kinase and p38 mitogen-activated protein kinase in mIgM-induced apoptosis of human B lymphocytes. *Proc Natl Acad Sci USA* 93:13814-13818.

13. Han, J.W., Zheng, H.F., Cui, Y., Sun, L.D., Ye, D.Q., Hu, Z., Xu, J.H., Cai, Z.M., Huang, W., Zhao, G.P., et al. 2009. Genome-wide association study in a Chinese Han population identifies nine new susceptibility loci for systemic lupus erythematosus. *Nat Genetics* 41:1234-1237.

14. Cunninghame Graham, D.S., Morris, D.L., Bhangale, T.R., Criswell, L.A., Syvanen, A.C., Ronnblom, L., Behrens, T.W., Graham, R.R., and Vyse, T.J. 2011. Association of NCF2, IKZF1, IRF8, IFIH1, and TYK2 with systemic lupus erythematosus. *PLoS Genet* 7:e1002341.

15. Wang, J.H., Nichogiannopoulou, A., Wu, L., Sun, L., Sharpe, A.H., Bigby, M., and Georgopoulos, K. 1996. Selective defects in the development of the fetal and adult lymphoid system in mice with an Ikaros null mutation. *Immunity* 5:537-549.

16. Kirstetter, P., Thomas, M., Dierich, A., Kastner, P., and Chan, S. 2002. Ikaros is critical for B cell differentiation and function. *Eur J Immunol* 32:720-730.

17. Reynaud, D., Demarco, I.A., Reddy, K.L., Schjerven, H., Bertolino, E., Chen, Z., Smale, S.T., Winandy, S., and Singh, H. 2008. Regulation of B cell fate commitment

and immunoglobulin heavy-chain gene rearrangements by Ikaros. *Nat Immunol* 9:927-936.

18.   Thompson, E.C., Cobb, B.S., Sabbattini, P., Meixlsperger, S., Parelho, V., Liberg, D., Taylor, B., Dillon, N., Georgopoulos, K., Jumaa, H., et al. 2007. Ikaros DNA-binding proteins as integral components of B cell developmental-stage-specific regulatory circuits. *Immunity* 26:335-344.

19.   Goldmit, M., Ji, Y., Skok, J., Roldan, E., Jung, S., Cedar, H., and Bergman, Y. 2005. Epigenetic ontogeny of the Igk locus during B cell development. *Nat Immunol* 6:198-203.

20.   Liu, Z., Widlak, P., Zou, Y., Xiao, F., Oh, M., Li, S., Chang, M.Y., Shay, J.W., and Garrard, W.T. 2006. A recombination silencer that specifies heterochromatin positioning and ikaros association in the immunoglobulin kappa locus. *Immunity* 24:405-415.

21.   Wojcik, H., Griffiths, E., Staggs, S., Hagman, J., and Winandy, S. 2007. Expression of a non-DNA-binding Ikaros isoform exclusively in B cells leads to autoimmunity but not leukemogenesis. *Eur J Immunol* 37:1022-1032.

22.   Dumortier, A., Jeannet, R., Kirstetter, P., Kleinmann, E., Sellars, M., Dos Santos, N.R., Thibault, C., Barths, J., Ghysdael, J., Punt, J.A., et al. 2006. Notch activation is an early and critical event during T-cell leukemogenesis in Ikaros-deficient mice. *Mol Cell Biol* 26:209-220.

23.   Sellars, M., Reina-San-Martin, B., Kastner, P., and Chan, S. 2009. Ikaros controls isotype selection during immunoglobulin class switch recombination. *J Exp Med* 206:1073-1087.

24.   Jacobson, E.M., and Tomer, Y. 2007. The CD40, CTLA-4, thyroglobulin, TSH receptor, and PTPN22 gene quintet and its contribution to thyroid autoimmunity: back to the future. *J Autoimmunity* 28:85-98.

25.   Tuscano, J.M., Harris, G.S., and Tedder, T.F. 2003. B lymphocytes contribute to autoimmune disease pathogenesis: current trends and clinical implications. *Autoimmunity Rev* 2:101-108.

26.   Crissman, H.A., and Steinkamp, J.A. 1982. Rapid, one step staining procedures for analysis of cellular DNA and protein by single and dual laser flow cytometry. *Cytometry* 3:84-90.

27.   Levenson, R., Macara, I.G., Smith, R.L., Cantley, L., and Housman, D. 1982. Role of mitochondrial membrane potential in the regulation of murine erythroleukemia cell differentiation. *Cell* 28:855-863.

28.   Zamzami, N., Marchetti, P., Castedo, M., Zanin, C., Vayssiere, J.L., Petit, P.X., and Kroemer, G. 1995. Reduction in mitochondrial potential constitutes an early irreversible step of programmed lymphocyte death in vivo. *J Exp Med* 181:1661-1672.

29.   Avitahl, N., Winandy, S., Friedrich, C., Jones, B., Ge, Y., and Georgopoulos, K. 1999. Ikaros sets thresholds for T cell activation and regulates chromosome propagation. *Immunity* 10:333-343.

30.   Dembele, D., and Kastner, P. 2003. Fuzzy C-means method for clustering microarray data. *Bioinformatics* 19:973-980.

31.   Han, A., Saijo, K., Mecklenbrauker, I., Tarakhovsky, A., and Nussenzweig, M.C. 2003. Bam32 links the B cell receptor to ERK and JNK and mediates B cell proliferation but not survival. *Immunity* 19:621-632.

32.   Favata, M.F., Horiuchi, K.Y., Manos, E.J., Daulerio, A.J., Stradley, D.A., Feeser, W.S., Van Dyk, D.E., Pitts, W.J., Earl, R.A., Hobbs, F., et al. 1998. Identification of a novel inhibitor of mitogen-activated protein kinase kinase. *J Biol Chem* 273:18623-18632.

33. Lee, J.C., Laydon, J.T., McDonnell, P.C., Gallagher, T.F., Kumar, S., Green, D., McNulty, D., Blumenthal, M.J., Heys, J.R., Landvatter, S.W., et al. 1994. A protein kinase involved in the regulation of inflammatory cytokine biosynthesis. *Nature* 372:739-746.

34. Swart, J.M., and Chiles, T.C. 2000. Rescue of CH31 B cells from antigen receptor-induced apoptosis by inhibition of p38 MAPK. *Biochem Biophys Res Comm* 276:417-421.

35. Badea, T.C., Wang, Y., and Nathans, J. 2003. A noninvasive genetic/pharmacologic strategy for visualizing cell morphology and clonal relationships in the mouse. *J Neurosci* 23:2314-2322.

36. Kraus, M., Alimzhanov, M.B., Rajewsky, N., and Rajewsky, K. 2004. Survival of resting mature B lymphocytes depends on BCR signaling via the Igalpha/beta heterodimer. *Cell* 117:787-800.

37. Gomez-del Arco, P., Maki, K., and Georgopoulos, K. 2004. Phosphorylation controls Ikaros's ability to negatively regulate the G(1)-S transition. *Mol Cell Biol* 24:2797-2807.

38. Nera, K.P., Alinikula, J., Terho, P., Narvi, E., Tornquist, K., Kurosaki, T., Buerstedde, J.M., and Lassila, O. 2006. Ikaros has a crucial role in regulation of B cell receptor signaling. *Eur J Immunol* 36:516-525.

39. Hashimoto, A., Okada, H., Jiang, A., Kurosaki, M., Greenberg, S., Clark, E.A., and Kurosaki, T. 1998. Involvement of guanosine triphosphatases and phospholipase C-gamma2 in extracellular signal-regulated kinase, c-Jun NH2-terminal kinase, and p38 mitogen-activated protein kinase activation by the B cell antigen receptor. *J Exp Med* 188:1287-1295.

40. Wang, C., Morley, S.C., Donermeyer, D., Peng, I., Lee, W.P., Devoss, J., Danilenko, D.M., Lin, Z., Zhang, J., Zhou, J., et al. 2010. Actin-bundling protein L-plastin regulates T cell activation. *J Immunol* 185:7487-7497.

41. Su, M.W., Dorocicz, I., Dragowska, W.H., Ho, V., Li, G., Voss, N., Gascoyne, R., and Zhou, Y. 2003. Aberrant expression of T-plastin in Sezary cells. *Cancer Res* 63:7122-7127.

42. Begue, E., Jean-Louis, F., Bagot, M., Jauliac, S., Cayuela, J.M., Laroche, L., Parquet, N., Bachelez, H., Bensussan, A., Courtois, G., et al. 2012. Inducible expression and pathophysiologic functions of T-plastin in cutaneous T-cell lymphoma. *Blood* 120:143-154.

43. Tse, K.W., Dang-Lawson, M., Lee, R.L., Vong, D., Bulic, A., Buckbinder, L., and Gold, M.R. 2009. B cell receptor-induced phosphorylation of Pyk2 and focal adhesion kinase involves integrins and the Rap GTPases and is required for B cell spreading. *J Biol Chem* 284:22865-22877.

44. Shi, G.X., Harrison, K., Wilson, G.L., Moratz, C., and Kehrl, J.H. 2002. RGS13 regulates germinal center B lymphocytes responsiveness to CXC chemokine ligand (CXCL)12 and CXCL13. *J Immunol* 169:2507-2515.

45. Wang, J.H., Avitahl, N., Cariappa, A., Friedrich, C., Ikeda, T., Renold, A., Andrikopoulos, K., Liang, L., Pillai, S., Morgan, B.A., et al. 1998. Aiolos regulates B cell activation and maturation to effector state. *Immunity* 9:543-553.

46. Sun, J., Matthias, G., Mihatsch, M.J., Georgopoulos, K., and Matthias, P. 2003. Lack of the transcriptional coactivator OBF-1 prevents the development of systemic lupus erythematosus-like phenotypes in Aiolos mutant mice. *J Immunol* 170:1699-1706.

47. Lessard, C.J., Adrianto, I., Ice, J.A., Wiley, G.B., Kelly, J.A., Glenn, S.B., Adler, A.J., Li, H., Rasmussen, A., Williams, A.H., et al. 2012. Identification of IRF8, TMEM39A, and IKZF3-ZPBP2 as susceptibility loci for systemic lupus erythematosus in a large-scale multiracial replication study. *Amer J Hum Genet* 90:648-660.

48. Barrett, J.C., Hansoul, S., Nicolae, D.L., Cho, J.H., Duerr, R.H., Rioux, J.D., Brant, S.R., Silverberg, M.S., Taylor, K.D., Barmada, M.M., et al. 2008. Genome-wide association defines more than 30 distinct susceptibility loci for Crohn's disease. *Nat Genetics* 40:955-962.

49. Hu, W., Sun, L., Gao, J., Li, Y., Wang, P., Cheng, Y., Pan, T., Han, J., Liu, Y., Lu, W., et al. 2011. Down-regulated expression of IKZF1 mRNA in peripheral blood mononuclear cells from patients with systemic lupus erythematosus. *Rheumatol Int* 31:819-822.

50. Lacotte, S., Dumortier, H., Decossas, M., Briand, J.P., and Muller, S. 2010. Identification of new pathogenic players in lupus: autoantibody-secreting cells are present in nephritic kidneys of (NZBxNZW)F1 mice. *J Immunol* 184:3937-3945.

51. Eisen, M.B., Spellman, P.T., Brown, P.O., and Botstein, D. 1998. Cluster analysis and display of genome-wide expression patterns. *Proc Natl Acad Sci USA* 95:14863-14868.

FIGURE LEGENDS

Figure 1 - Ik$^{L/L}$ mice produce autoantibodies.

(A) Indirect staining for antinuclear activity of HEp-2 cells by serum of Ik$^{L/L}$ vs. WT mice. MRL/lpr serum was used as a positive control. BALB/c serum was used as a negative control. Representative stainings from the serum of 2 Ik$^{L/L}$ mice are shown: one shows high ANA and the other shows weaker ANA. **(B)** Serum of Ik$^{L/L}$ (n=32, 6-8 weeks of age) and WT (n=18, 6-9 weeks of age) mice were tested for IgM antibodies to the indicated antigens by ELISA. MRL/lpr serum (n=4, ~20 weeks of age) was used as a positive control. Black bars show the mean of the indicated values. Statistical significance was determined by the Wilcoxon signed-rank test.

Figure 2 - Increased proliferation and early entry into cell cycle by Ik$^{L/L}$ B cells.

(A) CFSE-labeled Ik$^{L/L}$ and WT splenic FO B cells were stimulated for 72h in the presence of anti-IgM, anti-IgM + anti-CD40 (2 μg/ml), or anti-CD40 (2 μg/ml) + IL-4, then analyzed by flow cytometry. The number of divisions completed for the cells of each genotype is indicated. Gray histograms denote the CFSE labeling for non-stimulated WT and Ik$^{L/L}$ cells; both gave similar results. Representative of >3 independent experiments. **(B)** Ik$^{L/L}$ and WT B cells were stimulated for the indicated times with anti-IgM + anti-CD40 (10 μg/ml) antibodies. DNA content was measured by PI staining. The percentage of cells in the indicated phases (G0/G1, S, G2/M) of cell cycle are indicated. Representative of 2 independent experiments. **(C)** Ik$^{L/L}$ and WT cells were stimulated with anti-IgM + anti-CD40 (10 μg/ml), and analyzed at the indicated timepoints with PI and fluorescein isothiocyanate (FITC) staining. Representative of 2 independent experiments.

Figure 3 - The transcriptional response to BCR stimulation is intact in Ik$^{L/L}$ B cells.

Ik$^{L/L}$ and WT splenic FO B cells were cultured without stimulation for 3h, or with anti-IgM antibodies for 3 and 12h. Genome-wide expression analysis was performed on samples from two independent experiments, using Affymetrix 430 2.0 arrays. **(A)** The 10,747 genes with the greatest variance were selected and Fuzzy C-means clustering was used to define probe set clusters according to expression patterns (see Fig. S4). Clusters depicted are visualized globally with red/green coloration, where the red and green color scales indicate high and low expression values, respectively. **(B)** Probe sets up- or down-regulated >2-fold in non-stimulated Ik$^{L/L}$ cells were selected and clustered using the Cluster 3.0 software (see Table S1).

Figure 4 - Ik$^{L/L}$ B cells show hyper-phosphorylation of ERK and p38 after BCR stimulation.

(**A**) Ik$^{L/L}$ and WT splenic FO B cells were stimulated with anti-IgM or anti-IgM + anti-CD40 (10 µg/ml) for the indicated times. Immunoblotting was performed to determine the phosphorylation levels of the indicated kinases. GAPDH was used as a loading control. (**B**) Cells were stimulated as in (A), and P-ERK, P-p38 and P-Akt levels were measured by intracellular flow cytometry. Staining was performed after 15 min stimulation. Blue histograms indicate the Ik$^{L/L}$ samples; solid red histograms indicate the WT samples. Values indicate the mean fluorescence intensities (MFI). (**C**) U0126 and SB203580 inhibitors block ERK and p38 phosphorylation. Ik$^{L/L}$ and WT FO B cells were pretreated with the indicated inhibitors or vehicle (DMSO) for 45 min, then stimulated with anti-IgM + anti-CD40 (10 µg/ml) for 15 min. P-ERK and P-p38 were analyzed by flow cytometry. (**D**) Inhibition of ERK and p38 signaling rescue the hyper-proliferative phenotype of Ik$^{L/L}$ B cells. CFSE-labeled Ik$^{L/L}$ and WT FO B cells were pretreated with the indicated inhibitors, then stimulated with anti-IgM or anti-IgM + anti-CD40 (10 µg/ml) for 72h. Representative of >3 independent experiments.

Figure 5 - Ikaros deletion in mature B cells is sufficient to initiate the hyper-response to BCR stimulation and autoantibody production.

(**A**) Splenic FO B cells from TAM-treated Ik$^{f/f}$ Rosa26-CreERT2^{+} mice show enhanced ERK phosphorylation and hyper-proliferation following BCR stimulation. Cells from TAM-treated Ik$^{f/f}$ Rosa26-CreERT2^{+} or Ik$^{f/f}$ Rosa26-CreERT2^{-} mice were stimulated as indicated for 15 min and then measured for P-ERK (left panels). CFSE-labeled cells were stimulated for 72h and then measured for CFSE dilution (right panels). The number of divisions completed is indicated. Red histograms denote the cells from TAM-treated Ik$^{f/f}$ Rosa26-CreERT2^{+} mice; blue histograms denote the cells from TAM-treated Ik$^{f/f}$ Rosa26-CreERT2^{-} mice. Solid gray histograms indicate non-stimulated cells from either condition; both gave similar results. Representative of 2 experiments. (**B**) Splenic FO B cells from Ik$^{f/f}$ CD21-Cre^{+} mice show enhanced ERK phosphorylation after BCR stimulation. Cells from Ik$^{f/f}$ CD21-Cre^{+} and Ik$^{f/f}$ CD21-Cre^{-} mice were stimulated as indicated and P-ERK levels were measured. Red histograms indicate cells from Ik$^{f/f}$ CD21-Cre^{+} mice; blue histograms indicate cells from Ik$^{f/f}$ CD21-Cre^{-} mice. Solid gray histrograms indicate non-stimulated cells from either genotype; both gave similar results. Representative of 2 experiments. (**C**) Serum of Ik$^{f/f}$ CD21-Cre^{+} (n=14, 7-11 weeks of age) and Ik$^{f/f}$ CD21-Cre^{-} (n=10, 7-12 weeks of age) mice were tested for IgM antibodies to the indicated antigens by ELISA. (-)

indicates $Ik^{f/f}$ CD21-Cre$^-$. (+) indicates $Ik^{f/f}$ CD21-Cre$^+$. MRL/lpr serum (n=12, 10 weeks of age) was used as a positive control. Black bars show the mean of the indicated values. Statistical significance was determined by the Wilcoxon signed rank-test.

Figure S1 - Detection of ANA and IgG autoantibodies in $Ik^{L/L}$ serum.

(A) Scoring of ANA intensities using the indicated images to establish a standard scale (top). Relative ANA staining intensities of serum from $Ik^{L/L}$ vs. WT mice (bottom). **(B)** Serum of $Ik^{L/L}$ (n=32, 6-8 weeks of age) and WT (n=18, 6-9 weeks of age) mice were tested for IgG antibodies to the indicated antigens by ELISA. MRL/lpr serum (n=4, ~20 weeks of age) was used as a positive control. The graphs on the right for each ELISA indicate the same values presented on a smaller scale to highlight the statistical significance between the $Ik^{L/L}$ and WT samples. Black bars show the mean of the indicated values. Statistical significance was determined by the Wilcoxon signed rank-test.

Figure S2 - Detection of rheumatoid factor and anti-thyroglobulin antibodies in $Ik^{L/L}$ serum and the activation state of freshly isolated $Ik^{L/L}$ B cells.

(A) Serum of $Ik^{L/L}$ (n=41, 6-10 weeks of age) and WT (n=26, 32-52 weeks of age) mice were tested for IgM and IgG antibodies to the indicated antigens by ELISA. MRL/lpr serum (n=10, ~20 weeks of age) was used as a positive control. Black bars show the mean of the indicated values. Statistical significance was determined by two-tailed Student's t-test assuming unequal variance. **(B)** Freshly isolated splenic FO B cells from $Ik^{L/L}$ and WT mice were analyzed by flow cytometry for the indicated antigens. The MFI values are displayed relative to WT expression where WT values are defined as 1.0. Values shown were obtained from one representative experiment out of 3 performed.

Figure S3 - Response to IgM + IL-4 stimulation and reduced apoptosis in $Ik^{L/L}$ B cells.

(A) CFSE-labeled $Ik^{L/L}$ and WT splenic FO B cells were stimulated for 72h in the presence of anti-IgM + IL-4, then analyzed by flow cytometry. The number of divisions completed for the cells of each genotype is indicated. Gray histograms denote the CFSE labeling for non-stimulated WT and $Ik^{L/L}$ cells; both gave similar results. Representative of 2 experiments. **(B)** $Ik^{L/L}$ and WT B cells were stimulated for 18h with anti-IgM or anti-IgM + anti-CD40 (10 μg/ml), then incubated for 30 min with $DiOC_6$ to stain active mitochondria (live cells). The percentage of live cells as measured by flow cytometry is indicated. Representative of 3 experiments.

Figure S4 - Profile of FCM clusters.

Transcriptomic data from Ik$^{L/L}$ and WT B cells stimulated with anti-IgM for 0, 3 and 12h, was analyzed by Fuzzy C-means (FCM) partitional clustering. FCM was applied to 10,747 probe sets with a coefficient of variation >0.75 across all samples. 30 clusters of probe sets with similar expression profiles were generated, and probe sets that exhibited a membership value 0.7 were retained. Expression profiles of the 30 clusters are shown.

Figure S5 - Pan-tyrosine phosphorylation analysis of Ik$^{L/L}$ B cells.

Pan-tyrosine phosphorylation was analyzed in the samples from Fig. 4a by immunoblotting. GAPDH was used as a loading control.

Figure S6 - Analysis of early cell cycle regulators in Ik$^{L/L}$ B cells.

Ik$^{L/L}$ and WT splenic FO B cells were stimulated with anti-IgM or anti-IgM + anti-CD40 (2 µg/ml) for the indicated times and analyzed by Western blot using antibodies to the indicated cell cycle regulators. β-actin was used as a loading control.

Figure S7 - Deletion of the Ik$^{f/f}$ allele in mutant mice.

(A) Splenic FO B cells from TAM-treated Ik$^{f/f}$ Rosa26-CreERT2^{+} and Ik$^{f/f}$ Rosa26-CreERT2^{-} mice were analyzed by PCR (top) and Western blot (bottom) to detect the indicated PCR products and Ikaros proteins, respectively. β-actin was used as a loading control (bottom). **(B)** Splenic FO B cells from Ik$^{f/f}$ CD21-Cre^{+} and Ik$^{f/f}$ CD21-Cre^{-} mice were analyzed by PCR (top) and Western blot (bottom) to detect the indicated PCR products and Ikaros proteins, respectively. CD43^{+} cells were used to evaluate the lack of deletion and presence of Ikaros proteins in non-B cells. β-actin was used as a loading control (bottom).

Table S1 - Genes dysregulated >2-fold in freshly isolated Ik$^{L/L}$ FO B cells.

Probe sets up- or down-regulated >2x in all 4 pair-wise Ik$^{L/L}$ vs. WT comparisons were selected. Expression values have been generated by the MAS5 software.

Table S1: Genes dysregulated >2-fold in freshly isolated Ik$^{L/L}$ FO B cells

Gene Title	Gene Symbol	WT1	WT2	IkL/L1	IkL/L2	Fold Change
plastin 3 (T-isoform)	Pls3	0.7	2	58.1	44.6	38.04
cytochrome P450, family 4, subfamily f, polypeptide 16	Cyp4f16	1.4	0.8	35.4	24.8	27.36
---	---	1.8	1	35.3	30	23.32
growth factor receptor bound protein 7	Grb7	5.7	3	64	52.6	13.40
paraoxonase 3	Pon3	3.6	3.3	42	31.4	10.64
transmembrane protein 176B	Tmem176b	19	33.3	254.9	272.1	10.08
amyloid beta (A4) precursor protein	App	22.8	17.8	137	194.4	8.16
rhomboid family 1 (Drosophila)	Rhbdf1	113.8	41.5	538.3	558.9	7.07
dedicator of cytokinesis 7	Dock7	2.8	15.5	67.5	54	6.64
latexin	Lxn	15.8	24.4	160.1	102.7	6.54
lysosomal-associated protein transmembrane 4B	Laptm4b	39.4	70.4	342.6	293.2	5.79
tight junction protein 2	Tjp2	35.8	38.4	225.2	203.1	5.77
chemokine (C-C motif) ligand 3	Ccl3	78.7	38.4	189	447.1	5.43
endoglin	Eng	32.4	7.8	119.7	92	5.27
endoglin	Eng	43.4	31.7	160.3	227.5	5.16
arachidonate 5-lipoxygenase activating protein	Alox5ap	5.2	17.8	59.3	56.1	5.02
RAS, dexamethasone-induced 1	Rasd1	54.3	56.7	225.4	330.1	5.00
fos-like antigen 2	Fosl2	97.7	70.9	294.6	547.5	4.99
p21 protein (Cdc42/Rac)-activated kinase 1	Pak1	14.6	16.8	63.8	89.9	4.89
claudin 12	Cldn12	19	15.8	93.7	73.9	4.82
tight junction protein 2	Tjp2	17.3	30.8	102.6	123.2	4.69
p21 protein (Cdc42/Rac)-activated kinase 1	Pak1	30.9	20.6	75.5	158.7	4.55
PTK2 protein tyrosine kinase 2	Ptk2	26.6	21.8	120.8	94	4.44
adrenomedullin	Adm	99	55.6	249	432.2	4.41

Description	Gene					
glycoprotein 49 A /// leukocyte immunoglobulin-like receptor, subfamily B, member 4	Gp49a /// Lilrb4	152.1	185.6	474.9	983.8	4.32
tissue factor pathway inhibitor	Tfpi	42.3	28.7	176.8	110.6	4.05
G protein-coupled receptor 177	Gpr177	23.3	7	75.2	42.6	3.89
ornithine decarboxylase, structural 1	Odc1	271.9	272.8	808	1293.7	3.86
inhibitor of DNA binding 2	Id2	36.9	42.7	169.1	135.7	3.83
lamin B1	Lmnb1	41.7	33.7	130.3	157.1	3.81
coiled coil domain containing 88A	Ccdc88a	18.7	15.5	72	53.9	3.68
family with sequence similarity 129, member A	Fam129a	20.4	41.8	80.3	145.2	3.63
Rho guanine nucleotide exchange factor (GEF) 12	Arhgef12	38.3	33.3	112.1	146.9	3.62
membrane-spanning 4-domains, subfamily A, member 6C	Ms4a6c	42.9	54.7	201.9	149.5	3.60
CD9 antigen	Cd9	98.2	111.2	358.6	388.5	3.57
zinc finger and BTB domain containing 46	Zbtb46	11.4	30.9	65.9	84.1	3.55
brain expressed gene 1	Bex1	25.4	12.8	70.7	63.9	3.52
kallikrein related-peptidase 8	Klk8	19.3	10.7	54.6	50.9	3.52
cytoplasmic FMR1 interacting protein 1	Cyfip1	429.5	291.2	1165.9	1343.6	3.48
bone morphogenic protein receptor, type II (serine/threonine kinase)	Bmpr2	40.6	43.6	128.6	156.1	3.38
fatty acid binding protein 5, epidermal	Fabp5	115.8	120.5	373.5	415.5	3.34
galactosidase, alpha	Gla	34.4	27.8	69.4	136.9	3.32
RIKEN cDNA 2210013O21 gene	2210013O21Rik	17	22.7	73.6	54.8	3.23
prion protein	Prnp	58.4	37.9	124.7	183.7	3.20
limb region 1	Lmbr1	10.5	16.1	44.7	40	3.18
expressed sequence AI324046	AI324046	46.4	2.9	95.2	61.7	3.18
---	---	23.5	26.1	79.9	75.1	3.13
zinc finger CCCH type containing 12C	Zc3h12c	57	75.3	150.7	260.6	3.11
family with sequence similarity 129, member A	Fam129a	30.4	50.9	100.6	148.4	3.06
Immunoglobulin heavy chain (gamma polypeptide)	Ighg	61.4	49	128.3	209.8	3.06
lamin A	Lmna	42.3	29	97	119.8	3.04
Rho guanine nucleotide exchange factor (GEF) 12	Arhgef12	53.8	38.6	126.3	151.6	3.01

Description	Symbol					
cytochrome P450, family 27, subfamily a, polypeptide 1	Cyp27a1	37.8	47.9	118.5	138.6	3.00
predicted gene, 100041874	100041874	29	40.7	108.5	97.8	2.96
SET binding factor 2	Sbf2	133.2	108.7	285	428.4	2.95
nibrin	Nbn	57.7	39.7	124.3	161.4	2.93
melanoregulin	Mreg	184.2	132	545.5	375.3	2.91
adrenomedullin	Adm	52	33.2	79.2	166.1	2.88
integral membrane protein 2C	Itm2c	72.2	66.3	179.4	217.4	2.86
RIKEN cDNA 1110004E09 gene	1110004E09Rik	5.5	32.4	55.7	52.5	2.85
transmembrane and tetratricopeptide repeat containing 3	Tmtc3	33.7	6.3	74.5	39.1	2.84
suppressor of cytokine signaling 3	Socs3	74.2	115.5	284.1	253.1	2.83
transmembrane BAX inhibitor motif containing 1	Tmbim1	42	71	183.5	136.4	2.83
SCAN domain containing 3	Scand3	88.8	82.4	195.3	287.2	2.82
cytoplasmic FMR1 interacting protein 1	Cyfip1	334.5	256.9	861.6	779.5	2.77
H1 histone family, member 0	H1f0	10.5	43.2	79.7	69.1	2.77
nuclear receptor subfamily 4, group A, member 3	Nr4a3	328.8	305.7	529.2	1220.4	2.76
dishevelled associated activator of morphogenesis 1	Daam1	42.4	62.3	116.8	171.8	2.76
RIKEN cDNA 2810025M15 gene	2810025M15Rik	37.5	23.1	88.9	78.1	2.76
expressed sequence AA467197	AA467197	47.6	37.5	91.6	142.9	2.76
KDEL (Lys-Asp-Glu-Leu) containing 1	Kdelc1	93.5	120.1	299	283.2	2.73
fatty acid binding protein 5, epidermal	Fabp5	42.6	57.8	125.2	147	2.71
expressed sequence AI324046	AI324046	29.6	21.7	60	76.6	2.66
protein tyrosine phosphatase, non-receptor type 14	Ptpn14	33.5	33.5	96.4	81.2	2.65
potassium channel tetramerisation domain containing 14	Kctd14	57.1	73.6	165.4	179.9	2.64
G protein-coupled receptor 177	Gpr177	46.2	15.2	95.5	66.6	2.64
---	---	78.4	117.6	224.3	290.7	2.63
Myristoylated alanine rich protein kinase C substrate	Marcks	33.8	42.5	95.8	102.1	2.59
FBJ osteosarcoma oncogene	Fos	243.5	217	415.9	776.2	2.59
glycophorin C	Gypc	75	64.7	139.9	219.9	2.58
chemokine (C-C motif) ligand 4	Ccl4	107.8	145.8	211.3	441.2	2.57

Description	Symbol					Ratio
TNF receptor-associated factor 1	Traf1	327.4	144.1	573.9	635.2	2.56
annexin A4	Anxa4	83.3	78.2	199.3	214.5	2.56
---	---	171.1	79.9	311	327.4	2.54
solute carrier family 7 (cationic amino acid transporter, y+ system), member 7	Slc7a7	39	36.6	60	131.5	2.53
insulin-like growth factor I receptor	Igf1r	24.3	34.4	72.5	73.6	2.49
annexin A1	Anxa1	53.6	64.9	123.5	169.2	2.47
solute carrier family 43, member 3	Slc43a3	40.5	67.5	116.5	148.7	2.46
ST8 alpha-N-acetyl-neuraminide alpha-2,8-sialyltransferase 6	St8sia6	113.8	95.1	255.4	255.9	2.45
aryl-hydrocarbon receptor	Ahr	272.4	270.4	527.6	797.2	2.44
GRP1 (general receptor for phosphoinositides 1)-associated scaffold protein	Grasp	311.5	225.1	509.8	788.2	2.42
DIP2 disco-interacting protein 2 homolog C (Drosophila)	Dip2c	30	22.5	53.1	73.3	2.41
potassium channel tetramerisation domain containing 14	Kctd14	98.5	71	195.3	212.7	2.41
---	---	95	91.5	239.8	208.4	2.40
abhydrolase domain containing 4	Abhd4	116	106.7	201.5	322.1	2.35
malignant T cell amplified sequence 2	Mcts2	28	4.6	41.9	33.9	2.33
synaptogyrin 2	Syngr2	1588.3	1403.8	3149.6	3794.9	2.32
tetraspanin 31	Tspan31	112	94.5	269.5	209.4	2.32
Epstein-Barr virus induced gene 3	Ebi3	78	68	128.3	206.8	2.30
mitochondrial ribosomal protein L52	Mrpl52	462.4	531.8	1280.5	995.6	2.29
ornithine decarboxylase, structural 1	Odc1	2129.1	1801.7	4519.5	4390.2	2.27
potassium channel tetramerisation domain containing 14	Kctd14	212.1	156.3	474.1	360.7	2.27
S100 calcium binding protein A8 (calgranulin A)	S100a8	27.2	127.5	69	280.5	2.26
synaptogyrin 2	Syngr2	1400.1	1167.4	2530.7	3190.8	2.23
solute carrier family 20, member 1	Slc20a1	665.9	552.9	1005.2	1707.9	2.23
plakophilin 4	Pkp4	54.3	56	102.2	143.3	2.23
---	---	102.3	61.2	200.7	160.8	2.21
immunoglobulin joining chain	Igj	92.1	332.3	157.4	780.3	2.21

Description	Symbol					Ratio
interleukin 1 beta	Il1b	45.4	38	94.8	88.6	2.20
MAD homolog 1 (Drosophila)	Smad1	36.4	40.7	89.2	80.2	2.20
neutrophilic granule protein	Ngp	16.1	157.6	115.6	264.1	2.19
RIKEN cDNA 2010002N04 gene	2010002N04Rik	62	60.1	133.2	131.5	2.17
pogo transposable element with KRAB domain	Pogk	132.8	124.9	223.2	332.8	2.16
Ras suppressor protein 1	Rsu1	138.3	94	253.7	243.3	2.14
ankyrin repeat domain 33B	Ankrd33b	402.2	307.4	769.5	743.1	2.13
S100 calcium binding protein A9 (calgranulin B)	S100a9	23.8	97.3	55.1	202.5	2.13
ChaC, cation transport regulator-like 1 (E. coli)	Chac1	85.1	103	138.9	260.7	2.12
CD36 antigen	Cd36	46.2	42.9	93.3	94.5	2.11
hairy and enhancer of split 1 (Drosophila)	Hes1	57.9	31.8	102.4	86.2	2.10
insulin-like growth factor I receptor	Igf1r	81.4	102.7	182.8	202.8	2.09
BCL2-like 11 (apoptosis facilitator)	Bcl2l11	1188.6	1053.1	2065.9	2627.3	2.09
brain abundant, membrane attached signal protein 1	Basp1	79.8	126.3	194.9	235.8	2.09
catenin (cadherin associated protein), alpha 1	Ctnna1	71.5	54.4	141.8	120.7	2.08
asparagine synthetase	Asns	117.9	116.9	263.6	225	2.08
cDNA sequence BC028789	BC028789	101.5	116.5	242.2	206.8	2.06
hepatitis A virus cellular receptor 1	Havcr1	26.5	66.7	73.8	118	2.06
---	---	90	122.4	216.7	216.8	2.04
TM2 domain containing 2	Tm2d2	73.5	78.1	134.4	172.8	2.03
mitochondrial ribosomal protein L52	Mrpl52	70.5	101.7	190.5	158.4	2.03
interleukin 1 receptor, type II	Il1r2	165.2	136.1	278.7	327.2	2.01
RIKEN cDNA 2610204M08 gene	2610204M08Rik	138.8	205.6	236.3	455.9	2.01
ankyrin repeat domain 11	Ankrd11	1126.9	1006.7	505.4	559.9	0.50
RIKEN cDNA 1700021K19 gene	1700021K19Rik	417.3	558.5	212.5	274.1	0.50
RAS guanyl releasing protein 1	Rasgrp1	667.6	717.6	375.9	314.1	0.50
myeloid-associated differentiation marker	Myadm	77.1	104	49.5	40.6	0.50
RIKEN cDNA A130040M12 gene	A130040M12Rik	1369.2	923.7	291.3		0.50

Description	Symbol					
transmembrane and coiled coil domains 3	Tmcc3	55.2	66.7	28.3	32.1	0.50
zinc finger protein 318	Zfp318	196.4	191	92	99.9	0.50
glucocorticoid induced transcript 1	Glcci1	470.9	657.5	235.4	323.5	0.50
interaction protein for cytohesin exchange factors 1	Ipcef1	66.3	75.6	35.1	35.1	0.49
mannosidase 2, alpha B1	Man2b1	230	257.5	116.6	123.7	0.49
---	---	233.5	210.9	128.2	90.6	0.49
---	---	436.6	586.9	245.5	257.6	0.49
lipin 2	Lpin2	114.3	150.9	60.9	69.4	0.49
ubiquitin-conjugating enzyme E2D 1, UBC4/5 homolog (yeast)	Ube2d1	194.9	214.6	126.1	74.9	0.49
---	---	265.3	187.7	128	94.1	0.49
SH3-binding kinase 1	Sbk1	373.8	634	232.2	261.7	0.49
CD2 antigen	Cd2	1062.9	1075.9	549.5	495.3	0.49
acid phosphatase 5, tartrate resistant	Acp5	419.1	505.8	273.8	177.9	0.49
carnitine palmitoyltransferase 1a, liver	Cpt1a	269.4	278.4	145.9	121	0.49
Rho guanine nucleotide exchange factor (GEF) 3	Arhgef3	583.4	604	318.6	259.9	0.49
protein tyrosine phosphatase, receptor type, S	Ptprs	58.3	82.8	30.3	38.3	0.49
---	---	349.9	384.9	176.5	180.5	0.49
B and T lymphocyte associated	Btla	2452.6	3305.4	1606.7	1190.3	0.49
---	---	268.1	184.9	164.2	55.4	0.48
ATPase, Na+/K+ transporting, beta 1 polypeptide	Atp1b1	113	171.7	72.8	65.2	0.48
sphingomyelin synthase 1	Sgms1	275.7	347.9	140.7	161	0.48
annexin A6	Anxa6	310.7	339	146.2	167.7	0.48
regulatory factor X, 7	Rfx7	725.3	574.5	367.8	258.6	0.48
chromobox homolog 6	Cbx6	99.5	70.5	40.5	41.4	0.48
---	---	59.2	40.9	31.1	17.1	0.48
---	---	197.5	132.6	97.3	61.6	0.48
dihydropyrimidinase-like 2	Dpysl2	295.8	297.3	171.2	113.2	0.48
GTPase, IMAP family member 7	Gimap7	402.7	431.7	175.5	224	0.48

Description	Symbol					
metastasis associated lung adenocarcinoma transcript 1 (non-coding RNA)	Malat1	3976.3	4680.1	2661.4	1476.5	0.48
---	---	58.5	40.7	25.6	21.7	0.48
CD93 antigen	Cd93	138.5	157.5	81.4	58.9	0.47
---	---	133.7	138.9	60.3	68	0.47
A kinase (PRKA) anchor protein 13	Akap13	146.3	95.4	76.9	36.8	0.47
---	---	360.3	419.5	155	207.9	0.47
guanylate binding protein 6	Gbp6	119.3	134.6	63.2	54.7	0.46
chromobox homolog 7	Cbx7	337.5	442.9	161.6	200.4	0.46
Ly6/neurotoxin 1	Lynx1	231.8	312.7	124.6	125.5	0.46
predicted gene 7202	Gm7202	244.1	268	138.3	96.8	0.46
protein-L-isoaspartate (D-aspartate) O-methyltransferase domain containing 1	Pcmtd1	362.6	320.5	166.1	146.7	0.46
RIKEN cDNA 4930453J04 gene	4930453J04Rik	116.8	145.9	48	72.2	0.46
sorting nexin 29	Snx29	202	287.2	90.5	132.8	0.46
metastasis associated lung adenocarcinoma transcript 1 (non-coding RNA)	Malat1	885.3	562.2	409.9	250.4	0.46
apoptotic chromatin condensation inducer 1	Acin1	404.9	412.3	239	133.6	0.46
structural maintenance of chromosomes 4	Smc4	256.9	260.2	119.8	115.8	0.46
carboxypeptidase M	Cpm	277.6	438.1	159.3	165.7	0.45
---	---	50.4	49.8	26.7	18.8	0.45
RIKEN cDNA A230048O21 gene	A230048O21Rik	123.5	104.9	54.4	48.8	0.45
catalase	Cat	322.6	328.9	192.7	101	0.45
AT rich interactive domain 3B (BRIGHT-like)	Arid3b	126.8	109.3	38.4	67.4	0.45
family with sequence similarity 78, member A	Fam78a	197.4	246.1	114.1	83.9	0.45
C-type lectin domain family 2, member i	Clec2i	368.3	512.4	220	171.8	0.44
tubulin, beta 2B	Tubb2b	368.2	290.7	214.5	78.6	0.44
tetratricopeptide repeat domain 3	Ttc3	146.4	183	67.6	78.9	0.44
MAD homolog 7 (Drosophila)	Smad7	165.6	195.1	71.5	88.6	0.44
cytidine monophospho-N-acetylneuraminic acid hydroxylase	Cmah	134.8	115.7	56.6	53.3	0.44

Description	Gene					
ST3 beta-galactoside alpha-2,3-sialyltransferase 2	St3gal2	29.8	33.2	15.8	11.8	0.44
expressed sequence AW112010	AW112010	226.9	322.9	112.9	127.6	0.44
CD93 antigen	Cd93	143.6	196.1	98.8	49.6	0.44
PDZ and LIM domain 1 (elfin)	Pdlim1	320.2	526.5	200.7	169.1	0.44
SAM domain and HD domain, 1	Samhd1	168.1	290.6	91.1	109.2	0.44
adducin 3 (gamma)	Add3	280.9	267.2	119.8	118.6	0.43
RIKEN cDNA 4930431H11 gene	4930431H11Rik	465	480.5	232.8	178.1	0.43
E26 avian leukemia oncogene 2, 3' domain	Ets2	850.8	752.7	325.2	371.2	0.43
solute carrier family 44, member 2	Slc44a2	450.7	457.5	180.8	213.5	0.43
rho/rac guanine nucleotide exchange factor (GEF) 18	Arhgef18	1410.6	2049.8	680.2	821.5	0.43
solute carrier family 28 (sodium-coupled nucleoside transporter), member 2	Slc28a2	406.2	385.9	170.8	172.9	0.43
microtubule-associated protein, RP/EB family, member 1	Mapre1	89.5	66.1	39	28.4	0.43
Angiopoietin-like 1	Angptl1	289.1	246.3	133.9	97.4	0.43
coiled-coil domain containing 123	Ccdc123	180.6	259.7	112.8	76.5	0.43
spectrin beta 2	Spnb2	1069.8	733.2	388.4	383.5	0.43
post-GPI attachment to proteins 1	Pgap1	333.4	334.7	154.7	130.4	0.43
---	---	209.2	188.1	91.5	77.9	0.43
phosphodiesterase 7A	Pde7a	227.4	217.7	91.9	97.4	0.43
coiled-coil domain containing 88C	Ccdc88c	132.7	115.9	74.5	31.2	0.43
a disintegrin-like and metallopeptidase (reprolysin type) with thrombospondin type 1 motif, 6	Adamts6	105	107	50.3	39.8	0.43
SUMO1/sentrin specific peptidase 7	Senp7	285.4	336	181.8	79.4	0.42
---	---	70.4	70.3	42.1	17	0.42
family with sequence similarity 101, member B	Fam101b	123.9	134.8	55.3	52.6	0.42
ATPase, aminophospholipid transporter (APLT), class I, type 8A, member 1	Atp8a1	329.6	355.2	174.3	110.5	0.42
adducin 3 (gamma)	Add3	1000.8	790.8	467.1	277.8	0.42
adducin 3 (gamma)	Add3	1599.5	2126.6	706.5	821.6	0.41
Phosphodiesterase 7B	Pde7b	110.5	153.6	47.4	60.8	0.41

Description	Symbol					Ratio
TRAF2 and NCK interacting kinase	Tnik	75.3	64.2	35.4	21.5	0.41
adducin 1 (alpha)	Add1	152.6	139.8	74.9	43.5	0.40
---	---	141.7	229.6	58.8	90.7	0.40
protein tyrosine phosphatase 4a3	Ptp4a3	1145.5	1657.5	600	520.3	0.40
cytochrome P450, family 39, subfamily a, polypeptide 1	Cyp39a1	72.9	74.8	37	21.8	0.40
MKL (megakaryoblastic leukemia)/myocardin-like 1	Mkl1	258.3	368.5	108.6	140.2	0.40
Fc receptor, IgG, alpha chain transporter	Fcgrt	74.4	165	36.1	58.7	0.40
SAM domain and HD domain, 1	Samhd1	773.5	1220.3	354.3	433.9	0.40
sestrin 3	Sesn3	377.9	335	174.3	107	0.39
integrin beta 7	Itgb7	441.6	635.3	184	240.9	0.39
cysteine and glycine-rich protein 2	Csrp2	208.4	250.8	109	72	0.39
---	---	87.7	113.7	45.2	33.4	0.39
transmembrane and coiled coil domains 3	Tmcc3	94.9	110.4	45.8	32.6	0.38
ring finger protein 144A	Rnf144a	420.3	567.9	171.1	205.6	0.38
RIKEN cDNA 5830407E08 gene	5830407E08Rik	190.1	201.3	64.2	84.4	0.38
lymphocyte transmembrane adaptor 1	Lax1	252.3	321	119.6	97.2	0.38
ATPase, aminophospholipid transporter (APLT), class I, type 8A, member 1	Atp8a1	68.7	49.4	28.1	16.3	0.38
bromodomain PHD finger transcription factor	Bptf	134.3	58.1	37.3	34.4	0.37
trinucleotide repeat containing 6b	Tnrc6b	189.2	188.4	35.4	105.2	0.37
SAM domain and HD domain, 1	Samhd1	331.2	391.5	115.5	151.1	0.37
phosphodiesterase 2A, cGMP-stimulated	Pde2a	340.2	426.2	130.8	146	0.36
RIKEN cDNA E030047P09 gene	E030047P09Rik	71.7	83.1	20.3	35.3	0.36
G protein-coupled receptor 155	Gpr155	254.9	257.3	118	65.4	0.36
carboxypeptidase M	Cpm	135.3	238.8	68	65.9	0.36
family with sequence similarity 46, member A	Fam46a	611.1	364	150.7	198.1	0.36
---	---	205.1	160.6	48.5	79.4	0.35
hypothetical protein A630043P06	A630043P06	302.7	317.5	127.1	89.6	0.35
guanylate binding protein 6	Gbp6	143.6	162.7	43.8	61.7	0.34

Description	Symbol					
bromodomain and WD repeat domain containing 1	Brwd1	158.2	99	43.1	43.5	0.34
cysteine-rich protein 1 (intestinal)	Crip1	952.2	1406.2	382.4	402.4	0.33
ethanolamine kinase 1	Etnk1	334.5	244.9	121.9	70.7	0.33
---	---	207.8	253.8	68.3	82.6	0.33
nuclear antigen Sp100	Sp100	256.4	197.9	65.1	79.6	0.32
X Kell blood group precursor related X linked	Xkrx	207.3	243.7	84.9	55.9	0.31
EDAR (ectodysplasin-A receptor)-associated death domain	Edaradd	94.7	93.3	29.2	29.2	0.31
SRY-box containing gene 4	Sox4	90.3	104.2	44.9	15.4	0.31
RIKEN cDNA 5830407E08 gene	5830407E08Rik	238.1	196.3	79.4	48.1	0.29
---	---	140.6	101	63	7	0.29
DENN/MADD domain containing 1C	Dennd1c	44.6	69.7	3.1	29.3	0.28
ring finger protein 125	Rnf125	143.1	120.9	33.5	40	0.28
A kinase (PRKA) anchor protein (gravin) 12	Akap12	235	383.8	62.1	108.5	0.28
cell division cycle 25 homolog B (S. pombe)	Cdc25b	262.4	448.5	97.5	97.3	0.27
transmembrane protein 71	Tmem71	553.7	667.2	159.3	170.1	0.27
RIKEN cDNA C730049O14 gene	C730049O14Rik	321	309.1	113.5	51.9	0.26
EDAR (ectodysplasin-A receptor)-associated death domain	Edaradd	202.4	176.7	56.7	36.9	0.25
nucleotide-binding oligomerization domain containing 1	Nod1	81.5	103.3	18.9	24.4	0.23
family with sequence similarity 101, member B	Fam101b	248.8	231.2	42.4	66.4	0.23
l(3)mbt-like 3 (Drosophila)	L3mbtl3	85.6	71.3	18.6	16.9	0.23
rho/rac guanine nucleotide exchange factor (GEF) 18	Arhgef18	78.5	107.9	4.3	37.8	0.23
syndecan 1	Sdc1	181.5	240.7	38.6	45.2	0.20
---	---	140.7	197.8	32.3	32.4	0.19
sarcospan	Sspn	163.6	415.7	56	42.2	0.17
paired-Ig-like receptor A2	Pira2	172.8	254.5	44.1	20.6	0.15
syndecan 1	Sdc1	139.8	141.4	24.4	16.5	0.15
---	---	80.7	86	2.7	14.5	0.10
regulator of G-protein signaling 13	Rgs13	37.1	24.2	4.2	1.1	0.09
placental protein 11 related	Pp11r	46	54.3	4.8	3.3	0.08

DNA segment, Chr 18, ERATO Doi 232, expressed   D18Ertd232e   51.7   71.9   8.9   0.7   0.08

A.

MRL/lpr

BALB/c

WT

Ik$^{L/L}$

B.

Chromatin / nucleosome
p=2.75x10^{-6}

ds DNA
p=4.26x10^{-5}

Histone 1
p=9.15x10^{-6}

Histone 2A
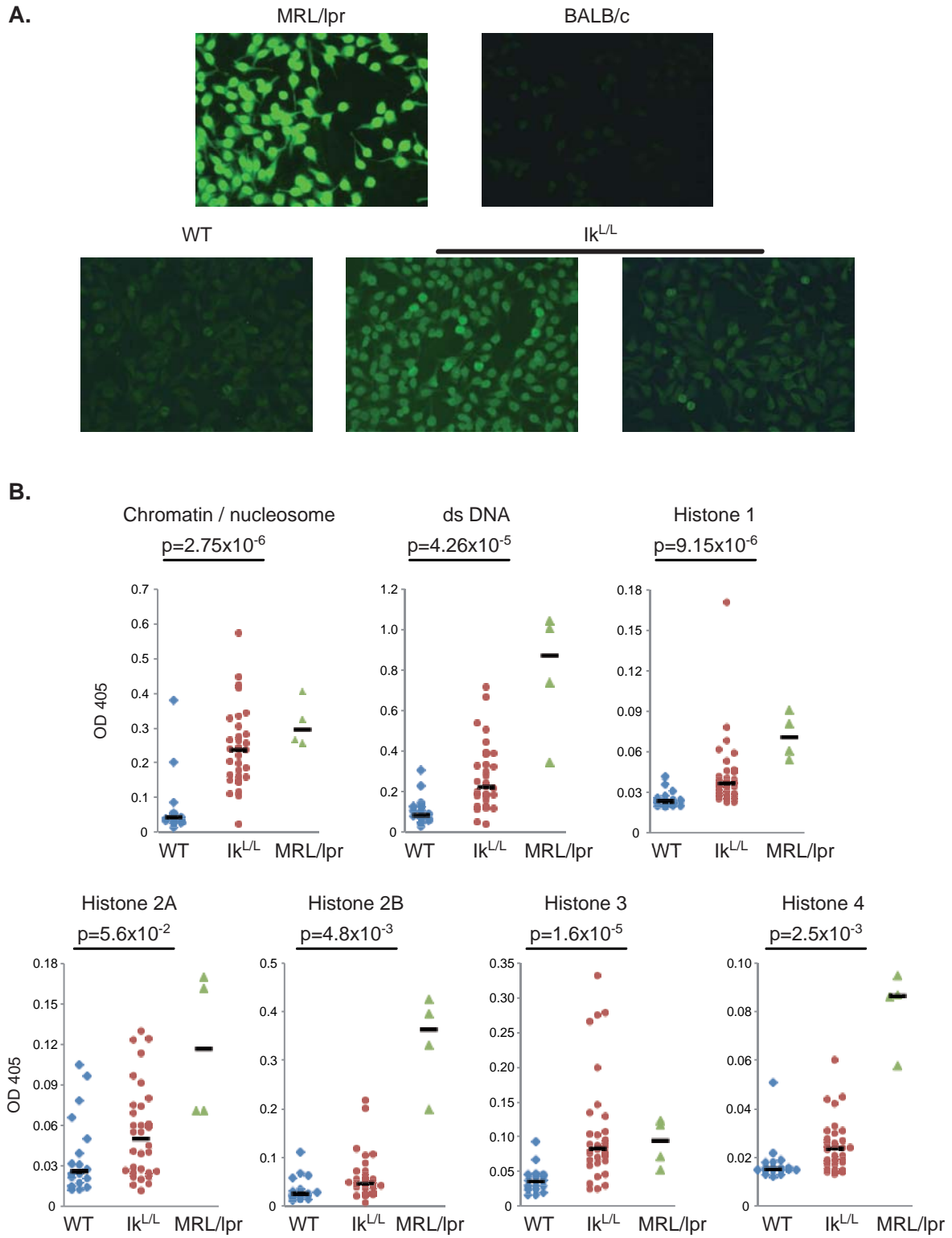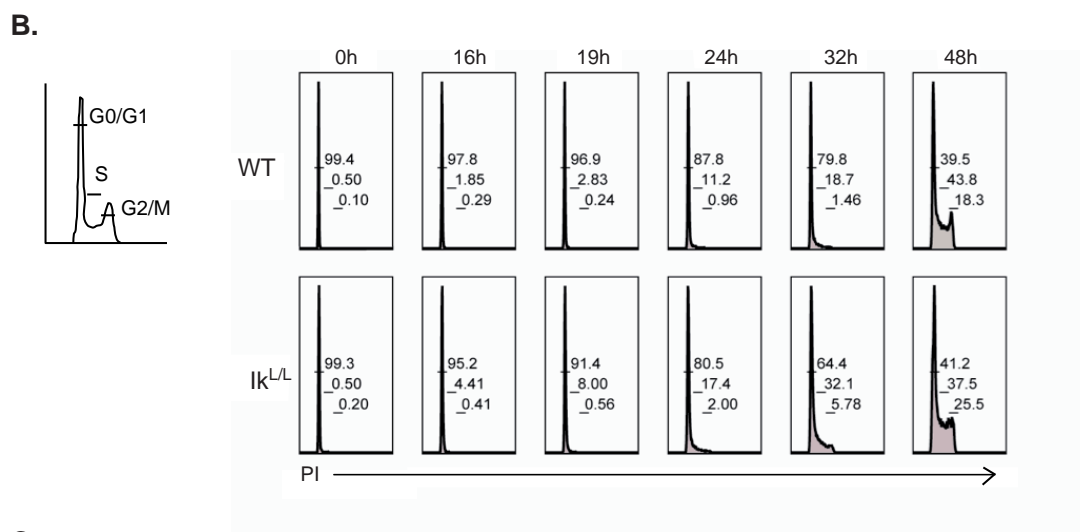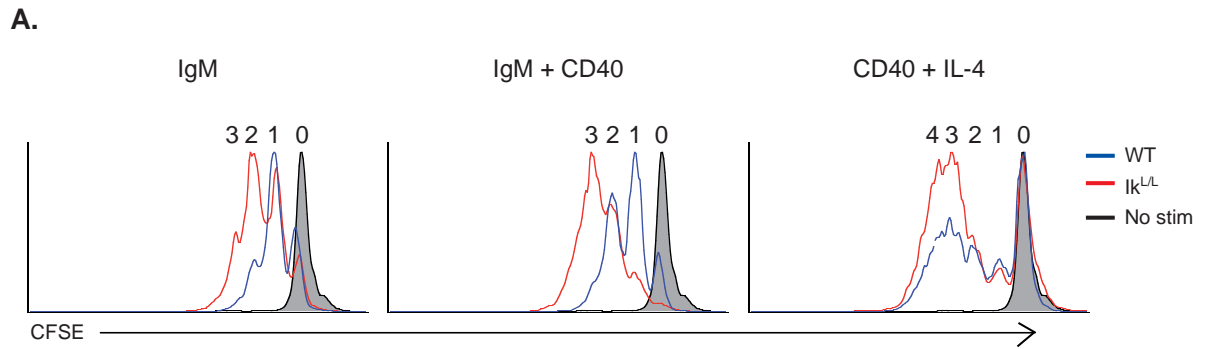p=5.6x10^{-2}

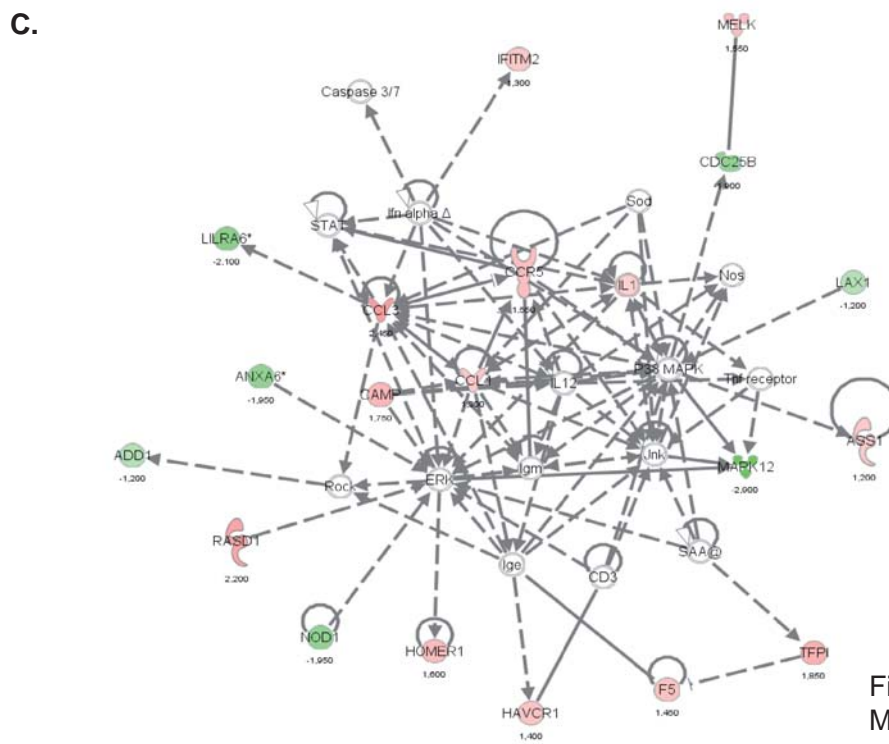**Histone 2B**
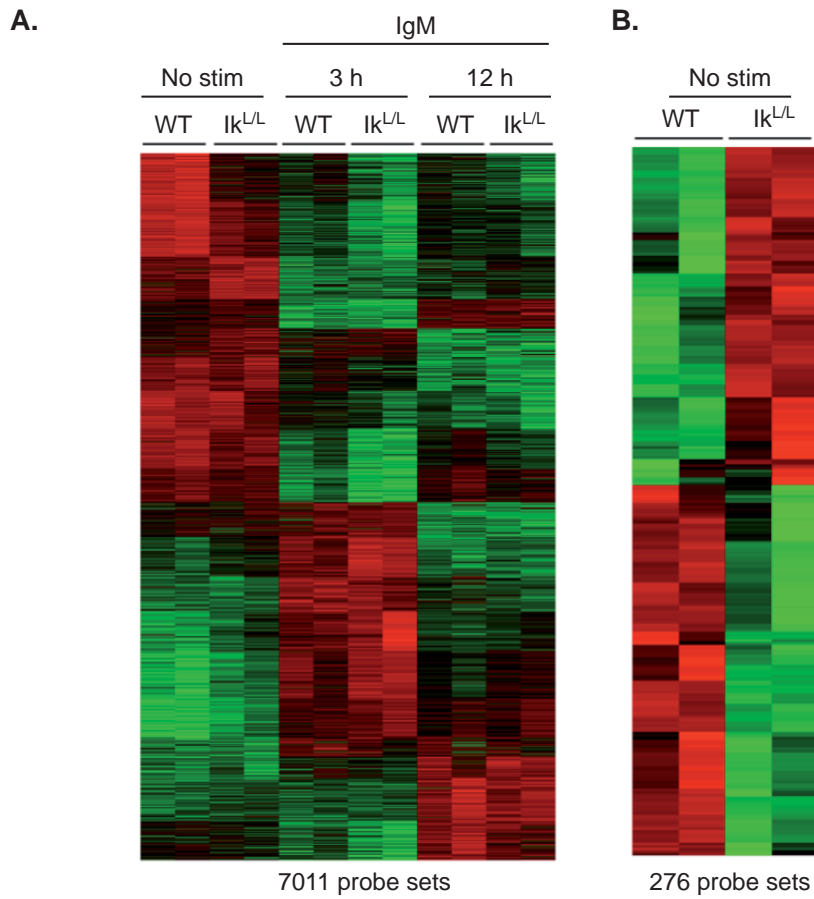p=4.8x10^{-3}

Histone 3
p=1.6x10^{-5}

Histone 4
p=2.5x10^{-3}

Figure 1
Macias-Garcia et al.

A.

IgM

3 2 1 0

IgM + CD40

3 2 1 0

CD40 + IL-4

4 3 2 1 0

WT
Ik$^{L/L}$
No stim

CFSE

B.

G0/G1

S

G2/M

	0h	16h	19h	24h	32h	48h
WT	99.4 / 0.50 / 0.10	97.8 / 1.85 / 0.29	96.9 / 2.83 / 0.24	87.8 / 11.2 / 0.96	79.8 / 18.7 / 1.46	39.5 / 43.8 / 18.3
Ik$^{L/L}$	99.3 / 0.50 / 0.20	95.2 / 4.41 / 0.41	91.4 / 8.00 / 0.56	80.5 / 17.4 / 2.00	64.4 / 32.1 / 5.78	41.2 / 37.5 / 25.5

PI

C.

G0/G1

S

G2/M

FITC

PI

WT

Ik$^{L/L}$

FITC

0h   12h   18h   24h   36h

PI
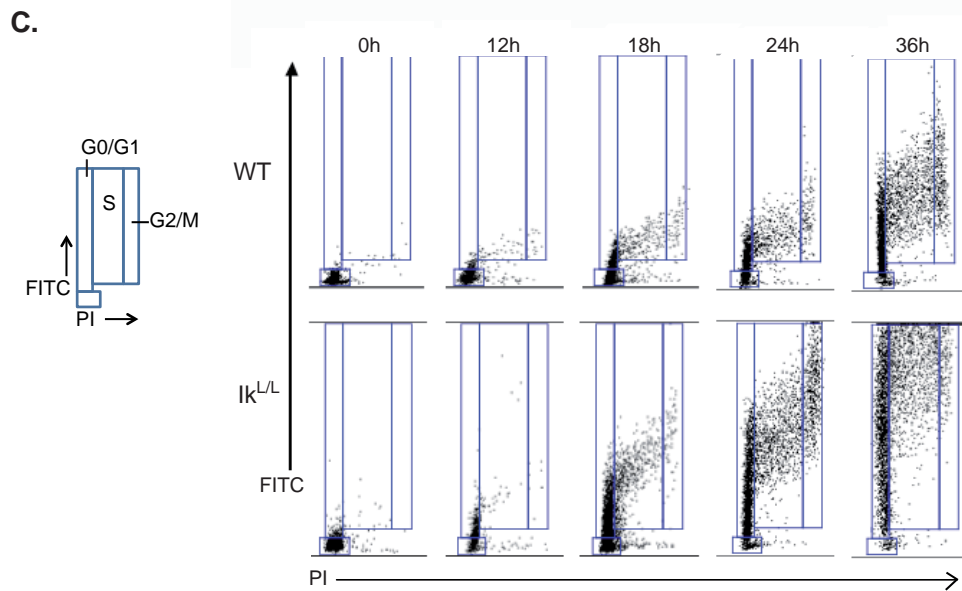
Figure 2
Macias-Garcia et al.

Figure 3
Macias-Garcia et al.

A.

B.

C.

No stim (MFI 39.5)
IgM + CD40 + DMSO (MFI 78)
IgM + CD40 + U0126 (MFI 33.7)

P-ERK

No stim (MFI 34.3)
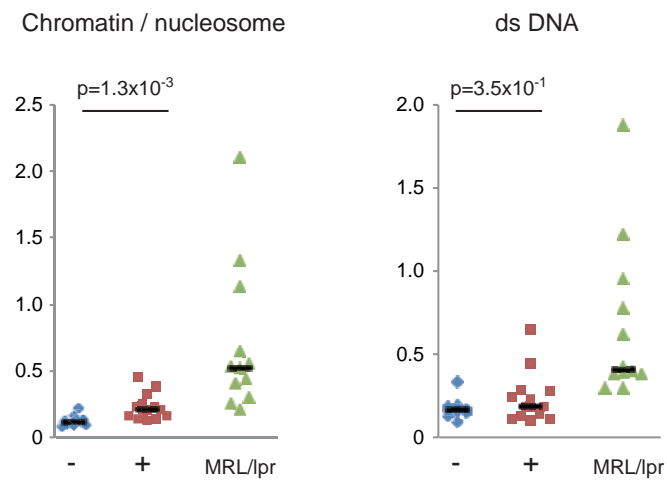IgM + CD40 + DMSO (MFI 67.5)
IgM + CD40 + SB203580 (MFI 33.7)

P-p38
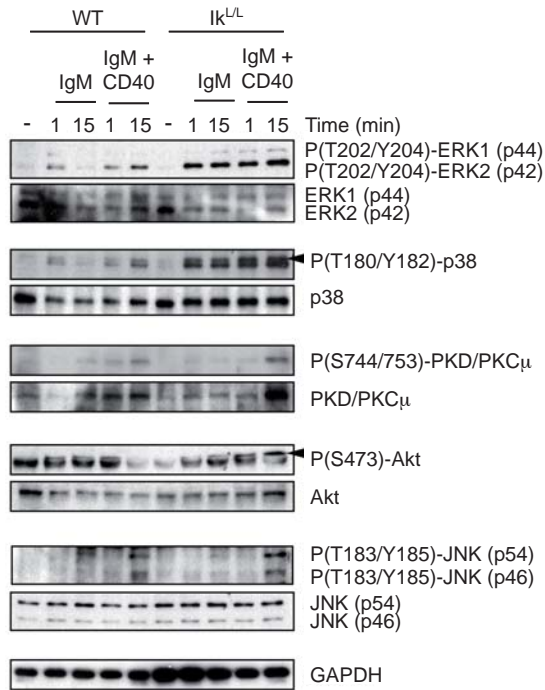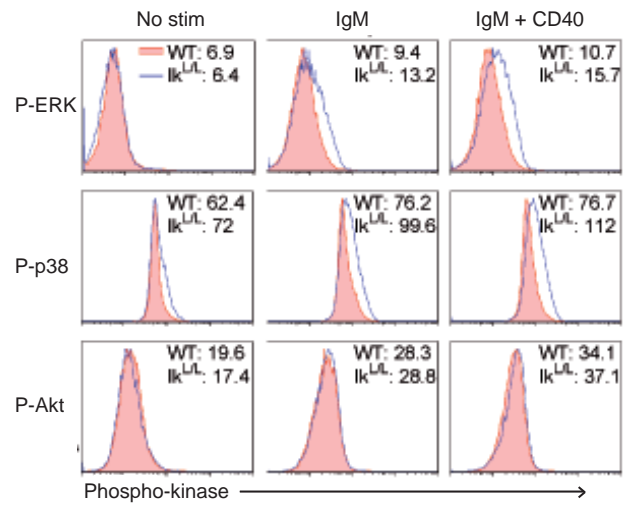
D.
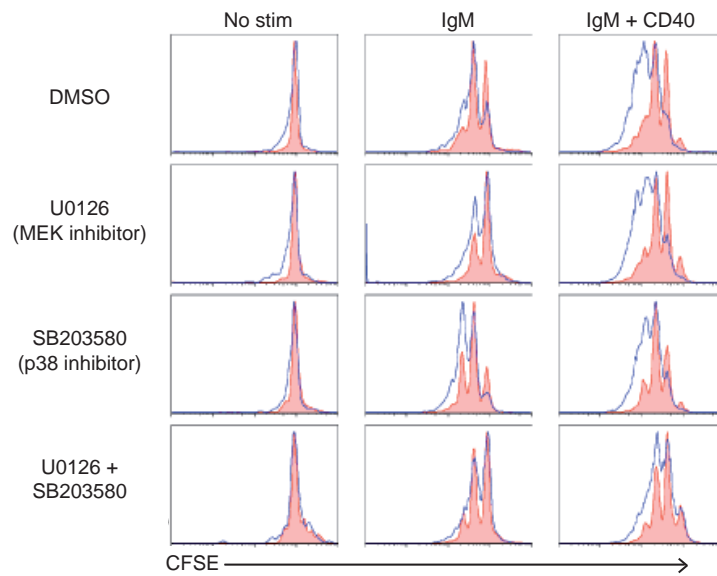
Figure 4
Macias-Garcia et al.

A.

IgM

IgM +
CD40

P-ERK   CFSE

2 1 0

4 3 2 1 0

— Ik$^{f/f}$ Rosa26-CreERT2$^-$
— Ik$^{f/f}$ Rosa26-CreERT2$^+$
— No stim

B.

IgM   IgM + CD40

P-ERK

— Ik$^{f/f}$ CD21-Cre$^-$
— Ik$^{f/f}$ CD21-Cre$^+$
— No stim

C.

Chromatin / nucleosome   ds DNA

p=1.3x10^{-3}

p=3.5x10^{-1}

-    +   MRL/lpr

-    +   MRL/lpr
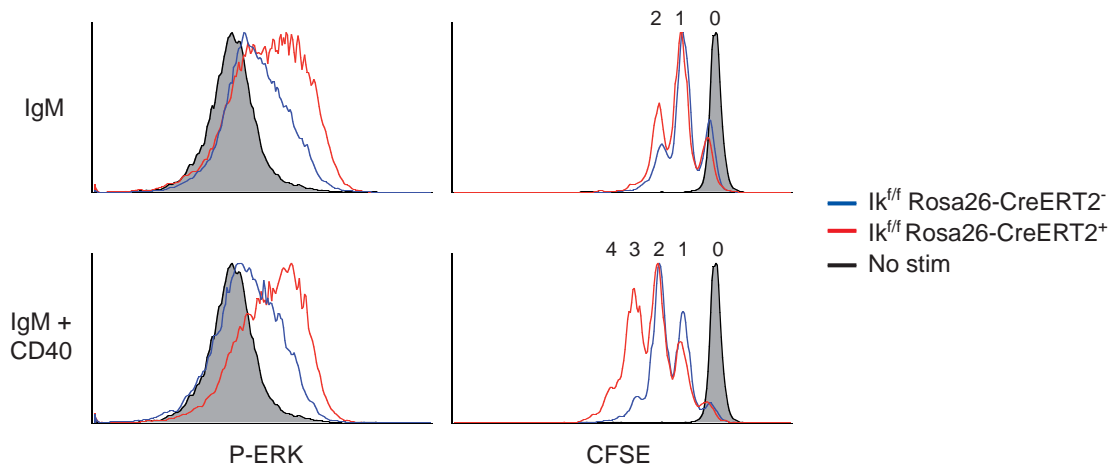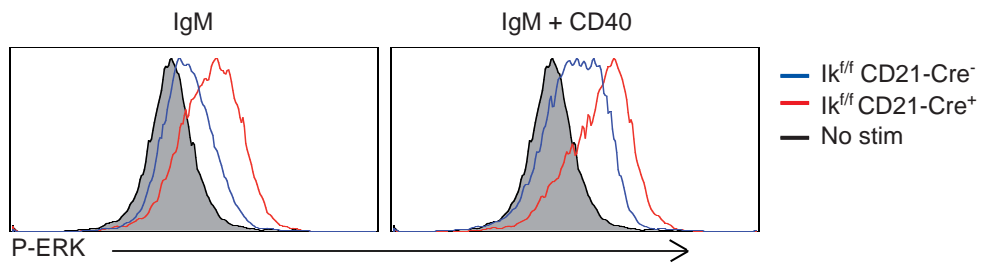
Figure 5
Macias-Garcia et al.

A.

Ik^{L/L}

Score 4.5   3   2   0.5

B.

Chromatin / nucleosome   ds DNA
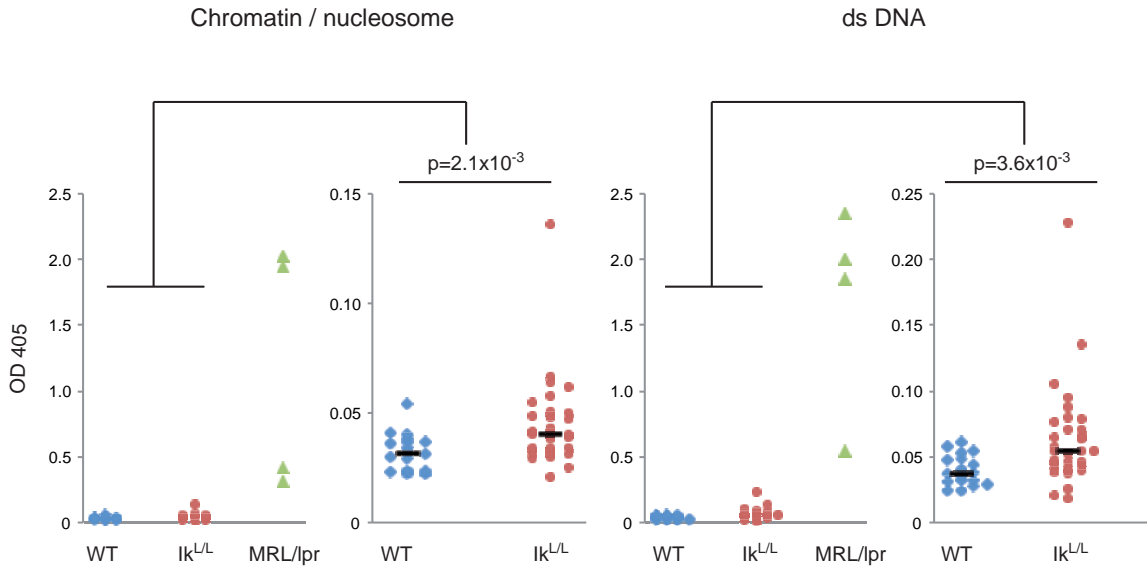

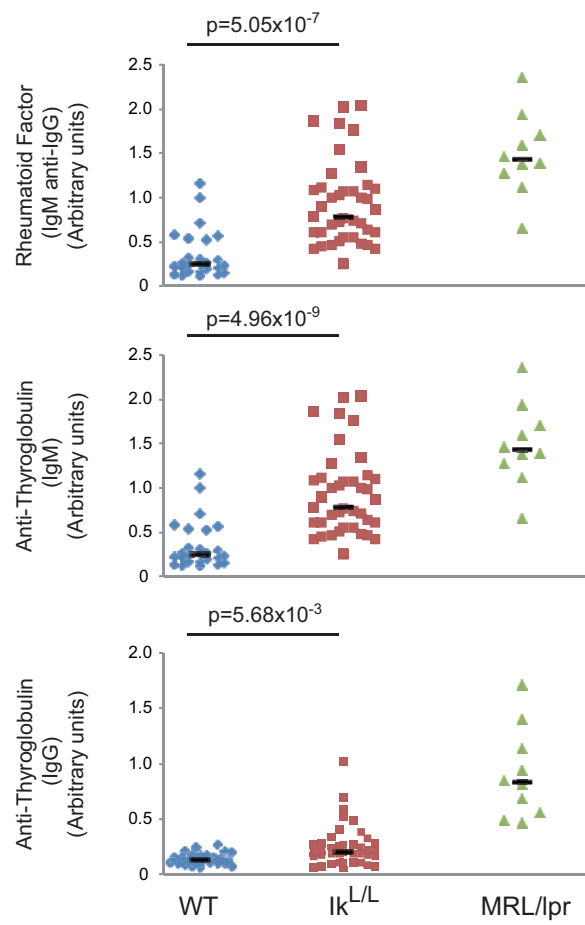p=2.1x10^{-3}

p=3.6x10^{-3}
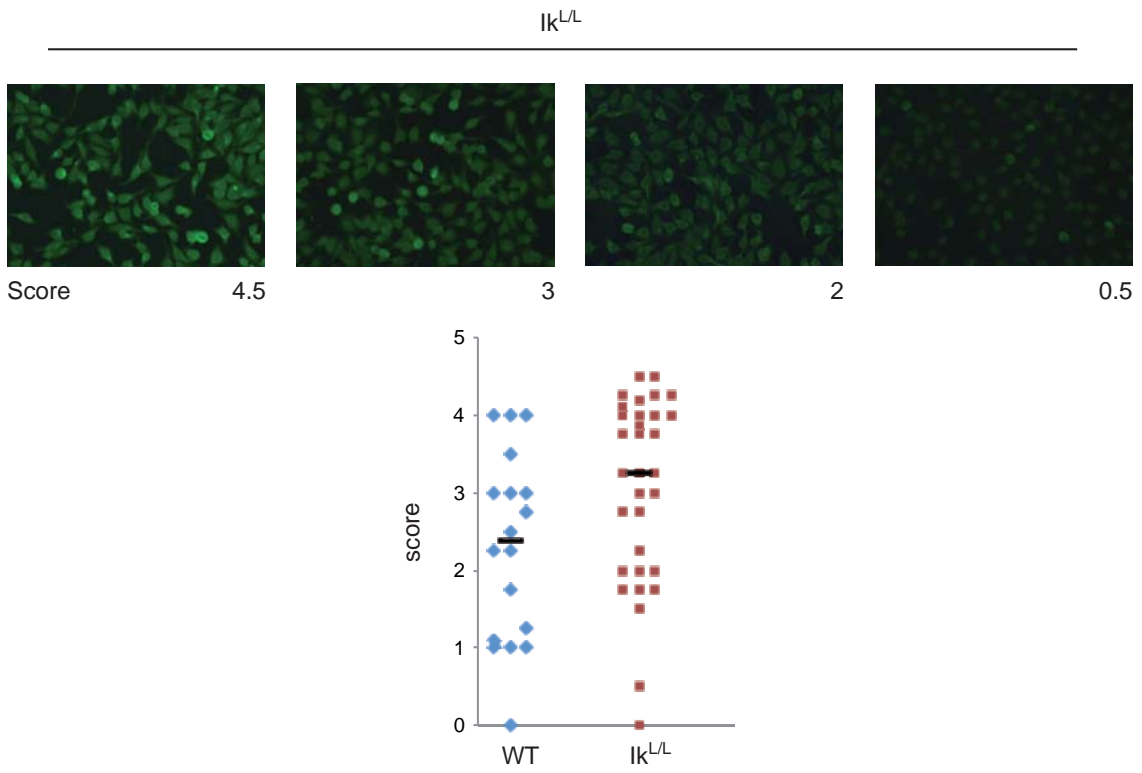
Figure S1
Macias-Garcia et al.

A.

B.

Figure S2
Macias-Garcia et al.

A.

IgM + IL-4

3 2 1 0

— WT
— Ik$^{L/L}$
— No stim

CFSE

B.

| No stim | IgM | IgM + CD40 |

WT

Ik$^{L/L}$

DiOC$_6$ (Mitochondrial membrane potential)
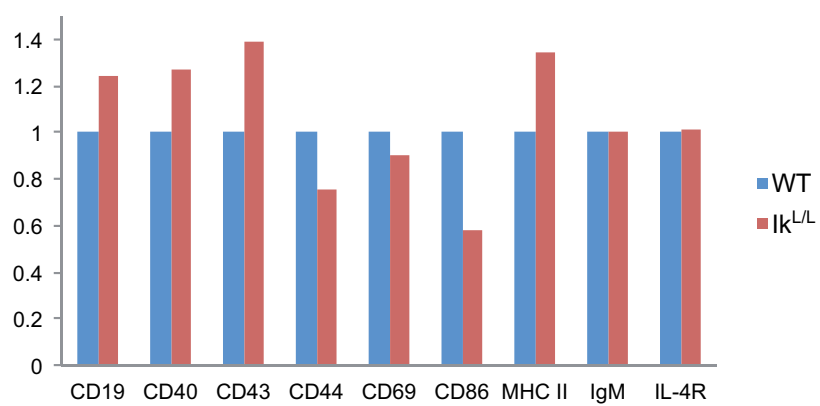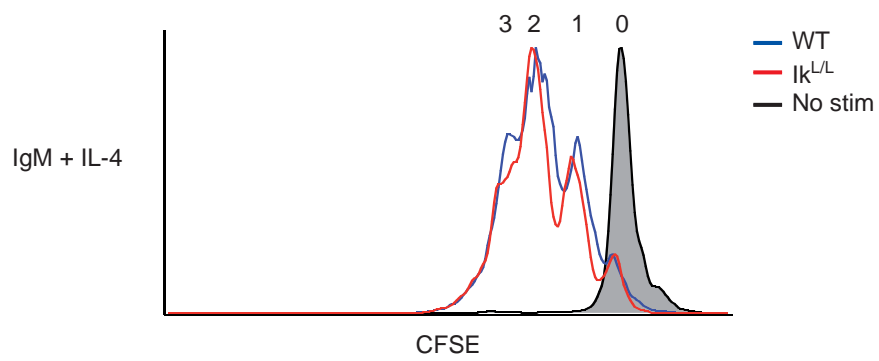
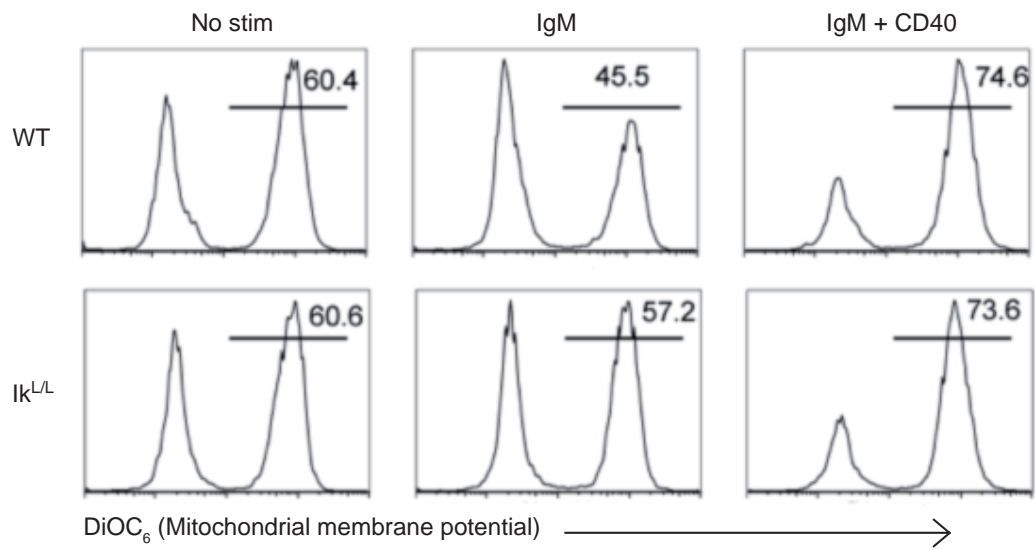60.4 45.5 74.6

60.6 57.2 73.6

Figure S3
Macias-Garcia et al.
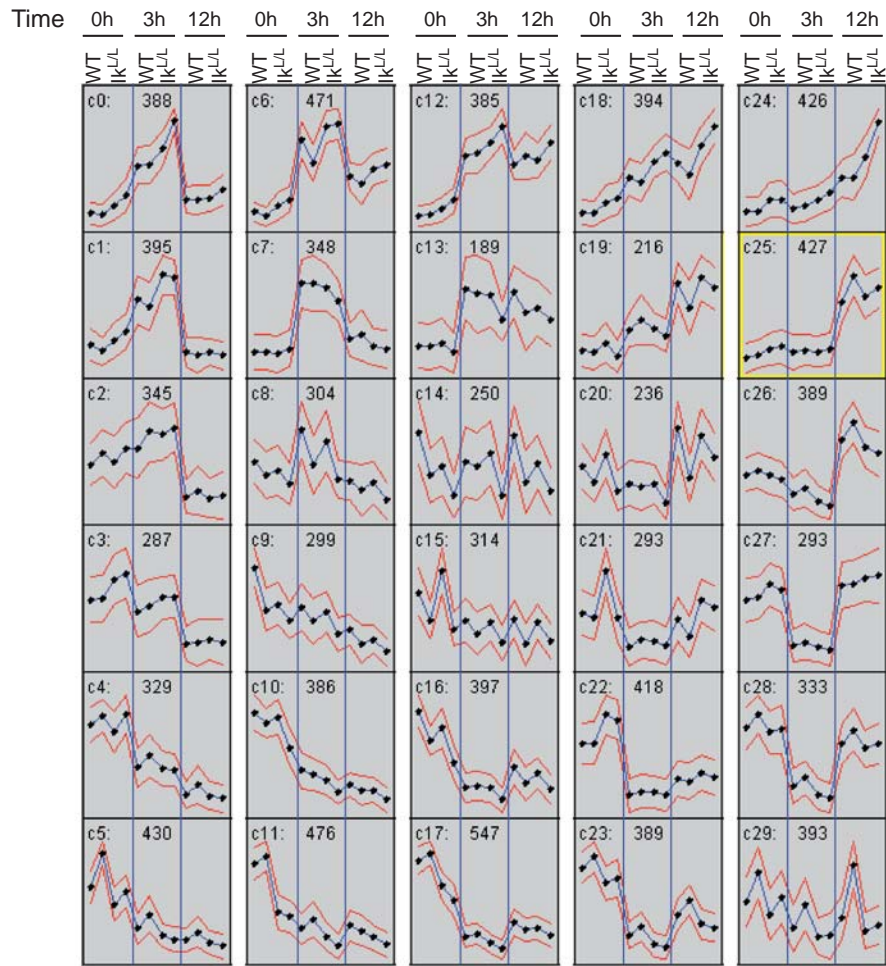
Figure S4
Macias-Garcia et al.
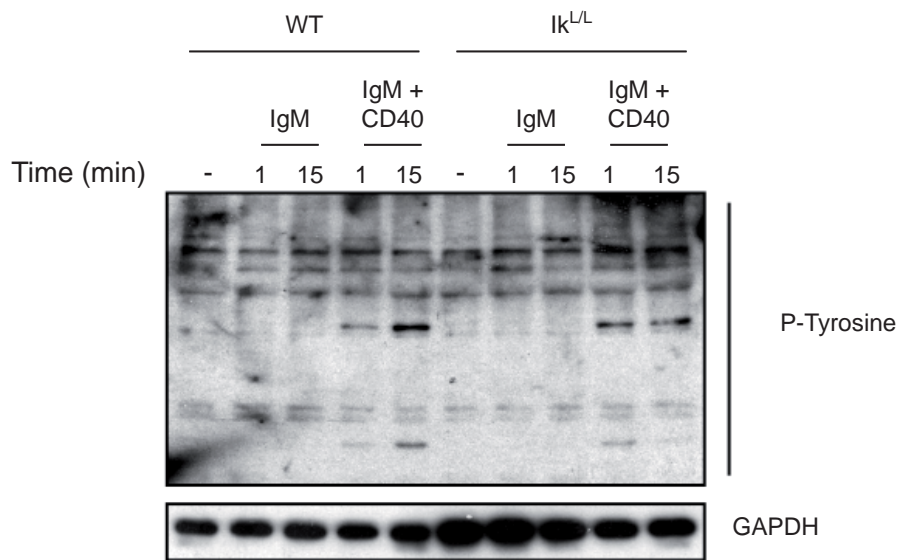
Figure S5
Macias-Garcia et al.

Figure S6
Macias-Garcia et al.

A.

Ik^{f/f} Rosa26-CreERT2

Cre   −   +
TAM   +   +

deleted

floxed

Cre   −   +
TAM   +   +

Ikaros

long exposure

short exposure

β-actin

B.

Ik^{f/f} CD21-Cre

CD43⁺ cells   FO B cells

Cre   −   +   −   +

deleted

floxed

CD43⁺ cells   FO B cells

Cre   −   +   −   +

Ikaros

β-actin

Figure S7
Macias-Garcia et al.

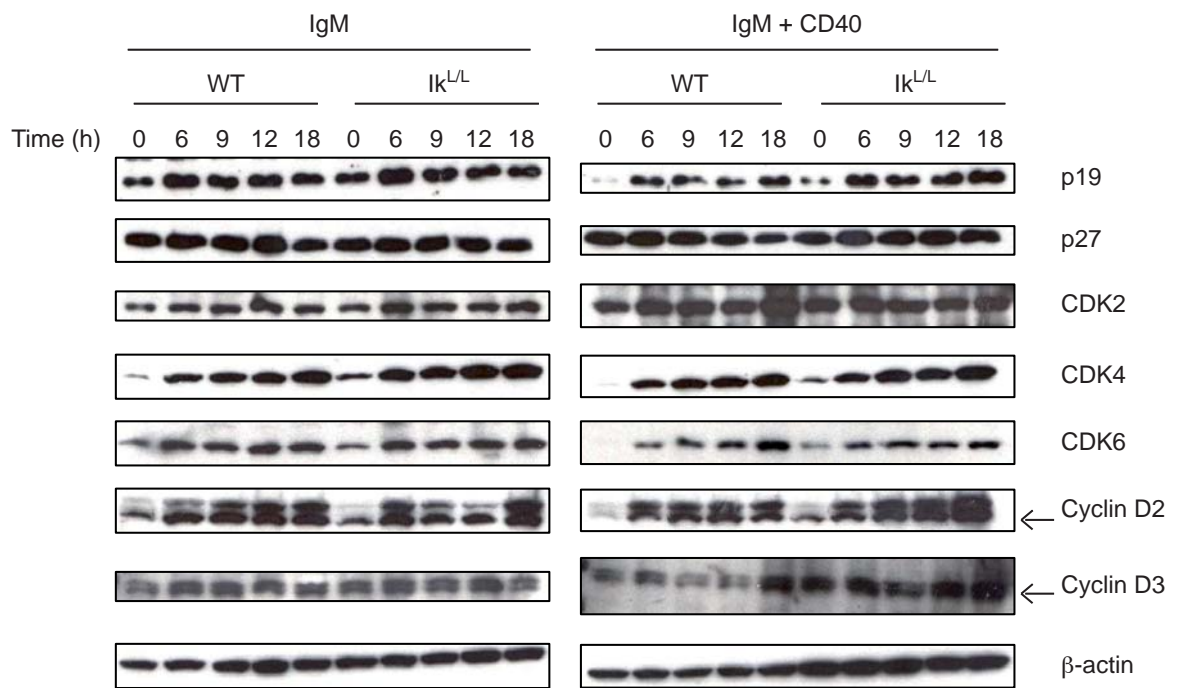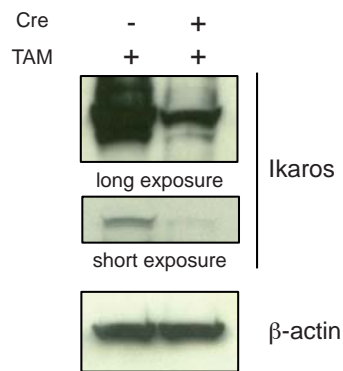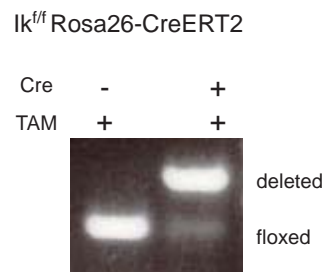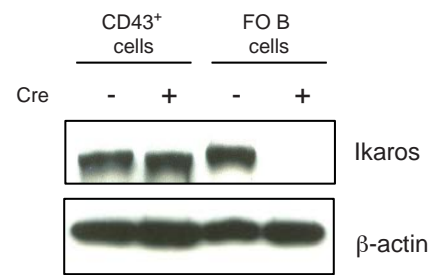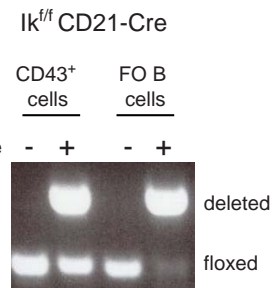# Section IV. B CELL ACTIVATION AND ITS RELATION WITH AUTO-IMMUNE SYMPTOMS IN THE IK$^{L/L}$ MOUSE

COMPLEMENTARY RESULTS

IV.6. The IL-4 dependent ERK phosphorylation

We have found that Ik$^{L/L}$ B cells show enhanced ERK phosphorylation and hyper-proliferation upon BCR stimulation. This phenotype could be due to several mechanisms. Guo et al. (2007) described an alternate pathway in which BCR signaling enhances ERK phosphorylation after the exposure of B cells to IL-4. This signaling was independent of PI-3K and PLC signalosome mediators, but dependent on Lyn and an unknown Rottlerin sensitive, molecule. To test if the alternate pathway could be responsible for the hyper-phosphorylation of ERK, Ik$^{L/L}$ and WT FO B cells were incubated with the PI-3K inhibitor Ly294002 to block the BCR signaling mediated by PI-3K, and with Rottlerin to inhibit the alternate pathway. Thereafter, the cells were stimulated with anti-IgM and the phosphorylation of ERK was measured by flow cytometry. While treatment with Ly294002 decreased ERK phosphorylation in WT cells, Rottlerin showed less effect. In contrast, ERK phosphorylation in the Ik$^{L/L}$ cells was severely affected by Rottlerin but not by Ly294002 (Fig. IV.4A). It is important to note that neither of the inhibitors alone abolished the phosphorylation of ERK in WT or IK$^{L/L}$ B cells. Moreover, use of both inhibitors in WT B cells decreased ERK phosphorylation to the same levels as non stimulated cells. This drastic effect was not seen in Ik$^{L/L}$ cells, where the use of both inhibitors demonstrated a synergistic effect in reducing ERK phosphorylation but did not completely inhibit phosphorylation (Fig. IV.4A). These results suggest that both pathways were activated in the Ik$^{L/L}$ cells.

If the alternate pathway is activated in Ik$^{L/L}$ cells, we hypothesized that the activation of this pathway in the WT cells would generate the same phenotype. To test this, WT and Ik$^{L/L}$ cells were exposed to IL-4 for 24 hours before incubation with the inhibitors and BCR stimulation. IL-4 exposure increased the ERK phosphorylation in WT cells to levels
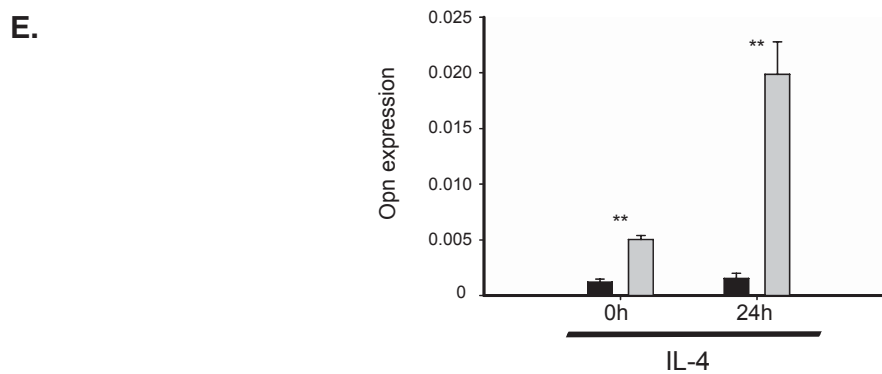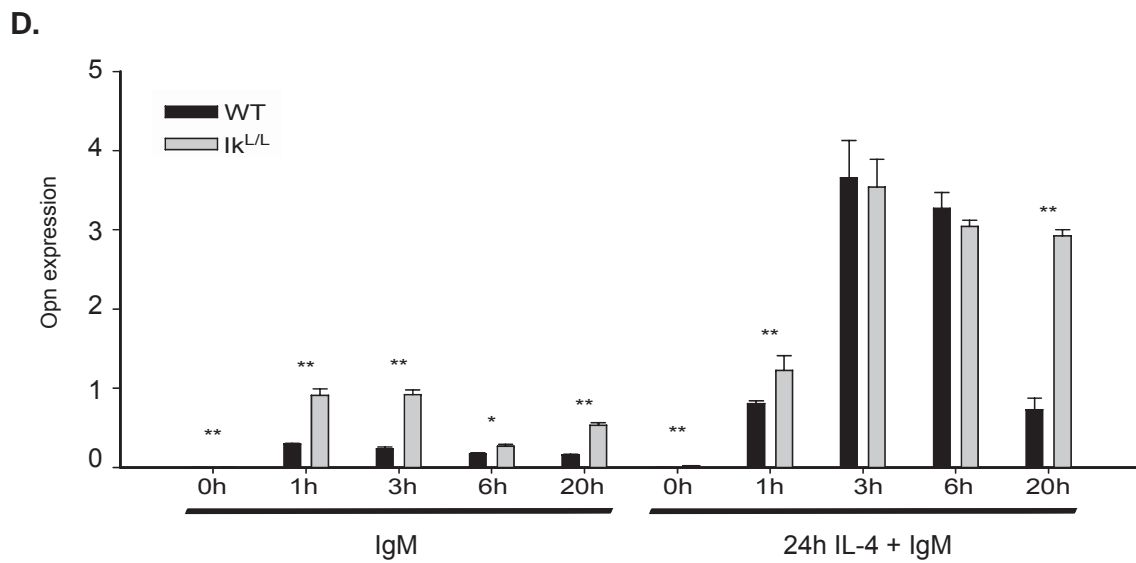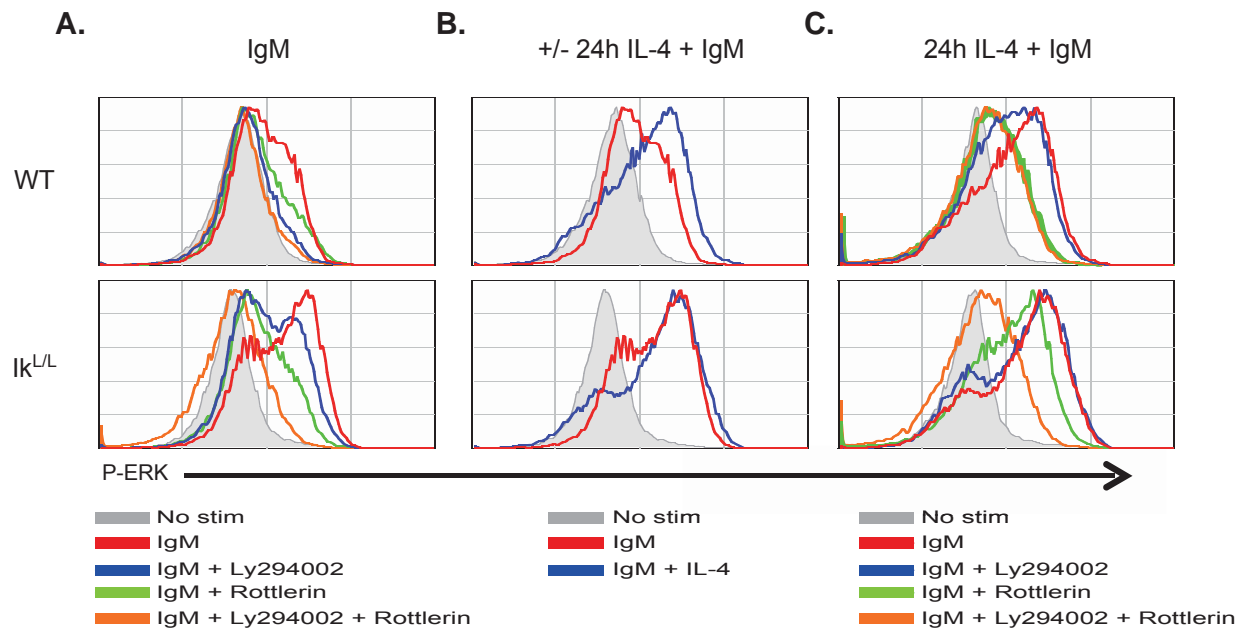
comparable to Ik$^{L/L}$ cells (Fig. IV.4B). However, the IL-4 treatment did not enhance the ERK phosphorylation in the Ik$^{L/L}$ cells, suggesting that these cells do not require exogenous IL-4 to activate the alternate pathway or that ERK phosphorylation is saturated in these cells. Indeed, while the IL-4 mediated ERK phosphorylation was not affected by Ly294002 in both genotypes, Rottlerin inhibited less ERK phosphorylation in Ik$^{L/L}$ cells than in WT cells (Fig. IV.4C). Moreover, both inhibitors did not reduce ERK phosphorylation to basal levels. Thus, IL-4 activates the alternate pathway in WT cells and increases ERK phosphorylation to levels similar to Ik$^{L/L}$, but Ik$^{L/L}$ did not require exogenous IL-4 for ERK activation.

It was described that the consequence of the alternate pathway is the production of Opn, an autoimmunity-associated cytokine (Rothstein and Guo, 2009). We evaluated Opn mRNA expression in WT and Ik$^{L/L}$ FO B cells exposed or not to IL-4 and BCR stimulation. BCR stimulation in cells without IL-4 exposure revealed 3x higher Opn expression in Ik$^{L/L}$ than in WT cells (Fig. IV.4D, left panel). As expected, Opn expression was increased in WT cells exposed to IL-4. Both WT and Ik$^{L/L}$ cells increased Opn expression after IL-4 exposure, and WT cells reached levels similar to Ik$^{L/L}$. Interestingly, Opn levels remained high in Ik$^{L/L}$ cells after 20 hours of stimulation, in contrast to WT cells where they were significantly decreased (Fig. IV.4D, right panel). Indeed, the basal levels of Opn were significantly higher in Ik$^{L/L}$ cells than in WT cells even in the absence of IL-4 (Fig. IV.4E). These data, together with the unaltered ERK phosphorylation after IL-4 exposure in Ik$^{L/L}$ cells, suggest that freshly isolated Ik$^{L/L}$ B cells are constitutively primed for better responsiveness through constitutive activation of the alternate pathway.

It was previously reported that Ikaros represses IL-4 expression in CD4+SP T cells (Quirion et al, 2009). This and our observation that Ik$^{L/L}$ B cells behave like IL-4-primed WT B cells suggested the possibility that elevated IL-4 levels *in vivo* may have primed Ik$^{L/L}$ B cells for better responsiveness. The analysis of IL-4 mRNA levels in total splenocytes revealed a ~3x increase in Ik$^{L/L}$ compared to WT cells (data not shown). Thus, it seems that the hyper-phosphorylation of ERK in Ik$^{L/L}$ B cells is mediated by a higher exposure to IL-4 and this could generate the different gene expression signature observed in the resting Ik$^{L/L}$. Therefore, we determined the genes induced or repressed after 24h of IL-4 exposure in

WT FO B cells (Affymetrix 430 2.0 arrays), and compared them to the genes over-expressed or down-regulated in naive Ik$^{L/L}$ B cells. 119 and 150 probe sets were induced or repressed, respectively, >2-fold by IL-4 in WT B cells (data not shown). However, there was no significant overlap between these genes and those overexpressed or repressed in freshly isolated Ik$^{L/L}$ B cells. Thus, the priming of Ik$^{L/L}$ B cells may not result from *in vivo* exposure to IL-4.

Fig. IV.4. WT and Ik$^{L/L}$ B cells activate ERK via different pathways after anti-IgM stimulation. A. ERK phosphorylation in cells incubated in absence or presence of Ly294002 and/or Rottlerin and stimulated with anti-IgM for 15 min. B. Levels of ERK phosphorylation in WT or Ik$^{L/L}$ FO B cells cultured for 24h with or without IL-4 and then stimulated with anti-IgM for 15 min. C. ERK phosphorylation of cells exposed 24h to IL-4 prior to treatment with IgM and inhibitors. D. RT-qPCR analysis of osteopontin (Opn) transcripts in FO B cells exposed or not to IL-4, and stimulated with anti-IgM for the indicated times. Arbitrary units. E. Increased basal Opn expression prior to anti-IgM stimulation (magnification of the 0h time point from D). Values are mean +/- sem. *p<0.05 and **p<0.005. Representative of 2 experiments (A-E).

A. IgM

B. +/- 24h IL-4 + IgM

C. 24h IL-4 + IgM

WT

Ik$^{L/L}$

P-ERK

No stim	No stim	No stim
IgM	IgM	IgM
IgM + Ly294002	IgM + IL-4	IgM + Ly294002
IgM + Rottlerin		IgM + Rottlerin
IgM + Ly294002 + Rottlerin		IgM + Ly294002 + Rottlerin

D.

E.

IV.7. B cell specific Ikaros deletion results in autoantibody production.

To complement the data obtained with the Ik$^{f/f}$ CD21-Cre mice, which indicated that Ikaros deficiency in mature B cells is sufficient for autoantibody production, we tested the serum of Ik$^{f/f}$ CD19-Cre mice (at 10 weeks of age) for anti-chromatin/nucleosome and anti-dsDNA antibodies. Ik$^{f/f}$ CD19-Cre^{+} mice delete Ikaros at Fr. B-C in the BM (see Fig.I.4). Serum from Ik$^{f/f}$ CD19-Cre^{+} mice showed increased levels of these antibodies of the IgM isotype compared to the littermate control Ik$^{f/f}$ CD19-Cre^{-} mice (Fig. IV.5). The levels of these antibodies were higher than the ones found in Ik$^{L/L}$ or in Ik$^{f/f}$ CD21-Cre^{+} mice of the same age. Indeed, some Ik$^{f/f}$ CD19-Cre^{+} mice showed higher levels than MRL/lpr mice (at 10 weeks of age). However, the IgG isotype was absent, which may be due to the young age of these mice. Further analysis should be performed in older mice. Thus, the Ik$^{f/f}$ CD19-Cre^{+} mice produce auto-antibodies related with SLE at levels comparable to those of MRL/lpr mice at 10 weeks of age.
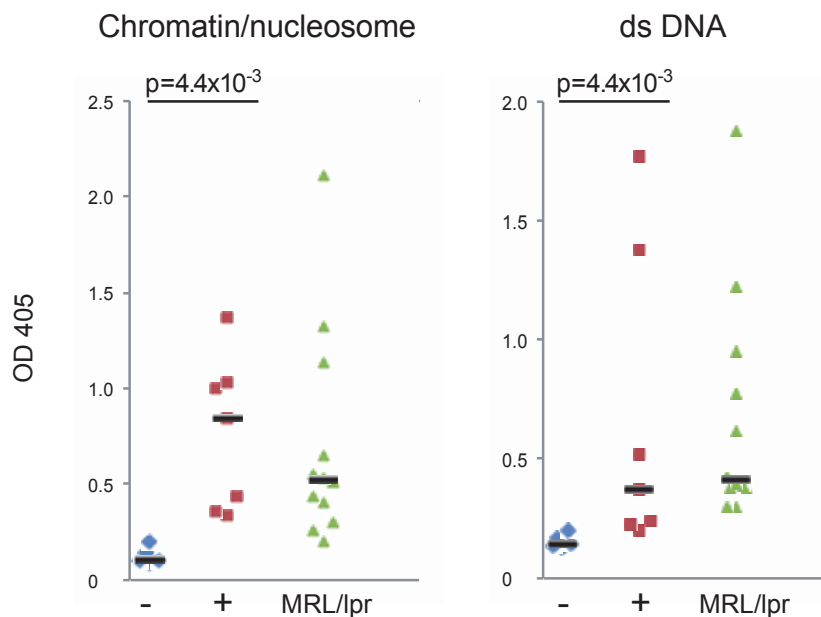
Figure IV.5. Ik$^{f/f}$ CD19-Cre^{+} mice produce autoantibodies. Serum from Ik$^{f/f}$ CD19-Cre^{+} (indicates as +) (n=7), Ik$^{f/f}$ CD19-Cre^{-} (indicates as -) (n=5) mice were tested for IgM antibodies to the indicated antigens by ELISA. Serum from MRL/lpr mice (n=12) were used as a positive control. Black bars show the mean of the indicated values. Statistical significance was determined by the Wilcoxon signed-rank test.

Section IV. **B CELL ACTIVATION AND ITS RELATION WITH AUTO-IMMUNE SYMPTOMS IN THE IK$^{L/L}$ MOUSE**

DISCUSSION

Here, we showed that Ikaros is a crucial regulator of the MAP kinase signaling that mediates the proliferation, cell growth and apoptotic response of follicular B cells upon the BCR and CD40 stimulation. Ikaros deficiency results in hyper-proliferation, increased growth and apoptosis inhibition. We found that a network of genes related to BCR, p38 and ERK signaling are deregulated in unstimulated Ik$^{L/L}$ FO B cells. The ERK and p38 MAP kinases exhibit striking increases in phosphorylation, and thus enhanced activation, in Ik$^{L/L}$ cells in response to stimulation. We also demonstrated that Ikaros deficiency leads to the production of autoantibodies associated with SLE. Importantly, this seems to be an intrinsic event as the specific deletion of Ikaros in mature B cells also induces autoantibody production. These results indicate that Ikaros is a negative regulator of B cell activation.

Is the enhanced ERK activation responsible for the hyper-proliferation in Ikaros-deficient cells? ERK and p38 are thought to be important for B cell proliferation and survival, respectively, in response to stimulation through the BCR and CD40 (Craxton et al., 1998; Han et al., 2003; Richards et al., 2001). We demonstrated that only the simultaneous inhibition of ERK and p38 decreases the proliferative advantage of Ik$^{L/L}$ cells over WT cells. However, we found that the sensitivity of ERK phosphorylation to inhibitors of the classical PI-3K dependent and the alternate Rottlerin sensitive pathway, was not the same in Ik$^{L/L}$ B cells compared to WT, suggesting the activation of different pathways of BCR signaling. Contrary to what was observed in WT cells, the PI-3K inhibitor have little effect in the Ik$^{L/L}$ ERK phosphorylation while the Rottlerin inhibitor have strong effect. However, the use of both inhibitors did not reduce the ERK phosphorylation to basal levels. The activation of the Rottlerin sensitive pathway in the WT cells by the exposure to IL-4, increased the ERK phosphorylation to levels comparable to Ik$^{L/L}$. This suggests that ERK hyper-phosphorylation in Ik$^{L/L}$ cells may be due, at least in part, to the alternate IL-4 pathway. Moreover, we found that Ik$^{+/L}$ FO B cells display increased proliferation compared to WT

but they do not reach the levels seen in Ik$^{L/L}$ FO B cells after anti-IgM +/- anti-CD40 stimulation (data not shown). However, Ik$^{+/L}$ B cells exhibit similar ERK phosphorylation as WT B cells after anti-IgM +/- anti-CD40 stimulation, suggesting that different mechanisms could be involved in the BCR mediated proliferation and ERK activation, and that proliferation is more sensitive to Ikaros levels. The analysis of the different kinases upstream ERK should be performed to clarify how ERK is activated in Ik$^{L/L}$ B cells and to test if the specific inhibition of these kinases affects proliferation.

Is the alternate ERK activation responsible for the auto-immune symptoms in the Ik$^{L/L}$ mice? Our results suggest that ERK phosphorylation in Ik$^{L/L}$ cells is mediated in different ways. It is possible that one of them is necessary to sustain the proliferation as ERK inhibition decreases the proliferation. Others may be important for the autoimmune phenotype seen in Ik$^{L/L}$ mice. The elevated expression of Opn has been reported in human autoimmune diseases such as SLE, rheumatoid arthritis and multiple sclerosis, as well as in murine models of human lupus (Patarca et al. 1990; Katagiri et al., 1995; Hudkins et al., 2000; Yumoto et al., 2002; Ohsima et al., 2002; Comabella et al., 2005; Weber et al., 2001). Ik$^{L/L}$ B cells show increased levels of Opn compared to WT, before and after BCR stimulation. IL-4 mediated ERK activation in WT cells triggers the production of Opn to similar levels as Ik$^{L/L}$, suggesting that the ERK phosphorylation due to IL-4 could be important for the autoimmune phenotype in Ik$^{L/L}$ mice. In addition, the B cell signature of a subgroup of quiescent SLE patients revealed an IL-4 signature, suggesting that an IL-4 pathway can be involved in the development of lupus (Garaud et al., 2011). Thus, it will be interesting to analyze the effect of IL-4 for the phenotype seen in Ik$^{L/L}$ mice (hyper-proliferation, ERK phosphorylation and Opn and antibody production), This could be done by crossing an IL-4 knockout mouse with the Ik$^{L/L}$ mouse, which should indicate if the deficiency of IL-4 affects or enhances Ik$^{L/L}$ phenotype.

How does Ikaros control cell cycle entry and BCR mediated apoptosis? The increased proliferation in Ik$^{L/L}$ cells could be supported by accelerated cell cycle entry and/or reduced apoptosis. We showed that Ik$^{L/L}$ B cells display accelerated cell cycle entry/progression after anti-IgM + anti-CD40 stimulation. One important molecule for cell cycle entry following

the BCR stimulation is Cyclin D2 (Solvason et al., 2000). Its expression is controlled by BCR-ERK signaling (Piatelli et al., 2002; Piatelli et al., 2004). However, the analysis of Cyclin D2 protein levels after anti-IgM +/- anti-CD40 revealed no difference between Ik$^{L/L}$ and WT B cells at the time points analyzed (0, 6, 9, 12 and 18h). Moreover, intracellular Cyclin D2 staining showed higher expression of Cyclin D2 in WT cells after 24h with anti-IgM stimulation (data not shown). These results suggest that the hyper-proliferation in Ik$^{L/L}$ cells could be independent of Cyclin D2. In addition, the other components of the G0/G1 to S transition were expressed at similar levels in both genotypes. This means that the components for the cell cycle entry are not affected. Another possibility is that the time points that we analyzed were not the correct ones to a difference in the cell cycle regulators and that we should investigate earlier time points.

Besides the accelerated cell cycle entry, we found less apoptotic cells in the Ik$^{L/L}$ samples compared to WT upon anti-IgM + anti-CD40 stimulation. ERK can down regulate Bim in response to co-stimulatory signals (e.g. BAFF), and influence the BCR mediated apoptosis (Craxton et al., 2005; Enders et al., 2003). Thus, increased ERK activation in Ik$^{L/L}$ cells may promote survival by the down regulating Bim. It would be interesting to measure Bim expression after BCR stimulation. Thus, although the mechanisms by which Ik$^{L/L}$ cells have accelerated cell cycle entry and reduced apoptosis are not clear, they seem to be driven by increased MAP kinase activation. The use of inhibitors or enhancer for ERK and p38 activation could determine the contribution of these MAP kinases to the cell cycle and apoptosis. Furthermore, a better understanding of the mechanism that drives apoptosis in Ik$^{L/L}$ cells would be helpful to determine if the diminution of apoptosis is involved in B cell tolerance, like what has been shown for lupus-prone mice (Tsubata, 2005).

Is the Ikaros deficiency an important factor to B cell tolerance? We showed here that the Ik$^{L/L}$ mice produce autoantibodies and that Ikaros deficiency in mature B cells was enough to generate the autoantibodies as well as alter ERK phosphorylation. This is in line with the diminution of Ikaros function by the expression of dn Ikaros isoforms in B cells that results in reduced B cell activation thresholds and the expression of higher levels of autoantibodies (Wojcik et al., 2007). In addition, we found higher autoantibody levels in the

serum of Ik$^{f/f}$ CD19-Cre$^+$ mice compared to Ik$^{f/f}$ CD21-Cre$^+$ mice. The CD19-Cre mediated Ikaros deletion occurs in the BM at Fr. B-C, before the tolerance checkpoints (at Fr. E). The CD21-Cre mediated Ikaros deletion takes place in the spleen in cells already exposed to some of this checkpoints. These results suggest that deletion of Ikaros at an early stage of B cell development enhances autoantibody production, and that this could be due to alterations in B cell tolerance. However, the analysis of ERK phosphorylation levels and proliferation has to be performed in Ik$^{f/f}$ CD19-Cre B cells. To test the contribution of Ikaros to B cell tolerance, a transgenic mouse model for auto-reactive B cells, such as the hen egg lysozome (HEL) model (Goodnow et al., 1989), can be used. The MD4 mouse line expresses the HEL specific immunoglobulin, and breeding this line to one that expresses soluble HEL (sHEL) induces anergic MD4 B cells. These anergic cells are able to pass the tolerance checkpoints, go to the periphery and produce little, if any, spontaneous HEL-specific antibody (Goodnow et al., 1989). It was shown that the reduction of the activation threshold by the over-expression of CD19 in the MD4/sHEL mouse results in the production of anti-HEL antibodies suggesting the breakdown of peripheral tolerance (Inaoki et al., 1997). Breeding the MD4/sHEL line with the Ik$^{f/f}$ CD19-Cre and Ik$^{f/f}$ CD21-Cre mouse lines and the analysis of antibody production would help to determine if Ikaros is required to maintain B cell anergy, and if this is important in early or late tolerance checkpoints.

Does Ikaros deficiency contribute to SLE development? Genome-wide studies have identified Ikaros polymorphisms in SLE patients (Han et al, 2009; Cunninghame Graham et al, 2011). We found that Ikaros deletion in the germ line and specifically in B cells, results in SLE-associated antibody production. However, it is not clear if Ikaros is involved only in the production of autoantibodies or in other parts of SLE development. To verify the contribution of B cell specific Ikaros deficiency in the development of lupus, we could cross of a lupus-prone mouse such as MRL/lpr with the Ik$^{f/f}$ CD21-Cre$^+$ to delete Ikaros specifically in mature B cells. If Ikaros deficiency contributes to SLE, the lupus phenotype would be enhanced in the MRL/lpr mice and the development of the disease should appear at early age.

Is Ikaros involved in the control of the proliferation only in B cells? Is the proliferation sensitive to Ikaros levels? The proliferative response of both B and T cells is sensitive to Ikaros levels. It was previously shown in the lab that T cells of Ik$^{L/L}$ and Ik$^{+/L}$ mice hyper-proliferate in response to anti-CD3 stimulation *in vitro* (Dumortier et al., 2006). Thus, in both, B and T cells, loss of Ikaros leads to enhanced proliferation, even after loss of a single allele. Furthermore, Ikaros may control the proliferation of DN4 T cells, through signals via the pre-T cell receptor (Kleinmann et al., 2008; Winandy et al., 1999). Ikaros deficiency also leads to pro-B cell accumulation, although it is currently unclear if this reflects increased proliferation downstream of the pre-BCR (Kirstetter et al, 2002). These observations suggest that a common mechanism, for B and T cells, could mediate the control of proliferation by Ikaros. It will be important to test if Ikaros-dependent modulation of ERK and p38-signalling pathways also controls the pre-BCR, pre-TCR and TCR signaling responses as this may have implications for the tumor suppressor function of Ikaros in T cells.

In conclusion, our results suggest that ERK phosphorylation in Ik$^{L/L}$ B cells are activated differently than in WT cells. Altered B cell activation may lead to predisposition to SLE. The evidence that enhanced ERK and p38 phosphorylation are involved in the hyper-activation of B cells suggests that pharmacological inhibition of these molecules may be useful for the therapy of SLE patients.

MATERIAL AND METHODS

1. Cell culture

Follicular B cells were enriched by depletion of CD43$^+$ cells followed by positive selection of CD23$^+$ cells with MACS beads (CD43 (Ly-48) beads and Streptavidin beads after CD23-biotin staining) (>90% purity, Miltenyi Biotech). Cells were incubated 24h with/without 10ng/ml IL4 (Peprotech). Cells were stimulated with 10µg/mL goat anti-mouse IgM F(ab') (Jackson Immunoresearch) and 10µg/mL mouse anti-CD40 (clone 1C10; ebiosience). The following inhibitors were used: Ly294002 (2µM, Cell Signalling), Rottlerin (10µM, Calbiochem).

2. Flow cytometry

For intracellular staining for phospho-ERK, cells were fixed in 2% Ultra-pure Formaldehyde (Electron Microscopy Science) for 10 min at RT. Cells were pelleted and permeablized with 100% ice cold methanol and incubated for >30 min on ice or at -20°C. Cells were then blocked in PBS supplemented with 10% FCS, 1% mouse serum, 1% rat serum and Fc Block (1:50). Samples were stained with Phospho-ERK (p44/42-Thr202/Tyr204) followed by biotin conjugated anti-rabbit IgG and Streptavidin-PE. Cells were analyzed with a FACSCalibur (BD BioSciences) and FlowJo software (TreeStar).

3. RT-qPCR

Total RNA was extracted from 1.50×10^5 cells using the RNeasy micro kit (Qiagen). RNAs were reverse-transcribed with SuperScript II reverse transcriptase (Invitrogen). qPCR reactions were performed in triplicate with cDNA from an equivalent of 15×10^4 cells with the Quantitect SYBR Green PCR kit (Qiagen; 40 cycles of 95°C 30 sec, 58°C 30 sec and 72°C 30 sec) and the LightCycler 480 Real-time PCR System (Roche). PCRs were analyzed with the LightCycler 480 basic software and the concentration of amplified cDNA was calculated relative to that of HPRT. Primers for Opn were from the Qiagen Quantitect assay Mm_Spp1_1_SG. HPRT primers were: 5'-GTTGGATACAGGCCAGACTTTGTTG and 5'-GATTCAACTTGCGCTCATCTTAGGC.

Ikaros deficiency: from T-ALL to auto-immune disease

CONCLUSIONS

The transcription factor Ikaros is essential for lymphopoiesis. The results shown here display how Ikaros deficiency affects B and T cells. Ikaros plays mainly a role of a transcriptional repressor, and it could be that this function is the same in all cells where it is expressed. However the expression of specific lineage genes and the epigenetic factors in each cell influences how Ikaros affects different pathways and functions, resulting in distinct phenotypes such as leukemia and autoimmune disease.

Ikaros function can be associated with the principal pathways that affect the normal development and function of lymphocytes. In B cells, Ikaros deficiency could affect the pathways downstream BCR signaling. We found that Ik$^{L/L}$ B cells have enhanced ERK and p38 activation after BCR stimulation which results in increased proliferation, reduced apoptosis and autoantibody production. In T cells, Ikaros competes with RBP-J of the Notch pathway to affect the normal development of T cells. Ikaros deficiency results in an aberrant activation of the Notch pathway that results in leukemia. We found that the deletion of the Notch1 promoter results in the generation of truncated ligand-independent Notch1 proteins which accelerate the development of leukemia. However, we observed that Notch activation is not sufficient for the development of leukemia, as the deletion of the Notch1 promoter in a WT background does not generate tumors. This suggests that Ikaros function may touch other pathways perhaps downstream of the TCR to affect proliferation and activation, similar to B cells where Ikaros affects the BCR signaling. It is important to note that not all the effects of Ikaros deficiency in the germ line may be observed, as some of them would have stronger consequences, like the fast development of leukemia which could hide a later susceptibility to SLE.

Ikaros affects the proliferation of B and T cells, and this is sensitive for Ikaros levels. Abnormal proliferation in both cell lineages can be observed, not only in homo- but also in heterozygote mice. The enhanced proliferation could be a consequence of the lower

activation threshold. However, the effect could be cell-specific, and altered proliferation could affect apoptosis-mediated selection differently in different cells. In B cells, this might affect tolerance. In T cells, it would lead an accumulation and expansion of immature cells.

Thus, Ikaros is an important transcription factor that affects both the development and the function of lymphocytes.

REFERENCES

Adachi T, Flaswinkel H, Yakura H, Reth M, Tsubata T, 1998. The B cell surface protein CD72 recruits the tyrosine phosphatase SHP-1 upon tyrosine phosphorylation. J Immunol 160(10):4662–4665.

Adachi T, Wienands J, Wakabayashi C, Yakura H, Reth M, Tsubata T, 2001. SHP-1 requires inhibitory co-receptors to down-modulate B cell antigen receptor-mediated phosphorylation of cellular substrates. J Biol Chem 276(28):26648–26655.

Al-Hajj M, Wicha MS, Benito-Hernandez A, Morrison SJ, Clarke MF, 2003. Prospective identification of tumorigenic breast cancer cells. Proc Natl Acad Sci U S A 100(7):3983-3988.

Allman D, Dalod M, Asselin-Paturel C, Delale T, Robbins SH, Trinchieri G, Biron CA, Kastner P, Chan S, 2006. Ikaros is required for plasmacytoid dendritic cell differentiation. Blood 108(13):4025-4034.

Allman D, Lindsley RC, DeMuth W, Rudd K, Shinton SA, Hardy RR, 2001. Resolution of three nonproliferative immature splenic B cell subsets reveals multiple selection points during peripheral B cell maturation. J Immunol 167(12), 6834-6840.

Allman D, Sambandam A, Kim S, Miller JP, Pagan A, Well D, Meraz A, Bhandoola A, 2003. Thymopoiesis independent of common lymphoid progenitors. Nature Immunol 4(2):168-174.

Amsen D, Blander JM, Lee GR, Tanigaki K, Honjo T, Flavell RA, 2004. Instruction of distinct CD4 T helper cell fates by different notch ligands on antigen-presenting cells. Cell 117(4):515-526.

Anolik JH, 2007. B cell biology and dysfunction in SLE. Bull NYU Hosp Jt Dis 65(3):182-186.

Arbuckle MR, McClain MT, Rubertone MV, Scofield RH, Dennis GJ, James JA, Harley JB, 2003. Development of autoantibodies before the clinical onset of systemic lupus erythematosus. N Engl J Med 349(16):1526-1533.

Armstrong F, Brunet de la Grange P, Gerby B, Rouyez MC, Calvo J, Fontenay M, Boissel N, Dombret H, Baruchel A, Landman-Parker J, Roméo PH, Ballerini P, Pflumio F, 2009. NOTCH is a key regulator of human T-cell acute leukemia initiating cell activity. Blood 113(8):1730-1740.

Ashworth TD, Pear WS, Chiang MY, Blacklow SC, Mastio J, Xu L, Kelliher M, Kastner P, Chan S, Aster JC, 2010. Deletion-based mechanisms of Notch1 activation in T-ALL: key roles for RAG recombinase and a conserved internal translational start site in Notch1. Blood 116(25):5455-5464.

Aster JC, Pear WS, Blacklow SC, 2008. Notch signaling in leukemia. Annu Rev Pathol 3:587-613.

Avitahl N, Winandy S, Friedrich C, Jones B, Ge Y, Georgopoulos K, 1999. Ikaros sets thresholds for T cell activation and regulates chromosome propagation. Immunity 10(3):333-343.

Ballen KK, Valinski H, Greiner D, Shultz LD, Becker PS, Hsieh CC, Stewart FM, Quesenberry PJ, 2001. Variables to predict engraftment of umbilical cord blood into immunodeficient mice: usefulness of the non-obese diabetic—severe combined immunodeficient assay. Br J Haematol 114(1):211–218.

Ballestar E, Esteller M, Richardson BC, 2006. The epigenetic face of systemic lupus erythematosus. J Immunol 176(12):7143-7147.

Bateman CM, Colman SM, Chaplin T, Young BD, Eden TO, Bhakta M, Gratias EJ, van Wering ER, Cazzaniga G, Harrison CJ, Hain R, Ancliff P, Ford AM, Kearney L, Greaves M, 2010. Acquisiton of genome-wide copy number alterations in monozygotic twins with acute lymphoblastic leukemia. Blood 115:3553-3558.

Batista FD, Arana E, Barral P, Carrasco YR, Depoil D, Eckl-Dorna J, Fleire S, Howe K, Vehlow A, Weber M, Treanor B, 2007. The role of integrins and coreceptors in refining thresholds for B-cell responses. Immunol Rev 218:197-213.

Baylin SB, Jones PA, 2011. A decade of exploring the cancer epigenome - biological and translational implication. Nat Rev Cancer 11(10):726-734.

Bellacosa A, Chan TO, Ahmed NN, Datta K, Malstrom S, Stokoe D, McCormick F, Feng J, Tsichlis P, 1998. Akt activation by growth factors is a multiple-step process: the role of the PH domain. Oncogene 17(3):313–325.

Bellacosa A, Testa JR, Staal SP, Tsichlis PN, 1991. A retroviral oncogene, akt, encoding a serine-threonine kinase containing an SH2-like region. Science 254(5029):274-277.

Bellavia D, Mecarozzi M, Campese AF, Grazioli P, Talora C, Frati L, Gulino A, Screpanti I, 2007. Notch3 and the Notch3-upregulated RNA-binding protein HuD regulate Ikaros alternative splicing. EMBO J 26(6):1670-1680.

Bellavia D, Mecarozzi M, Campese AF, Grazioli P, Talora C, Frati L, Gulino A, Screpanti I, 2007. Notch3 and the Notch3-upregulated RNA-binding protein HuD regulate Ikaros alternative splicing. EMBO J. 26(6):1670–1680.

Beverly LJ, Capobianco AJ, 2003. Pertubation of Ikaros isoforms selection by MLV integration is a cooperative event in Notch(IC)-induced T cell leukemogenesis. Cancer Cell 3(6):551-564.

Boggs SS, Trevisan M, Patrene K, Georgopoulos K, 1998. Lack of NK cell precursors in fetal liver of Ikaros knockout mutant mice. Nat Immun 16(4):137-145.

Bonnet D, Dick JE, 1997. Human acute myeloid leukemia is organized as a hierarchy that originates from a primitive hematopoietic cell. Nat Med 3(7):730-737.

Bonnet M, Loosveld M, Montpellier B, Navarro JM, Quilichini B, Picard C, Di Cristofaro J, Bagnis C, Fossat C, Hernandez L, Mamessier E, Roulland S, Morgado E, Formisano-Treziny C, Dik WA, Langerak AW, Prebet T, Vey N, Michel G, Gabert J, Soulier J, Macintyre EA, Asnafi V, Payet-Bornet D, Nadel B, 2011. Posttranscriptional deregulation of MYC via PTEN constitutes a major alternative pathway of MYC activation in T-cell acute lymphoblastic leukemia. Blood 117(24):6650-6659.

Bosma GC, Custer RP, Bosma MJ, 1983. A severe combined immunodeficiency mutation in the mouse. Nature 301(5900):527–530.

Brown KE, Baxter J, Graf D, Merkenschlager M, Fisher AG, 1999. Dynamic repositioning of genes in the nucleus of lymphocytes preparing for cell division. Mol Cell 3(2):207-217.

Brown KE, Guest SS, Smale ST, Hahm K, Merkenschlager M, Fisher AG, 1997. Association of transcriptionally silent genes with Ikaros complexes at centromeric heterochromatin. Cell 91(6):845-854.

Bruce WR, Van Der Gaag H, 1963. A quantitative assay for the number of murine lymphoma cells capable of proliferation in vivo, Nature 199:79-80.

Buhl AM, Cambier JC, 1999. Phosphorylation of CD19 Y484 and Y515, and linked activation of phosphatidylinositol 3-kinase, are required for B cell antigen receptor-mediated activation of Bruton's tyrosine kinase. J Immunol 162(8):4438–4446.

Burnet FM, 1972. A reassessment of the forbidden clone hypothesis of autoimmune disease. Aust J Exp Biol Med Sci 50(1):1-9.

Busslinger M, 2004. Transcriptional control of early B cell development. Annu Rev Immunol 22:55-79.

Carsetti R, Kohler G, Lamers MC, 1993. A role for immunoglobulin D: interference with tolerance induction. Eur J Immunol 23, 168-178.

Carsetti R, Kohler G, Lamers MC, 1995. Transitional B cells are the target of negative selection in the B cell compartment. J Exp Med 181(6):2129-2140.

Castor A, Nilsson L, Astrand-Grundstrom I, Buitenhius M, Ramirez C, Anderson K, Strombeck B, Garwicz S, Bekassy AN, Schmiegelow K, Lausen B, Hokland P, Lehmann S, Juliusson G, Johansson B, Jacobsen SE, 2005. Distinct patterns of hematopoietic stem cell involvement in acute lymphoblastic leukemia. Nat Med 11(6):630:637.

Chang NH, McKenzie T, Bonventi G, Landolt-Marticorena C, Fortin PR, Gladman D, Urowitz M, Wither JE, 2008. Expanded population of activated antigen-engaged cells within the naïve B cell compartment of patients with systemic lupus erythematosus. J Immunol 2008;180(2):1276-1284.

Chao DT, Korsmeyer SJ, 1998. BCL-2 family: regulators of cell death. Annu Rev Immunol 16:395–419.

Chari S, Umetsu SE, Winandy S, 2010. Notch target gene deregulation and maintenance of the leukemogenic phenotype do not require RBP-J kappa in Ikaros null mice. J Immunol 185(1):410-417.

Chiba T, Kita K, Zheng YW, Yokosuka O, Saisho H, Iwama A, Nakauchi H, Taniguchi H, 2006. Side population purified from hepatocellular carcinoma cells harbors cancer stem cell-like properties. Hepatology 44(1):240-251.

Chiu CW, Dalton M, Ishiai M, Kurosaki T, Chan AC, 2002. BLNK: molecular scaffolding through 'cis'-mediated organization of signaling proteins. Embo J 21(23):6461-6472.

Chiu PP, Jiang H, Dick JE, 2010. Leukemia-initiating cells in human T-lymphoblastic leukemia exhibit glucocorticoid resistance. Blood 116(24):5268-5279.

Chua C, Zaiden N, Chong KH, See SJ, Wong MC, Ang BT, Tang C, 2008. Characterization of a side population of astrocytoma cells in response to temozolomide. J Neurosurg 109(5):856-866.

Chung JB, Silverman M, Monroe JG, 2003. Transitional B cells: step by step towards immune competence. Trends Immunol 24(6):343-349.

Ciofani M, Knowles GC, Wiest DL, von Boehmer H, Zuñiga-Pflucker JC, 2006. Stage-specific and differential notch dependency at the alphabeta and gammadelta T lineage bifurcation. Immunity 25(1):105-116.

Ciofani M, Zuñiga-Pflucker JC, 2005. Notch promotes survival of pre-T cells at the beta-selection checkpoint by regulating cellular metabolism. Nat Immunol 6(9):881-888.

Clappier E, Gerby B, Sigaux F, Delord M, Touzri F, Hernandez L, Ballerine P, Baruchel A, Pflumio F, Soulier J, 2011. Clonal selection in xenografted human T cell acute lymphoblastic leukemia recapitulates gain of malignancy at relapse. J Exp Med 208(4):653-661.

Clark MR, Campbell KS, Kazlauskas A, Johnson SA, Hertz M, Potter TA, Pleiman C, Cambier JC, 1992. The B cell antigen receptor complex: association of Ig-alpha and Ig-beta with distinct cytoplasmic effectors. Science 258(5079):123–126.

Clarke MF, Dick JE, Dirks PB, Eaves CJ, Jamieson CH, Jones DL, Visvader J, Weissman IL, Wahl GM, 2006. Cancer Stem Cells--perspectives on current status and future directions: AACR Workshop on cancer stem cells. Cancer Res 66(19):9339-9344.

Clarkson B, Fried J, Strife A, Sakai Y, Ota K, Okita T, 1970. Studies of cellular proliferation in human leukemia. 3. Behavior of leukemic cells in three adults with acute leukemia given continous infusion of 3H-thymidine for 8 or 10 days. Cancer 25(6):1237-1260.

Clarkson BD, 1969. Review of recent studies of cellular proliferation in acute leukemia. Natl Cancer Inst Monogr 30:81-120.

Clarkson BD, 1974. The survival value of the dormant state in neoplastic and normal populations. In: Clarkson B, Basega R, eds. Control of proliferation in animal cells. New York, NY: Cold Spring Harbor Laboratory 945-972.

Cobaleda C, Gutiérrez-Cianca N, Pérez-Losada J, Flores T, García-Sauz R, González M, Sánchez-García I, 2000. A primitive hematopoietic cell is the target for the leukemic transformation in human Philadelphia-positive acute lymphoblastic leukemia. Blood 95(3):1007-1013.

Cobaleda C, Jochum W, Busslinger M, 2007. Conversion of mature B cells into T cells by dedifferentiation to uncommitted progenitors. Nature 449(7161):473-477.

Cobb BS, Morales-Alcelay S, Kleiger G, Brown KE, Fisher AG, Smale ST, 2000. Targeting of Ikaros to pericentromeric heterochromatin by direct DNA binding. Genes Dev 14(17):2146-2160.

Cobb RM, Oestreich KJ, Osipovich OA, Oltz EM, 2006. Accessibility control of V(D)J recombination. Adv Immunol 91:45-109.

Comabella M, Pericot I, Goertsches R, Nos C, Castillo M, Blas Navarro J, Rio J, Montalban X, 2005. Plasma osteopontin levels in multiple sclerosis. J Neuroimmunol 158(1-2):231–239.

Cooke MP, Heath AW, Shokat KM, Zeng Y, Finkelman FD, Linsley PS, Howard M, Goodnow CC, 1994. Immunoglobulin signal transduction guides the specificity of B cell-T cell interactions and is blocked in tolerant self-reactive B cells. J Exp Med 179(2):425-438.

Cooray HC, Blackmore CG, Maskell L, Barrand MA, 2002. Localisation of breast cancer resistance protein in microvessel endothelium of human brain. Neuroreport 13(16):2059-2063.

Cope AP, Feldmann M, 2004. Emerging approaches for the therapy of autoimmune and chronic inflamatory disease. Curr Opin Immunol 16(6):780-786.

Corcoran AE, 2005. Immunoglobulin locus silencing and allelic exclusion. Semin Immunol 17(2):141-154.

Cox CV, Diamanti P, Evely RS, Kearns PR, Blair A, 2009. Expression of CD133 on leukemia-initiating cells in childhood ALL. Blood 113(14):3287-3296.

Cox CV, Martin HM, Kearns PR, Virgo P, Evely RS, Blair A, 2007. Characterization of a progenitor cell propulation in childhood T-cell acute lymphoblastic leukemia. Blood 109(2):674-682.

Craxton A, Draves KE, Gruppi A, Clark EA, 2005. BAFF regulates B cell survival by downregulating the BH3-only family member Bim via the ERK pathway. J Exp Med 202(10):1363-1374.

Craxton A, Shu G, Graves JD, Saklatvala J, Krebs EG, Clark EA, 1998. p38 MAPK is required for CD40-induced gene expression and proliferation in B lymphocytes. J Immunol 161(7):3225-3236.

Crispín JC, Liossis SN, Kis-Toth K, Lieberman LA, Kyttaris VC, Juang YT, Tsokos GC, 2010. Pathogenesis of human systemic lupus erythematosus: recent advances. Trends Mol Med 16(2):47-57.

Cross DA, Alessi DR, Cohen P, Andjelkovich M, Hemmings BA,1995. Inhibition of glycogen synthase kinase-3 by insulin mediated by protein kinase B. Nature 378(6559):785–789.

Cunninghame Graham DS, Morris DL, Bhangale TR, Criswell LA, Syvanen AC, Ronnblom L, Behrens TW, Graham RR, Vyse TJ, 2011. Association of NCF2, IKZF1, IRF8, IFIH1, and TYK2 with systemic lupus erythematosus. Plos Genet 7(10):e1002341.

Dal Porto JM, Gauld SB, Merrell KT, Mills D, Pugh-Bernard AE, Cambier J, 2004. B cell antigen receptor signaling 101. Mol Immunol 41(6-7), 599-613.

D'Ambrosio D, Hippen KL, Cambier JC, 1996. Distinct mechanisms mediate SHC association with the activated and resting B cell antigen receptor. Eur J Immunol 26(8):1960-1965.

Datta K, Franke TF, Chan TO, Makris A, Yang SI, Kaplan DR, Morrison DK, Golemis EA, Tsichlis PN, 1995. AH/PH domain-mediated interaction between Akt molecules and its potential role in Akt regulation. Mol Cell Biol 15(4):2304-2310.

Datta SR, Dudek H, Tao X, Masters S, Fu H, Gotoh Y, Greenberg ME, 1997. Akt phosphorylation of BAD couples survival signals to the cell-intrinsic death machinery. Cell 91(2):231–241.

Dean M. Fojo T, Bates S, 2005. Tumor stem cells and drug resistance. Nat Rev Cancer 5(4):275-284.

DeFranco AL, 1993. Structure and function of the B cell antigen receptor. Annu Rev Cell Biol 9:377-410.

del Peso L, Gonzalez-Garcia M, Page C, Herrera R, Nunez G, 1997. Interleukin-3-induced phosphorylation of BAD through the protein kinase Akt. Science 278(5338):687–689.

Deng CH, Zhang QP, 2010. Leukemia stem cells in drug resistance and metastasis. Chin Med J (Engl) 123(7):954-960.

Diamanti, Blair, 2009. Stem cells in childhood acute lymphoblastic leukemia: identifying the most revelant targets for therapy. Blood 113(18):4477.

Dick J.E., 2008. Stem cell concepts renew cancer research. Blood. 112(13):4793-4807.

Dolmetsch RE, Lewis RS, Goodnow CC, Healy JI, 1997. Differential activation of transcription factors induced by Ca2+ response amplitude and duration. Nature 386(6627):855–858.

Dong C, Davis RJ, Flavell RA, 2002. MAP kinases in the immune response. Annu Rev Immunol 20:55-72.

Donjerkovic D, Scott DW, 2000. Activation-induced cell death in B lymphocytes. Cell Res 10(3):179-192.

Dovat S, Ronni T, Russell D, Ferrini R, Cobb BS, Smale ST, 2002. A common mechanism for mitotic inactivation of C2H2 zinc finger DNA-binding domains. Genes Dev 16(23):2985-2990.

Dumortier A, Kirstetter P, Kastner P, Chan S., 2003. Ikaros regulates neutrophil differentiation. Blood 101(6):2219-2226.

Dumortier A, Jeannet R, Kirstetter P, Kleinmann E, Sellars M, dos Santos NR, Thibault C, Barths J, Ghysdael J, Punt JA, Kastner P, Chan S., 2006. Notch activation is an early and critical event during T-Cell leukemogenesis in Ikaros deficient mice. Mol Cell Biol. 26(1):209-220.

Dupuis A, Gaub MP, Legrain M, Drenou B, Mauvieux L, Lutz P, Herbrecht R, Chan S, Kastner P, 2012. Biclonal and biallelec deletion occur in 20% of B-ALL cases with IKZF1 mutations. Leukemia leu.2012.204.

Eeva J, Pelkonen J, 2004. Mechanisms of B cell receptor induced apoptosis. Apoptosis 9(5):525-531.

Ellisen LW, BirdJ, West DC, Soreng AL, Reynolds TC, Smith SD, Sklar J, 1991. TAN-1, the human homolog of the Drosophila notch gene, is broken by chromosomal translocations in T lymphoblastic neoplasms. Cell 66(4):649-661.

Enders A, Bouillet P, Puthalakath H, Xu Y, Tarlinton DM, Strasser A, 2003. Loss of the pro-apoptotic BH3-only Bcl-2 family member Bim inhibits BCR stimulation-induced apoptosis and deletion of autoreactive B cells. J Exp Med 198(7):1119-1126.

Engel I, Mure C, 2002. Disruption of pre-TCR expression accelerates lymphomagenesis in E2A-deficient mice. Proc Natl Acad Sci U S A 99(17):11322-11327.

Ezzat S, Zhu X, Loeper S, Fischer S, Asa SL, 2006. Tumor-derived Ikaros 6 acetylates the Bcl-XL promoter to up-regulate a survival signal in pituitary cells. Mol Endocrinol 20(11):2976-2986.

Flaswinkel H, Reth M, 1994. Dual role of the tyrosine activation motif of the Ig-alpha protein during signal transduction via the B cell antigen receptor. Embo J 13(1):83-89.

Floto RA, Clatworthy MR, Heilbronn KR, Rosner DR, MacAry PA, Rankin A, Lehner PJ, Ouwehand WH, Allen JM, Watkins NA, Smith KG, 2005. Loss of function of a lupus-associated FcgammaRIIb polymorphism through exclusion from lipid rafts. Nat Med 11(10):1056-1058.

Frech M, Andjelkovic M, Ingley E, Reddy KK, Falck JR, Hemmings BA, 1997. High affinity binding of inositol phosphates and phosphoinositides to the pleckstrin homology domain of RAC/protein kinase B and their influence on kinase activity. J Biol Chem 272(13):8474-8481.

Fruman DA, Snapper SB, Yballe CM, Alt FW, Cantley LC, 1999. Phosphoinositide 3-kinases knockout mice: role of p85alpha in B cell development and prolifeation. Biochem Soc Trans 27(4):624-629.

Fu C, Turck CW, Kurosaki T, Chan AC, 1998. BLNK: a central linker protein in B cell activation. Immunity 9(1):93–103.

Fujimoto M, Fujimoto Y, Poe JC, Jansen PJ, Lowell CA, DeFranco AL, Tedder TF, 2000. CD19 regulates Src family protein tyrosine kinase activation in B lymphocytes through processive amplification. Immunity 13(1):47–57.

Fukuyama H, Nimmerjahn F, Ravetch JV, 2005. The inhibitory Fcgamma receptor modulates autoimmunity by limiting the accumulation of immunoglobulin G+ anti-DNA plasma cells. Nat Immunol 6(1):99-106.

Furth J, Kahn M, 1937. The transmission of leukaemia of mice with a single cell. Am J Cancer 31:276-282.

Garaud JC, Schickel JN, Blaison G, Knapp AM, Dembele D, Ruer-Laventie J, Korganow AS, Martin T, Soulas-Sprauel P, Pasquali JL, 2011. B cell signature during inactive systemic lupus is heterogeneous: toward a biological dissection of lupus. PlusOne 6(8):e23900.

Garcia-Cozar FJ, Okamura H, Aramburu JF, Shaw KT, Pelletier L, Showalter R, Villafranca E, Rao A, 1998. Two-site interaction of nuclear factor of activated T cells with activated calcineurin. J Biol Chem 273(37):23877-23883.

Gauld SB, Blair D, Moss CA, Reid SD, Harnett MM, 2002. Differential roles for extracellularly regulated kinase-mitogen-activated protein kinase in B cell antigen receptor-induced apoptosis and CD40-mediated rescue of WEHI-231 immature B cells. J Immunol 168(8):3855–3864.

Gauld SB, Merrell KT, Cambier JC, 2006. Silencing of autoreactive B cells by anergy: a fresh perspective. Curr Opin Immunol 18(3):292-297.

Georgopoulos K, Bigby M, Wang JH, Molnar A, Wu P, Winandy S, Sharpe A, 1994. The Ikaros gene is required for the development of all lymphoid lineages. Cell 79(1):143-156.

Georgopoulos K, Moore DD, Derfler B., 1992. Ikaros, an early lymphoid-specific transcription factor and a putative mediator for T cell commitment. Science 258(5083):808-812.

Georgopoulos K, Winandy S, Avitahl N., 1997. The role of the Ikaros gene in lymphocyte development and homeostasis. Annu Rev Immunol. 15:155-176.

Gerby B, Clappier E, Armstrong F, Deswarte C, Calvo J, Poglio S, Soulier J, Boissel N, Leblanc T, Baruchel A, Landman-Parker J, Roméo PH, Ballerini P, Pflumio F, 2011. Expression of CD34 and CD7 on human T-cell acute lymphoblastic leukemia discriminates functionally heterogeneous cell populations. Leukemia 25(8):1249-1258.

Goitsuka R, Fujimura Y, Mamada H, Umeda A, Morimura T, Uetsuka K, Doi K, Tsuji S, Kitamura D, 1998. BASH, a novel signaling molecule preferentially expressed in B cells of the bursa of Fabricius. J Immunol 161(11):5804–5808.

Gold MR, Chan VW, Turck CW, DeFranco AL, 1992. Membrane Ig cross-linking regulates phosphatidylinositol 3-kinase in B lymphocytes. J Immunol 148(7):2012–2022.

Gold MR, Ingham RJ, McLeod SJ, Christian SL, Scheid MP, Duronio V, Santos L, Matsuuchi L, 2000. Targets of B-cell antigen receptor signaling: the phosphatidylinositol 3-kinase/Akt/glycogen synthase kinase-3 signaling pathway and the Rap1 GTPase. Immunol Rev 176:47-68.

Golebiewska A, Brons NH, Bjerkvig R, Niclou SP, 2011. Critical appraisal of the side population assay in stem cell and cancer stem cell research. Cell Stem Cell 8(2):136-147.

Gómez-del Arco P, Koipally J, Georgopoulos K, 2005. Ikaros SUMOylation: switching out of repression. Mol Cell Biol 25(7):2688-2697.

Gómez-del Arco P, Maki K, Georgopoulos K, 2004. Phosphorylation controls Ikaros's ability to negatively regulate the G(1)-S transition. Mol Cell Biol 24(7):2797-2807.

Gómez-del-Arco P, Kashiwagi M, Jackson AF, Naito T, Zhang J, Liu F, Kee B, Vooijs M, Radtke F, Redondo JM, Georgopoulos K, 2010. Alternative promoter usage at the Notch1 locus supports ligand-independent signaling in T cell development and leukemogenesis. Immunity 33(5):685-698.

Goodell MA, Brose K, Paradis G, Conner AS, Mulligan RC, 1996. Isolation and functional properties of murine hematopoietic stem cells that are replicating in vivo. J Exp Med 183(4):1797-1806.

Goodnow CC, Crosbie J, Jorgensen H, Brink RA, Basten A, 1989. Induction of self-tolerance in mature peripheral B lymphocytes. Nature 342(6248):385-391.

Graves JD, Draves KE, Craxton A, Saklatvala J, Krebs EG, Clark EA, 1996. Involvement of stress-activated protein kinase and p38 mitogen-activated protein kinase in mIgM-induced apoptosis of human B lymphocytes. Proc Natl Acad Sci U S A 93(24):13814-13818.

Grawunder U, Leu TM, Schatz DG, Werner A, Rolink AG, Melchers F, Winkler TH, 1995. Down-regulation of RAG1 and RAG2 gene expression in preB cells after functional immunoglobulin heavy chain rearrangement. Immunity 3(5):601-608.

Guo B, Blair D, Chiles TC, Lowell CA, Rothstein TL, 2007. Cutting Edge: B cell receptor (BCR) cross-talk: the IL-4 induced alternate pathway for BCR signaling operates in parallel with the classical patway, is sensitive to Rottlerin, and depends on Lyn. J Immunol 178(8):4726-4730.

Guo B, Tumang JR, Rothstein L, 2009. B cell receptor crosstalk: B cells express osteopontin through the combined action of the alternate and classical BCR signaling pathways. Mol Immunol 46(4):587-591.

Hahm K, Cobb BS, McCarty AS, Brown KE, Klug CA, Lee R, Akashi K, Weissman IL, Fisher AG, Smale ST, 1998. Helios, a T cell-restricted Ikaros family member that quantitatively associates with Ikaros at centromeric heterochromatin. Genes Dev 12(6):782-796.

Hahm K, Ernst P, Lo K, Kim GS, Turck C, Smale ST, 1994. The lymphoid transcription factor LyF-1 is encoded by specific, alternatively spliced mRNAs derived from the Ikaros gene. Mol Cell Biol 14(11):7111-7123.

Halverson R, Torres RM, Pelanda R, 2004. Receptor editing is the main mechanism of B cell tolerance toward membrane antigens. Nat Immunol 5(6):645-650.

Han A, Saijo K, Mecklenbrauker I, Tarakhovsky A, Nussenzweig MC, 2003. Bam32 links the B cell receptor to ERK and JNK and mediates B cell proliferation but not survival. Immunity 19(4):621-632.

Han H, Tanigaki K, Yamamoto N, Kuroda K, Yashimoto M, Nakahata T, Ikuta K, Honjo T, 2002. Inducible gene knockout of transcription factor recombination signal binding protein-J reveals its essential role in T versus B lineage decision. Int Immunol 14(6):637-645.

Han JW, Zheng HF, Cui Y, Sun LD, Ye DQ, Hu Z, Xu JH, Cai ZM, Huang W, Zhao GP, Xie HF, Fang H, Lu QJ, Xu JH, Li XP, Pan YF, Deng DQ, Zeng FQ, Ye ZZ, Zhang XY, Wang QW, Hao F, Ma L, Zuo XB, Zhou FS, Du WH, Cheng YL, Yang JQ, Shen SK, Li J, Sheng YJ, Zuo XX, Zhu WF, Gao F, Zhang PL, Guo Q, Li B, Gao M, Xiao FL, Quan C, Zhang C, Zhang Z, Zhu KJ, Li Y, Hu DY, Lu WS, Huang JL, Liu SX, Li H, Ren YQ, Wang ZX, Yang CJ, Wang PG, Zhou WM, Lv YM, Zhang AP, Zhang SQ, Lin D, Li Y, Low HQ, Shen M, Zhai ZF, Wang Y, Zhang FY, Yang S, Liu JJ, Zhang XJ, 2009. Genome-wide association study in a Chinese Han population identifies nine new susceptibility loci for systemic lupus erythematosus. Nat Genetics 41(11):1234-1237.

Haraguchi N, Utsunomiya T, Inoue H, Tanaka F, Mimori K, Barnard GF, Mori M, 2006. Characterization of a side population of cancer cells from human gastrointestinal system. Stem Cells 24(3):506-513.

Hardy RR, Carmack CE, Shinton SA, Kemp JD, Hayakawa K, 1991. Resolution and characterization of pro-B and pre-pro-B cell stages in normal mouse bone marrow. J Exp Med 173(5):1213-1225.

Hardy RR, Hayakawa K, 2001. B cell development pathways. Annu Rev Immunol 19:595-621.

Harker N, Naito T, Cortes M, Hostert A, Hirschberg S, Tolaini M, Roderick K, Georgopoulos K, Kioussis D, 2002. The CD8alpha gene locus is regulated by the Ikaros family of proteins. Mol Cell 10(6):1403-1415.

Hashimoto A, Okada H, Jiang A, Kurosaki M, Greenberg S, Clark EA, Kurosaki T, 1998. Involvement of guanosine triphosphatases and phospholipase C-gamma2 in extracellular signal-regulated kinase, c-Jun NH2-terminal kinase, and p38 mitogen-activated protein kinase activation by the B cell antigen receptor. J Exp Med 188(7):1287-1295.

Hashimoto S, Iwamatsu A, Ishiai M, Okawa K, Yamadori T, Matsushita M, Baba Y, Kishimoto T, Kurosaki T, Tsukada S, 1999. Identification of the SH2 domain binding protein of Bruton's tyrosine kinase as BLNK-- functional significance of Btk-SH2 domain in B-cell antigen receptor-coupled calcium signaling. Blood 94(7):2357-2364.

Haydu JE, De Keersmaecker K, Duff MK, Paietta E, Racevskis J, Wiernik PH, Rowe JM, Ferrando A, 2012. An activating intragenic deletion in Notch1 in human T-ALL. Blood 119(22):5211-5214.

He CF, Liu YS, Cheng YL, Gao JP, Pan TM, Han JW, Quan C, Sun LD, Zheng HF, Zuo XB, Xu SX, Sheng YJ, Yao S, Hu WL, Li Y, Yu ZY, Yin XY, Zhang XJ, Cui Y, Yang S, 2010. TNIP1, SLC15A4, ETS1, RasGRP3 and IKZF1 are associated with clinical features of systemic lupus erythematosus in a Chinese Han population. Lupus 19(10):1181-1186.

Heidenreich O, Vormoor J, 2009. Malignant stem cells in childhood ALL: the debate continues! Blood 113(18):4476-4477.

Hirschmann-Jax C, Foster AE, Wulf GG, Nuchtern JG, Jax TW, Gobel U, Goodell MA, Brenner MK, 2004. A distinct "side population" of cells with high drug efflux capacity in human tumor cells. Proc Natl Acad Sci U S A 101(39):14228-14233.

Ho AD, Wanger W, 2006. Bone marrow niche and leukemia. Ernst Schering Found Symp Proc 5:125-139.

Hoflinger S, Kesavan K, Fuxa M, Hutter C, Heavey B, Radtke F, Busslinger M, 2004. Analysis of Notch1 function by in vitro T cell differentiation of Pax5 mutant lymphoid progenitors. J Immunol 173(6):3935-3944.

Hong D, Gupta R, Ancliff P, Atzberger A, Brown J, Soneji S, Green J, Colman S, Piacibello W, Buckle V, Tsuzuki S, Greaves M, Enver T, 2008. Initiating and cancer-propagating cells in TEL-AML1-associated childhood leukemia. Science 319(5861):336-339.

Hu W, Sun L, Gao J, Li Y, Wang P, Cheng Y, Pan T, Han J, Liu Y, Lu W, Zuo X, Sheng Y, Yao S, He C, Yu Z, Yin X, Cui Y, Yang S, Zhang X, 2011. Down-regulated expression of IKZF1 mRNA in peripheral blood mononuclear cells from patients with systemic lupus erythematosus. Rheumatol Int 31(6):819-822.

Hudkins KL, Giachelli CM, Eitner F, Couser WG, Johnson RJ, Alpers CE, 2000. Osteopontin expression in human crescentic glomerulonephritis. Kidney Int 57(1):105–116.

Ishiai M, Kurosaki M, Pappu R, Okawa K, Ronko I, Fu C, Shibata M, Iwamatsu A, Chan AC, Kurosaki T, 1999. BLNK required for coupling Syk to PLC gamma 2 and Rac1-JNK in B cells. Immunity 10(1):117-125.

Ito M, Hiramatsu H, Kobayashi K, Suzue K, Kawahata M, Hioki K, Ueyama Y, Koyanagi Y, Sugamaru K, Tsuji K, Heike T, Nakahata T, 2002. NOD/SCID/gamma(c)(null) mouse: an excellent recipient mouse model for engraftment of human cells. Blood 100(9):3175–3182.

Jacob A, Cooney D, Pradhan M, Coggeshall KM, 2002. Convergence of signaling pathways on the activation of ERK in B cells. J Biol Chem 277(26):23420-23426.

Jager R, Gisslinger H, Passamonti F, Rumi E, Berg T, Gisslinger B, Pietra D, Harutyunyan A, Klampfl T, Olcaydu D, Cazzola M, Kralovics R, 2010. Deletions of the transcription factor Ikaros in myeloproliferative neoplasms. Leukemia 24(7):1290-1298.

Jastrzebski K, Hannan KM, Tchoubrieva EB, Hannan RD, Pearson RB, 2007. Coordinate regulation of ribosome biogenesis and function by the ribosomal protein S6 kinase, a key mediator of mTOR function. Growth Factors 25(4):209-226.

Jeannet R, Mastio J, Macias-Garcia A, Oravecz A, Ashworth T, Geimer Le Lay AS, Jost B, Le Gras S, Ghysdael J, Gridley T, Honjo T, Radtke F, Aster JC, Chan S, Kastner P, 2010. Oncogenic activation of the Notch1 gene by deletion of its promoter in Ikaros-deficient T-ALL. Blood 116(25):5443-5454.

Jiang R, Lan Y, Chapman HD, Shawber C, Norton CR, Serreze DV, Weinmaster G, Gridley T, 1998. Defects in limb, craniofacial, and thymic development in Jagged2 mutant mice. Genes Dev 12(7):1046-1057.

John L, Ward A., 2011. The Ikaros gene family: Transcriptional regulators of hematopoiesis and immunity. Mol Immunol 48(9-10):1272-1278.

Johnson GL, Lapadat R, 2002. Mitogen-activated protein kinase pathways mediated by ERK, JNK, and p38 protein kinases. Science 298(5600):1911-1912.

Johnson SA, Pleiman CM, Pao L, Schneringer J, Hippen K, Cambier JC, 1995. Phosphorylated immunoreceptor signaling motifs (ITAMs) exhibit unique abilities to bind and activate Lyn and Syk tyrosine kinases. J Immunol 155(10):4596-4603.

Kakinuma S, Kodama Y, Amasaki Y, Yi S, Tokairin Y, Arai M, Nishimura M, Monobe M, Kojima S, Shimada Y, 2007. Ikaros is a mutational target for lymphomagenesis in Mlh1-deficient mice. Oncogene 26(20):2945-2949.

Kakinuma S, Nishimura M, Sasanuma S, Mita K, Suzuki G, Katsura Y, Sado T, Shimida Y, 2002. Spectrum of Znfn1a1 (Ikaros) inactivation and its association with loss of heterozygosity in radiogenic T-cell lymphomas in susceptible B6C3F1 mice. Radiat Res 157(3):331-340.

Kastner P, Chan S, 2011. Role of Ikaros in T-cell acute lymphoblastic leukemia. World J Biol Chem 2(6):108-114.

Katagiri Y, Mori K, Hara T, Tanaka K, Murakami M, Uede T, 1995. Functional analysis of the osteopontin molecule. Ann N Y Acad Sci 760:371–374.

Kathrein KL, Chari S, Winandy S, 2008. Ikaros directly represses the notch target gene Hes1 in a leukemia T cell line: implication for CD4 regulation. J Biol Chem 283(16):10476-10484.

Katz E, Lord C, Ford CA, Gauld SB, Carter NA, Harnett MM, 2004. Bcl-(xL) antagonism of BCR-coupled mitochondrial phospholipase A(2) signaling correlates with protection from apoptosis in WEHI-231 B cells. Blood 103(1):168-176.

Kelly PN, Dakic A, Adams JM, Nutt SL, Strasser A, 2007. Tumor growth need not be driven by rare cancer stem cells. Science 317(5836):337.

Kennedy JA, Barabé F, Poeppl AG, Wang JC, Dick JE, 2007. Comment on "Tumor growth need not be driven by rare cancer stem cells". Science 318(5857):1722.

Kil LP, de Bruijn MJ, van Nimwegen M, Corneth OB, van Hamburg JP, Dingjian GM, Thaiss F, Rimmelzwaan GF, Elewaut D, Delsing D, van Loo PF, Hendriks RW, 2012. Btk levels set the threshold for B-cell activation and negative selection of autoreactive B cells in mice. Blood 119(16):3744-3756.

Killmann SA, Cronkite EP, Robertson JS, Fliedner TM, Bond VP, 1963. Estimation of phases of the life cycle of leukemic cells from labeling in human beings in vivo with tritiated thymidine. Lab Invest 12:671-684.

Kim J, Sif S, Jones B, Jackson A, Koipally J, Heller E, Winandy S, Viel A, Sawyer A, Ikeda T, KingstK, 1999. Ikaros DNA-binding proteins direct formation of chromatin remodeling complexes in lymphocytes. Immunity 10(3):345-355.

Kirstetter P, Thomas M, Dierich A, Kastner P, Chan S., 2002. Ikaros is critical for B cell differentiation and function. Eur J Immunol 32(3):720-730.

Kitamura D, Kudo A, Schaal S, Muller W, Melchers F, Rajewsky K, 1992. A critical role of lambda 5 protein in B cell development. Cell 69(5):823-831.

Kleinmann E, Geimer Le Lay AS, Sellars M, Kastner P, Chan S, 2008. Ikaros represses the transcriptional response to Notch Signaling in T-cell development. Mol Cell Biol 28(24):7465-7475.

Koipally J, Georgopoulos K, 2002. A molecular dissection of the repression circuitry of Ikaros. J Biol Chem 277(31):27697-27705.

Koncz G, Bodor C, Kovesdi D, Gati R, Sarmay G, 2002. BCR mediated signal transduction in immature and mature B cells. Immunol Lett 82(1-2):41-49.

Krivtsov AV, Twomey D, Feng Z, Stubbs MC, Wang Y, Faber J, Levine JE, Wang J, Hahn WC, Gilliland DG, Golub TR, Armstrong SA, 2006. Transformation from committed progenitor to leukaemia stem cell initiated by MLL-AF9. Nature 442(7104):818-822.

Kuiper RP, Schoenmakers EF, van Reijmersdal SV, Hehir-Kwa JY, van Kessel AG, van Leeuwen FN, Hoogerbrugge PM, 2007. High-resolution genomic profiling of childhood ALL reveals novel recurrent genetic lesions affecting pathways involved in lymphocyte differentiation and cell cycle progression. Leukemia 21(6):1258-1266.

Kuiper RP, Waanders E, var der Velden VHJ, van Reijmersdal SV, Venkatachalam R, Scheijen B, Sonneveld E, van Dongen JJ, Veerman AJ, van Leeuwen FN, van Kessel AG, Hoogerbrugge PM, 2010. IKZF1 deletion predict relapse in uniformly treated pediatric precursor B-ALL. Leukemia 24(7):1258-1264.

Kurosaki T, 1999. Genetic analysis of B cell antigen receptor signaling. Annu Rev Immunol 17:555–592.

Lalande ME, Miller RG, 1979. Fluorescence flow analysis of lymphocyte activation using Hoechst 33342 dye. J Histochem Cytochem 27(1):394-397.

Landolt-Marticorena C, Wither R, Reich H, Herzenberg A, Scholey J, Gladman DD, Urowitz MB, Fortin PR, Wither J, 2011. Increased expression of B cell activation factor supports the abnormal expansion of transitional B cells in systemic lupus erythematosus. J Rheumatol 38(4):642-651.

Lapidot T, Sirard C, Vormoor J, Murdoch B, Hoang T, Caceres-Cortes J, Minden M, Paterson B, Caligiuri MA, Dick JE, 1994. A cell initiating human acute myeloid leukaemia after transplantation into SCID mice. Nature 367(6464):645-648.

Le Viseur C, Hotfilder M, Bomken S, Wilson K, Rottgers S, Schrauder A, Rossemann A, Irving J, Stam RW, Shultz LD, Harbott J, Jurgens H, Schrappe M, Pieters R, Vormoor J, 2008. In childhood acute lymphoblastic leukemia, blasts at different stages of immunophenotypic maturation have stem cell properties. Cancer Cell 14(1):47-58.

Li X, Gounari F, Protopopov A, Khazaie K, von Boehmer H, 2008. Oncogenesis of T-ALL and nonmalignant consequences of overexpressing intracellular NOTCH1. J Exp Med 205(12):2851-2861.

Liu S, Velez MG, Humann J, Rowland S, Conrad FJ, Halverson R, Torres RM, Pelanda R, 2005. Receptor editing can lead to allelic inclusion and development of B cells that retain antibodies reacting with high avidity autoantigens. J Immunol 175(8):5067-5076.

Lo K, Landau NR, Smale ST, 1991. LyF-1, a transcriptional regulator that interacts with a novel class of promoters for lymphocyte-specific genes. Mol Cell Biol 11(10):5229-5243.

Loeser RF, Erickson EA, Long DL, 2008. Mitogen-activated protein kinases as therapeutic targets in osteoarthritis. Curr Opin Rheumatol. 20(5):581-586.

Lopez RA, Schoetz S, DeAngelis K, O'Neill D, Bank A, 2002. Multiple hematopoietic defects and delayed globin switching in Ikaros null mice. Proc Natl Acad Sci USA 99(2):602–607.

Ma S, Pathak S, Mandal M, Trinh L, Clark MR, Lu R, 2010. Ikaros and Aiolos inhibit pre-B-cell proliferation by directly suppressing c-Myc expression. Mol Cell Biol 30(17):4149-4158.

Ma W, Gutierrez A, Goff DJ, Geron I, Sadarangani A, Jamieson CA, Court AC, Shih AY, Jiang Q, Wu CC, Li K, Smith KM, Crews LA, Gibson NW, Deichaite I, Morris SR, Wei P, Carson DA, Look AT, Jamieson CH, 2012. NOTCH1 signaling promotes human T-cell acute lymphoblastic leukemia initiating cell regeneration in supportive niches. PLos One 7(6) e39725.

Mackay F, Woodcock SA, Lawton P, Ambrose C, Baetscher M, Schneider P, Tschopp J, Browning JL, 1999. Mice transgenic for BAFF develop lymphocytic disorders along with autoimmune manifestations. J Exp Med 190(11):1697-1710.

Maillard I, Fang T, Pear WS, 2005. Regulation of lymphoid development, differentiation, and function by the Notch pathwat. Annu Rev Immunol 23:945-974.

Makino S, 1956. Further evidence favoring the concept of the stem cell in ascites tumors of rats. Ann N Y Acad Sci 63(5):818-830.

Malissein E, Verdier M, Ratinaud MH, Troutaud D, 2003. Changes in Bad phosphorylation are correlated with BCR-induced apoptosis of WEHI-231 immature B cells. Biochimie 85, 733-740.

Mantha S, Ward M, McCafferty J, Herron A, Palomero T, Ferrando A, Bank A, Richardson C, 2007. Activating Notch 1 mutations are an early event in T-cell malignancy of Ikaros point mutation Plastic/+ mice. Leuk Res 31(3):321-327.

Marcais A, Jeannet R, Hernandez L, Soulier J, Sigaux F, Chan S, Kastner P, 2010. Genetic inactivation of Ikaros is a rare event in human T-ALL. Leuk Res 34(4):426-429.

Maser RS, Choudhury B, Campbell PJ, Feng B, Wong KK, Protopopov A, O'Neil J, Gutierrez A, Ivanoca E, Perna I, Lin E, Mani V, Jiang S, McNamara K, Zaghlul S, Edkins S, Stevens C, Brennan C, Martin ES, Wiedemeyer R, Kabbarah O, Nogueira C, Histen G, Aster J, Mansour M, Duke V, Foroni L, Fielding AK, Goldstone AH, Rowe JM, Wang YA, Look AT, Stratton MR, Chin L, Futreal PA, DePinho RA, 2007. Chromosomally unstable mouse tumours have genomic alterations similar to diverse human cancers. Nature 447(7147):966-971.

McGaha TL, Sorrentino B, Ravetch JV, 2005. Restoration of tolerance in lupus by targeted inhibitory receptor expression. Science 307(5709):590-593.

McQueen F, 2012. A B cell explanation for autoimmune disease: the forbidden clone returns. Postgrad Med J 88(1038):226-233.

Meier R, Alessi DR, Cron P, Andjelkovic M, Hemmings BA, 1997. Mitogenic activation, phosphorylation, and nuclear translocation of protein kinase Bbeta. J Biol Chem 272(48):30491-30497.

Meleshko AN, Movchan LV, Belevtsev MV, Savitskaja TV, 2008. Relative expression of different Ikaros isoforms in childhood acute leukemia. Blood Cells Mol Dis 41(3):278-283.

Meyer LH, Debatin KM. 2011. Diversity of human keukemia xenograft mouse models: Implications for disease biology. Cancer Res 71(23):7141-7144.

Miosge LA, Goodnow CC, 2005. Genes, pathways and checkpoints in lymphocyte development and homeostasis. Immunol Cell Biol 83(4):318-335.

Mishra N, Reilly CM, Brown DR, Ruiz P, Gilkeson GS, 2003. Histone deacetylase inhibitors modulate renal disease in the MRL-lpr/lpr mouse. J Clin Invest 111(4):539-552.

Mizuno T, Rothstein T L, 2005. B cell receptor (BCR) cross-talk: CD40 engagement enhances BCR-induced ERK activation. J Immunol 174(6):3369-3376.

Molnar A, Georgopoulos K, 1994. The Ikaros gene encodes a family of functionally diverse zinc finger DNA-binding proteins. Mol Cell Biol 14(12):8292-8303.

Molnar A, Wu P, Largespada DA, Vortkamp A, Scherer S, Copeland NG, Jenkins NA, Bruns G, Georgopoulos K, 1996. The Ikaros gene encodes a family of lymphocyte-restricted zinc finger DNA binding proteins, highly conserved in human and mouse. J Immunol 156(2):585-592.

Morisot S, Wayne AS, Bohana-Kashtan O, Kaplan IM, Gocke CD, Hildreth R, Stetler-Stevenson M, Walker RL, Davis S, Meltzer PS, Wheelan SJ, Brown P, Jones RJ, Shultz LD, Civin CI, 2010. High frequencies of leukemia stem cells in poor-outcome childhood precursor-B acute lymphoblastic leukemias. Leukemia 24(11):1859-1866.

Mullighan CG, Goorha S, Radtke I, Miller CB, Coustan-Smith E, Dalton JD, Girtman K, Mathew S, Ma J, Pounds SB, Su X, Pui CH, Relling MV, Evans WE, Shurtleff SA, Downing JR, 2007. Genome-wide analysis of genetic alterations in acute lymphoblastic leukemia. Nature 446(7137):758-764.

Mullighan CG, Miller CB, Radtke I, Phillips LA, Dalton J, Ma J, White D, Hughes TP, Le Beau MM, Pui CH, Relling MV, Shurtleff SA, Downing JR, 2008. BCR-ABL1 lymphoblastic leukaemia is characterized by the deletion of Ikaros. Nature 453(7191):110-114.

Mullighan CG, Phillips LA, Su X, Ma J, Miller CB, Shurtleff SA, Downing JR, 2008. Genomic analysis of the clonal origins of relapsed acute lymphoblastic leukemia. Science 322(5906):1377-1380.

Mundt C, Licence S, Shimizu T, Melchers F, Martensson IL, 2001. Loss of precursor B cell expansion but not allelic exclusion in VpreB1/VpreB2 double-deficient mice. J Exp Med 193(4):435-445.

Nagai K, Takata M, Yamamura H, Kurosaki T, 1995. Tyrosine phosphorylation of Shc is mediated through Lyn and Syk in B cell receptor signaling. J Biol Chem 270(12):6824-6829.

Nakase K, Ishimaru F, Avitahl N, Dansako H, Matsuo K, Fujii K, Sezaki N, Nakayama H, Yano T, Fukuda S, Imajoh K, Takeuchi M, Miyata A, Hara M, Yasukawa M, Takahashi I, Taguchi H, Matsue K, Nakao S, Niho Y, Takenaka K, Shinagawa K, Ikeda K, Niiya K, Harada M, 2000. Dominat negative isoform of the Ikaros gene in patients with adult B cell acute lymphoblastic leukemia. Cancer Res 60(15):4062-4065.

Nemazee D, 2006. Receptor editing in lymphocyte development and central tolerance. Nat Rev Immunol 6(10):728-740.

Nguyen LV, Vanner R, Dirks P, Eaves CJ, 2012. Cancer stem cells: an envolving concept. Nat Rev Cancer 12(2):133-143.

Nichogiannopoulou A, Trevisan M, Neben S, Friedrich C, Georgopoulos K, 1999. Defects in hemopoietic stem cell activity in Ikaros mutant mice. J Exp Med 190(9):1201-1214.

Nie L, Xu M, Vladimirova A, Sun XH, 2003. Notch-induced E2A ubiquitination and degradation are controlled by MAP kinase activities. EMBO J 22(21):5780-5792.

Niiro H, Clark EA, 2002. Regulation of B-cell fate by antigen-receptor signals. Nat Rev Immunol 2(12):945-956.

Norvell A, Mandik L, Monroe JG, 1995. Engagement of the antigen-receptor on immature murine B lymphocytes results in death by apoptosis. J Immunol 154(9):4404-4413.

Notta F, Doulatov S, Dick JE, 2010. Engraftment of human hematopoietic stem cells is more efficient in female NOD/SCID/IL-2Rgc-null recipients. Blood 115(18):3704–3707.

Notta F, Mullighan CG, Wang JC, Poeppl A, Doulatov S, Phillips LA, Ma J, Minden MD, Downing JR, Dick JE, 2011. Evolution of human BCR-ABL1 lymphoblastic leukaemia-initiating cells. Nature 469(7330):362-367.

Nowell PC, 1976. The clonal evolution of tumor cell populations. Science 194(4260):23-28.

Nutt SL, Kee BL, 2007. The transcriptional regulation of B cell lineage commitment. Immunity 26(6):715-725.

Odendahl M, Jacobi A, Hansen A, Feist E, Hiepe F, Burmester GP, Lipsky PE, Radbrunch A, Dorner T, 2000. Disturbed peripheral B lymphocyte homeostasis in systemic lupus erythematosus. J Immunol 165(10):5970-5979.

Ohshima S, Yamaguchi N, Nishioka K, Mima T, Ishii T, Umeshita-Sasai M, Kobayashi H, Shimizu M, Katada Y, Wakitani S, Murata N, Nomura S, Matsuno H, Katayama R, Kon S, Inobe M, Uede T, Kawase I, Saeki Y, 2002. Enhanced local production of osteopontin in rheumatoid joints. J Rheumatol 29(10):2061–2067.

Olivero S, Maroc C, Beillard E, Gabert J, Nietfeld W, Chabannon C, Tonnelle C, 2000. Detection of different Ikaros isoforms in human leukaemias using real-time quantitative polymerase chain reaction. Br J Haematol 110(4):826-830.

Palomero T, Lim WK, Odom DT, Sulis ML, Real PJ, Margolin A, Barnes KC, O'Neil J, Neuberg D, Weng AP, Aster JC, Sigaux F, Soulier J, Look AT, Young RA, Califano A, Ferrando AA, 2006. NOTCH1 directly regulates c-MYC and activates a feedforward-loop transcriptional network promoting leukemic cell growth. Proc Natl Acad Sci U S A 103(48):18261-18266.

Pao LI, Famiglietti SJ, Cambier JC, 1998. Asymmetrical phosphorylation and function of immunoreceptor tyrosine-based activation motif tyrosines in B cell antigen receptor signal transduction. J Immunol 160(7):3305–3314.

Papathanasiou P, Perkins AC, Cobb BS, Ferrini R, Sridharan R, Hoyne GF, Nelms KA, Smale ST, Goodnow CC., 2003. Widespread failure of hematolymphoid differentiation caused by a recessive niche-filling allele of the Ikaros transcription factor. Immunity 19(1):131-144.

Patarca R, Wei FY, Singh P, Morasso MI, Cantor H, 1990. Dysregulated expression of the T cell cytokine Eta-1 in CD4-8- lymphocytes during the development of murine autoimmune disease. J Exp Med 172(4):1177–1183.

Payne KJ, Dovat S, 2011. Ikaros and tumor suppression in acute lymphoblastic leukemia. Crit Rev Oncog 16(1-2): 3-12.

Pear WS, Aster JC, 2004. T cell acute lymphoblastic leukemia/lymphoma: a human cancer commonlcy associated with aberrant Notch1 signaling. Curr Opin Hematol 11(6):426-433.

Pear WS, Aster JC, Scott ML, Hasserjian RP, Soffer B, Sklar J, Baltimore D, 1996. Exclusive development of T cell neoplasm in mice transplanted with bone marrow expressing activated Notch alleles. J Exp Med 183(5):2283-2291.

Perdomo J, Holmes M, Chong B, Crossley M., 2000. Eos and Pegasus, two members of the Ikaros family of proteins with distinct DNA binding activities. J Biol Chem 275(49):38347-38354.

Petro JB, Khan WN, 2001. Phospholipase C-gamma 2 couples Bruton's tyrosine kinase to the NF-kappaB signaling pathway in B lymphocytes. J Biol Chem 276(3):1715-1719.

Piatelli MJ, Doughty C, Chiles TC, 2002. Requirement for a hsp90 chaperone-dependent MEK1/2-ERK pathway for B cell antigen receptor-induced cyclin D2 expression in mature B lymphocytes. J Biol Chem 277(14):12144-12150.

Piatelli MJ, Wardle C, Blois J, Doughty C, Schram BR, Rothstein TL, Chiles TC, 2004. Phosphatidylinositol 3-kinase-dependent mitogen-activated protein/extracellular signal-regulated kinase kinase 1/2 and NF-kappa B signaling pathways are required for B cell antigen receptor-mediated cyclin D2 induction in mature B cells. J Immunol 172(5):2753-2762.

Pierce GB Jr, Dixon FJ Jr, Verney EL, 1960. Teratocarcinogenic and tissue-forming potentials of the cell types comprising neoplastic embryoid bodies. Lab Invest 9:583-602.

Pierce GB, Speers WC, 1988. Tumors as caricatures of the process of tissue renewal: prospects for therapy by directing differentiation, Cancer Res 48(8):1996-2004.

Pierce GB, Wallace C, 1971. Differentiation of malignant to benign cells. Cancer Res 31(2):127-134.

Pleiman CM, Abrams C, Gauen LT, Bedzyk W, Jongstra J, Shaw AS, Cambier JC, 1994. Distinct p53/56lyn and p59fyn domains associate with nonphosphorylated and phosphorylated Ig-alpha. Proc Natl Acad Sci U S A 91(10):4268–4272.

Polyak K, Haviv I, Campbell IG, 2009. Co-evolution of tumor cells and their microenvironment. Trends Genet 25(1):30-38.

Pongubala JM, Northrup DL, Lancki DW, Medina KL, Treiber T, Bertolino E, Thomas M, Grosschedl R, Allman D, Singh H, 2008. Transcription factor EBF restricts alternative lineage options and promotes B cell fate commitment independently of Pax5. Nat Immunol 9(2):203-215.

Pui JC, Allman D, Xu L, DeRocco S, Karnell FG, Bakkour S, Lee JY, Kadesch T, Hardy RR, Aster JC, Pear WS, 1999. Notch1 expression in early lymphopoiesis influences B versus T lineage determination. Immunity 11(3):299-308.

Quintana E, Shackleton M, Sabel MS, Fullen DR, Johnson TM, Morrison SJ, 2008. Efficient tumour formation by single human melanoma cells. Nature 456(7222):593-598.

Quirion MR, Gregory GD, Umetsu SE, Winandy S, Brown MA, 2009. Cutting edge: Ikaros is a regulator of Th2 cell differentiation. J Immunol 182(2):741-745.

Radke F, Wilson A, Stark G, Bauer M, van Meerwijk J, MacDonald HR, Aguet M, 1999. Deficient T cell fate specification in mice with an induced inactivation of Notch1. Immunity 10(5):547-558.

Radtke F, Schweisguth F, Pear W, 2005. The Notch "gospel". EMBO Rep Meeting report 6(12):1120-1125.

Radtke F, Wilson A, MacDonald HR, 2004. Notch signaling in T- and B-cell development. Curr Opin Immunol 16(2):174-179.

Rebollo A, Schmitt C, 2003. Ikaros, Aiolos and Helios: transcription regulators and lymphoid malignancies. Immunol Cell Biol 81(3):171-175.

Reichlin A, Hu Y, Meffre E, Nagaoka H, Gong S, Kraus M, Rajewsky K, Nussenzweig MC, 2001. B cell development is arrested at the immature B cell stage in mice carrying a mutation in the cytoplasmic domain of immunoglobulin beta. J Exp Med 193(1):13–23.

Ren M, Cowell JK, 2011. Constitutive Notch pathway activation in murine ZMYM2-FGFR1- induced T-cell lymphomas associated with atypical myeloproliferative disease. Blood 117(25):6837-6847.

Reschly EJ, Spaulding C, Vilimas T, Graham WV, Brumbaugh RL, Aifantis I, Pear WS, Kee BL, 2006. Notch1 promotes survival of E2A-deficient T cell lymphomas through pre-Tcell receptor-dependent and - independent mechanisms. Blood 107(10):4115-4121.

Resh MD, 1999. Fatty acylation of proteins: new insights into membrane targeting of myristoylated and palmitoylated proteins. Biochim Biophys Acta 1451(1):1-16.

Reth M, 1989. Antigen receptor tail clue. Nature 338(6214):383–384.

Reth M, 1992. Antigen receptors on B lymphocytes. Annu Rev Immunol 10:97-121.

Reynaud D, Demarco IA, Reddy KL, Schjerven H, Bertolino E, Chen Z, Smale ST, Winandy S, Singh H, 2008. Regulation of B cell fate commitment and immunoglobulin heavy-chain gene rearrangements by Ikaros. Nat Immunol 9(8):927-936.

Reynolds TC, Smith SD, Sklar J, 1987. Analysis of DNA surrounding the breakpoints of chromosomal translocations involving the beta T cell receptor gene in human lymphoblastic neoplasm. Cell 50(1):107-117.

Richards JD, Dave SH, Chou CH, Mamchak AA, DeFranco AL, 2001. Inhibition of the MEK/ERK signaling pathway blocks a subset of B cell responses to antigen. J Immunol 166(6):3855-3864.

Rohn JL, Lauring AS, Linenberger ML, Overbaugh J,1996. Transduction of Notch2 in feline leukemia virus- induced thymic lymphoma. J. Virol 70(11):8071–8080.

Rolink A, Grawunder U, Winkler TH, Karasuyama H, Melchers F, 1994. IL-2 receptor alpha chain (CD25, TAC) expression defines a crucial stage in pre-B cell development. Int Immunol 6(8):1257-1264.

Rothenberg EV, More JE, Yui MA, 2008. Launching the T-cell-lineage developmental programme. Nat Rev Immunol 8(1):9-21.

Rothstein TL, Guo B, 2009. Receptor crosstalk: reprogramming B cell receptor signalling to an alternate pathway results in expression and secretion of the autoimmunity-associated cytokine, osteopontin. J Intern Med 265(6):632-643.

Rowley RB, Burkhardt AL, Chao HG, Matsueda GR, Bolen JB, 1995. Syk protein-tyrosine kinase is regulated by tyrosine-phosphorylated Ig alpha/Ig beta immunoreceptor tyrosine activation motif binding and autophosphorylation. J Biol Chem 270(19):11590-11594.

Roy M, Pear W, Aster JC, 2007. The multifaceted role of Notch in cancer. Curr Opin Genet Dev 17(1):52-59.

Rui L, Vinuesa CG, Blasioli J, Goodnow CC, 2003. Resistance to CpG DNA-induced autoimmunity through tolerogenic B cell antigen receptor ERK signaling. Nat Immunol 4(6):594–600.

Ruiz A, Jiang J, Kempski H, Brady HJ, 2004. Overexpression of the Ikaros 6 isoform is restricted to t(4;11) acute lymphoblastic leukaemia in children and infants and has a role in B-cell survival. Br J Haematol 125(1):31-37.

Ruland J, Mak TW, 2003. Transducing signals from antigen receptors to nuclear factor kappaB. Immunol Rev 193:93-100.

Saito K, Scharenberg AM, Kinet JP 2001. Interaction between the Btk PH domain and phosphatidylinositol-3,4,5-trisphosphate directly regulates Btk. J Biol Chem 276(19):16201-16206.

Sato S, Miller AS, Inaoki M, Bock CB, Jansen PJ, Tang ML, Tedder TF, 1996. CD22 is both a positive and negative regulator of B lymphocyte antigen receptor signal transduction: altered signaling in CD22-deficient mice. Immunity 5(6):551–562.

Scharenberg AM, El-Hillal O, Fruman DA, Beitz LO, Li Z, Lin S, Gout I, Cantley LC, Rawlings DJ, Kinet JP, 1998. Phosphatidylinositol-3,4,5-trisphosphate (PtdIns-3,4,5-P3)/Tec kinase-dependent calcium signaling pathway: a target for SHIP-mediated inhibitory signals. Embo J 17(7):1961-1972.

Schmitt TM, Ciofani M, Petrie HT, Zuñiga-Pflucker JC, 2004. Maintenance of T cell specification and differentiation requires recurrent Notch receptor-ligand interactions. J Exp Med 200(4):469-479.

Sellars M, Kastner P, Chan S, 2011. Ikaros in B cell development and function. World J Biol Chem 26(6):132-139.

Sellars M, Reina-SanMartin B, Kastner P, Chan S, 2009. Ikaros controls isotype selection during immunoglobulin class switch recombination. J Exp Med 206(5):1073-1087.

Shimada Y, Nishimura M, Kakinuma S, Okumoto M, Shiroishi T, Clifton KH, Wakana S, 2000. Radiaton-associated loss of heterozygosity at the Znfn1a1 (Ikaros) locus on chromosome 11 in murine thymic lymphomas. Radiat Res 154(3): 293:300.

Shlomchik MJ, 2008. Sites and stages of autoreactive B cell activation and regulation. Immunity 28(1):18-28.

Shultz LD, Lyons BL, Burzenski LM, Gott B, Chen X, Chaleff S, et al. Human lymphoid and myeloid cell development in NOD/LtSz-scid IL2R gamma null mice engrafted with mobilized human hemopoietic stem cells. J Immunol 174(10):6477–6489.

Shultz LD, Schweitzer PA, Christianson SW, Gott B, Schweitzer IB,Tennent B, McKenna S, Mobraaten L, Rajan TV, Greiner DL et al. 1995 Multiple defects in innate and adaptive immunologic function in NOD/LtSz-scid mice. J Immunol 154(1):180–191.

Singh SK, Hawkins C, Clarke ID, Squire JA, Bayani J, Hide T, Hekelman RM, Cusimano MD, Dirks PB, 2004. Identification of human brain tumour initiating cells. Nature 432(7015):396-401.

Sitnicka E, Brakebusch C, Martensson IL, Svensson M, Agace WW, Sigvardsson M, Buza-Vidas N, Bryder D, Cilio CM, Ahlenius H, Maraskovsky E, Peschon JJ, Jacobsen SE, 2003. Complementary signaling through flt3 and interleukin-7 receptor alpha is indispensable for fetal and adult B cell genesis. J Exp Med 198(10):1495-1506.

Smith-Bouvier DL, Divekar AA, Sasidhar M, Du S, Tiwari-Woodruff SK, Arnold AP, Singh RR, Voskuhl RR, 2008. A role for sex chromosome complement in the female bias in autoimmune disease. J Exp Med 205(5):1099-1108.

Solvason N, Wu WW, Kabra N, Wu X, Lees E, Howard MC, 1996. Induction of cell cycle regulatory proteins in anti-immunoglobulin-stimulated mature B lymphocytes. J Exp Med 184(2):407-417.

Solvason N, Wu WW, Parry D, Mahony D, Lam EW, Glassford J, Klaus GG, Sicinski P, Weinberg R, Liu YJ,Howard M, Lees E, 2000. Cyclin D2 is essential for BCR-mediated proliferation and CD5 B cell development. Int Immunol 12(5):631-638.

Sridharan R, Smale ST, 2007. Predominant interaction of both Ikaros and Helios with the NuRD complex in immature thymocytes. J Biol Chem 282(41):30227-30238.

Su TT, Rawlings DJ, 2002. Transitional B lymphocyte subsets operate as distinct checkpoints in murine splenic B cell development. J Immunol 168(5):2101-2110.

Sun L, Crotty ML, Sensel M, Sather H, Navara C, Nachman J, Steinherz PG, Gaynon PS, Seibel N, Mao C, Vassilev A, Reaman GH, Uckun FM, 1999. Expression of dominant-negative Ikaros isoforms in T-cell acute lymphoblastic leukemia. Clin Cancer Res 5(8):2112-2120.

Suzuki H, Terauchi Y, Fujiwara M, Aizawa S, Yazaki Y, Kadowaki T, Koyasu S, 1999. Xid-like immunodeficiency in mice with disruption of the p85alpha subunit of phosphoinositide 3-kinase. Science 283(5400):390-392.

Taghon T, Yui MA, Pant R, Diamond RA, Rothenberg EV, 2006. Developmental and molecular characterization of emerging beta- and gammadelta-selected pre-T cells in the adult mouse thymus. Immunity 24(1):53-64.

Taghon TN, David ES, Zúñiga-Pflucker JC, Rothenberg EV, 2005. Delayed, asynchronous, and reversible T-lineage specification induced by Notch/Delta signaling. Genes Dev 19(8):965-978.

Talora C, Campese AF, Bellavia D, Pascucci M, Checquolo S, Groppioni M, Frati L, von Boehmer H, Gulino A, Screpanti I, 2003. Pre-TCR-triggered ERK signalling-dependent downregulation of E2A activity in Notch3-induced T-cell lymphoma. EMBO Rep 4(11):1067-1072.

Tan JB, Visan I, Yuan JS, Guidos CJ, 2005. Requirement for Notch1 signals at sequential early stages of intrathymic T cell development. Nature Immunol 6(7): 671-679.

Tanaka S, Tsukada J, Suzuki W, Hayashi K, Tanigaki K, Tsuji M, Inoue H, Honjo T, Kubo M, 2006. The interleukin-4 enhancer CNS-2 is regulated by Notch signals and controls initial expression in NKT cells and memory-type CD4 T cells. Immunity 24(6):689-701.

Tang L, Bergevoet SM, Gilissen C, de Witte T, Jansen JH, van der Reijden BA, Raymakers RA, 2010. Hematopoietic stem cells exhibit a specific ABC transporter gene expression profile clearly distinct from other stem cells. BMC Pharmacol 10:12.

Tatarek J, Cullion K, Ashworth T, Gerstein R, Aster JC, Kelliher MA, 2011. Notch1 inhibition targets the leukemia-initiating cells in a Tal1/Lmo2 mouse model of T-ALL. Blood 118(6):1579-1590.

Taussig DC, Miraki-Moud F, Anjos-Afonso F, Pearce DJ, Allen K, Ridler C, Lillington D, Oakervee H, Cavenagh J, Agrawal SG, Lister TA, Gribben JG, Bonnet D, 2008. Anti-CD38 antibody-mediated clearance of human repopulating cells masks the heterogeneity of leukemia-initiating cells. Blodd 112(3):568-575.

Taussig DC, Vargaftig J, Miraki-Moud F, Griessinger E, Sharrock K. Luke T, Lillington D, Oakervee H, Cavenagh J, Agrawal SG, Lister TA, Gribben JG, Bonnet D, 2010. Leukemia-initiating cells from some acute myeloid leukemia patients with mutated nucleophosmin reside in the CD34(-) fraction. Blood 115(10):1976-1984.

Tefferi A, 2010. Novel mutations and their functional and clinical relevance in myeloproliferative neoplasms: JAK2, MPL, TET2, ASXL1, CBL, IDH, and IKZF1. Leukemia 24(6):1128-1138.

Thomas M, Calamito M, Srivastava B, Maillard I, Pear WS, Allman D, 2007. Notch activity synergizes with B-cell-receptor and CD40 signaling to enhance B-cell activation. Blood 109(8):3342-3350.

Thompson EC, Cobb BS, Sabbattini P, Meixlsperger S, Parelho V, Liberg D, Taylor B, Dillon N, Georgopoulos K, Jumaa H, Smale ST, Fisher AG, Merkenschlager M, 2007. Ikaros DNA-binding proteins as integral components of B cell developmental-stage-specific regulatory circuits. Immunity 26(3):355-344.

Trinh LA, Ferrini R, Cobb BS, Weinmann AS, Hahm K, Ernst P, Garraway IP, Merkenschlager M, Smale ST, 2001. Down-regulation of TDT transcription in CD4(+)CD8(+) thymocytes by Ikaros proteins in direct competition with an Ets activator. Genes Dev 15(14):1817-1832.

Tsubata T, 2005. B cell abnormality and autoimmune disorders. Autoimmunity 38(5):331-337.

Tsubata T, Murakami M, Honjo T, 1994. Antigen-receptor cross-linking induces peritoneal B-cell apoptosis in normal but not autoimmunity-prone mice. Curr Biol 4(1):8–17.

Tsubata T, Wu J, Honjo T, 1993. B-cell apoptosis induced by antigen receptor crosslinking is blocked by a T-cell signal through CD40. Nature 364(6438):645-648.

Tsujimoto Y, 2003. Cell death regulation by the Bcl-2 protein family in the mitochondria. J Cell Physiol 195(2):158–167.

Urban JA, Winandy S, 2004. Ikaros null mice display defects in T cell selection and CD4 versus CD8 lineage decisions. J Immunol 173(7):4470-4478.

Uren AG, Kool J, Matentzoglu K, de Ridder J, Mattison J, van Uitert M, Lagcher W, Sie D, Tanger E, Cox T, Reinders M, Hubbard TJ, Rogers J, Jonkers J, Wessels L, Adams DJ, van Lohuizen M, Berns A, 2008. Large-scale mutagenesis in p19(ARF)-and p53-deficient mice identifies cancer genes and their collaborative networks. Cell 133(4):727-741.

Varnum-Finney B, Dallas MH, Kato K, Bernstein ID, 2008. Notch target Hes5 ensures appropriate Notch induced T-versus B-cell choices in the thymus. Blood 111(5):2615-2620.

Wang HC, Peng V, Zhao Y, Sun XH, 2012. Enhanced Notch activation is advantageous but not essential for T cell lymphomagenesis in Id1 transgenic mice. PLos One 7(2):e32944.

Wang JC, 2007. Evaluating therapeutic efficacy cancer stem cells: new challenges posed by a new paradigm. Cell Stem Cell 1(5):497-501.

Wang JC, Dick JE, 2005. Cancer stem cells: lessons from leukemia. Trends Cell Biol 15(9):494-501.

Wang JH, Nichogiannopoulou A, Wu L, Sun L, Sharpe AH, Bigby M, Georgopoulos K, 1996. Selective defects in the development of the fetal and adult lymphoid system in mice with an Ikaros null mutation. Immunity 5(6):537-549.

Wang W, 2003. The SWI/SNF family of ATP-dependent chromatin remodelers: similar mechanisms for diverse functions. Curr Top Microbiol Immunol 274:143-169.

Wardemann H, Yurasov S, Schaefer A, Young JW, Meffre E, Nussenzweig MC, 2003. Predominant autoantibody production by early human B cell precursors. Science 301(5638):1374-1377.

Washburn T, Schweighoffer E, Gridley T, Chang D, Fowlkes BJ, Cado D, Robey E, 1997. Notch activity influences the alphabeta versus gammadelta T cell lineage decision. Cell 88(6):833-843.

Watanabe-Fukunaga R, Brannan CI, Copeland NG, Jenkins NA, Nagata S, 1992. Lymphoproliferation disorder in mice explained by defects in Fas antigen that mediates apoptosis. Nature 356(6367):314–317.

Weber GF, Cantor H, 2001. Differential roles of osteopontin/Eta-1 in early and late lpr disease. Clin Exp Immunol 126(3):578–583.

Weng AP, Ferrando AA, Lee W, Morris JP 4th, Silverman LB, Sanchez-Irizarry C, Blacklow SC, Look AT, Aster JC, 2004. Activating mutations of Notch1 in human T cell acute lymphoblastic leukemia. Science 306(5694): 269-271.

Weng AP, Millholland JM, Yashiro-Ohtani Y, Arcangel ML, Lau A, Wai C, Del Bianco C, Rodriguez CG, Sai H, Tobias J, Li Y, Wolfe MS, Shachaf C, Feisher D, Blacklow SC, Pear WS, Aster JC, 2006. c-Myc is an important direct target of Notch1 in T-cell acute lymphoblastic leukemia/lymphoma. Genes Dev 20(15):2096-2109.

Wienands J, Schweikert J, Wollscheid B, Jumaa H, Nielsen PJ, Reth M, 1998. SLP-65: a new signaling component in B lymphocytes which requires expression of the antigen receptor for phosphorylation. J Exp Med 188(4):791–795.

Wilson A, MacDonald HR, Radke F, 2001. Notch 1-deficient common lymphoid precursors adopt a B cell fate in the thyumus. J Exp Med 194(7):1003-1012.

Winandy S, Wu L, Wang JH, Georgopoulos K, 1999. Pre-T cell receptor (TCR) and TCR-controlled checkpoints in T cell differentiation are set by Ikaros. J Exp Med 190(8):1039-1048.

Winandy S, Wu P, Georgopoulos K, 1995. A dominant mutation in the Ikaros gene leads to rapid development of leukemia and lymphoma. Cell 83(2):289-299.

Wojcik H, Griffiths E, Staggs S, Hagman J, Winandy S, 2007. Expression of a non-DNA-binding Ikaros isoform exclusively in B cells leads to autoimmunity but not leukemogenesis. Eur J Immunol 37(4):1022-1032.

Wu C, Wei Q, Utomo V, Nadesan P, Whetstone H, Kandel R, Wunder JS, Alman BA, 2007. Side population cells isolated from mesenchymal neoplasms have tumor initiating potential. Cancer Res 67(17):8216-8222.

Wu L, Nichogiannopoulou A, Shortman K, Georgopoulos K, 1997. Cell-autonomous defects in dendritic cell populations of Ikaros mutant mice point to a developmental relationship with the lymphoid lineage. Immunity 7(4):483-492.

Yagi T, Hibi S, Takanashi M, Kano G, Tabata Y, Imamura T, Inaba T, Morimoto A, Todo S, Imashuku S, 2002. High frequency of Ikaros isoform 6 expression in acute myelomonocytic and monocytic leukemias: implications for up-regulation of the antiapoptotic protein Bcl-XL in leukemogenesis. Blood 99(4):1350-1355.

Yamazaki J, Mizukami T, Takizawa K, Kuramitsu M, Momose H, Masumi A, Ami Y, Hasegawa H, Hall WW, Tsujimoto H, Hamaguchi I, Yamaguchi K, 2009. Identification of cancer stem cells in Tax-transgenic (Tax-Tg) mouse model of adult T-cell leukemia/lymphoma. Blood 114(13):2709-2720.

Yoshida T, Higuchi T, Hagiyama H, Strasser A, Nishioka K, Tsubata T, 2000. Rapid B cell apoptosis induced by antigen receptor ligation does not require Fas (CD95/APO-1), the adaptor protein FADD/MORT1 or CrmA-sensitive caspases but is defective in both MRL-+/+ and MRL-lpr/lpr mice. Int Immunol 12(4):517–526.

Yoshida T, Ng SY, Zuniga-Pflucker JC, Georgopoulos K, 2006. Early hematopoietic lineage restrictions directed by Ikaros. Nat Immunol 7(4):382-391.

Yumoto K, Ishijima M, Rittling SR, Tsuji K, Tsuchiya Y, Kon S, Nifuji A, Uede T, Denhardt DT, Noda M, 2002. Osteopontin deficiency protects joints against destruction in anti-type II collagen antibody-induced arthritis in mice. Proc Natl Acad Sci U S A 99(7):4556–4561.

Yurasov S, Wardemann H, Hammersen J, Tsuiji M, Meffre E, Pascual V, Nussenzweing MC, 2005. Defective B cell tolerance checkpoints in systemic lupus erythematosus. J Exp Med 201(5):703-711.

Zhang J, Ding L, Holmfeldt L, Wu G, Heatley SL, Payne-Turner D, Easton J, Chen X, Wang J, Rusch M, Lu C, Chen SC, Wei L, Collins-Underwood JR, Ma J, Roberts KG, Pounds SB, Ulyanov A, Becksfort J, Gupta

P, Huether R, Kriwacki RW, Parker M, McGoldrick DJ, Zhao D, Alford D, Espy S, Bobba KC, Song G, Pei D, Cheng C, Roberts S, Barbato MI, Campana D, Coustan-Smith E, Shurtleff SA, Raimondi SC, Kleppe M, Cools J, Shimano KA, Hermiston ML, Doulatov S, Eppert K, Laurenti E, Notta F, Dick JE, Basso G, Hunger SP, Loh ML, Devidas M, Wood B, Winter S, Dunsmore KP, Fulton RS, Fulton LL, Hong X, Harris CC, Dooling DJ, Ochoa K, Johnson KJ, Obenauer JC, Evans WE, Pui CH, Naeve CW, Ley TJ, Mardis ER, Wilson RK, Downing JR, Mullighan CG, 2012. The genetic basis of early T-cell precursor acute lymphoblastic leukaemia. Nature 481(7380):157-163.

Zhang L, Yang S, He YJ, Shao HY, Wang L, Chen H, Gao YJ, Qing FX, Chen XC, Zhao LY, Tan S, 2010. Fluorouracil selectively enriches stem-like leukemic cells in a leukemic cell line. Int J Biol Sci 6(5):419-427.

RESUME EN FRANÇAIS

Ikaros, un facteur de transcription à doigt de zinc, est un régulateur essentiel de la lymphopoïèse. Ikaros est nécessaire á l'engagement des précurseurs lymphoïdes dans le lignage B (Wang et al. 1996), ainsi qu'á la différenciation des lymphocytes B matures (Kirstetter et al. 2002). Ikaros joue aussi un rôle important dans la répression des gènes cibles de Notch pendant le développement des thymocytes T (Dumortier et al. 2006; Kleinmann et al. 2008).

 La lignée de souris Ikaros $^{L/L}$ a été générée dans notre laboratoire par insertion du gène rapporteur LacZ dans l'exon 2 d'Ikzf1 (le gène codant d'Ikaros). Cette insertion entraîne la délétion de la séquence protéique codée par l'exon2 et une expression réduite (environs 10% du niveau normal) d'une protéine Ikaros comportant les domaines de liaison à l'ADN et de dimérisation. Cependant, bien que le phénotype lymphoïde de ces souris soit atténué par rapport aux souris mutantes nulles pour Ikaros (qui ne possèdent pas de cellules B), les souris Ik$^{L/L}$ développent des lymphocytes B après la naissance. Avec l'âge, toutes les souris Ik $^{L/L}$ développent des leucémies T. Ces tumeurs sont dépendantes de la voie de signalisation Notch et présentent souvent des mutations du gène Notch1 similaires à celles trouvées chez les patients atteints de leucémie aiguë lymphoblastique T (LAL-T).

Au cours de mon travail de thèse, j'ai étudié différents phénotypes liés á la perte d'Ikaros dans les cellules B et T chez les souris Ikaros $^{L/L}$. J'ai tout d'abord étudié les leucémies T chez ces souris, notamment par rapport à leur dépendance vis-à-vis de la voie de signalisation Notch et la présence de cellules initiatrices de leucémie. Plus récemment, je me suis impliquée dans l'étude du mécanisme par lequel Ikaros contrôle la tolérance de lymphocytes B, par régulation de la signalisation des MAP kinases.

1) Rôle de Notch dans les leucémies T déficientes pour Ikaros

Plus de 50% de LAL-T humaines ont des mutations activatrices du gène Notch1. Ces mutations facilitent le clivage (activation) ou augmentent la stabilité de la protéine activée (Weng et al. 2004). Par ailleurs, un pourcentage élevé de LAL-T ont des niveaux accrus d'ARN messager du gène Notch3 (Bellavia et al. 2002). Malgré ces données, il n'était pas connu si ces gènes sont requis dans le processus de leucémogenèse T.

Pour étudier la dépendance du développement des leucémies T Ik$^{L/L}$ vis-à-vis de la voie Notch, nous avons délété RBPJ (le facteur de transcription médiateur de la réponse de la voie Notch) chez les souris Ik$^{L/L}$, par croisement avec des allèles floxés de RBPJ et le transgène CD4-Cre. Nous avons aussi étudié les rôles de Notch1 et Notch3 par croisement avec des animaux nuls pour Notch3, ou par délétion de Notch1 dans les cellules T Ik$^{L/L}$ (allèles floxés de Notch1 et transgène CD4-Cre). La suppression de RBP-J retarde l'apparition de la leucémie de 18 semaines á 30 semaines, montrant l'importance de la voie Notch. L'absence de Notch3 par contre n'a pas impact sur la cinétique de développement et le phénotype des tumeurs. De façon surprenante, la suppression spécifique du promoteur et de l'exon1 de Notch1 accélère la leucémogenèse. Ces tumeurs montrent encore une forte activation de la voie Notch et expriment de façon constitutive

des protéines Notch1 activée. Nous avons montré que la délétion du promoteur de Notch1 est un événement oncogénique, car elle conduit à l'activation de promoteurs cryptiques intragéniques dans la région 3' du gène, qui génèrent des transcrits codant pour des protéines Notch1 constitutivement actives.

2) Analyse des cellules initiatrices de leucémie dans le modèle murin de LAL-T déficient pour Ikaros

Alors que la vision traditionnelle était qu'un cancer est un ensemble de cellules toutes équivalentes entre elles qui se divisent de façon incontrôlée, de nombreux travaux récents ont suggéré qu'il existe une grande hétérogénéité cellulaire dans les cancers, et que seules certaines cellules rares possèdent la capacité de se diviser de façon indéfinie. Ces cellules ont été appelées cellules souches tumorales. En se divisant, elles peuvent donner naissance à une cellule équivalente, ou à une cellule tumorale qui ne possède qu'un pouvoir réduit à proliférer. Ce concept a été établi pour de nombreux cancers, mais sa validité pour les leucémies T reste à confirmer. Les cellules souches tumorales sont en général des cellules qui prolifèrent peu, et qui sont épargnées par les thérapies traditionnelles qui ciblent les cellules en prolifération. Leur préservation pourrait être à l'origine des rechutes et des échecs thérapeutiques. Il est donc essentiel de mieux comprendre la biologie de ces cellules pour pouvoir définir dans l'avenir des stratégies thérapeutiques pour les éliminer.

J'ai entrepris d'analyser les tumeurs $Ik^{L/L}$ pour déterminer si des cellules souches leucémiques existent ou pas. Par des essais de transplantation j'ai testé la capacité des cellules tumorales $Ik^{L/L}$ à initier des tumeurs chez les souris receveuses irradiées de façon létale. Les transplantations effectuées par dilution limite indiquent que le nombre de cellules initiatrices de leucémie présentes dans les tumeurs $Ik^{L/L}$ n'est pas si rare, puisqu'il est possible de générer des tumeurs avec l'injection d'au moins 500 cellules tumorales. J'ai aussi montré que toutes les cellules leucémiques de ces souris ne sont pas équivalentes et que certaines d'entre elles sont plus agressives. Par des transplantations en série, où la tumeur générée dans les premières souris receveuses est utilisée pour générer des tumeurs chez des souris receveuses secondaires puis tertiaires, j'ai montré que les cellules tumorales $Ik^{L/L}$ ont une capacité d'auto-renouvellement à long-terme, une caractéristique importante de cellules souches. J'ai par ailleurs détecté une population minoritaire (environ 1% des cellules leucémiques) qui possède des propriétés normalement associées aux cellules souches, et qui est fortement enrichie parmi les cellules résistantes à la thérapie par le 5-fluorouracil.

3. Ikaros contrôle la tolérance de lymphocytes B en limitant la signalisation des MAP kinases

Des études récentes d'association génétique ont montré qu'un polymorphisme du gène humain IKZF1 prédispose au lupus érythémateux systémique (SLE) (Han et al, 2009), maladie caractérisée par la production d'auto-anticorps anti-nucléaires et de lésions rénales.

La cellule B peut être activée par liaison des antigènes au récepteur des cellules B (BCR), où un seuil de signal est nécessaire pour provoquer une réponse proliférative qui est déterminée par l'affinité de l'antigène pour le BCR et la densité de l'antigène (Batista and Neuberger, 1998). La cellule B peut aussi être activée par les cellules T après l'engagement des molécules CD40 exprimées à la surface des cellules B avec leur ligand CD40L. Cette co-stimulation supprime la réponse apoptotique et favorise l'entrée dans le cycle cellulaire (Niiro and Clark, 2002). Dans le laboratoire, nous avons précédemment montré que les cellules B $Ik^{L/L}$ sont hyper-prolifératives suite à la stimulation par le BCR (Kirstetter et al. 2002).

Nous avons montré que la réponse transcriptionnelle provoquée par la stimulation du BCR dans les cellules B déficientes pour Ikaros est similaire à celle cellules B de type sauvage. Par contre, Ikaros contrôle des réseaux de gènes dans les cellules B naïves qui limitent la réactivité des MAP kinases Erk et p38, après signalisation par le BCR. Nous avons montré que l'activation excessive d'Erk et p38 dans les cellules B $Ik^{L/L}$ stimulées par le BCR et CD40L détermine leur phénotype d'hyper-prolifération. Nous avons également analysé la production d'auto-anticorps chez ces souris, et avons observé que les souris $Ik^{L/L}$ produisent des auto-anticorps caractéristiques du SLE comme les anticorps anti-chromatine, anti-ADN et anti-nucléaire. J'ai montré que les phénotypes d'hyper-prolifération des cellules B après stimulation, d'hyper-activation d'Erk et de production d'auto-anticorps sont également présents chez les souris où la suppression d'Ikaros est induite spécifiquement dans les cellules B matures. Ces résultats suggèrent qu'Ikaros contrôle la tolérance des lymphocytes B en régulant l'activation de la voie des MAP kinases.

Déficit en Ikaros: de LAL-T à la maladie auto-immune

Le facteur de transcription Ikaros est un régulateur essentiel de la lymphopoïèse. Ikaros est nécessaire à la différenciation des lymphocytes B et joue aussi un rôle important dans la suppression des leucémies leucémie aiguës lymphoblastique T (LAL-T). Contrairement aux souris mutantes nulles pour Ikaros, les souris mutantes hypomorphes Ik$^{L/L}$ développent des lymphocytes B matures après la naissance. Avec l'âge, toutes les souris Ik$^{L/L}$ développent des leucémies T Notch dépendantes avec des mutations similaires à celles trouvées chez les patients atteints de LAL-T. La souris Ik$^{L/L}$ est donc un excellent modèle pour étudier l'activation des cellules B matures et la pathogenèse des LAL-T. Nous avons montré que la délétion spécifique du promoteur et de l'exon 1 de Notch1 dans les cellules T conduit à l'activation de promoteurs cryptiques dans la région 3' du gène, qui génèrent des transcrits codant pour des protéines Notch1 constitutivement actives qui accélèrent la leucémogenèse dans la souris Ik$^{L/L}$. De plus, nous mettrons en évidence l'existence de cellules initiatrices de leucémie dans les tumeurs Ik$^{L/L}$ puisque nous avons trouvé que des cellules ayant la capacité de s'auto-renouveler représentent 1 sur 500. En outre, nous avons démontré que certaines cellules tumorales ont la capacité de rejeter le colorant de Hoechst et que ces cellules sont enrichies dans les cellules quiescentes. Enfin, nous avons montré que les cellules B Ik$^{L/L}$ ont une activation excessive de ERK et de p38 après la stimulation du BCR, ce qui résulte en une hyper-prolifération et une production d'autoanticorps liés au lupus systémique érythémateux. Nos résultats suggèrent qu'Ikaros est un régulateur négatif de l'activation des lymphocytes B.

Ikaros deficiency: from T-ALL to auto-immune disease

The Ikaros transcription factor is a critical regulator of lymphopoeisis. Ikaros is needed for the differentiation of B cell and plays an important role in tumor suppression in T cells. Contrary to the other Ikaros targeted mutant mice, the Ik$^{L/L}$ mouse develops mature B cells after birth. With age, it develops Notch dependent tumors with similar mutations as those found in human T cell acute lymphoblastic leukemia (T-ALL). Thus, the Ik$^{L/L}$ mouse is an excellent model to study mature B cell activation and T-ALL tumor development. Here, we have shown that the deletion of the promoter and exon1 of the Notch1 gene in Ik$^{L/L}$ T cells activates a cryptic promoter in the 3' region which leads to the production of truncated, constitutively activated Notch1 proteins that accelerate tumorigenesis in the Ik$^{L/L}$ mice. Moreover, we give evidence for the existence of LICs in the Ik$^{L/L}$ tumors as we have found a specific subpopulation of cells with a frequency of 1 in 500 which show self-renewal capacity. In addition, we demonstrated that some tumor cells have the ability to efflux the Hoechst dye and that this side population is enriched in quiescent cells. Finally, we elucidate that Ik$^{L/L}$ B cells display an enhanced activation of ERK and p38 after BCR stimulation that results in hyper-proliferation and the production of autoantibodies related to systemic lupus erythematosus (SLE). Our results suggest that Ikaros is a negative regulator of B cell activation.